

**Engineering Gelatin-Based
Biomatrices *for*
Pre-vascularisation *of*
Bone Analogues**

Barbara Klotz

Engineering Gelatin-Based Biomatrices for Pre-vascularisation of Bone Analogues

Barbara Klotz

Copyright © B.J.Klotz 2020. All rights reserved. No parts of this thesis may be reproduced, stored in a retrieval system of any nature or transmitted in any form or by any means, without prior written consent of the author. The copyright of the articles that have been published has been transferred to the respective journals.

ISBN: 978-94-6380-647-3

Cover and design: Pattern from Freepik.com
ProefschriftMaken, proefschriftmaken.nl

Layout and print: ProefschriftMaken, proefschriftmaken.nl

Financial support for the printing of this thesis was kindly provided by the Dutch society for Biomaterials and Tissue Engineering (NBTE) and the 'Utrechtse Stichting tot Bevordering der Mondziekten, Kaak- en Aangezichtschirurgie'.

Engineering Gelatin-Based Biomatrices for Pre-vascularisation of Bone Analogues

**Ontwerp van biomaterialen
voor pre-vascularisatie van botanalogen**

(met een samenvatting in het Nederlands)

**Konstruktion von Biomaterialien
zur Vaskularisation von Knochenanaloga**

(mit einer Zusammenfassung in deutscher Sprache)

Proefschrift

ter verkrijging van de graad van doctor aan de Universiteit Utrecht
op gezag van de rector magnificus, prof. dr. H.R.B.M. Kummeling,
ingevolge het besluit van het college voor promoties
in het openbaar te verdedigen op vrijdag 7 februari 2020 des middags te 12.45 uur

door

Barbara Judith Klotz

geboren op 26 november 1988 te Filderstadt, Duitsland

Promotoren

Prof. dr. A.J.W.P. Rosenberg

Prof. dr. ir. J. Malda

Copromotoren

Dr. ir. D. Gawlitta

Dr. K.S. Lim

Table of contents

Chapter 1	General introduction and research aims	7
Chapter 2	Gelatin-Methacryloyl Hydrogels: Towards Biofabrication-Based Tissue Repair	21
Chapter 3	Visible light crosslinking of gelatin hydrogels offers an enhanced cell microenvironment with improved light penetration depth	45
Chapter 4	Enzymatically crosslinked gelatin hydrogels for engineering pre-vascularised bone-like tissue analogues	73
Chapter 5	A versatile bio-synthetic hydrogel platform for engineering of tissue analogues	93
Chapter 6	Engineering of a complex bone tissue model with endothelialised channels and capillary-like networks	121
Chapter 7	General discussion and future perspectives	147
Appendices		159
	Supporting Information Chapter 6	161
	List of abbreviations	165
	Nederlandse samenvatting	167
	Deutsche Zusammenfassung	171
	Acknowledgements	175
	Curriculum Vitae	179

Chapter 1

General introduction and
research aims



From autologous bone flaps to engineered tissue analogues for bone regeneration

In the last 10 years, bone remains as the second most transplanted tissue in the human body. The current treatment of a missing bone segment is the replacement with autologous bone [1]. While smaller bone defects *e.g.* in the mandible can be replaced by non-vascularised bone tissue transplants, defects exceeding approximately 5 cm in length also require immediate vascular supply. Consequently, for such large bone defects, vascularised bone flaps are used [2]. These vascularised flaps are conventionally harvested from the fibula, scapula or the iliac crest [3]. Anastomosis of such a relatively large implant is critical to guarantee immediate blood supply through the full thickness of the implanted graft and therefore survival of the implant. However, the limitation of such reconstructive surgeries are the burdens on the patient of donor site morbidity [4] and the requirement of long surgery times [5].

The field of tissue engineering, as defined by Langer and Vacanti in 1993, holds the promise to develop tissue substitutes with the aim to maintain, restore or augment the functions of a patient's diseased tissue [6]. To engineer such a tissue analogue, primary human cells are used and cultured in a carrier material provided by additional stimuli. Over the course of almost 30 years, successes were reached for thin or avascular tissues and organs such as cartilage [7-9], skin [10] and bladder [11].

For tissue engineering of bone and other tissues, the major bottleneck is vascularisation for creation of up-scaled tissue constructs of clinically-relevant size [12]. Another challenge in engineering vascularised bone tissues lies in the requirement of a carrier material that allows for efficient tissue development. Furthermore, next to the desired biological, mechanical and chemical requirements of a biomaterial [12], also its clinical applicability is critical [13].

Above named challenges are currently addressed in the field of tissue engineering to enable the fabrication of vascularised bone tissue analogues. Once strategies are found to successfully fabricate bone tissue analogues in the laboratory from the patient's own (stem) cells, in future such implants could replace autologous bone flaps.

Tissue engineering of pre-vascularised bone analogues

Tissue engineering of clinically-relevant sized constructs, requires the simultaneous development of vasculature and bone. Pre-vascularisation of a tissue analogue is a strategy to enable direct blood-perfusion of the engineered construct after implantation at the defect site. Key ingredients for engineering bone with an intricate pre-vascular network include stem cell co-cultures and a carrier material. In this section, approaches to create these co-cultures and state-of-the-art in material development will be introduced.

Co-cultures to engineer pre-vascularised bone tissue

To engineer pre-vascularised bone tissue, co-cultures of cells are required containing endothelial functions, pericyte-like cells [14] that can stabilise endothelial networks and cells that undergo osteogenesis (Figure 1). Furthermore, it has been shown that independent of the differentiation status of the endothelial cells, they can induce osteoblastic differentiation of the multipotent mesenchymal stromal cells (MSCs) that they are co-cultured with [15]. In the present thesis, cell types were chosen for the co-cultures that could be used in an autologous clinical setting.

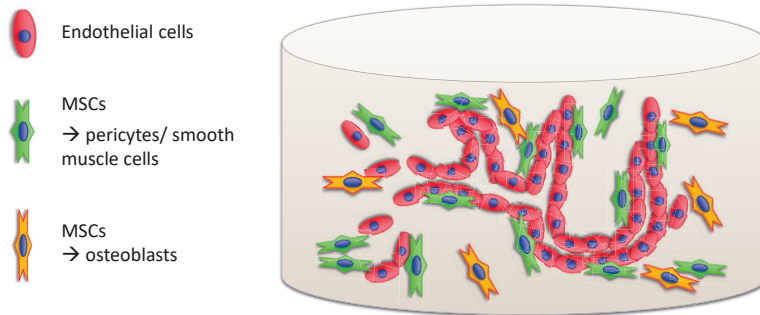


Figure 1. Co-cultures of endothelial cells and differentiated MSCs into pericyte-like cells and osteoblasts. Endothelial cells selforganise into capillary-like structures which are stabilised by pericyte-like cells. A fraction of MSCs differentiates into osteogenic cells.

Endothelial progenitor cells can be derived from bone marrow, peripheral blood or cord blood and can differentiate into a mature endothelial phenotype [16] and stimulate *de novo* formation of vascular networks [17]. Endothelial colony forming cells (ECFCs) or outgrowth endothelial cells (OECs/EOCs) have potent proliferative capacities [18] and physically contribute to vasculogenesis [19, 20]. When derived from cord blood, both higher cell numbers and higher colony numbers can be obtained compared to isolation from adult peripheral blood. Furthermore, secondary and tertiary colonies can arise from umbilical cord blood, which is not possible from peripheral blood [21]. Additionally, the immune privilege [22] of these cells makes them valuable for clinical applications [15].

When MSCs are used in the co-culture, they can differentiate into pericytes that support and stabilise self-assembled endothelial networks. For the osteoblastic phenotype either isolated primary osteoblasts or undifferentiated stem cells are used, which need to be stimulated to undergo osteogenic differentiation. The benefit of using undifferentiated cells like MSCs (derived from *e.g.* bone marrow, adipose tissue or from dental tissue), is the clinical relevance of these cells. In contrast to (pre) osteoblasts, these cells can be expanded in high numbers.

For the above reasons, in present thesis, ECFCs and MSCs were selected to engineer pre-vascularised bone tissue.

While *in vitro*, the clear beneficial effect of endothelial/ osteogenic co-cultures was shown, *in vivo*, a significantly added effect on bone regeneration of using endothelial cells for co-implantation with bone-forming cells was not yet clearly shown [23]. To aim for a clinically significant effect of endothelial cells combined with osteogenically committed cells on bone regeneration *in vivo*, a supporting carrier material needs to be found by selection *in vitro*.

Natural versus synthetic hydrogels

As a cell carrier material for tissue regeneration, hydrogels are very popular, since they closely resemble the natural extracellular matrix (ECM), which is composed of a protein network with high water content. Furthermore, hydrogels provide the residing stem cells with a three dimensional (3D) environment in which cells can secrete matrix and remodel the ECM into tissue-like constructs [24]. The increased attention of hydrogels is, moreover, also attributed to a paradigm shift. Cells cultured in 3D compared to 2D behave differently and their behaviour better resembles the responses that cells elicit in native tissues [25].

Hydrogels can be composed of either synthetic polymers and/or natural materials. While natural hydrogels are bioactive and biodegradable, synthetic materials need to be enriched with cell adhesion sites and with biodegradable linkers between polymers. These natural hydrogels or enriched synthetic environments need to allow for cell migration and matrix deposition.

For synthetic hydrogels, polyethylene glycol (PEG) is an often used base-material since it is readily available, easily modified and does generally not elicit an immune response upon implantation [26]. Furthermore, PEG is an often used compound for medical applications such as to stabilise active ingredients when injected into the blood stream [27]. Since it is a biologically inert and hydrophilic polymer, it is especially suitable as a base-material for tissue engineering applications.

Despite the progress in the field of polymers, it still remains a challenge to build synthetic materials that can cover the pleiotropic functions of a biologic material and consequently these materials remain reductionist [28]. Furthermore, the natural ECM can still be considered as a black box with different features that are only slowly beginning to be understood. For instance, recently, it was established that fast stress-relaxation properties of a material are critical for cell differentiation [29]. These dynamics are inherently present in natural ECMs, meaning that residing cells in a material are able to deform it. In contrast, synthetic materials typically exhibit an elastic behaviour instead [29].

On the other hand, biologic materials such as collagen, fibrin and alginate are extensively used, but early degradation is a well-known disadvantage. Furthermore, immunogenicity and batch-to-batch variation can be additional drawbacks of using these biologic materials for tissue engineering.

Among the biologic materials, gelatin is an exemption. Via acid- or base-extraction it is derived from collagen, the most abundant protein in mammals. As the heat-denatured form of collagen, it retains its bioactive sequences, while the immunogenicity is limited [30, 31]. Gelatin is characterised by bioactive sequences that mediate cell functions such as proliferation, migration and differentiation, and furthermore, cell-mediated enzymatic degradation is enabled [31-33]. Gelatin is used in the clinics since several decades as plasma expander and as stabiliser in vaccines [34]. In Chapter 2 gelatin is discussed more in detail.

Design and development of novel hydrogels

In order to select or develop a suitable hydrogel for endothelial and MSC co-cultures, both base-material(s) and crosslinking mechanism are critical.

For tissue engineering purposes, gelatin-based materials are very attractive due to the intrinsic biological activity of the material, the biodegradability and the limited immunogenicity as outlined above. Therefore, all studies of this thesis were based on gelatin as a base-material for the creation of different hydrogel platforms.

For the formation of the capillary network, soft hydrogels with an elastic modulus below 4 kPa are required [35-37]. In general, such soft gels can be achieved by applying low polymer, protein or peptide concentrations, but also by introducing a low number of crosslinks of the chains [36, 38]. However, as a consequence, soft hydrogels are prone to early degradation and low shape stability [37]. Ideally, the hydrogel degradation would be in balance with the matrix deposition of the residing cells [39]. In contrast to vasculogenesis, pronounced osteogenic differentiation can be stimulated in rather stiff matrices with E-moduli between 15 and 30 kPa [40, 41]. While it was shown that osteogenic cell differentiation is improved when co-cultured with endothelial cells [42], osteogenesis might be even further enhanced in soft hydrogels.

Next to the base material itself, also the crosslinking mechanism of a hydrogel critically determines the characteristics of a biomaterial. The crosslinking mechanism of a hydrogel contributes to the biological performance of a material. While radicals are generated during photo-crosslinking, enzymatic crosslinking such as by transglutaminases is mimicking the physiological way of crosslinking proteins. These are all considerations to take into account when selecting or developing a clinically-relevant hydrogel platform for engineering functional vascularised bone tissue analogues.

Fabrication approaches of hydrogel-based constructs

For 3D cell cultures, conventionally, millimetre to centimetre-scale disc-shaped hydrogels are used (see Chapter 2, Key Figure). Such model constructs allow for the study of cell-material interactions. Upscaling of such model constructs is required to fabricate clinically-relevant sized constructs. Biofabrication is a technique that emerged in recent years, which could help to scale-up. Bioprinting or robotic assembly of cell-laden modules are strategies to fabricate spatially defined, complex

tissue constructs, composed of multiple cell types and materials (*e.g.* hydrogels and thermoplastic materials) [43-47]. Also, moulding approaches are often combined with 3D bioprinting. Kolesky and co-workers suggest to divide the different components of a tissue analogue over multiple bioinks that are 3D printed, after which an ECM-like hydrogel is moulded around the biofabricated scaffold [48]. To generate channels that could serve as channels for the vascular system, fugitive/sacrificial materials are used [48].

This thesis is focussing on the design of biologically active hydrogels that support cell differentiation and ultimately can support the formation of pre-vascularised bone tissue analogues. Therefore, co-cultures in mm-sized hydrogel discs of various materials are used to investigate the cell-material interactions and cell behaviour such as migration and differentiation during material development and selection. A next step could be the inclusion of the selected material in biofabrication approaches. The here investigated or developed hydrogel platforms could be fine-tuned for use in direct biofabrication processes or as moulding materials that are combined with biofabrication.

Research aims and thesis outline

The goal of this thesis is to develop hydrogel platforms that are suitable for engineering pre-vascularised bone-like tissue analogues. Suitability in this context means that the material allows for formation of vascular networks, stabilised by pericyte-like cells and osteogenic differentiation *in vitro*. Furthermore, the clinical relevance was a strong motivator for the choices of both the biomaterials and the cell sources to facilitate its translatability into putative clinical applications in the future. In table 1 the main aim of the thesis and the underlying specific research questions are summarised.

The work of this thesis takes advantage of previously established co-culture methods for ECFCs from umbilical cord blood and MSCs from bone marrow [49]. However, in order to successfully engineer a pre-vascularised bone-like tissue construct, it is of critical relevance to find a carrier material that can support this tissue development process.

First of all, the potential and limitations of an often used material, gelatin-methacryloyl (gelMA), will be described in a literature review in **Chapter 2**. It particularly focusses on gelMA hydrogels for tissue engineering and biofabrication approaches. Specifically, the literature is evaluated regarding the use of gelMA as a matrix material for vascularised bone engineering and aspects towards clinical application of gelMA are reviewed. Due to the promising characteristics of gelMA, this material was used as a starting point in experimental studies. In **Chapter 3**, the potential cytotoxic concerns around the UV-initiated crosslinking of gelMA hydrogels will be addressed and a new photo-initiator set will be investigated that could be activated in the visible light spectrum. In particular, it will be investigated

whether a visible light crosslinking system could outperform UV light-mediated gelMA crosslinking in terms of biofunctionality of the encapsulated cells and light penetration depth to create up-scaled hydrogel constructs. For better comparison to existing literature chondrocytes were used, since gelMA hydrogels were mainly used for cartilage engineering. Next, the effects of crosslinking reactions that are mediated via enzymatic reactions, rather than by radicals, and that can occur under physiological conditions will be investigated. In **Chapter 4**, the focus is to explore the enzymatic crosslinking of gelatin by microbial transglutaminase and the additional option to immobilise native proteins in the hydrogel. More specifically, osteogenesis is enhanced in soft gelatin-transglutaminase hydrogels by the incorporation of tissue-specific laminins. In a next step, the objective is to overcome the premature degradation of low-concentration gelatin by incorporation of a synthetic component into a hydrogel platform. Furthermore, required characteristics of the novel material include the possibility of tissue-specific tailoring of the hydrogel with native, unmodified proteins and to allow for robust vascularisation and bone formation. Therefore, **Chapter 5** describes a novel hydrogel platform based on clinically-relevant components including gelatin, PEG and factor XIIIa (a factor involved in the blood coagulation cascade) for crosslinking. Moreover, the hydrogel will be tailored with different proteins for the engineering of various tissue types.

As a subaim of this thesis, also an explorative study will be undertaken to estimate the feasibility of engineering complex vascularised bone-like constructs (**Chapter 6**). Importantly, clinically relevant cells will be used, which require cell differentiation during co-culture. An endothelial-lined channelled construct will be made which is surrounded by a co-culture in the bulk hydrogel. The potential strategies will be explored to achieve parallel divergent cellular differentiation, *i.e.* towards pericytes and osteogenic lineages, within a single biomaterial within the same culture medium. In **Chapter 7**, the most important differences between the employed hydrogel systems and their relevance for pre-vascularised bone tissue engineering is discussed.

Table 1. Overview of the research aims**Main aim:**

To design gelatin-based hydrogel platforms that are clinically relevant, support vasculogenesis and osteogenic differentiation, and can be utilised to stimulate the formation of pre-vascularised bone tissue analogues.

Specific aims:

1. To investigate whether visible light-induced hydrogel crosslinking is superior to UV-light in terms of biofunctional performance of embedded cells and light penetration depth in up-scaled hydrogel constructs. (**Chapter 3**)
2. To investigate the potential of enzymatically crosslinked gelatin hydrogels to fabricate pre-vascularised, osteogenically differentiated tissue analogues. (**Chapter 4**)
3. To develop a semi-synthetic platform that is tunable and stable at low polymer concentrations; has comparable biological functionality as the clinically not relevant material Matrigel; and the option to immobilise tissue-specific proteins that can guide tissue development. (**Chapter 5**)

Subaim:

4. Explorative feasibility study to engineer a complex bone tissue model with an endothelialised channel and capillary-like networks with osteogenically differentiated cells in the bulk hydrogel. (**Chapter 6**)

References

1. Shegarfi, H. and O. Reikeras, *Review article: bone transplantation and immune response*. J Orthop Surg (Hong Kong), 2009. **17**(2): p. 206-11.
2. Sándor, G.K.B., T.C. Lindholm, and C.M.L. Clokie, *Bone Regeneration of the Cranio-maxillofacial and Dento-alveolar Skeletons in the Framework of Tissue Engineering*. Topics in Tissue Engineering, 2003.
3. Haumer, A., et al., *From Autologous Flaps to Engineered Vascularized Grafts for Bone Regeneration*. Vascularization for Tissue Engineering and Regenerative Medicine, 2017: p. 1-34.
4. Ling, X.F. and X. Peng, *What is the price to pay for a free fibula flap? A systematic review of donor-site morbidity following free fibula flap surgery*. Plast Reconstr Surg, 2012. **129**(3): p. 657-74.
5. Pogrel, M.A., et al., *A comparison of vascularized and nonvascularized bone grafts for reconstruction of mandibular continuity defects*. Journal of Oral and Maxillofacial Surgery, 1997. **55**(11): p. 1200-1206.
6. Langer, R. and J.P. Vacanti, *Tissue engineering*. Science, 1993. **260**(5110): p. 920-6.
7. Brittberg, M., et al., *Matrix-Applied Characterized Autologous Cultured Chondrocytes Versus Microfracture: Five-Year Follow-up of a Prospective Randomized Trial*. Am J Sports Med, 2018. **46**(6): p. 1343-1351.
8. Saris, D., et al., *Matrix-Applied Characterized Autologous Cultured Chondrocytes Versus Microfracture: Two-Year Follow-up of a Prospective Randomized Trial*. Am J Sports Med, 2014. **42**(6): p. 1384-94.
9. Basad, E., et al., *Matrix-induced autologous chondrocyte implantation versus microfracture in the treatment of cartilage defects of the knee: a 2-year randomised study*. Knee Surg Sports Traumatol Arthrosc, 2010. **18**(4): p. 519-27.
10. Yannas, I.V., et al., *Synthesis and characterization of a model extracellular matrix that induces partial regeneration of adult mammalian skin*. Proc Natl Acad Sci U S A, 1989. **86**(3): p. 933-7.
11. Atala, A., et al., *Tissue-engineered autologous bladders for patients needing cystoplasty*. Lancet, 2006. **367**(9518): p. 1241-6.
12. Khademhosseini, A. and R. Langer, *A decade of progress in tissue engineering*. Nat Protoc, 2016. **11**(10): p. 1775-81.
13. Fatehullah, A., S.H. Tan, and N. Barker, *Organoids as an in vitro model of human development and disease*. Nat Cell Biol, 2016. **18**(3): p. 246-54.
14. Au, P., et al., *Bone marrow-derived mesenchymal stem cells facilitate engineering of long-lasting functional vasculature*. Blood, 2008. **111**(9): p. 4551-4558.
15. Thebaud, N.B., et al., *Whatever their differentiation status, human progenitor derived - or mature - endothelial cells induce osteoblastic differentiation of bone marrow stromal cells*. Journal of Tissue Engineering and Regenerative Medicine, 2012. **6**(10): p. e51-e60.
16. Asahara, T., et al., *Isolation of putative progenitor endothelial cells for angiogenesis*. Science, 1997. **275**(5302): p. 964-967.
17. Yoder, M.C., *Human endothelial progenitor cells*. Cold Spring Harb Perspect Med, 2012. **2**(7): p. a006692.
18. Melero-Martin, J.M., et al., *In vivo vasculogenic potential of human blood-derived endothelial progenitor cells*. Blood, 2007. **109**(11): p. 4761-8.

19. Yoon, C.H., et al., *Synergistic neovascularization by mixed transplantation of early endothelial progenitor cells and late outgrowth endothelial cells: the role of angiogenic cytokines and matrix metalloproteinases*. *Circulation*, 2005. **112**(11): p. 1618-27.
20. Chong, M.S., W.K. Ng, and J.K. Chan, *Concise Review: Endothelial Progenitor Cells in Regenerative Medicine: Applications and Challenges*. *Stem Cells Transl Med*, 2016. **5**(4): p. 530-8.
21. Lavergne, M., et al., *Cord blood-circulating endothelial progenitors for treatment of vascular diseases*. *Cell Proliferation*, 2011. **44**: p. 44-47.
22. Ladhoff, J., et al., *Immune privilege of endothelial cells differentiated from endothelial progenitor cells*. *Cardiovascular Research*, 2010. **88**(1): p. 121-129.
23. Shanbhag, S., et al., *Cell Cotransplantation Strategies for Vascularized Craniofacial Bone Tissue Engineering: A Systematic Review and Meta-Analysis of Preclinical In Vivo Studies*. *Tissue Eng Part B Rev*, 2017. **23**(2): p. 101-117.
24. Klotz, B.J., et al., *Gelatin-Methacryloyl Hydrogels: Towards Biofabrication-Based Tissue Repair*. *Trends Biotechnol*, 2016. **34**(5): p. 394-407.
25. Pampaloni, F., E.G. Reynaud, and E.H. Stelzer, *The third dimension bridges the gap between cell culture and live tissue*. *Nat Rev Mol Cell Biol*, 2007. **8**(10): p. 839-45.
26. Zalipsky, S. and J.M. Harris, *Poly(Ethylene Glycol)* 1997. **680**(ACS Symposium Series): p. 1-13.
27. Davis, F.F., *The origin of peganology*. *Adv Drug Deliv Rev*, 2002. **54**(4): p. 457-8.
28. Ehrbar, M., et al., *Enzymatic formation of modular cell-instructive fibrin analogs for tissue engineering*. *Biomaterials*, 2007. **28**(26): p. 3856-66.
29. Rosales, A.M. and K.S. Anseth, *The design of reversible hydrogels to capture extracellular matrix dynamics*. *Nature Reviews Materials*, 2016. **1**(2).
30. Gorgieva, S. and V. Kokol, *Collagen- vs. Gelatine-Based Biomaterials and Their Biocompatibility: Review and Perspectives*. INTECH Open Access Publisher 2011.
31. Van den Steen, P.E., et al., *Biochemistry and molecular biology of gelatinase B or matrix metalloproteinase-9 (MMP-9)*. *Crit Rev Biochem Mol Biol*, 2002. **37**(6): p. 375-536.
32. Nichol, J.W., et al., *Cell-laden microengineered gelatin methacrylate hydrogels*. *Biomaterials*, 2010. **31**(21): p. 5536-44.
33. Heino, J., et al., *Evolution of collagen-based adhesion systems*. *Int J Biochem Cell Biol*, 2009. **41**(2): p. 341-8.
34. Elzoghby, A.O., *Gelatin-based nanoparticles as drug and gene delivery systems: reviewing three decades of research*. *J Control Release*, 2013. **172**(3): p. 1075-91.
35. Occhetta, P., et al., *VA-086 methacrylate gelatine photopolymerizable hydrogels: A parametric study for highly biocompatible 3D cell embedding*. *Journal of Biomedical Materials Research Part A*, 2015. **103**(6): p. 2109-2117.
36. Chen, Y.C., et al., *Functional Human Vascular Network Generated in Photocrosslinkable Gelatin Methacrylate Hydrogels*. *Advanced Functional Materials*, 2012. **22**(10): p. 2027-2039.
37. Klotz, B.J., et al., *Engineering of a complex bone tissue model with endothelialised channels and capillary-like networks*. *Eur Cell Mater*, 2018. **35**: p. 335-348.
38. Celikkin, N., et al., *Gelatin methacrylate scaffold for bone tissue engineering: The influence of polymer concentration*. *Journal of Biomedical Materials Research Part A*, 2018. **106**(1): p. 201-209.
39. Hutmacher, D.W., *Scaffolds in tissue engineering bone and cartilage*. *Biomaterials*, 2000. **21**(24): p. 2529-43.
40. Tan, S., et al., *The synergetic effect of hydrogel stiffness and growth factor on osteogenic differentiation*. *Biomaterials*, 2014. **35**(20): p. 5294-306.

41. Wen, J.H., et al., *Interplay of matrix stiffness and protein tethering in stem cell differentiation*. Nature Materials, 2014. **13**(10): p. 979-987.
42. Tae, J.Y., et al., *Enhanced Osteogenic Differentiation Potential of Stem-Cell Spheroids Created From a Coculture of Stem Cells and Endothelial Cells*. Implant Dent, 2017. **26**(6): p. 922-928.
43. Kolesky, D.B., et al., *Three-dimensional bioprinting of thick vascularized tissues*. Proc Natl Acad Sci U S A, 2016. **113**(12): p. 3179-84.
44. Mekhileri, N.V., et al., *Automated 3D bioassembly of micro-tissues for biofabrication of hybrid tissue engineered constructs*. Biofabrication, 2018. **10**(2): p. 024103.
45. Schuurman, W., et al., *Bioprinting of hybrid tissue constructs with tailorable mechanical properties*. Biofabrication, 2011. **3**(2): p. 021001.
46. Boere, K.W., et al., *Covalent attachment of a three-dimensionally printed thermoplast to a gelatin hydrogel for mechanically enhanced cartilage constructs*. Acta Biomater, 2014. **10**(6): p. 2602-11.
47. Visser, J., et al., *Reinforcement of hydrogels using three-dimensionally printed microfibrils*. Nature Communications, 2015. **6**.
48. Kolesky, D.B., et al., *3D bioprinting of vascularized, heterogeneous cell-laden tissue constructs*. Adv Mater, 2014. **26**(19): p. 3124-30.
49. Pennings, I., et al., *Effect of donor variation on osteogenesis and vasculogenesis in hydrogel cocultures*. J Tissue Eng Regen Med, 2019. **13**(3): p. 433-445.

Chapter 2

Gelatin-Methacryloyl Hydrogels: Towards Biofabrication-Based Tissue Repair

Barbara J. Klotz | Debby Gawlitta | Antoine J.W.P. Rosenberg
Jos Malda | Ferry P.W. Melchels

Trends in Biotechnology 2016 May;34(5):394-407



Abstract

Research over the past decade on the cell–biomaterial interface has shifted to the third dimension. Besides mimicking the native extracellular environment by 3D cell culture, hydrogels offer the possibility to generate well-defined 3D biofabricated tissue analogs. In this context, gelatin-methacryloyl (gelMA) hydrogels have recently gained increased attention. This interest is sparked by the combination of the inherent bioactivity of gelatin and the physicochemical tailorability of photo-crosslinkable hydrogels. GelMA is a versatile matrix that can be used to engineer tissue analogs ranging from vasculature to cartilage and bone. Convergence of biological and biofabrication approaches is necessary to progress from merely proving cell functionality or construct shape fidelity towards regenerating tissues. GelMA has a critical pioneering role in this process and could be used to accelerate the development of clinically relevant applications.

Trends

In gelMA hydrogels, the inherent bioactivity of gelatin is combined with the tailorability of photo-crosslinking.

3D-generated tissue analogs need to be geometrically natural mimics that are biofunctionally and mechanically stable.

GelMA will accelerate the development of cell-laden biofabricated constructs and will have a pioneering role in their translation to clinically relevant applications.

Hydrogels and the Paradigm Shift to the Third Dimension

Over the past decade, cell culture research has witnessed a paradigm shift into the third dimension. 3D cultured cells behave differently compared with those cultured in monolayers (2D) and their responses better resemble those in the native tissue [1]. In this shift from the second to the third dimension, hydrogel-based approaches are driving current biomaterial research in tissue engineering. In tissue engineering, hydrogels are used that ideally resemble the natural extracellular matrix (ECM) to stimulate cells to form functional tissue with mechanical integrity to ensure survival of the graft upon implantation. While current synthetic hydrogels are often still too reductionist compared with biopolymers and, therefore, lack important biological cues [2,3], biological materials generally lack the necessary strength and precise mechanical tunability. In present-day biomaterial research, there is a strong need for a merger of both biologically active and physicochemically tailorable hydrogels [3]. Gelatin modified by methacryloyl (methacrylamide and methacrylate) side groups (gelMA) has recently gained increasing attention, because it satisfies the requirements of biofunctionality and mechanical tunability to a reasonable extent, particularly compared with other available hydrogel-forming biomaterials [4–9]. By using this 3D cell culture platform, not only is the natural extracellular environment represented, but it also provides the possibility to generate well-defined 3D tissue constructs [10–12]. In this respect, conventional 3D casting techniques for cell-laden hydrogels are replaced by advanced fabrication techniques. The emerging field of biofabrication (see Glossary) has as its aim the automated generation of biologically functional, hierarchical 3D constructs using living cells, bioactive molecules, biomaterials, cell aggregates, or hybrid cell-material and their subsequent maturation [13]. This advanced technology, which encompasses both bioassembly and bioprinting, allows for the generation of architecturally complex tissue analogs, which comprise a spatially organized assembly of various cell types potentially mimicking the native situation. This development of 3D tissue analogs reflects the evolutionary stages from cell culture in monolayers to 3D culture in disc-shaped hydrogels, to biofabricating 3D constructs undergoing biological maturation to ultimately repair a tissue defect *in vivo* (Figure 1, Key Figure).

Key Figure

Evolutionary Stages from 2D Cell Culture to the Development of 3D Tissue Analogs

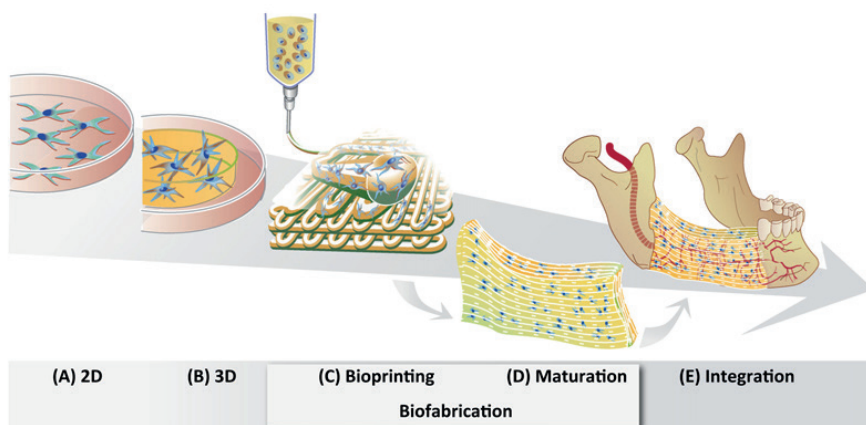


Figure 1 (A) 2D cell culture on plastic; (B) 3D cell culture inside hydrogel constructs; (C) bioprinting of 3D constructs; (D) biological maturation of the 3D bioprinted construct forming a tissue analog; and (E) implantation and integration of the tissue analog into the defect site.

In this review, we provide an overview of the uses of gelMA as a cell-encapsulating hydrogel, serving as a base material for a multitude of tissue-engineering strategies. We provide a picture of the diverse modifications of gelatin and its crosslinking systems, detailing the trends in gelatin- based biomaterial research, and the place of gelMA therein. In particular, we describe the use of gelMA in state-of-the-art biofabrication approaches to obtain complex tissue analogs, and we highlight the functional aspects of these developments. By doing so, we put into perspective the usefulness of gelMA-based engineered constructs in terms of the translational aspect of regenerative medicine.

Gelatin-Based Hydrogels for Cell Encapsulation

Gelatin is widely used in applications ranging from the food industry [14] to medicine and pharmaceutical processing [15]. In tissue engineering and regenerative medicine, gelatin is an attractive base material for engineering ‘smart’ hydrogels for drug delivery (e.g., [16,17]). Increasing interest in the use of gelatin in these fields stems from its various desirable features, including biocompatibility, biodegradability, low cost, and ease of manipulation [18]. Additionally, gelatin is a material that is generally recognized as safe (GRAS) by the US Food and Drug Administration (FDA) for food processing. Furthermore, it is routinely used in the clinic as a plasma expander and as a stabilizer in several protein formulations, including vaccines [16]. Gelatin is a proteinaceous substance comprising denatured and partially hydrolyzed native

collagen, mainly type I [17] (Box 1). In contrast to collagen, gelatin exhibits limited antigenicity due to heat denaturation [19]. Importantly, the bioactive sequences of collagen [e.g., the arginine- glycine-aspartic acid (RGD) peptide] for cell attachment and matrix metalloproteinase (MMP)- sensitive degradation sites are retained in the gelatin backbone [20]. As such, essential cellular functions, such as migration, proliferation, and differentiation, can be facilitated via integrin- mediated cell adhesion and cell-mediated enzymatic degradation [21,22].

Box 1. *Gelatin: A Versatile Biomaterial*

Typically, for the extraction of gelatin, collagen is obtained from bovine or porcine skin or bone as a by-product of the meat-processing industry. Extracts from collagen compositions are commonly obtained under either acidic or basic conditions, which are referred to as type A or type B gelatin, respectively. These collected protein fragments form a gelatinous mixture. The Bloom strength, which typically ranges from 90 g to 300 g for porcine skin, is a measure of the strength of the physical gel that is formed upon cooling. This depends on species and molecular weight, among other factors. For example, fish gelatin is characterized by lower Bloom strength compared with porcine or bovine gelatin [68] and, therefore, is less suitable for biofabrication purposes, because these often make use of these gelation properties.

To use gelatin as a biomaterial, its instability at body temperature is overcome by covalent crosslinking methods [23]. Gelatin can be crosslinked either without prior modification or after functionalization of its side groups. Unmodified gelatin can be crosslinked in various ways to form a covalent network, such as by chemical or enzymatic crosslinking (Box 2). The application of gelatin-based hydrogels based on prior modification, such as gelMA, are the main focus of this review.

Box 2. Covalent Crosslinking without Chemical Modification

Unmodified gelatin is crosslinkable without any prior modification, which is the strategy traditionally used to fabricate gelatin hydrogels. For instance, aldehydes are well-known crosslinking agents for proteins [69,70], but are typically not suitable for simultaneous cell encapsulation due to the cytotoxicity, immunogenicity, and inflammatory effects of their degradation products [71]. In addition, genipin, a natural crosslinking agent, which is considered less cytotoxic compared with aldehydes, must be used at a low dose when the hydrogel is employed to encapsulate cells [72]. Overall, most crosslinking agents that enable generation of gels with high mechanical stability exhibit considerable cytotoxicity [70]. By contrast, enzymatic crosslinking of gelatin under physiological conditions by means of transglutaminases or tyrosinases provides a more cell-friendly approach [73–75]. However, this crosslinking system exhibits limited tailorability in the design of the hydrogels. Major disadvantages of direct crosslinking methods (without prior modification of gelatin) include poor control over the crosslinking density and the resulting stiffness of the hydrogel. For these reasons, using functionalized gelatin has become a favored approach over the direct crosslinking of gelatin.

Covalent Crosslinking after Chemical Modification

The addition of functional groups to the gelatin backbone is a crosslinking strategy with a high degree of control over hydrogel design and properties, compared with direct crosslinking techniques. Crosslinking of functional groups can be initiated using various systems. However, only a few are suitable for simultaneous crosslinking and cell encapsulation [24] (Table 1). Both (photo)radical-initiating systems and enzymatic crosslinking of functionalized gelatin are frequently used. In contrast to indirect enzymatic crosslinking, photoinitiation provides good temporal and spatial control over the crosslinking process [25], which is essential for creating an architecturally complex tissue analog. For this, both ultraviolet light (UV) and visible light (VIS) are used for photoinitiation [10,26].

Table 1 Modifications of Gelatin and Crosslinking Systems Used for Cell Encapsulation^a

Functional Group	Initiating System	Biological Response after Cell Encapsulation	Refs
Acrylamide	Irgacure 2959 (UV-A, 365 nm)	>90% viability after 1 day (HepG2)	[76]
Ferulic acid	Laccase + O ₂	>91% viability (fibroblasts, ECFCs), angiogenesis	[77]
Furfurylamine	Rose Bengal (VIS)	87% viability after 1 day (MSCs), used for osteochondral tissue formation	[26]
	APS/TEMED	>80% viability after 1 day (chondrocytes)	[51]
	Irgacure 2959 (UV-A, 365 nm)	70% to >90% viability depending on, e.g., crosslinking conditions, cell type, macromer concentration; various differentiations investigated	E.g., [3,4,6–8, 10,11,21,28, 33,35,37,38, 40,42–45,48, 50,52,55,58, 62,76,78]
Methacryloyl	VA-086 (UV-A, 365 nm)	MSC/HUVEC coculture, vascularization; >97% viability after extrusion printing (HepG2)	[5,12]
	LAP (VIS 430–490 nm)	>96% viability after 1 day (MSCs), chondrogenic differentiation; cell proliferation increase of 23% over 2 weeks (MSC); adipocyte culture	[9,79,80]
	G2CK or P2CK (near-infrared femtosecond laser 800 nm)	26% viability (MG63 cells) after two-photon polymerization	[81]
Methacryloyl and acetylation	Irgacure 2959 (UV)	Chondrocyte encapsulation, used for inkjet printing	[28]
Methacryloyl galactosylation	Irgacure 2959	90% viability (HepG2), functional testing of hepatocytes	[27]
Norborene	DTT or LAP (UV 365 nm)	>91% viability (MSCs)	[82]
Phenolation	HRP + H ₂ O ₂	>94% viability or not quantified; various differentiations investigated (e.g., neurogenesis, osteogenesis, and vascularization)	E.g., [83–89]
Styrenation	Camphor-quinone (VIS 400–520 nm)	26% viability (chondrocytes)	[90]

A variety of functional groups have been used for crosslinking in (photo)radical-initiating or enzymatic-catalyzing systems (Table 1). Moreover, some double modifications have been used to improve cell behavior [27] or enhance processability [28]. Yet, most of the reported literature uses gelMA with the photoinitiator 1-[4-(2-hydroxyethoxy)-phenyl]-2-hydroxy-2-methyl-1-propane-1-one, which is better known under its trade name Irgacure® 2959 from BASF (formerly Ciba Specialty Chemicals). This water-soluble initiator, which dissociates into a benzoyl and ketyl-free radical upon UV light irradiation through a cleavage reaction [29], has a relatively low cytotoxicity compared with other photoinitiators [30]. Interestingly, deviations from the gold standard of using gelMA with Irgacure 2959, except for the use of styrenated gelatin with camphorquinone (which showed low cell

viability), are all recent and one-off demonstrations. The introduction of acrylamide, furfurylamine, and norborene-substituted gelatin may have specific advantages compared with gelMA, although these await further research.

The use of VIS (with suitable initiators) has a strong rationale, since UV is known to have detrimental effects on biological components. Although cell viability is generally assessed 1 day after crosslinking, more subtle damage may be incurred by UV that could affect cell functionality and tissue formation in the longer term [31]. Moreover, the long-term effects of Irgacure 2959, albeit relatively cell friendly compared with other UV photoinitiators [32], have not yet been studied fully.

Box 3. GelMA Synthesis

GelMA is generally prepared by reacting gelatin with methacrylic anhydride in phosphate buffered saline (PBS) at pH 7.5. Methacrylic anhydride is added slowly to the gelatin solution under vigorous stirring at 50 °C. During the reaction, methacrylic acid is formed. After 1 h, the reaction is diluted with water. To remove unreacted methacrylic anhydride from the reaction mixture, it is dialyzed against distilled water. The obtained reaction product, gelMA, is freeze-dried to a white porous foam [33]. The DoF of the synthesized gelMA batch can be tailored by varying the methacrylic anhydride:gelatin ratio [21,33]. The DoF was characterized by van den Bulcke *et al.* as the percentage of functionalized primary amine groups over total primary amine groups [33] and is generally determined by the Habeeb method [91].

Gelatin-Methacryloyl Hydrogels for Cell Encapsulation

GelMA was first introduced in 2000 by Van den Bulcke and coworkers [33]. Subsequently, it gained considerable interest in the tissue-engineering community due to its inherent bioactivity and physicochemical tailorability [34]. The first step in the hydrogel design of gelMA is the selection of an appropriate degree of functionalization (DoF) of gelatin (Box 3). This is tailored by the amount of methacrylic anhydride that is used for the synthesis of gelMA macromers (Box 3). By using these macromers, hydrogels can be fabricated in the presence of a (light) initiator and an energy source. Via radical polymerization, gelatin chains are connected through short polymethacryloyl chains (Figure 2).

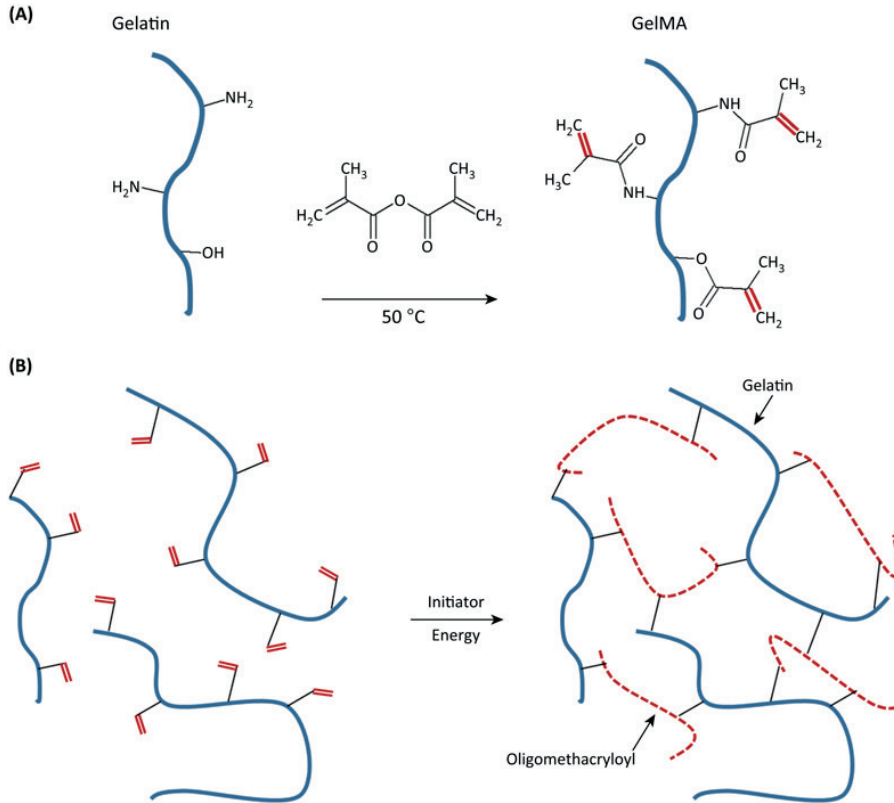


Figure 2. Gelatin-Methacryloyl (GelMA) Synthesis and Hydrogel Formation. (A) Reaction of methacrylic anhydride with amine and hydroxyl groups on gelatin gives rise to gelMA macromers. (B) Upon generation of a free radical (e.g., by light exposure in the presence of a photoinitiator), the methacrylamide and methacrylate side groups on the gelMA chains polymerize via radical addition-type polymerization to yield a network of gelatin chains connected through short poly-methacryloyl chains.

The biomaterial can be further tailored to form specific tissues by designing the desired physicochemical properties. As an example, spreading of cartilage cells needs to be prevented within the gel. This can be achieved by using increased polymer concentrations (conventionally 10%) that may sterically prevent cells from spreading. In addition, highly functionalized gels with a DoF approaching 80% can hamper cell spreading, possibly by extensive crosslinks throughout the hydrogel. Typically, gelMA macromers with DoF of 20–80% are used to generate stable hydrogels [10,21,35], with increasing percentages of methacryloyl substitution leading to hydro- gels that are stiffer and more durable, with smaller pore sizes [35]. Typically, by varying the macromer concentration from 5% to 20%, hydrogels are generated with compressive moduli in the range of 5–180 kPa [10]. Next to the DoF of a synthesized gelMA batch and its macromer concentration, the parameters of photo-crosslinking critically influence the properties of the resulting hydrogel. These parameters include the light exposure time, light intensity, and initiator concentration. Over time, these parameters can be affected by degradation. The

gelMA network is susceptible to local degradation by enzymes, most notably by MMPs, which are secreted by the (embedded) cells [3,36].

All design parameters need to be carefully balanced for each specific application. These include the stiffness, degradation profile, and intended cellular behavior in the resulting hydrogel. For a detailed summary on the design parameters, the reader is referred to a recent review by Khademhosseini and colleagues [34]. Due to this tunability of gelMA properties, it is used in a variety of strategies in tissue engineering. Indeed, gelMA has been applied in approaches aiming to regenerate neural tissue, vascularization, cartilage, bone, skin, skeletal muscle, cardio, liver, and kidney [34].

Biofabrication Techniques

Conventionally, research on cell-encapsulating gelMA hydrogels is often based on casted or molded disk-shaped microtissues that serve as models to study cell-material interactions. To obtain a tissue-like construct with a defined 3D structure, more advanced technologies have now emerged. The excellent spatial and temporal control over gelMA crosslinking, and its rheological behavior enable deposition by various biofabrication-related techniques (Figure 3).

Fabricating Cell-Laden Modules by Microfluidic Strategies

Microfluidic strategies were developed to encapsulate cells in gelMA droplets (Figure 3A) for a bottom-up tissue-engineering approach, or as micromodule for advanced assembling strategies to build more complex tissues [37]. Furthermore, a microfluidic spinning technique was introduced to fabricate photo-crosslinkable gelMA fibers with encapsulated cells [38]. It was shown that engraving of gelMA fibers induced cell alignment on the surface of the fibers [38]. To enhance the potential of these cell-laden fibers, encapsulation within a bulk hydrogel may be beneficial. Such 3D patterns in the fibers can be used as templates for creating tissues that exhibit preferential cell orientations, such as blood vessels or muscle fibers. Recently, an alternative set-up was introduced to create highly viable cell-laden microfibers in a straightforward and high-throughput manner. Upon stretching of the loaded fibers, cell alignment within the constructs was achieved [39].

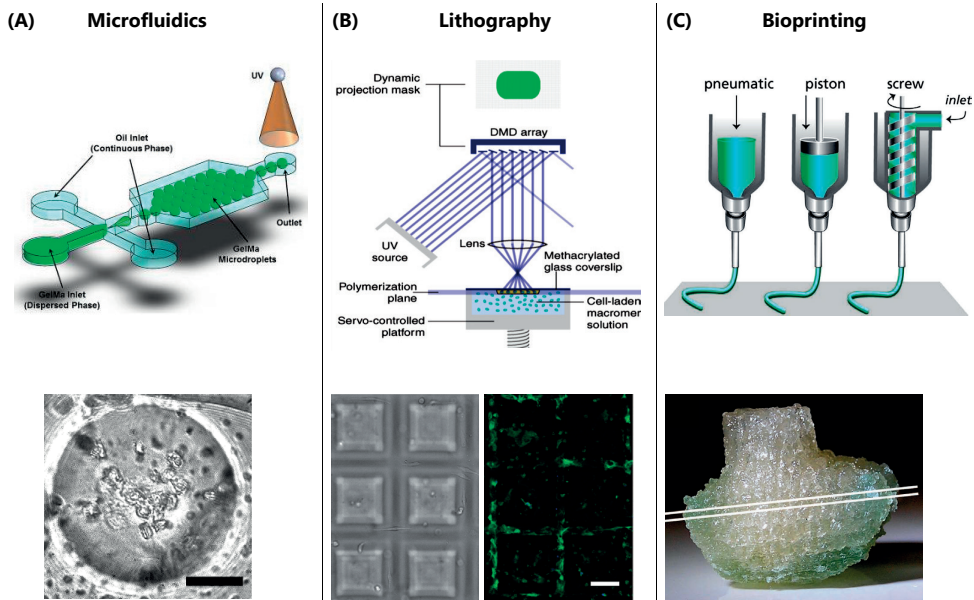


Figure 3. Categories of Gelatin-Methacryloyl (GelMA)-Based Biofabrication-Related Techniques and their Generated Constructs. (A) Preparation of cell-laden microspheres by microfluidics (scale bar = 30 μm). (B) Stereolithographic fabrication of pyramid-shaped scaffolds by spatially controlled light-initiated crosslinking of a gelMA macromer-cell mixture in a computer-controlled platform. By using this approach, cells are encapsulated while building the construct. Encapsulated cells stained for actin expression (scale bar = 100 μm). (C) Computer-controlled robotic dispensing of cell-laden gelMA to build a 3D construct, for instance, a bioprinted analog of the distal femur from a human knee. Reproduced, with permission, from [92] (A), [42] (B), and (upper picture) [93] and (lower picture) [45] (C). Abbreviation: UV, ultraviolet.

Using Soft- and Stereolithography for Cell Encapsulation

GelMA is also used in various soft lithography techniques to fabricate micropatterned tissues that involve cell encapsulation. Construct features on the micrometer scale, down to 100 nm in resolution, were successfully fabricated, resulting in robust cell-laden gelMA microtissues [21]. Such a micropatterning procedure was also used in a ‘layer-by-layer’ bottom-up approach by means of masks to build an osteon-like hydrogel with microchannel networks based on gelMA [40,41]. These approaches demonstrate the localized deposition of cells to form the vasculogenic and osteogenic parts of bone tissue. However, when moving towards creating larger constructs for tissue repair strategies, such a mask-based approach in micromolding is limited due to high costs, its time-consuming nature, and lack of automation.

In contrast to micromolding, stereolithography circumvents these challenges since it can be performed as a maskless photopatterning technique able to directly build up 3D structures. The design is processed by software and sliced into several layers. By a dynamic stereolithographic technique, 100–250 μm-thin slices with various shapes could be fabricated (Figure 2B) with high cell survival of approximately 80%

after 8 h of cell encapsulation [42]. Overall, stereolithography is a valuable means to create complex 3D architectures to guide cell alignment and behavior within a generated construct. However, stereolithography is limited to one resin-composition containing one biomaterial (mixture) and homogeneously distributed cells.

Bioprinting of Tissues with Cell-Containing GelMA-Based Inks

In addition to lithographic approaches, tissue analogs can be also generated in a layer-by-layer fashion with bioprinting. Tissue construction by 3D printing of cells by means of a hydrogel-based ink has recently become an attractive approach in tissue engineering [10,43]. By a direct-write bioprinting strategy, researchers showed that it was possible to build gelMA-based constructs with varying architectures [44]. To embrace the complexity of a tissue in a printed analog, a bioprinting approach was proposed that comprises heterogeneous subunits [43]. In this approach, a poloxamer gel was used as a sacrificial material to create the vascular luminal space for seeding of endothelial cells. Around the vascular bed, fibers were coprinted containing heterogeneous cell types with high cell viability and the bulk material was molded using gelMA [43]. Furthermore, for engineering bone, a microcarrier technology was combined with printing technology. Mesenchymal stromal cells (MSCs) were seeded on polylactide microspheres for extensive cell expansion and these multicellular aggregates were printed within a gelMA-gellan gum ink [8].

Several strategies were introduced to allow for the well-defined deposition of cell-laden gelMA. To improve the rheological characteristics of gelMA for printing, viscosity-enhancing components were mixed into the bioink. For instance, adding gellan gum [11] or hyaluronic acid [10] to the gelMA-precursor solution optimized the ink rheological properties for dispensing. Another method for improving biofabrication of gelMA is codeposition with reinforcing biomaterials. Thermoplastics, such as polycaprolactone (PCL), can serve a dual role here. First, the deposition of gelMA is more defined because the PCL can delineate the boundaries of the gelMA compartment and, second, constructs can be generated with enhanced mechanical properties [10,45]. A third approach to improving the printability of cell-laden gelMA hydrogels relies on the inherent temperature-dependent sol-gel transition of gelatin and not on viscosity-enhancing materials or codeposition techniques [12]. Cooling of the printed fibers on the collecting plate to 5 °C, immediately after deposition, enhanced physical crosslinking of gelMA and provided sufficient mechanical integrity to build up layers. However, the rapid change in temperature may affect the behavior of more fragile cell types. This approach was suitable for high gelMA concentrations between 10% and 20% and allowed encapsulation of a liver cell line (HepG2) with high viability.

To generate complex anatomically shaped constructs, sacrificial components, such as poly (vinylalcohol) (PVA) and alginate, have been codeposited with gelMA and PCL. These sacrificial materials, which were removed in aqueous solution after the fabrication process, were used as temporary structures for the support of overhanging geometries. By using this approach, porous constructs were obtained of clinically relevant sizes without affecting cell viability during the fabrication process [45].

GelMA Composite Structures for Enhanced Tissue-Specific Functionality

Analogous to the use of gelatin [46], gelMA is increasingly being used in combination with other materials. GelMA will not always be suitable on its own and may need further biologic stimuli for improved cell behavior or enhanced mechanical properties (Figure 4).

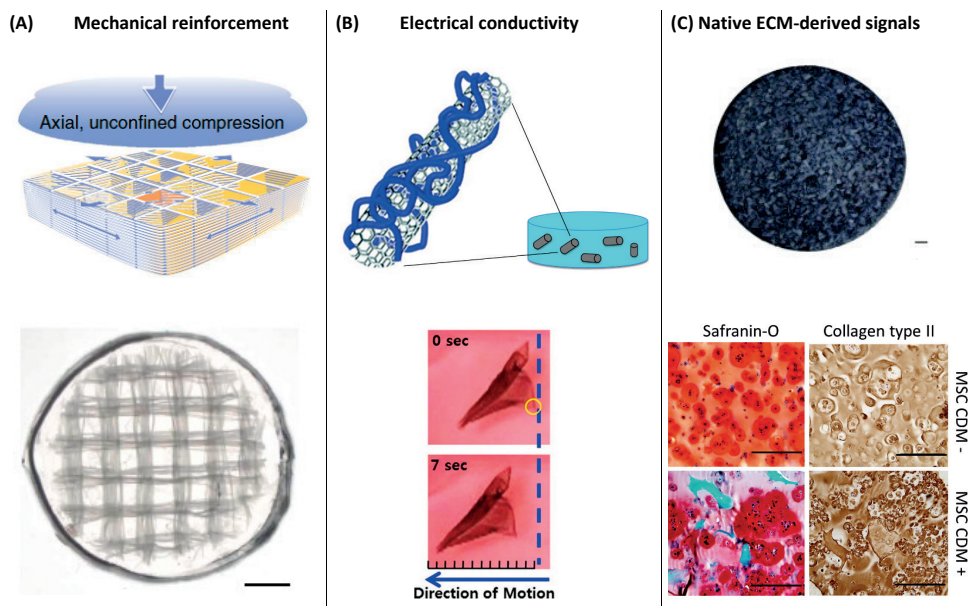


Figure 4. Examples of Combining Gelatin-Methacryloyl (GelMA) with Different Materials to Obtain Tissue-Specific Functionalities. (A) Mechanical reinforcement of hydrogels by combination with electrospun box structures that form a macroscopic network structure (scale bar = 1 mm). (B) (i) Providing gelMA with electrical conductivity by the addition of carbon nanotubes to the bulk hydrogel. (ii) The cardiomyocyte-seeded composite showed improved contraction behavior, resulting in movement of the construct of about 2.5 mm. (C) Optimizing gelMA by addition of cartilage-derived matrix particles [1.5% (w/v)] to the hydrogel (scale bar = 500 μm). Mesenchymal stromal cells (MSCs) produced pronounced cartilage-specific matrix, of GAGs and collagen type II. Compared with non-laden gelMA (scale bar = 200 μm). Reproduced, with permission, from [51] (A), [55] (B, i), [58] (B, ii), and [50] (C). Abbreviation: ECM, extracellular matrix.

In composites, a synergistic effect of the materials can be achieved that enhances the (bio)functionality of gelMA-based hydrogels. For example, GelMA composites were developed with calcium phosphates [40], polysaccharides [47], hyaluronan [10,48], silk [49], and ECM particles [50]. Furthermore, synthetic polymers, such as PCL [45,51] and poly(ethylene glycol) (PEG) [52–54], and nanoparticles have also been combined with gelMA [55].

Mechanical Reinforcement

The mechanical properties of gelMA can be tailorable, resulting in considerable strength and stiffness. However, this will not be sufficient for some applications, particularly when low stiffness is chosen for the sake of biofunctionality. In these cases, reinforcement strategies are available, including codeposition with reinforcing biomaterials (hybrid printing) [56], infusion of gelMA into 3D printed scaffolds followed by covalent binding between gel and scaffold [6], and reinforcement of cell-laden gels with 3D printed microfibers, leading to an increase in stiffness of up to 54 times compared with hydrogel or fiber mesh alone [51] (Figure 4A).

Engineering Vascular Networks in gelMA

A major hurdle in tissue engineering is the limited supply of oxygen and nutrients in generated tissue constructs. This limitation is addressed by introducing a minute vascular network in tissue-engineered constructs to prevent a necrotic core. The feasibility to engineer vascular-like networks in gelMA constructs has been investigated mainly by two approaches. First, by using a scaffold-based strategy, relatively large-diameter vascular beds are engineered that are seeded with endothelial cells after fabrication of the construct [57]. Second, smaller, capillary-like structures are generated by encapsulation of endothelial cells within the bulk material [57]. The latter approach is based on the intrinsic capability of endothelial cells to self-assemble de novo into capillary-like structures.

Capillary-like structures have been formed by self-organization of MSCs and endothelial colony-forming cells (ECFCs) [7,35] or human umbilical vein endothelial cells (HUVECs) [5] that were combined within a gelMA bulk hydrogel. The next step in engineering vasculature-like structures within a tissue-engineered construct could be taken by offering appropriate (blood) flow conditions for improved cell maturation. Accordingly, a coculture of ECFCs and MSCs, embedded in a pure gelMA carrier, was implanted subcutaneously into immunodeficient mice [7,35]. After 7 days, an evenly distributed endothelial network was formed throughout the construct. This provided proof of concept of functional anastomoses of bioengineered vascular-like structures in gelMA [7].

Tissue-Specific Differentiation in gelMA

Next to general approaches for vascularizing cell-laden constructs, gelMA has been used in a broad spectrum of tissue-specific applications. For the engineering of cardiac patches, gelMA was combined with carbon nanotubes and graphene oxide microspheres for introducing electrical conductivity [55,58,59]. Functional assessment of neonatal rat cardiomyocytes on a 2D composite patch highlighted higher and more synchronous beating rates and a lower excitation threshold compared with a culture on pure gelMA [58]. These 2D patches are thought to be rolled up or folded to form 3D tissues [58]. For a direct 3D approach that encapsulates cells within the composite, a cell line (NIH-3T3 fibroblasts) was used that demonstrated good cellular function [59].

In liver tissue engineering, hepatocyte microaggregates were generated in a high-throughput manner and encapsulated in gelMA [60]. Analysis confirmed that the encapsulation did not interfere with cell viability, and primary hepatocytes could be maintained with a stable phenotype for 21 days. Furthermore, gelMA containing the cell aggregates could serve as a bioink for 3D liver printing [60].

In bone tissue engineering, the combination of cells, minerals, and proteins, such as occurs in the native tissue, is increasingly used [46]. GelMA has been combined with calcium phosphates and human osteoblast-like cells (MG63) [40]. Although the addition of ceramics resulted in higher mechanical strength, no significant effect on osteogenicity has been shown so far.

In addition to the direct intramembranous route, bone can also be formed via an indirect endochondral route, with cartilage tissue as an intermediate stage. Endochondral ossification was shown in gelMA constructs in a subcutaneous rat model [50]. First, gelMA-encapsulated MSCs were cultured *in vitro* for 2 weeks to provide a cartilage template that was subsequently remodeled *in vivo* into mineralized bone tissue harboring bone marrow cavities. The gelMA hydrogel was almost completely degraded during this process, while the newly formed matrix assured construct integrity [50].

Cartilage is another load-bearing tissue that requires prolonged mechanical performance of tissue-engineered constructs, for which gelMA has been demonstrated useful. Although dedifferentiation of chondrocytes can occur within gelMA gel of low stiffness (1.5 kPa) [61], in stiffer gelMA gels (approximately 30 kPa) chondrogenic redifferentiation occurs, both *in vitro* [10] and *in vivo* [6]. Yet, hyaluronic acid has been shown to be a valuable additive to gelMA-based constructs for cartilage tissue engineering, because it directly influences chondrocyte differentiation in a concentration-dependent manner [10,48,62]. Moreover, for cartilage engineering, a sophisticated construct was designed with high mechanical strength. In this approach, methacrylated PCL was 3D printed and covalently crosslinked with chondrocyte-laden gelMA [6]. It is vital that reinforcing strategies do not impede tissue formation. This broad application of gelMA for numerous tissue-engineering strategies underscores its versatility. However, it still remains to be determined which tissue analogs gelMA is most suitable for (see Outstanding Questions). This may largely depend on the potency of gelMA within composite structures that can give tissue-specific functionality to gelatin.

Tissue Architecture

The architecture of a tissue analog is mainly dictated by (bio)functional and mechanical aspects. Currently, the main challenge lies in up-scaling microtissues to clinically relevant-sized constructs. This cannot be achieved by simply applying the same methods and creating a larger tissue. The complexity of the construct is increased, together with the number of challenges. For example, up scaling of a construct comprises nutrient transfer throughout the construct and provision of the

required mechanical stability. Whereas gelMA has proven its potency in creating microtissues, in future research yet more focus is expected on up-scaling.

Furthermore, an essential aspect of tissue architecture is to embrace the complexity of a tissue in its engineered analog. For example, Kolesky and coworkers divided different tissue components (vasculature, ECM, and specific cells) over multiple bioinks [43]. However, this biofabrication approach, similar to most others, focused on short-term cell behavior rather than on long-term features, such as matrix remodeling and tissue maturation. Such long-term outcomes of biofabricated tissues will be of great value to determine the level of architectural complexity that will need to be imposed to obtain functional human tissue analogs.

GelMA from A (Pre-)Clinical Perspective

Promising results were obtained in a preclinical study, demonstrating the potential of gelMA for clinical application. The aforementioned endochondral bone regeneration [50] is an example of impressive balance between degradation of a biomaterial and replacement by neotissue, which is one of the key and most challenging goals in tissue engineering. GelMA degradability can be tailored to the remodeling rate of the target tissue within limits. Increasing the DoF will improve mechanical properties and extend the required degradation period [36,63].

For clinical translation, gelMA as a base material has to meet several requirements. First, the *in vitro* and *in vivo* biocompatibility of gelMA and its degradation products, particularly oligomethacrylates, has to be considered. An extensive *in vitro* study showed good biocompatibility for gelatin type B-based gelMA, while type A-based gelMA elicited inflammatory reactions [64], possibly caused by high levels of endotoxins in the latter material. So far, only one immunocompetent animal (mouse) model has been used to test gelMA biocompatibility. The absence of proinflammatory activity provided a first proof of immunocompatibility for type B-based gelMA [64]. While endotoxin-free gelatin was used (type B-based gelMA) in this study, most research is currently conducted with gelMA that is based on gelatin with high endotoxin levels. These endotoxins can cloud the observations by influencing cell behaviour (e.g., stimulation of osteogenesis [65]), or may elicit other undesired effects. This aspect is generally underestimated in the field.

Other challenges in clinical translation are in batch-to-batch variations and possible disease transfer associated with animal-derived materials. Nonetheless, clinical grade gelatin is now routinely used in the clinic, which indicates that the benefits are believed to outweigh the risks.

Future Directions

The current major bottleneck in the translation of tissue-engineered constructs to the clinic is to convert a successful regenerative approach to procedures adhering to good manufacturing practice (GMP) while retaining the intended regenerative capacity. The conversion extends from the gelMA synthesis and bioprinting to the cell-culturing protocols. For example, the gold standard for gelMA crosslinking is now by Irgacure 2959 and UV light. However, to circumvent the associated drawbacks of UV light, alternative crosslinking systems, such as by VIS, may receive more attention for crosslinking gelMA. The incorporation of cells further complicates translation because tissue-engineering products need to conform to the legislation for advanced therapy medicinal products (ATMPs), which is still an underexplored field [66]. Thus, given its general potency, gelMA might not only be a pioneer for translating semisynthetic biomaterials to ATMPs, but could also act as a 'transitional technology' [67]. In this way, we could understand further how to accelerate the translation of the technology from bench to bedside. During this process, gelMA could serve as a stepping-stone for the design of next-generation tissue analogs.

Concluding Remarks

GelMA has become an attractive biomaterial in recent years for engineering various tissues since the gelatin backbone provides cells with biological cues and its functionalization enables one to tailor specific physicochemical properties. At present, research is either mainly focused on the generation of viable well-defined 3D constructs or on long-term cell performance in nonbiofabricated constructs.

The greatest challenge is to scale up construct dimensions to clinically relevant sizes. Therefore, future research with gelMA should focus on converging biofabrication and tissue-engineering technologies to create large, well-defined, and functional tissue equivalents upon maturation. The design of smart geometries, combinations of various materials and tissue types, and maintenance of the complex tissues under ATMP guidelines will be next. In conclusion, gelMA has a valuable pioneering role and is likely to accelerate the clinical translation of biofabrication-based tissue repair.

Acknowledgments

The authors' research work is supported by the Dutch Arthritis Foundation; the European Community's Seventh Framework Programme (FP7/2007-2013) under grant agreement 309962 (HydroZONES); and the European Research Council under grant agreement 647426 (3D-JOINT).

References

1. Pampaloni, F. *et al.* (2007) The third dimension bridges the gap between cell culture and live tissue. *Nat. Rev. Mol. Cell Biol.* 8, 839–845
2. Ehrbar, M. *et al.* (2007) Enzymatic formation of modular cell- instructive fibrin analogs for tissue engineering. *Biomaterials* 28, 3856–3866
3. Benton, J.A. *et al.* (2009) Photocrosslinking of gelatin macromers to synthesize porous hydrogels that promote valvular interstitial cell function. *Tissue Eng. Part A* 15, 3221–3230
4. Bertassoni, L.E. *et al.* (2014) Hydrogel bioprinted microchannel networks for vascularization of tissue engineering constructs. *Lab Chip* 14, 2202–2211
5. Occhetta, P. *et al.* (2014) VA-086 methacrylate gelatine photo- polymerizable hydrogels: a parametric study for highly biocompatible 3D cell embedding. *J. Biomed. Mater. Res. Part A* 103, 2109–2117
6. Boere, K.W.M. *et al.* (2014) Covalent attachment of a three- dimensionally printed thermoplast to a gelatin hydrogel for mechanically enhanced cartilage constructs. *Acta Biomater.* 10, 2602–2611
7. Lin, R.Z. *et al.* (2013) Transdermal regulation of vascular network bioengineering using a photopolymerizable methacrylated gelatin hydrogel. *Biomaterials* 34, 6785–6796
8. Levato, R. *et al.* (2014) Biofabrication of tissue constructs by 3D bioprinting of cell-laden microcarriers. *Biofabrication* 6, 035020
9. Lin, H. *et al.* (2014) Cartilage tissue engineering application of injectable gelatin hydrogel with in situ visible-light-activated gelation capability in both air and aqueous solution. *Tissue Eng. Part A* 20, 2402–2411
10. Schuurman, W. *et al.* (2013) Gelatin-methacrylamide hydrogels as potential biomaterials for fabrication of tissue-engineered cartilage constructs. *Macromol. Biosci.* 13, 551–561
11. Melchels, F.P.W. *et al.* (2014) Development and characterisation of a new bioink for additive tissue manufacturing. *J. Mater. Chem. B* 2, 2282–2289
12. Billiet, T. *et al.* (2014) The 3D printing of gelatin methacrylamide cell-laden tissue-engineered constructs with high cell viability. *Biomaterials* 35, 49–62
13. Groll, J. *et al.* (2016) Biofabrication: reappraising the definition in an evolving field. *Biofabrication* 8, 013001
14. Gomez-Guillen, M.C. *et al.* (2011) Functional and bioactive properties of collagen and gelatin from alternative sources: a review. *Food Hydrocolloids* 25, 1813–1827
15. Djagny, K.B. *et al.* (2001) Gelatin: a valuable protein for food and pharmaceutical industries: review. *Crit. Rev. Food Sci.* 41, 481–492
16. Elzoghby, A.O. (2013) Gelatin-based nanoparticles as drug and gene delivery systems: reviewing three decades of research. *J. Controlled Release* 172, 1075–1091
17. Young, S. *et al.* (2005) Gelatin as a delivery vehicle for the controlled release of bioactive molecules. *J. Controlled Release* 109, 256–274
18. Lai, J-Y. and Li, Y-T. (2010) Functional assessment of cross-linked porous gelatin hydrogels for bioengineered cell sheet carriers. *Biomacromolecules* 11, 1387–1397
19. Gorgieva, S. and Kokol, V. (2011) Collagen- vs. Gelatine-Based Biomaterials and Their Biocompatibility: Review and Perspectives, INTECH Open Access Publisher
20. Van den Steen, P.E. *et al.* (2002) Biochemistry and molecular biology of gelatinase B or matrix metalloproteinase-9 (MMP-9). *Crit. Rev. Biochem. Mol. Biol.* 37, 375–536

21. Nichol, J.W. *et al.* (2010) Cell-laden microengineered gelatin methacrylate hydrogels. *Biomaterials* 31, 5536–5544
22. Heino, J. *et al.* (2009) Evolution of collagen-based adhesion systems. *Int. J. Biochem. Cell Biol.* 41, 341–348
23. Reddy, N. *et al.* (2015) Crosslinking biopolymers for biomedical applications. *Trends Biotechnol.* 33, 362–369
24. Mironi-Harpaz, I. *et al.* (2012) Photopolymerization of cell-encapsulating hydrogels: crosslinking efficiency versus cytotoxicity. *Acta Biomater.* 8, 1838–1848
25. Nguyen, K.T. and West, J.L. (2002) Photopolymerizable hydrogels for tissue engineering applications. *Biomaterials* 23, 4307–4314
26. Mazaki, T. *et al.* (2014) A novel, visible light-induced, rapidly crosslinkable gelatin scaffold for osteochondral tissue engineering. *Sci. Rep.* 4, 4457
27. Gevaert, E. *et al.* (2014) Galactose-functionalized gelatin hydrogels improve the functionality of encapsulated Hepg2 cells. *Macromol. Biosci.* 14, 419–427
28. Hoch, E. *et al.* (2013) Chemical tailoring of gelatin to adjust its chemical and physical properties for functional bioprinting. *J. Mater. Chem. B* 1, 5675–5685
29. Liu, M. *et al.* (2014) Time-resolved spectroscopic and density functional theory study of the photochemistry of irgacure-2959 in an aqueous solution. *J. Phys. Chem. A* 118, 8701–8707
30. Williams, C.G. *et al.* (2005) Variable cytocompatibility of six cell lines with photoinitiators used for polymerizing hydrogels and cell encapsulation. *Biomaterials* 26, 1211–1218
31. Fedorovich, N.E. *et al.* (2009) The effect of photopolymerization on stem cells embedded in hydrogels. *Biomaterials* 30, 344–353
32. Bryant, S.J. *et al.* (2000) Cytocompatibility of UV and visible light photoinitiating systems on cultured NIH/3T3 fibroblasts *in vitro*. *J. Biomaterials Sci. Polym. Ed.* 11, 439–457
33. Van Den Bulcke, A.I. *et al.* (2000) Structural and rheological properties of methacrylamide modified gelatin hydrogels. *Biomacromolecules* 1, 31–38
34. Yue, K. *et al.* (2015) Synthesis, properties, and biomedical applications of gelatin methacryloyl (GelMA) hydrogels. *Biomaterials* 73, 254–271
35. Chen, Y.C. *et al.* (2012) Functional human vascular network generated in photocrosslinkable gelatin methacrylate hydrogels. *Adv. Funct. Mater.* 22, 2027–2039
36. Koshy, S.T. *et al.* (2014) Injectable, porous, and cell-responsive gelatin cryogels. *Biomaterials* 35, 2477–2487
37. Jung, J. and Oh, J. (2014) Swelling characterization of photo-cross-linked gelatin methacrylate spherical microgels for bioencapsulation. *e-Polymers* 14, 161–168
38. Shi, X. *et al.* (2015) Microfluidic spinning of cell-responsive grooved microfibers. *Adv. Funct. Mater.* 25, 2250–2259
39. Li, Y. *et al.* (2015) Chinese-noodle-inspired muscle myofiber fabrication. *Adv. Funct. Mater.* 25, 5999–6008
40. Zuo, Y. *et al.* (2015) Photocrosslinkable methacrylated gelatin and hydroxyapatite hybrid hydrogel for modularly engineering biomimetic osteon. *ACS Appl. Mater. Interfaces* 7, 10386–10394
41. Zuo, Y. *et al.* (2012) Bottom-up approach to build osteon-like structure by cell-laden photocrosslinkable hydrogel. *Chem. Commun. (Camb.)* 48, 3170–3172
42. Soman, P. *et al.* (2013) Digital microfabrication of user-defined 3D microstructures in cell-laden hydrogels. *Biotechnol. Bioeng.* 110, 3038–3047

43. Kolesky, D.B. *et al.* (2014) 3D bioprinting of vascularized, heterogeneous cell-laden tissue constructs. *Adv. Mater.* 26, 3124–3130
44. Bertassoni, L.E. *et al.* (2014) Direct-write bioprinting of cell-laden methacrylated gelatin hydrogels. *Biofabrication* 6, 024105
45. Visser, J. *et al.* (2013) Biofabrication of multi-material anatomically shaped tissue constructs. *Biofabrication* 5, 035007
46. Santoro, M. *et al.* (2014) Gelatin carriers for drug and cell delivery in tissue engineering. *J. Control. Release* 190, 210–218
47. Wang, H. *et al.* (2014) Cell-laden photocrosslinked GelMA–DexMA copolymer hydrogels with tunable mechanical properties for tissue engineering. *J. Mater. Sci. Mater. Med.* 25, 2173–2183
48. Levett, P.A. *et al.* (2014) Hyaluronic acid enhances the mechanical properties of tissue-engineered cartilage constructs. *PLoS ONE* 9, e113216
49. Xiao, W. *et al.* (2011) Synthesis and characterization of photocrosslinkable gelatin and silk fibroin interpenetrating polymer network hydrogels. *Acta Biomater.* 7, 2384–2393
50. Visser, J. *et al.* (2015) Endochondral bone formation in gelatin methacrylamide hydrogel with embedded cartilage-derived matrix particles. *Biomaterials* 37, 174–182
51. Visser, J. *et al.* (2015) Reinforcement of hydrogels using three-dimensionally printed microfibres. *Nat. Commun.* 6, 6933
52. Cha, C.Y. *et al.* (2014) Structural reinforcement of cell-laden hydrogels with microfabricated three dimensional scaffolds. *Biomater. Sci.* 2, 703–709
53. Hutson, C.B. *et al.* (2011) Synthesis and characterization of tunable poly (ethylene glycol): gelatin methacrylate composite hydrogels. *Tissue Eng. Part A* 17, 1713–1723
54. Daniele, M.A. *et al.* (2014) Interpenetrating networks based on gelatin methacrylamide and PEG formed using concurrent thiol click chemistries for hydrogel tissue engineering scaffolds. *Biomaterials* 35, 1845–1856
55. Shin, S.R. *et al.* (2011) Carbon nanotube reinforced hybrid microgels as scaffold materials for cell encapsulation. *ACS Nano* 6, 362–372
56. Schuurman, W. *et al.* (2011) Bioprinting of hybrid tissue constructs with tailorable mechanical properties. *Biofabrication* 3, 021001
57. Novosel, E.C. *et al.* (2011) Vascularization is the key challenge in tissue engineering. *Adv. Drug Deliv. Rev.* 63, 300–311
58. Shin, S.R. *et al.* (2013) Carbon-nanotube-embedded hydrogel sheets for engineering cardiac constructs and bioactuators. *ACS Nano* 7, 2369–2380
59. Shin, S.R. *et al.* (2013) Cell-laden microengineered and mechanically tunable hybrid hydrogels of gelatin and graphene oxide. *Adv. Mater.* 25, 6385–6391
60. Gevaert, E. *et al.* (2014) High throughput micro-well generation of hepatocyte micro-aggregates for tissue engineering. *PLoS ONE* 9, e105171
61. Levett, P.A. *et al.* (2014) Chondrocyte redifferentiation and construct mechanical property development in single-component photocrosslinkable hydrogels. *J. Biomed. Mater. Res. Part A* 102, 2544–2553
62. Levett, P.A. *et al.* (2014) A biomimetic extracellular matrix for cartilage tissue engineering centered on photocurable gelatin, hyaluronic acid and chondroitin sulfate. *Acta Biomater.* 10, 214–223
63. Nguyen, A.H. *et al.* (2015) Gelatin methacrylate microspheres for controlled growth factor release. *Acta Biomater.* 13, 101–110

64. Sirova, M. *et al.* (2014) Immunocompatibility evaluation of hydrogel-coated polyimide implants for applications in regenerative medicine. *J. Biomed. Mater. Res. Part A* 102, 1982–1990
65. Croes, M. *et al.* (2015) Proinflammatory mediators enhance the osteogenesis of human mesenchymal stem cells after lineage commitment. *PLoS ONE* 10, e0132781
66. Leijten, J. *et al.* (2015) Cell based advanced therapeutic medicinal products for bone repair: keep it simple? *Adv. Drug Deliv. Rev.* 84, 30–44
67. Evans, C.H. (2011) Barriers to the clinical translation of orthopedic tissue engineering. *Tissue Eng. Part B: Rev.* 17, 437–441
68. Farris, S. *et al.* (2009) Development of polyion-complex hydrogels as an alternative approach for the production of bio-based polymers for food packaging applications: a review. *Trends Food Sci. Technol.* 20, 316–332
69. Bigi, A. *et al.* (2001) Mechanical and thermal properties of gelatin films at different degrees of glutaraldehyde crosslinking. *Biomaterials* 22, 763–768
70. Sisson, K. *et al.* (2009) Evaluation of cross-linking methods for electrospun gelatin on cell growth and viability. *Biomacromolecules* 10, 1675–1680
71. Speer, D.P. *et al.* (1980) Biological effects of residual glutaraldehyde in glutaraldehyde-tanned collagen biomaterials. *J. Biomed. Mater. Res.* 14, 753–764
72. Wang, C. *et al.* (2011) Cytocompatibility study of a natural bio-material crosslinker: Genipin with therapeutic model cells. *J. Biomed. Mater. Res. Part B: Appl. Biomater.* 97B, 58–65
73. Babin, H. and Dickinson, E. (2001) Influence of transglutaminase treatment on the thermoreversible gelation of gelatin. *Food Hydro- colloids* 15, 271–276
74. Chen, P-Y. *et al.* (2014) Fabrication of large perfusable macro- porous cell-laden hydrogel scaffolds using microbial transglutaminase. *Acta Biomater.* 10, 912–920
75. Das, S. *et al.* (2015) Bioprintable, cell-laden silk fibroin-gelatin hydrogel supporting multilineage differentiation of stem cells for fabrication of three-dimensional tissue constructs. *Acta Biomater.* 11, 233–246
76. Billiet, T. *et al.* (2013) Quantitative contrasts in the photopolymerization of acrylamide and methacrylamide-functionalized gelatin hydrogel building blocks. *Macromol. Biosci.* 13, 1531–1545
77. Park, K.M. and Gerecht, S. (2014) Hypoxia-inducible hydrogels. *Nat. Commun.* 5, 4075
78. Zhou, L. *et al.* (2014) Biomimetic mineralization of anionic gelatin hydrogels: effect of degree of methacrylation. *RSC Adv.* 4, 21997– 22008
79. Henrikson, K.J. *et al.* (2014) Nucleous pulposus tissue engineering using a novel photopolymerizable hydrogel and minimally invasive delivery. *Spine J.* 14, S173
80. Huber, B. *et al.* (2015) Methacrylated gelatin and mature adipocytes are promising components for adipose tissue engineering. *J. Biomater. Appl.* 30, 699–710
81. Ovsianikov, A. *et al.* (2014) Laser photofabrication of cell-containing hydrogel constructs. *Langmuir* 30, 3787–3794
82. Mu-noz, Z. *et al.* (2014) Gelatin hydrogels formed by orthogonal thiol-norbornene photochemistry for cell encapsulation. *Biomater. Sci.* 2, 1063–1072
83. Lee, Y. *et al.* (2014) Enzyme-catalyzed in situ forming gelatin hydrogels as bioactive wound dressings: effects of fibroblast delivery on wound healing efficacy. *J. Mater. Chem. B* 2, 7712– 7718
84. Amini, A.A. and Nair, L.S. (2012) Enzymatically cross-linked injectable gelatin gel as osteoblast delivery vehicle. *J. Bioact Compat. Pol.* 27, 342–355

85. Lee, Y. *et al.* (2013) In situ forming gelatin-based tissue adhesives and their phenolic content-driven properties. *J. Mater. Chem. B* 1, 2407–2414
86. Wang, L.S. *et al.* (2012) Enzymatically cross-linked gelatin-phenol hydrogels with a broader stiffness range for osteogenic differentiation of human mesenchymal stem cells. *Acta Biomater.* 8, 1826–1837
87. Lee, S.H. *et al.* (2014) In situ crosslinkable gelatin hydrogels for vasculogenic induction and delivery of mesenchymal stem cells. *Adv. Funct. Mater.* 24, 6771–6781
88. Li, Z. *et al.* (2015) Injectable gelatin derivative hydrogels with sustained vascular endothelial growth factor release for induced angiogenesis. *Acta Biomater.* 13, 88–100
89. Chuang, C-H. *et al.* (2015) Enzymatic regulation of functional vascular networks using gelatin hydrogels. *Acta Biomater.* 19, 85–99
90. Hoshikawa, A. *et al.* (2006) Encapsulation of chondrocytes in photopolymerizable styrenated gelatin for cartilage tissue engineering. *Tissue Eng.* 12, 2333–2341
91. Habeeb, A.S.A. (1966) Determination of free amino groups in proteins by trinitrobenzenesulfonic acid. *Anal. Biochem.* 14, 328–336
92. Jung, J. and Oh, J. (2014) Cell-induced flow-focusing instability in gelatin methacrylate microdroplet generation. *Biomicrofluidics* 8, 036503
93. Malda, J. *et al.* (2013) 25th anniversary article: engineering hydrogels for biofabrication. *Adv. Mater.* 25, 5011–5028

Chapter 3

Visible light crosslinking of gelatin hydrogels offers an enhanced cell microenvironment with improved light penetration depth

Khoon S. Lim | Barbara J. Klotz | Gabriella C. J. Lindberg
Ferry P. W. Melchels | Gary J. Hooper | Jos Malda
Debby Gawlitta | Tim B. F. Woodfield

Macromolecular Bioscience 19(6):1900098



Abstract

In this study, we investigated the cyto-compatibility and cellular functionality of cell-laden gelatin-methacryloyl (Gel-MA) hydrogels fabricated using a set of photo-initiators which absorb in 400 – 450 nm of the visible light range. Gel-MA hydrogels crosslinked using this combination of visible light photo-initiators, which consisted of ruthenium (Ru) and sodium persulfate (SPS), were characterised to have comparable physico-mechanical properties (sol fraction, mass swelling ratio and compressive modulus) as Gel-MA gels photo-polymerised using more conventionally adopted photo-initiators, such as 1-[4-(2-hydroxyethoxy)-phenyl]-2-hydroxy-2-methyl-1-propan-1-one (Irgacure® 2959) and lithium phenyl(2,4,6-trimethylbenzoyl) phosphinate (LAP). We demonstrated that the Ru/SPS system had a less adverse effect on the viability and metabolic activity of human articular chondrocytes encapsulated in Gel-MA hydrogels for up to 35 days. Furthermore, cell-laden constructs crosslinked using the Ru/SPS system had significantly higher glycosaminoglycan (GAG) content, and re-differentiation capacity as compared to cells embedded in gels crosslinked using UV + I2959 and Vis + LAP. We also demonstrated that the Vis + Ru/SPS system offered significantly greater light penetration depth as compared to the UV + I2959 system, allowing thick (10mm) Gel-MA hydrogels to be fabricated with homogenous crosslinking density throughout the construct. These results demonstrate the potential of these Ru/SPS visible light photo-initiators for use in fabricating cell-laden hydrogels, which offer considerable advantages over traditional UV polymerising systems in terms of clinical relevance and practicability for applications such as cell encapsulation, 3D constructs for tissue engineering, biofabrication and in situ crosslinking of injectable hydrogels.

Introduction

In recent years, scaffold-based strategies adopting hydrogels as biomaterials for tissue engineering have received significant attention and offer a number of advantages due to their highly hydrated polymeric network and their structural similarity to native extracellular matrix [1]. Among these, photo-polymerisable gelatin hydrogels are especially attractive as they offer the ability for spatial and temporal control over the polymerisation process. Additionally, the reaction can be performed at room or physiological temperature, with fast curing rates and minimal heat generation [2,3].

In general, the photo-polymerisation process requires grafting of functional photo-labile moieties, such as methacryloyl (methacrylamides and methacrylates), tyramine, or styrene to gelatin [4–10]. Amongst these different photo-crosslinkable gelatin materials, gelatin-methacryloyl (Gel-MA) has emerged as a promising biomaterial, due to the tailorable physical properties (crosslinking density, swelling and stiffness) depending on the degree of methacryloyl substitution and the initial macromer concentration, thereby making it a versatile platform for various tissue engineering applications [4,11]. To date, the most commonly used photo-initiator to crosslink Gel-MA is 1-[4-(2-hydroxyethoxy)-phenyl]-2-hydroxy-2-methyl-1-propan-1-one, which is also known as Irgacure® 2959 (I2959) [12,13]. When exposed to ultraviolet (UV) light, Gel-MA undergoes crosslinking through chain-growth radical polymerisation. Here, the I2959 molecules absorb photons of light and dissociate into radicals, which then propagate through the methacryloyl groups, forming covalent kinetic chains to hold the polymer chains together (Figure 1A) [13].

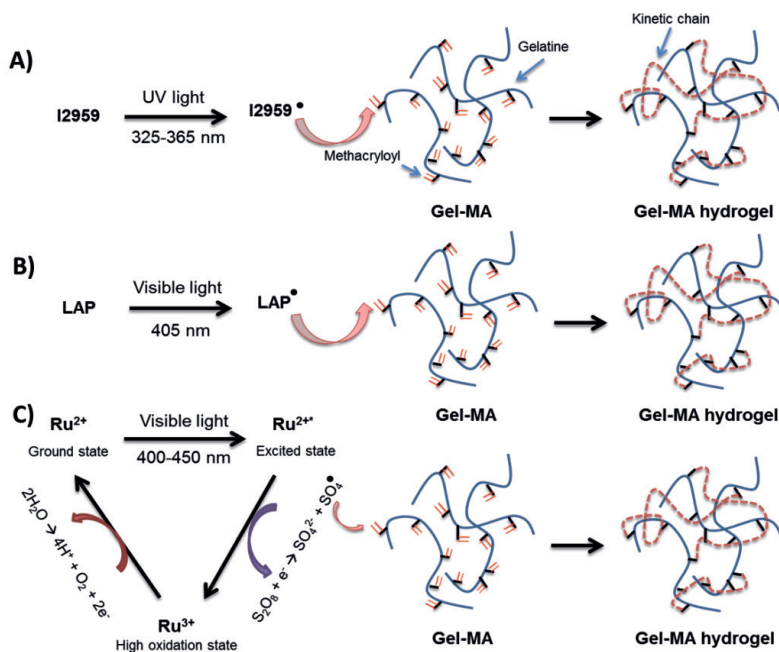


Figure 1. Schematic of the Gel-MA crosslinking process using A) UV light and I2959; B) Visible light and LAP; C) Visible light and Ru/SPS.

However, one major drawback of using I2959 is that it requires ultraviolet (UV) light for photo-excitation, which can potentially cause cellular DNA and tissue damage [14–16]. For example, previous studies conducted by Dahle *et al.* demonstrated that both UVA (320 – 400 nm) and UVB (290 – 320 nm) radiation can induce chromosomal, as well as genetic instability in mammalian cells [17,18]. Furthermore, Lavker *et al.* reported that repetitive exposure of human skin to low dose of UVA resulted in dermal alternations such as inflammation and lysozyme deposition [19]. UV light can also react with oxygen in the environment, forming reactive oxygen species (ROS), such as the superoxide radical ($O_2^{\cdot -}$), hydroxyl radical (OH^{\cdot}), singlet oxygen (1O_2) and ozone (O_3), which have also been shown to cause oxidative damage to DNA [19,20]. Additionally, for *in vivo* injectable hydrogel applications, UV light has been previously reported to have limited light penetration depth and can be attenuated by the native tissue [21,22] Elisseeff *et al.* showed that transmittance of UVA through human skin was significantly reduced, where visible light photo-initiating systems were more efficient for transdermal polymerisation [23]. Therefore, the development and cell-related characterisation of alternative photo-polymerisation systems that operate in the visible light (400-700 nm) spectrum may offer significant advantages for tissue engineering applications such as cell delivery or as space-fillers post augmentation, compared to more common UV photo-polymerisation.

To date, a number of visible light photo-initiating systems have been investigated to fabricate cell-laden Gel-MA hydrogels, and include: camphorquinone [24,25], fluorescein [24], rose bengal [26], riboflavin [24], lithium phenyl-2,4,6-trimethylbenzoylphosphinate (LAP) [27,28] and eosin Y [29]. In particular, LAP behaves very similarly to I2959, both being type 1 photo-initiators that undergo unimolecular bond cleavage to generate free radicals to facilitate polymerisation (Figure 1B) [14,27]. However, LAP has limited molar absorptivity in a narrow visible light range ($\epsilon \sim 30 \text{ M}^{-1}\text{cm}^{-1}$ at 405 nm), resulting in the need of using high concentrations to fabricate hydrogels [14,27]. On the other hand, although eosin-Y has a much higher molar absorptivity ($\epsilon \sim 100,000 \text{ M}^{-1}\text{cm}^{-1}$ at 525 nm), it often requires the presence of both a co-initiator (triethanolamine) and a co-monomer (N-vinylpyrrolidinone or N-vinylcaprolactam) to facilitate methacryloyl based photo-polymerisation [30–33] facilitate cellular adhesion or stimulate signaling pathways. Poly(ethylene glycol). In contrast, another emerging visible light initiating system, consisting of a ruthenium (Ru)-based transition metal complex ($\epsilon \sim 14600 \text{ M}^{-1}\text{cm}^{-1}$ at 450 nm) and sodium persulfate (SPS), has shown potential for tissue engineering applications [34–37]. When irradiated with visible light, the photo-excited Ru^{2+} oxidises into Ru^{3+} by donating electrons to SPS (Figure 1B). After accepting electrons, SPS dissociates into sulphate anions and sulphate radicals (Figure 1B). These radicals are subsequently able to crosslink Gel-MA by propagating through the methacryloyl groups [38] [39]. However, the cellular functionality such as cell differentiation and tissue formation in cell-laden constructs photo-crosslinked using this Ru/SPS visible light system has not been investigated. Moreover, the feasibility of this visible light photo-initiating system to allow fabrication of large and thick constructs for *in situ* photo-curing has also not been demonstrated.

Therefore, the aim of this study was to assess cyto-compatibility and cell functionality of cell-laden Gel-MA hydrogels fabricated using the Ru/SPS visible light photo-initiating system. We describe herein the systematic characterisation of physical properties of the visible light cross-linked Gel-MA hydrogels over a range of photo-initiator concentrations and irradiation conditions, compared to the two conventional and most commonly adopted systems, UV + I2959 and Vis + LAP. With clinical translation of this system in mind, we also evaluated the light penetration depth of the Ru/SPS system to assess the feasibility of developing thick, fully-crosslinked tissue engineered constructs while maximising cell viability. Given that one of the potential applications of cell-encapsulated visible light cross-linked Gel-MA hydrogels is in cartilage tissue engineering, we investigated the *in vitro* re-differentiation capacity of expanded human articular chondrocytes as a clinically relevant cell source for further characterisation of the Ru/SPS system.

Materials and methods

Materials

Gelatin (porcine skin, type A, 300g Bloom strength), phosphate buffered saline (PBS), methacrylic anhydride, cellulose dialysis membrane (14 kDa molecular weight cut-off), L-ascorbic acid-2-phosphate (AsAp), tris(2,2-bipyridyl)dichlororuthenium(II) hexahydrate (Ru), sodium persulfate (SPS), calcein-AM, Propidium Iodide (PI), proteinase K, dimethyl-methylene blue (DMMB), ethylenediaminetetraacetic acid disodium salt dihydrate (Di-sodium-EDTA), sodium chloride (NaCl), hyaluronidase, ITS+1, dexamethasone, hydrochloric acid (37%), sodium hydroxide (NaOH), chondroitin sulphate A (CS-A) and L-proline were purchased from Sigma-Aldrich (Missouri, USA). 1-[4-(2-hydroxyethoxy)-phenyl]-2-hydroxy-2-methyl-1-propan-1-one (Irgacure® 2959) was a gift from BASF (Ludwigshafen, Germany). Collagenase type II was purchased from Worthington biochemical corporation (Lakewood, USA). Lithium phenyl-2,4,6-trimethylbenzoylphosphinate (LAP) was purchased from Toyo Chemical Industry (Tokyo, Japan). Dulbecco's Modified Eagle's Medium (DMEM) high glucose, 4-(2-hydroxyethyl)-1-piperazine-ethanesulfonic acid (HEPES), Gibco non-essential amino acids (NEAA), foetal calf serum (FCS), 0.25% trypsin/EDTA, and penicillin-streptomycin (PS, 10,000 U/mL), AlamarBlue® reagent, bovine serum albumin (BSA), goat-anti-mouse secondary antibody (Alexa Fluor 488), F-actin rhodamine phalloidin (Alexa Fluor® 594 Phalloidin), 4,6-diamidino-2-phenylindole (D1306, DAPI), and the CyQUANT® cell proliferation assay kit were purchased from ThermoFisher Scientific (Auckland, New Zealand). Medical grade silicone sheets were obtained from BioPlexus (Ventura, USA). Cell strainers (100 µm) were purchased from BD Biosciences (Auckland, New Zealand). Di-sodium hydrogen phosphate (Na₂HPO₄) and acetic acid (glacial, 100%) was ordered from Merck Millipore (Darmstadt, Germany). Optimal cutting temperature compound (OCT) was obtained from VWR International (Auckland, New Zealand). Transforming growth factor β 1 (TGFβ-1) was purchased from R&D systems, Minneapolis, USA. Primary antibodies collagen II (II-II6B3-C) were purchased from DSHB (Iowa City,

USA). Primary antibodies for collagen I (Ab34710) and aggrecan (Ab3773) were obtained from Abcam (Melbourne, Australia).

Synthesis of gelatin-methacryloyl (Gel-MA)

Gelatin was dissolved in PBS at a 10wt% concentration, with 0.6 g of methacrylic anhydride per gram of gelatin added to the solution, and left to react for 1 h at 50°C under constant stirring⁴. This was followed by dialysis against deionised water to remove unreacted methacrylic anhydride. The purified Gel-MA solution was filtered through a 0.22 µm sterile filter, then lyophilised under sterile conditions. The degree of methacryloyl substitution was quantified to be 60% (data not shown) using ¹H-proton nuclear magnetic resonance spectroscopy (Bruker Avance 400 MHz).

Fabrication of Gel-MA hydrogels

Dried sterile Gel-MA (10wt%) was dissolved in PBS at 37°C and left to cool overnight at RT. Prior to crosslinking, the Gel-MA solution was heated to 37°C, then Ru and SPS were added, scooped into the silicon moulds (5 mm diameter x 1 mm thickness) on a glass slide and sandwiched with a cover slip. The samples were then irradiated (20 cm distance from light source for all experiments) under light (OmniCure® S1500, Excelitas Technologies). The light was irradiated through a light filter (Rosco IR/UV filter) where only light of the wavelength 400 – 450 nm and final intensity of 30 mW/cm² was allowed to pass through. A variety of initiator concentrations (0.1/1, 0.2/2 and 0.3/3 of Ru/SPS (mM/mM)) and exposure times (0.5, 1, 3, 5, 10 and 15 minutes) were studied to optimise the irradiation conditions. Gel-MA hydrogels fabricated using Vis (intensity = 30 mW/cm², 400 - 450 nm) + 0.05wt% LAP, UV (intensity = 30 mW/cm², 300 - 400 nm) + 0.05wt% I2959, and a variety of exposure times (0.5, 1, 3, 5, 10 and 15 minutes) were used as controls.

Swelling and mass loss analysis

All samples were weighed for the initial wet mass (m_{initial, t_0}) after crosslinking, and three samples were lyophilised immediately to obtain their dry weights (m_{dry, t_0}). The actual macromer fraction was calculated based on the equation below:

$$\text{Actual macromer fraction} = \frac{m_{\text{dry}, t=0}}{m_{\text{initial}, t=0}} \quad (1)$$

These samples were then submerged in a bath of PBS and incubated at 37°C. Samples were removed from the incubator after 1 day, blotted dry and weighed (m_{swollen}). The swollen samples were then freeze-dried and weighed again (m_{dry}). The sol fraction and mass swelling ratio (q) were calculated as follows:

$$m_{\text{initial}, \text{dry}} = m_{\text{initial}} \times \text{actual macromer fraction} \quad (2)$$

$$\text{Sol fraction} = \frac{m_{\text{initial}, \text{dry}} - m_{\text{dry}}}{m_{\text{initial}, \text{dry}}} \times 100\% \quad (3)$$

$$q = \frac{m_{\text{swollen}}}{m_{\text{dry}}} \quad (4)$$

Compression testing

The stiffness of the fabricated hydrogels was measured at room temperature using a dynamic mechanical analyser (TA instruments, DMA 2980). Unconfined compression testing was performed at 30% strain/min (5 mm diameter x 2 mm thickness) and the corresponding force was measured at a sampling frequency of 1.67 Hz. Sample diameter was measured using vernier callipers, and the compressive modulus was calculated from the slope of the linear region (10-15% strain range) of the stress-strain curves as previously reported ⁷.

Cartilage excision, chondrocyte isolation and expansion

Healthy human articular cartilage was harvested following ethics approval (New Zealand Health and Disability Ethics Committee - URB/07/04/014) from a consenting 28 year old female patient undergoing ligament reconstruction of the knee. The cartilage was diced into 1 to 2 mm³ cubes and digested overnight at 37°C with 0.15% w/v collagenase type II in basic chondrocyte medium (DMEM high glucose medium supplemented with 10% FCS, 10 mM HEPES, 0.2 mM L-ascorbic acid-2-phosphate, 0.4 mM L-proline and 1% Penicillin/Streptomycin). The resulting suspension was filtered through a 100-µm cell strainer to exclude the undigested tissue and centrifuged at 700g for 4 min. Isolated human articular chondrocytes (HACs) were cultured in basic chondrocyte medium and expanded at 37°C in a humidified 5% CO₂/95% air incubator. Media was refreshed twice per week.

HAC encapsulation in Gel-MA hydrogels

Expanded HACs at P2 were trypsinised and suspended in basic chondrocyte medium. The cell suspension was added to the macromer solution containing sterile filtered initiators to give a final concentration of 5 x 10⁶ HACs/ml. The cell-laden gels were then fabricated as outlined previously in section 2.3. Samples were then irradiated for 15 minutes at an intensity of 30 mW/cm² for both UV and visible light, where initiator concentrations were kept at 0.05wt% I2959, 0.05wt% LAP or 0.2/2 (mM/mM) Ru/SPS respective to the light source. Constructs were cultured in chondrogenic differentiation media (Dulbecco's DMEM high glucose supplemented with 0.4 mM L-proline, 10 mM HEPES, 0.1 mM NEAA, 100 U/mL penicillin, 0.1 mg/mL streptomycin, 0.2 mM AsAp, 1 x ITS+1 premix, 1.25 mg/mL BSA, 10 nM dexamethasone and 10 ng/mL TGFβ-1). Live/dead, AlamarBlue®, glycosaminoglycan (GAG) and DNA assays were performed on the samples after 1, 21, 35 days in culture as described below.

Live/dead assay

Harvested samples were washed with PBS, then stained with 1 µg/ml of Calcein-AM and 1 µg/ml of PI for 10 minutes. Live cells stained green whereas dead cell nuclei stained red. After staining, the gels were washed with PBS for three times before imaging them, using a fluorescence microscope (Zeiss Axio Imager Z1). The number of live and dead cells were quantified using the ImageJ software (Bio-Formats plugin) and the cell viability was calculated using the equation below:

$$\text{Viability (\%)} = \frac{\text{number of live cells}}{\text{number of live cells} + \text{dead cells}} \times 100\% \quad (5)$$

AlamarBlue® assay

An AlamarBlue assay was performed to determine the metabolic activity of cells according to the manufacturer's protocol. Samples were incubated in basic chondrocyte medium containing 10% (v/v) AlamarBlue® reagent for 24 hours. The AlamarBlue® reagent is reduced from blue to red/pink colour by metabolically active cells. The reduction in AlamarBlue® reagent was calculated after measuring the absorbance at 570 nm, using 600 nm as a reference wavelength (Fluostar Galaxy BMG Labtechnology).

Glycosaminoglycan (GAG) and DNA assay

Glycosaminoglycan (GAG) and DNA content were measured as described previously [3,40]. Briefly, cell-laden Gel-MA samples were digested overnight in 200 µL of 1 mg/ml proteinase-K solution at 56 °C. In order to quantify the amount of GAG retained in the gel, the digested samples were reacted with DMMB dye. The absorbance was then measured on a plate reader at 520 nm (Fluostar Galaxy BMG Labtechnology). GAG content was calculated from a standard curve constructed using known concentrations of chondroitin sulphate-A. The DNA content in the gels was measured using a CyQUANT kit. Following digestion, cells were lysed and RNA degraded using the provided lysis buffer with RNase A (1.35 KU/ml) added for 1 hour at RT. GR-dye solution was then added to the samples, incubated at RT for 15 minutes, then the fluorescence was measured (Fluostar Galaxy BMG Labtechnology). A standard curve was constructed using the DNA provided in the kit.

Immunofluorescence histological examination

The cell-laden constructs were fixed in 10% formalin for 1 hour at RT and washed in PBS supplemented with 0.1 M glycine. For histological evaluation, the samples were embedded in OCT then cryo-sectioned (30 µm thick sections)^{8,32} Weinhim Multicomponent gelatin-methacryloyl (GelMA). Sections were incubated in 0.1 wt.% hyaluronidase for 30 min at RT, washed with PBS and blocked with 2 wt.% bovine serum albumin (BSA) in PBS for 1 hour at RT. Primary antibodies for collagen type I (1:200, rabbit), collagen type II (1:200, mouse) or aggrecan (1:300, mouse), were diluted in blocking buffer and applied overnight at 4 °C. Samples were washed three times in blocking buffer for 10 min each followed by incubation with a goat-anti-mouse (Alexa Fluor® 488) and donkey-anti-rabbit (Alexa Fluor® 594) secondary antibodies, diluted in blocking buffer (1:400), in the dark for 1 hour at RT. For the last 10 min of the incubation, 4',6-Diamidino-2-Phenylindole, Dihydrochloride (DAPI,

1:1000 dilution) was added. Lastly, constructs were washed three times in PBS and visualised using the Zeiss Axioimager Z1 microscope.

Gene expression

Samples cultured for 1 week were collected, digested in 10mg/ml proteinase K solution at 55°C for 30 min, incubated with 1ml TRIzol reagent for 5 min at RT followed by RNA isolation in accordance with the manufacturer's guidelines. In brief, 200 μ l of chloroform was vigorously mixed with the samples, followed with 3 min RT incubation and 15 min centrifugation at 12000 g. The aqueous phase containing the RNA was transferred to tubes containing 500 μ l isopropanol then incubated at RT for 20 min followed by centrifugation for 10 min at 12000 g. The RNA pellet was washed twice in cold 70% ethanol and re-suspended in RNase free water. Ambion® DNA-free™ DNase Treatment was further used to remove any contaminating DNA according to manufacturer's instructions. Total RNA yield was determined using a spectrophotometer (Thermo Scientific, NanoDrop 8000) and the integrity was validated electrophoretically (Agilent Technologies, 2200 TapeStation). 300 ng total RNA per sample was reverse transcribed into complementary DNA (cDNA) using TaqMan™ first strand synthesis. Polymerase chain reaction (PCR) was then performed using an iCycler quantitative real-time PCR (qRT-PCR) machine (Roche, LightCycler®480 II), SYBRGreen™ and primers (Sigma Aldrich, KiCqStart® SYBR® Green Primers). The specific genes of interest were collagen type IA1 (GenBank accession no NM_000088), collagen type IIA1 (GenBank accession no NM_001844) and aggrecan (GenBank accession no NM_001135). Glyceraldehyde-3-phosphate dehydrogenase (GAPDH, Sigma Aldrich, GenBank accession no NM_002046) was selected as housekeeping gene. Each sample was run in duplicate and the threshold cycle and primer efficiency were analysed, where the geometric mean of the reference gene (GAPDH) was used to calculate the normalised mRNA expression of each target gene.

Light penetration depth study

10wt% Gel-MA macromers were prepared as outlined above in section 2.3. Prior to crosslinking, Ru and SPS were added to the Gel-MA solution for a final concentration of 0.2/2 (mM/mM) Ru/SPS, pipetted into silicon moulds (5 mm diameter x 10 mm thickness) on a glass slide and sandwiched with a cover slip. The samples were then irradiated under light (OmniCure® S1500, Excelitas Technologies) for 15 minutes through a light filter (Rosco IR/UV filter) where only light of 400 – 450 nm wavelength and final intensity of 30 mW/cm² was allowed to pass through. Gel-MA hydrogels fabricated using UV light (intensity = 30 mW/cm², 300 – 400 nm), 0.05wt% I2959 and 15 minutes of exposure time were used as controls. The fabricated hydrogels were then carefully removed from the mould and sliced into five 2mm thick sections and marked as regions (i to v) relative to the depth from the irradiation source. The sections were then subjected to mass loss and swelling studies as outlined in section 2.3.1. A similar setup was also adopted to fabricate HAC-laden constructs, with subsequent live/dead analysis (section 2.7) performed to evaluate cell viability within each of the five regions (i to v) relative to the depth from the irradiation source.

Transdermal polymerisation and in vivo subcutaneous implantation

Gel-MA hydrogels fabricated using either UV + I2959 or Vis + Ru/SPS were implanted subcutaneously in BALB/C mice as per ethics approval C3/16. All hydrogel macromer components were sterile filtered prior to usage, the samples were crosslinked sterily in a laminar flow hood, and incubated in sterile PBS overnight prior to implantation. Female BALB/C mice were anaesthetised using inhalational isoflurane. After shaving and disinfection, subcutaneous pockets of approximately 10mm deep were made by blunt dissection in a ventral direction from the incision down the side of the mouse in both directions. The pre-fabricated sterile Gel-MA hydrogels were then inserted into the base of the subcutaneous pocket, and the incision was closed using sutures and surgical glue. After 14 days, the mice were sacrificed and the implants with surrounding tissue and underlying muscle were carefully dissected from the subcutaneous site and fixed in 4% (v/v) phosphate buffered formalin for at least 1 day at 4 °C. The harvested samples were then cryo-sectioned (30 µm sections) and stained with haematoxylin (H) and eosin (E). For imitation of transdermal polymerisation, the mice were shaven after sacrificed, the skin from the dorsal region was harvested, and tissue hydration was maintained in a saline bath. 10wt% Gel-MA macromer solution with either 0.2/2 (mM/mM) Ru/SPS or 0.05wt% I2959 were pipetted into silicon moulds (5 mm diameter x 10 mm thickness) on a glass slide and sandwiched with a cover slip. The harvested skin sample were then placed on top of the samples, and light (OmniCure® S1500, Excelitas Technologies) was allowed to irradiate through the skin for 15 minutes to crosslink the samples. A final intensity of 30 mW/cm² was used for both the UV and visible light systems. Hydrogels fabricated with the same conditions without being covered by skin were used as controls. The fabricated hydrogels were then carefully removed from the mould and subjected to mass loss analysis as outlined in section 2.3.1.

Statistical analysis

All results were analysed using a two-way ANOVA with post-hoc Tukey's multiple comparisons tests unless stated. Data for mass loss and swelling studies were analysed using a one-way ANOVA. The models were constructed using GraphPad Prism (GraphPad Software, version 6). Samples in each study were all prepared in triplicate, and all studies were repeated 3 times ($n=3$). A $p<0.05$ was considered as statistically significant.

Results

Fabrication of Gel-MA hydrogels

Optimisation of initiator concentrations

Gel-MA hydrogels were successfully fabricated using the Ru/SPS photo-initiator system in the 400 - 450nm visible light range. Optimisation of the irradiation conditions required to fabricate Gel-MA hydrogels was investigated by examining a range of initiator concentrations whilst keeping the light intensity constant at 30 mW/cm². This was based on previously reported data indicating this light intensity as optimal for protein-protein crosslinking [42,43]. The crosslinking efficiency was measured by the sol fraction (eq 3), which is defined as the weight fraction of polymer chains that are not covalently bound to the hydrogel network after photo-polymerisation [1,44,45]. It was observed that at 0.1/1 Ru/SPS (mM/mM), a minimum of 5 minutes exposure time was required to fabricate stable hydrogels, with resultant sol fraction of approximately 35 - 42% (Figure 2A). Increasing the initiator concentration to 0.2/2 Ru/SPS (mM/mM) significantly increased the polymerisation rate ($p < 0.05$), resulting in the fabrication of hydrogels with sol fraction less than 30% within 0.5 min. The sol fraction values decreased as the exposure time increased, and plateaued at approximately 15%. This minimal sol fraction value achieved was also comparable to gels crosslinked using Vis + 0.05wt% LAP and UV + 0.05wt% I2959 (Fig 2A). Furthermore, increasing the initiator concentration to 0.3/3 Ru/SPS (mM/mM) resulted in identical sol fraction profiles as 0.2/2 Ru/SPS (mM/mM). This result indicates that complete crosslinking of the Gel-MA macromers was achieved using 0.2/2 Ru/SPS (mM/mM). One major observation was that gels crosslinked using UV + 0.05wt% I2959 had a faster polymerisation rate, where the sol fraction value plateaued after 0.5 min of UV exposure.

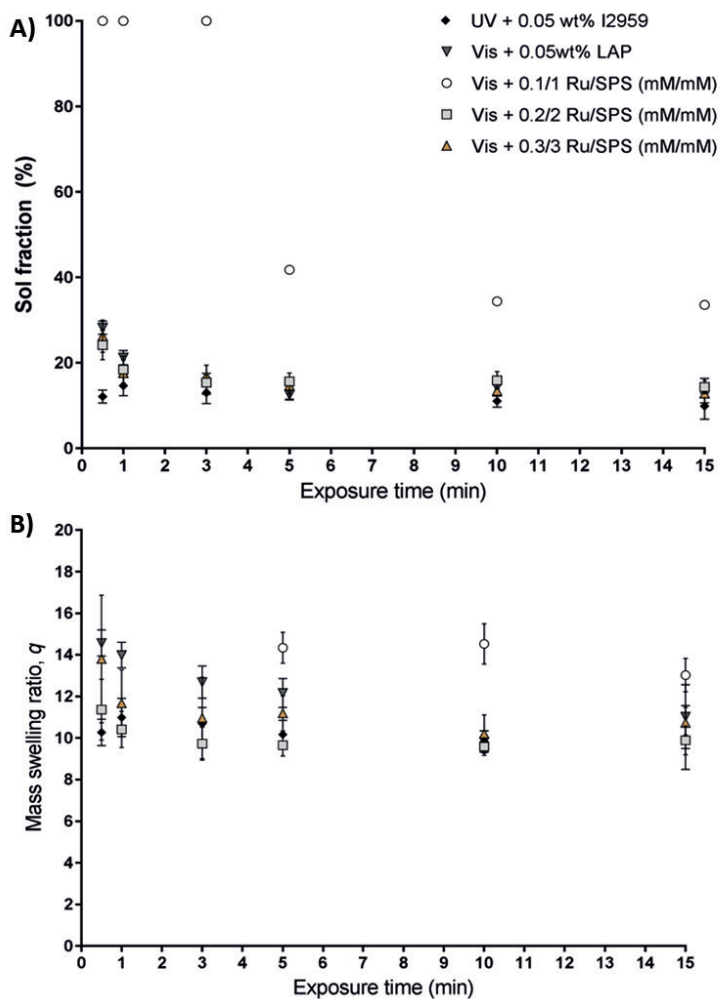


Figure 2. Physico-chemical properties of Gel-MA hydrogels fabricated using different concentrations of Ru/SPS as a function of exposure time: A) Sol fraction; B) Mass swelling ratio, q . Gel-MA gels crosslinked using UV + 0.05wt% I2959 and Vis + 0.05wt% LAP were used as controls. Light intensities for both UV and visible (Vis) light were kept constant at 30 mW/cm² for 15 minutes. Sol fraction values of 100% indicate no hydrogel formation.

Results obtained for the mass swelling ratio (q) complemented the sol-gel analysis, where a decrease in q was observed for longer exposure times (Figure 2B). Furthermore, samples with higher sol fraction possessed higher mass swelling ratios. Once again, increasing the initiator concentration from 0.2/2 Ru/SPS (mM/mM) to 0.3/3 Ru/SPS (mM/mM) did not show any significant differences in the mass swelling ratio ($p = 0.9680$), demonstrating that 0.2/2 Ru/SPS (mM/mM) was sufficient to completely crosslink the macromers.

Mechanical testing of Gel-MA hydrogels

It was observed that after 15 minutes of exposure at 30 mW/cm², Gel-MA hydrogels fabricated using 0.1/1 Ru/SPS (mM/mM) had a compressive modulus of 12.8 ± 1.7 kPa (Figure 3). Increasing the initiator concentration to 0.2/2 Ru/SPS (mM/mM) resulted in hydrogels of significantly greater compressive modulus (31.6 ± 0.8 kPa, $p < 0.0001$), which were comparable to Gel-MA hydrogels fabricated using the conventional Vis + 0.05wt% LAP (33.5 ± 1.6 kPa, $p = 0.5356$) and UV + 0.05wt% I2959 (33.6 ± 2.1 kPa, $p = 0.4740$). However, no significant difference was observed when the initiator concentration was further increased to 0.3/3 Ru/SPS (mM/mM) (29.4 ± 1.9 kPa, $p = 0.3626$). Again, this result indicated that 0.2/2 Ru/SPS (mM/mM) was sufficient to completely crosslink the Gel-MA macromers, which led to the selection of this concentration for all further studies described herein.

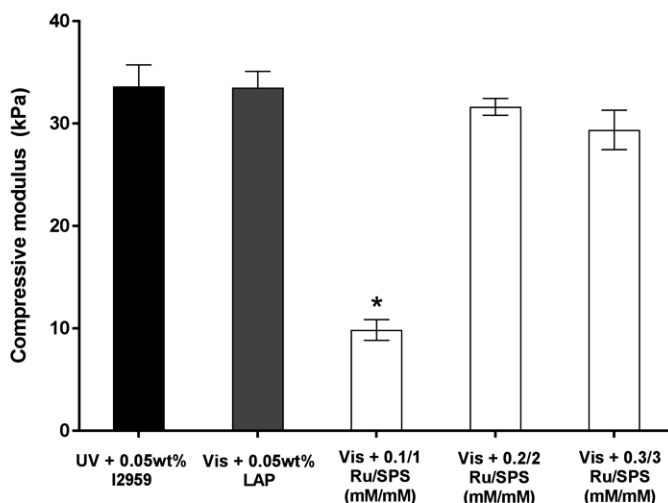


Figure 3. Compressive modulus of Gel-MA hydrogels fabricated using different concentrations of Ru/SPS. Light intensity and irradiation time were kept at 30 mW/cm² and 15 minutes, respectively. Gel-MA gels crosslinked using UV + 0.05wt% I2959 and Vis + 0.05wt% LAP were used as controls. *Indicates significant difference to other columns ($p < 0.05$).

HAC encapsulation in Gel-MA hydrogels

As the overall goal was to investigate the potential for the visible light cross-linking system to be used for 3D cell encapsulation in tissue engineering applications, expanded (passage 2) HACs were encapsulated into the 3D Gel-MA hydrogels. Live-dead fluorescence images following short (1 day) and long-term (35 days) *in vitro* culture showed that the cell-laden gels fabricated using the UV + I2959, Vis + LAP and Vis + Ru/SPS system demonstrated good viability and an abundance of live cells (Figure S1). In a 3D environment, chondrocytes typically exhibit a rounded morphology as an indication of their chondrogenic phenotype [41] scaffold

architecture could potentially restrict cell-cell communication and differentiation. This is particularly important when choosing the appropriate culture platform as well as scaffold-based strategy for clinical translation, that is, hydrogel or microtissues, for investigating differentiation of chondroprogenitor cells in cartilage tissue engineering. We, therefore, studied the influence of gap junction-mediated cell-cell communication on chondrogenesis of bone marrow-derived mesenchymal stromal cells (BM-MSCs). For all time points, it was observed that in all the UV + I2959, Vis + LAP and Vis + Ru/SPS system, the encapsulated cells were not only homogeneously distributed, but also remained rounded (Figure S2).

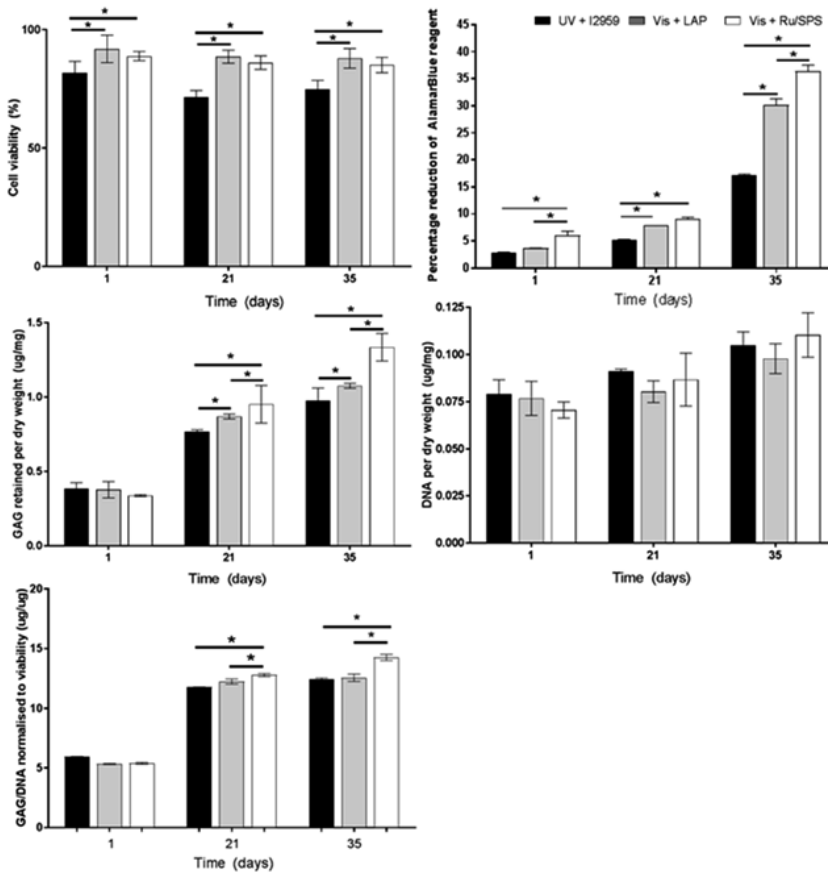


Figure 4. Encapsulation of HACs in Gel-MA hydrogels using UV + I2959, Vis + LAP, and Vis + Ru/SPS, at 1, 21 and 35 days in culture. A) Cell viability (%); B) Metabolic activity reported as percentage reduction of Alamarblue reagent; C) GAG retained per dry weight ($\mu\text{g}/\text{mg}$); D) DNA per dry weight ($\mu\text{g}/\text{mg}$); E) GAG/DNA normalised to cell viability. *Significant differences between columns below each end of lines ($p < 0.05$).

Total live/dead cell counts were used to evaluate viability of the encapsulated HACs. All systems demonstrated good cell viability over the 35-day culture period (>80%). Both the Vis + LAP and Vis + Ru/SPS system showed significantly higher cell viability than the UV + I2959 system for all three examined time points (Figure 4A). We also observed no significant differences between the two systems utilising visible light photo-initiation in terms of cell viability across all time points. After longer-term culture for 35 days, HACs encapsulated using the UV + I2959 system showed a reduction in viability, whereas cell viability in both the Vis + LAP and Vis + Ru/SPS samples remained greater than 85%. These results suggests that the visible light photo-initiator system presents a more cyto-compatible environment as compared to the UV crosslinking system.

Furthermore, metabolic activity of each of the samples was examined in order to evaluate the biological function of encapsulated cells. It was observed that the Vis + Ru/SPS samples had significantly higher metabolic activity at 1 ($p = 0.0016$), 21 ($p = 0.0001$) and 35 days ($p < 0.0001$) compared to UV + I2959 (Figure 4B). Similarly, the Vis + LAP samples also showed statistically higher metabolic activity compared to gels crosslinked using UV + I2959 at 21 ($p = 0.0146$) and 35 days ($p < 0.0001$). These results indicate that although cells encapsulated in Gel-MA using the conventional UV + I2959 system exhibit favourable cell viability and metabolic activity throughout the culture period, the visible light system showed an improvement on both measures, which was likely due to the lower overall photo-toxicity, radical toxicity and oxidative stress exerted on the cells.

To determine the ability of all UV + I2959, Vis + LAP and Vis + Ru/SPS Gel-MA hydrogels to support biological function and extracellular matrix formation, the chondrogenic differentiation capacity of the HACs post encapsulation was examined *in vitro*. Figure 4D demonstrates that the encapsulated HACs were able to proliferate within the gels, regardless of which photo-initiation system was used, where an increase in DNA content was observed from 1 day to 35 days. However, no significant differences were observed across all three systems at every examined time point. In terms of tissue formation, there was a clear increase in total GAG content from 1 to 35 days in the UV + I2959 ($p < 0.0001$), Vis + LAP ($p < 0.001$) and Vis + Ru/SPS ($p < 0.0001$) constructs (Figure 4C). Both visible light systems resulted in significantly higher GAG content of samples, compared to those crosslinked with the UV + I2959 system at 21 and 35 days. In addition, HACs encapsulated using Vis + Ru/SPS secreted more GAGs in the hydrogels at 21 ($p = 0.0033$) and 35 days ($p < 0.0001$) after encapsulation, compared to the Vis + LAP crosslinked samples.

If we consider the re-differentiation capacity of cell encapsulated Gel-MA constructs, GAG/DNA in the UV + I2959, Vis + LAP and Vis + Ru/SPS samples increased significantly from 1 to 35 days, indicating that these Gel-MA hydrogels are able to support chondrogenic differentiation of HACs (Figure 4E). However, most importantly, we observed that after 35 days in culture, constructs encapsulated using Vis + Ru/SPS had significantly higher GAG/DNA ($14.2 \pm 0.7 \mu\text{g}/\mu\text{g}$) than in the Vis + LAP ($12.5 \pm 0.9 \mu\text{g}/\mu\text{g}$, $p < 0.0001$) and UV + I2959 system ($12.4 \pm 0.4 \mu\text{g}/\mu\text{g}$, $p <$

0.0001). Immunofluorescence analysis confirms that the encapsulated HACs secreted collagen type I, collagen type II and aggrecan in the GelMA hydrogels, regardless of the applied photo-encapsulation system. Further quantitative analysis showed that there are no significant differences in terms of collagen type I and collagen type II production within the gels among all three photo-polymerisation systems (Figure 5J and K). However, the total coverage area for aggrecan was significantly higher in the Vis + Ru/SPS as compared to the UV + I2959 and Vis + LAP systems (Figure 5L) where a higher expression of aggrecan was stained in the pericellular regions of the HACs at day 35 in the Vis + Ru/SPS constructs (Figure 5G-I). Chondrogenic gene expressions at early culture time point (day 7) were evaluated to further study the effect of oxidative stress that is exerted on the cells during the photo-encapsulated process. We did observe that the gene expressions for collagen type II and aggrecan are indeed higher in the Vis + Ru/SPS systems (Figure 5M, N & O), further confirming our other observations that this photo-crosslinking system is more cell friendly, and exerts less damage to the cells during the encapsulation process.

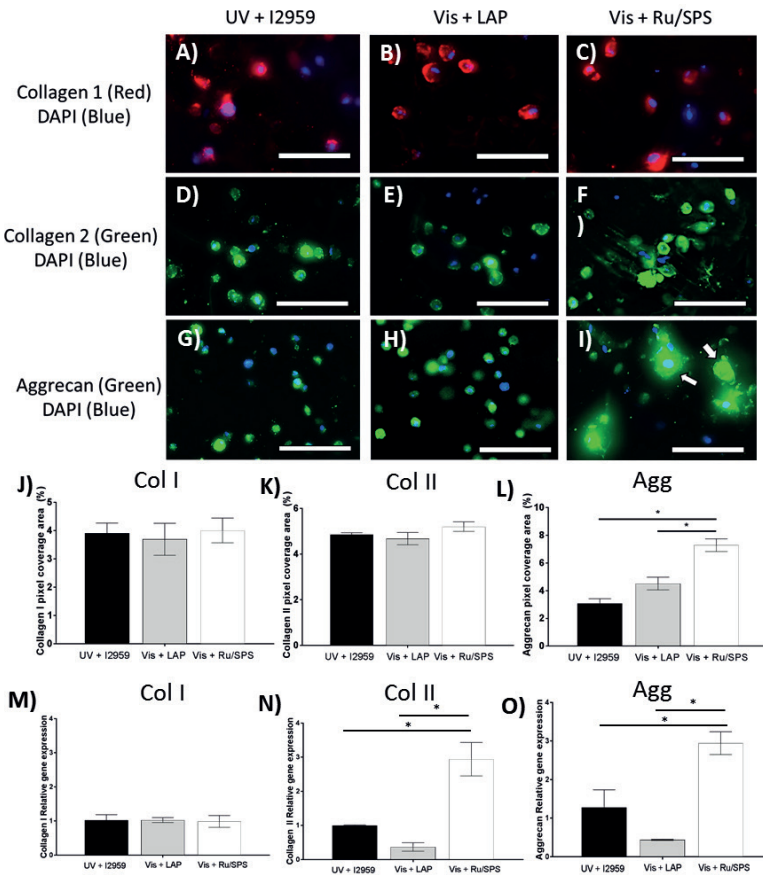


Figure 5. Immunofluorescence staining of HAC encapsulated in Gel-MA hydrogels using UV + I2959, Vis + LAP, or Vis + Ru/SPS after 35 days in culture: collagen type I (A-C); collagen type II (D-F); aggrecan (G-I). Pixel coverage area per panel for collagen I (J), collagen II (K) and aggrecan (L). Early relative gene expression after 7 days in culture: collagen I (M), collagen II (N) and aggrecan (O). Scale bar = 100 μ m. *Significant differences between columns below each end of lines ($p < 0.05$).

Light penetration depth study

As the photo-polymerisation processes can be applied to fabricate *in vivo* injectable hydrogels for tissue engineering applications, we further compared the effectiveness of the photo-polymerisation systems for fabrication of thick hydrogel constructs (10mm). One of the major advantage of using visible light is the better light penetration depth over UV that will be a beneficial for transdermal polymerisation or *in situ* crosslinking. As our cell encapsulation data suggested that the Vis + Ru/SPS is more superior over the Vis + LAP system in terms of HAC metabolic activity and re-differentiation capacity, we chose to only compare the Vis + Ru/SPS to the more conventional UV + I2959 for subsequent experiments. The UV + I2959 system demonstrated a limited penetration depth (6 - 8mm), whereas Vis + Ru/SPS system was able to penetrate through and completely polymerise the entire 10mm thick construct (Figure 6B). This observation was confirmed by mass loss data, where the Vis + Ru/SPS gels of different irradiation depths (i to v) had no significant difference in sol fraction values ($p > 0.98$). In contrast, for the UV + I2959 crosslinked samples, regions of the hydrogel farthest away from the irradiation source exhibited an increased sol fraction, with samples beyond 6mm (regions iv - v) completely dissolving after 1 day (sol fraction = 100%). A similar trend was observed for the mass swelling ratios, where no significant difference was observed for the Vis + Ru/SPS crosslinked samples across all regions (i to v). However, gels crosslinked using the UV + I2959 had distinctly different swelling ratios at different depths from the irradiation source (Figure 6D). These results further indicated that UV light has limited penetration depth as well as being attenuated through the z-axis during photo-crosslinking, resulting in varying crosslinking density with depth within the hydrogel.

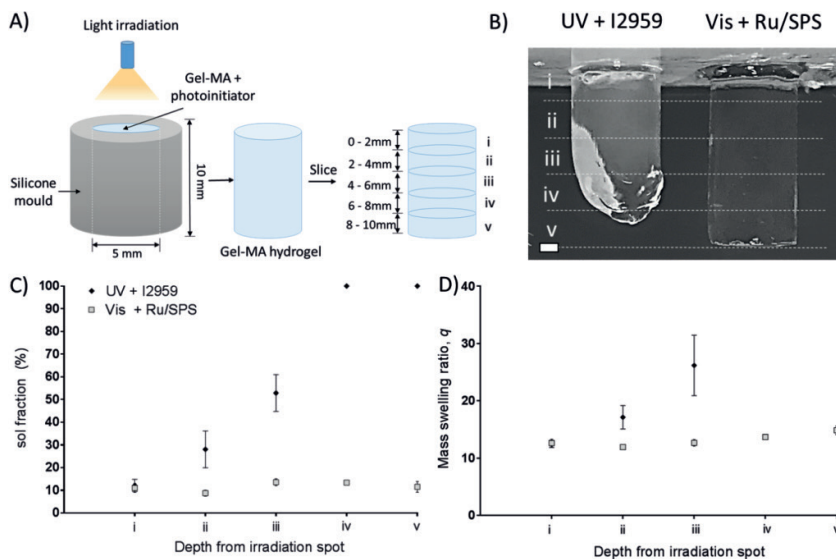


Figure 6. Fabrication of thick hydrogel constructs using both UV + I2959 and Vis + Ru/SPS systems: A) Schematic of light penetration depth setup; B) Macroscopic images of Gel-MA constructs post photo-polymerisation, scale bar = 1 mm; C) Sol fraction values; and D) Mass swelling ratios of samples as per depth from irradiation spot.

We further extended our studies to evaluate cell viability within the samples at different depths from the irradiation source (Figure 7). Interestingly, we observed an increase in cell viability at increasing depths for the UV crosslinked samples, where cells in the middle regions (iii, 4 – 6 mm from the irradiation source) had significantly higher viability ($p < 0.0001$) than those cells closer to the light source (i, < 2 mm from irradiation source). This data concurs with our previous mass loss results (Figure 6C), where UV light was likely being attenuated through the z-axis, with cells at different irradiation depths being subjected to different UV light intensity. In contrast, no significant differences in cell viability were observed for the Vis + Ru/SPS samples throughout the full 10mm depth of the construct (regions i-v)

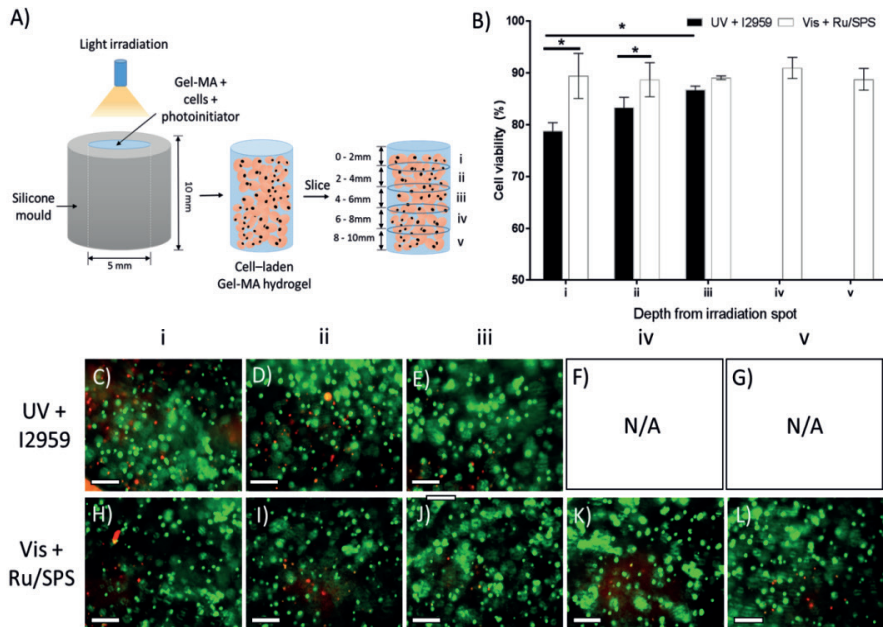


Figure 7. Fabrication of thick cell-laden constructs using both UV + I2959 and Vis + Ru/SPS systems: A) Schematic of light penetration depth setup; B) Cell viability at different depths from the light irradiation spot. Live dead images of UV + I2959 crosslinked samples (C - G) for different irradiation depths i, ii, iii, iv and v respectively, scale bar = 100 μm . Images F and G were not available due to the gels completely dissolved after 1 day in culture. Live dead images of Vis + Ru/SPS crosslinked samples (H - L) for different irradiation depths i, ii, iii, iv and v respectively, scale bar = 100 μm .

Transdermal polymerisation study and *in vivo* subcutaneous implantation

One of the major advantages of having a greater light penetration depth is the potential use of this visible light photo-crosslinking system for transdermal polymerisation. We evaluated the possibility to fabricate hydrogels transdermally using murine skin (0.5 mm) as a model (Figure 8A), and observed that UV light had limited transmission through skin resulting in the formation of a weak gel that was completely dissolved after 1 day (100% sol fraction, Figure 8B). In contrast, hydrogels were successfully crosslinked using visible light transmitted through the murine skin, with no statistically difference in sol fraction and swelling ratio to the control (Figure 8B). *In vivo* studies showed that after 14 days of subcutaneous implantation, there was limited cell infiltration into the hydrogels fabricated using both the UV + I2959 and Vis + Ru/SPS system. No significant differences were observed in terms of the host response to the gels fabricated using both these systems, again suggesting that there were no distinct differences in physico-chemical and mechanical properties of hydrogels crosslinked using either UV + I2959 or Vis + Ru/SPS, and is in agreement with our *in vitro* data.

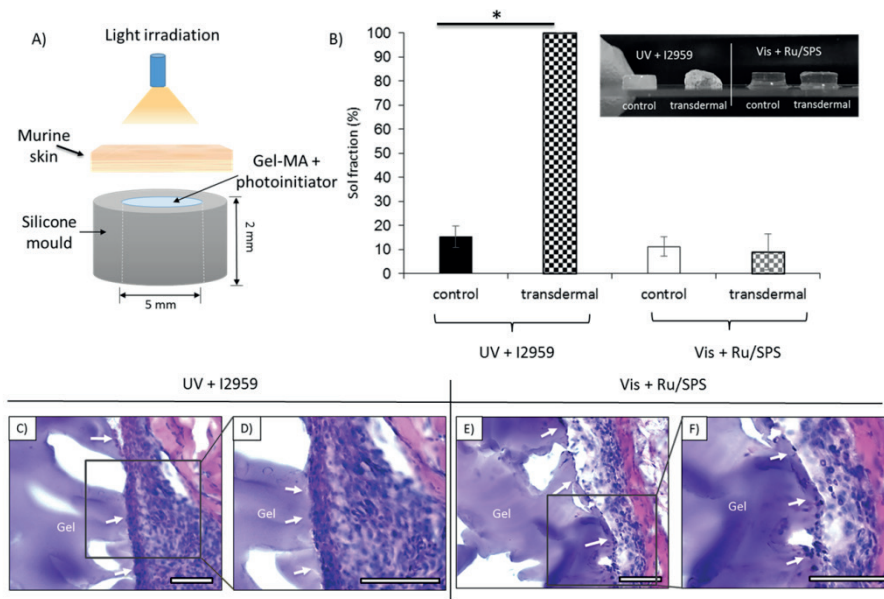


Figure 8. Transdermal polymerisation of Gel-MA constructs using both UV + I2959 and Vis + Ru/SPS systems: Schematic (A) and sol fraction (B) of Gel-MA hydrogels photo-crosslinked using light transmitted through murine skin; Immunohistochemical staining (H&E) of Gel-MA hydrogels fabricated using UV + I2959 (C & D) and Vis + Ru/SPS (E & F) post 14 days implanted subcutaneously. White arrows pointing to hydrogel and tissue interface. Scale bar = 100 μm .

Discussion

In this study, we demonstrated that the optimal irradiation conditions to fabricate Gel-MA hydrogels consisted of a visible light intensity of 30 mW/cm², photo-initiator concentration of 0.2/2 Ru/SPS (mM) and at least 3 minutes of exposure time. However more importantly, it should be recognised that the Ru/SPS concentration required to fully photo-crosslink Gel-MA hydrogels in this study was 10 times lower than the initiator concentrations reported to date in the literature to crosslink other polymers via their phenol moieties [4,46,47] such chemical modification processes can cause protein degradation, denaturation or loss of biological activity due to side chain disruption. This study exploited the observation that native tyrosine rich proteins could be crosslinked via radical initiated bi-phenol bond formation without any chemical modification of the protein. A new, tyramine functionalised poly(vinyl alcohol). This difference in initiator concentrations between Gel-MA and the other phenolated polymers such as gelatin, fibrinogen, resilin and tyraminated PVA, may likely be due to the reactivity of different functional groups, as well as different initiator components that are responsible for crosslinking. During the photo-polymerisation process, Ru²⁺ is photo-excited to Ru³⁺ by donating electrons to SPS [35,48] For other phenolated polymeric systems, Ru³⁺ is responsible for the crosslink formation. However in our case, the sulphate radicals which are products from the dissociation of SPS are responsible for reacting with methacryloyl groups on Gel-MA to form covalent crosslinks. As the reaction between the sulphate radicals and the methacryloyl groups is more effective than the reaction between the Ru³⁺ and phenol groups, less Ru/SPS is therefore required to crosslink the Gel-MA hydrogels. On the other hand, however, the Ru³⁺ component may contribute to crosslinking the phenol groups present in the gelatin backbone concurrently.

The sol fraction (10 – 15%), mass swelling ratio q (9 – 10) and compressive moduli (~20 kPa) obtained for Vis + 0.2/2 Ru/SPS (mM/mM) Gel-MA hydrogels in this study are comparable to properties obtained for Gel-MA gels fabricated using the UV + I2959 and Vis + LAP systems [49,50] This result indicates that the visible light system is capable of fabricating Gel-MA hydrogels of equivalent physico-mechanical properties to the other more conventional and widely adopted photo-initiated polymerisation system. Although we did observe that the UV + I2959 system had a faster crosslinking rate compared to both the Vis + LAP and Vis + Ru/SPS systems, the mass loss and swelling studies were conducted in an ideal environment without taking oxygen inhibition and light penetration depth into account, where the macromer was irradiated while sandwiched between a glass slide and cover slip, and is not an accurate representation of the downstream application. Moreover, in addition to Gel-MA hydrogels alone, we have successfully employed this visible light system to other polymers including heparin, hyaluronic acid, poly(vinyl alcohol) and gellan gum, all of which were functionalised with unsaturated vinyl moieties, such as methacryloyl or allyl groups [36,38,51]. Taking these factors into account, our work suggests that both synthetic and biological polymers modified with functional vinyl moieties can be crosslinked through different chemistries such as chain-growth methacryloyl or step-growth thiol-ene photo-click polymerisation, using Vis + Ru/SPS.

As expected, encapsulated cells had high cell viability (>80%) after 1 day for both photoinitiator systems. This result is comparable to a previous study reported by Schuurman *et al.* where after 1 day, the viability of equine articular chondrocytes encapsulated in 10wt% Gel-MA gels crosslinked using UV + I2959 was approximately 83% [52]. Nichol *et al.* also showed that fibroblasts encapsulated in 10wt% Gel-MA gels had viability of 82% after UV polymerisation [49]. In this study, applying either the Vis + LAP or Vis + Ru/SPS system resulted in cell-laden hydrogel constructs with an improved cell viability and significantly higher metabolic activity than UV gels. We believe that this result might be due to the negative effect of UV irradiation to the cells, which has been shown to cause genomic instability of cells [38,53,54] Previous work from Greene *et al.* describes that hepatocytes photo-encapsulated in gelatin-norbornene gels using visible light + eosin-Y had significantly higher metabolic activity compared to their UV counterparts [14]. Caliri *et al.* also showed that UV irradiation significantly reduced the cell viability of hepatic stellate cells when compared to visible light for encapsulation in methacrylated hyaluronic acid hydrogels [55]. Furthermore, UV is known to react with oxygen in the environment, forming reactive oxygen species (ROS) such as superoxide radical ($O_2^{\cdot -}$), hydroxyl radical (OH^{\cdot}), singlet oxygen (1O_2) and ozone (O_3), which can oxidise the lipid bilayer of cells [54,56,57] This lipid peroxidation may disrupt the cell membrane integrity and permeability, which can lead to upregulation of tissue degrading enzymes, and generation of toxic products [54,57] The chondrogenic differentiation study showed that GAG content and re-differentiation capacity (GAG/DNA) of HACs were significantly higher in the Vis + Ru/SPS samples than their Vis + LAP and UV + I2959 counterparts after long-term 35 day culture. As both LAP and Ru/SPS require visible light for photo-initiation, the difference observed in cell viability, metabolic activity and re-differentiation capacity, might be due to the diverse radical generation mechanism. We hypothesise that the Ru + SPS system has a slower but more sustained radical generation rate being a non-cleavage type 2 photoinitiator that undergoes a self-recycling mechanism (Figure 1) [35,39,48,58] It has been previously reported that this ability to re-initiate polymerisation allows type 2 photoinitiators to be less affected by oxygen inhibition [58]. Further covalent incorporation of chondrogenic factors or growth factor-binding peptides within Vis + Ru/SPS Gel-MA hydrogels (such as TGF- β 1, hyaluronic acid, heparin) would likely further enhance this chondrogenic niche [12,59].

The clinical relevance of these visible light initiating systems are particularly appealing for cell delivery or as space-fillers post augmentation, where *in situ* photo-curing typically requires high light intensity to minimise both oxygen inhibition and light attenuation. We demonstrated that the UV + I2959 system has a limited light penetration depth and can be attenuated during photo-crosslinking of constructs greater than 2 mm in thickness. Although a maximum penetration depth of 6 mm could be achieved with UV, variations in physical properties (sol fraction and mass swelling ratio) and cell viability were detected, indicating an inhomogeneous and sub-optimal crosslinking density throughout the construct. Our findings correlate to previous studies which also highlighted the limited penetration depth of UV light in either photo-curing of dental resin [60] have been used routinely as a filling material for both anterior and posterior teeth. The early RBCs were either chemically cured

two component materials or photo-initiated materials that used UV initiators in the beginning and then transitioned to visible light initiators such as camphorquinone which was introduced in 1978. The first report of a light curing material was of an ultraviolet (UV, photo-responsive polymers [61,62] or transdermal photopolymerisation [23]. The Vis + Ru/SPS system showed an added advantage in having enhanced penetration depth with homogenous crosslinking density and cell viability throughout a 10 mm thick construct. Furthermore, we have also reported that the Vis + Ru/SPS system is less susceptible to oxygen inhibition compared to the UV + I2959 system, allowing fabrication of large 3D bioprinted constructs with good shape fidelity [39]. In a transdermal polymerisation setup, we observed that a visible light intensity of 30 mW/cm² was enough to transmit through the murine skin and enable photo-crosslinking of the Gel-MA + 0.2/2 (mM/mM) Ru/SPS macromer. In contrast, using the same UV intensity and 0.05wt% I2959 did not result in successful hydrogel fabrication, highlighting the limited skin penetration and transmittance of light in the UV range. Lin *et al.* previously showed that a combination of higher UV intensity (40 mW/cm²) and I2959 concentration (0.5wt%) was indeed able to facilitate transdermal polymerisation of Gel-MA hydrogels [63]. However, we showed that the Vis + Ru/SPS system is significantly more efficient where lower visible light intensity and Ru/SPS concentrations were sufficient to transdermally fabricate hydrogels of similar quality to the controls. Although the murine skin model (0.5 mm) used in this study is thinner, it does consist of three distinctive layers (epidermis, dermis and hypodermis) similarly to human skin (1 – 2 mm). The cytotoxicity of the transition metal Ru might raise some concerns for use in clinical applications. Therefore, we conducted a cell growth inhibition assay to assess the toxicity of Ru in accordance to the ISO10993 standard. We observed that the concentration of Ru (0.2 mM) used in this study is below the accepted cytotoxicity threshold (<30%, Fig S1). This result is in agreement with a previous study conducted by Elvin *et al.*, where even a concentration as high as 1 mM of Ru was not cytotoxic [10]. In the same study, Elvin *et al.* also showed that gelatin-tyramines were fabricated into tissue sealants using 1/20 Ru/SPS (mM/mM) and showed minimal inflammatory response and no adverse cytotoxic reactions based on histological analysis [10]. Similarly, our *in vivo* subcutaneous study also displayed that the Gel-MA hydrogels fabricated using Vis + Ru/SPS showed no significant difference in host tissue reaction in comparison to the UV + I2959 counterparts (Figure 8C-F).

We believe that adopting the Vis + Ru/SPS system offers advantages over the UV irradiation system with respect to not only promoting cell viability and function within *in situ* photo-cured hydrogels or 3D constructs, but importantly to host cells in surrounding healthy tissue that would also be exposed to high light intensity, particularly during the photo-polymerisation of thick or large constructs. Furthermore, we purport that the applicability of the Vis + Ru/SPS system may be of particular benefit over Vis + LAP and UV + I2959 systems in the field of biofabrication or 3D bioprinting of thick, cell-laden constructs, where again, high light intensity or high photo-initiator concentration are generally necessary to maintain shape fidelity of biofabricated constructs as well as obtain maximum cell survival [39].

Conclusions

We have demonstrated and optimised the use of the visible light photo-initiators (Ru/SPS) to fabricate Gel-MA hydrogels. The fabricated gels offered similar physico-chemical and mechanical properties compared to those crosslinked using conventionally adopted UV + I2959 photo-initiator system. HACs encapsulated in visible light polymerised gels demonstrated superior cell viability and metabolic activity, as well as greater GAG content and re-differentiation capacity (GAG/DNA) as compared to UV crosslinked Gel-MA hydrogels. Furthermore, the enhanced penetration depth observed for the visible light system offers added benefits for *in situ* photo-curing applications and fabrication of thick hydrogel constructs. This study highlights the potential of this Vis + Ru/SPS system for fabrication of Gel-MA gels for not only cartilage engineering, but also other tissue engineering applications including cell delivery and *in-situ* photo-curing.

Acknowledgements

The authors wish to acknowledge Dr Ben Schon for his scientific input and his involvement in the subcutaneous implantation study. The authors also wish to acknowledge funding support from the Royal Society of New Zealand Rutherford Discovery Fellowship (RDF-U001204; TW), Health Research Council of New Zealand Emerging Researcher First Grant and Sir Charles Hercus Fellow (HRC 15/483 & 19/135; KL), the EU/FP7 'skelGEN' consortium under grant agreement n° [318553], the Dutch Arthritis Foundation (LLP-12; JM) and the European Research Council under grant agreement 647426 (3D-JOINT; JM).

References

1. Lim K S, Roberts J J, Alves M-H, Poole-Warren L A and Martens P J 2015 Understanding and tailoring the degradation of PVA-tyramine hydrogels *J. Appl. Polym. Sci.* **132** 42142
2. Nafea E H, Poole-Warren L A and Martens P J 2014 Structural and permeability characterization of biosynthetic PVA hydrogels designed for cell-based therapy *J. Biomater. Sci. Polym. Ed.* **25** 1771–90
3. Schon B S, Hooper G J and Woodfield T B F 2016 Modular Tissue Assembly Strategies for Biofabrication of Engineered Cartilage *Ann. Biomed. Eng.* **45** 100–14
4. Lim K S, Alves M H, Poole-Warren L A and Martens P J 2013 Covalent incorporation of non-chemically modified gelatin into degradable PVA-tyramine hydrogels *Biomaterials* **34** 7907–105
5. Bryant S, Nicodemus G and Villanueva I 2008 Designing 3D Photopolymer Hydrogels to Regulate Biomechanical Cues and Tissue Growth for Cartilage Tissue Engineering *Pharm. Res.* **25** 2379–86
6. Van Den Bulcke A I, Bogdanov B, De Rooze N, Schacht E H, Cornelissen M and Berghmans H 2000 Structural and Rheological Properties of Methacrylamide Modified Gelatin Hydrogels *Biomacromolecules* **1** 31–8
7. Manabe T, Okino H, Tanaka M and Matsuda T 2004 In situ-formed, tissue-adhesive co-gel composed of styrenated gelatin and styrenated antibody: potential use for local anti-cytokine antibody therapy on surgically resected tissues *Biomaterials* **25** 5867–73
8. Vuocolo T, Haddad R, Edwards G A, Lyons R E, Liyou N E, Werkmeister J A, Ramshaw J A M and Elvin C M 2012 A Highly Elastic and Adhesive Gelatin Tissue Sealant for Gastrointestinal Surgery and Colon Anastomosis *J. Gastrointest. Surg.* **16** 744–52
9. Hoshikawa A, Nakayama Y, Matsuda T, Oda H, Nakamura K and Mabuchi K 2006 Encapsulation of chondrocytes in photopolymerizable styrenated gelatin for cartilage tissue engineering *Tissue Eng.* **12** 2333–41
10. Elvin C M, Vuocolo T, Brownlee A G, Sando L, Huson M G, Liyou N E, Stockwell P R, Lyons R E, Kim M, Edwards G A, Johnson G, McFarland G A, Ramshaw J A M and Werkmeister J A 2010 A highly elastic tissue sealant based on photopolymerised gelatin *Biomaterials* **31** 8323–31
11. Melchels F P W, Dhert W J A, Hutmacher D W and Malda J 2014 Development and characterisation of a new bioink for additive tissue manufacturing *J. Mater. Chem. B* **2** 2282–9
12. Brown G C J, Lim K S, Farrugia B L, Hooper G J and Woodfield T B F 2017 Covalent Incorporation of Heparin Improves Chondrogenesis in Photocurable Gelatin-Methacryloyl Hydrogels *Macromol. Biosci.* **17** 1700158
13. Klotz B J, Gawliitta D, Rosenberg A J W P, Malda J and Melchels F P W 2016 Gelatin-Methacryloyl Hydrogels: Towards Biofabrication-Based Tissue Repair *Trends Biotechnol.* **34** 394–407
14. Greene T, Lin T, Ourania M A and Lin C 2016 Comparative study of visible light polymerized gelatin hydrogels for 3D culture of hepatic progenitor cells *J. Appl. Polym. Sci.* **134** 44585
15. Bryant S J, Nuttelman C R and Anseth K S 2000 Cytocompatibility of UV and visible light photoinitiating systems on cultured NIH/3T3 fibroblasts in vitro *J. Biomater. Sci. Polym. Ed.* **11** 439–57

16. de Gruijl F R, van Kranen H J and Mullenders L H F 2001 UV-induced DNA damage, repair, mutations and oncogenic pathways in skin cancer *J. Photochem. Photobiol. B Biol.* **63** 19–27
17. Dahle J and Kvam E 2003 Induction of Delayed Mutations and Chromosomal Instability in Fibroblasts after UVA-, UVB-, and X-Radiation *Cancer Res.* **63** 1464–9
18. Dahle J, Kvam E and Stokke T 2005 Bystander effects in UV-induced genomic instability: antioxidants inhibit delayed mutagenesis induced by ultraviolet A and B radiation *J. Carcinog.* **4** 11
19. Lavker R and Kaidbey K 1997 The Spectral Dependence for UVA-Induced Cumulative Damage in Human Skin *J. Invest. Dermatol.* **108** 17–21
20. Urushibara A, Kodama S and Yokoya A 2014 Induction of genetic instability by transfer of a UV-A-irradiated chromosome *Mutat. Res. Toxicol. Environ. Mutagen.* **766** 29–34
21. Peak J G and Peak M J 1991 Comparison of initial yields of DNA-to-protein crosslinks and single-strand breaks induced in cultured human cells by far- and near-ultraviolet light, blue light and X-rays *Mutat. Res. Mol. Mech. Mutagen.* **246** 187–91
22. Cooke M S, Evans M D, Dizdaroglu M and Lunec J 2003 Oxidative DNA damage: mechanisms, mutation, and disease *FASEB J.* **17** 1195–214
23. Elisseeff J, Anseth K, Sims D, McIntosh W, Randolph M and Langer R 1999 Transdermal photopolymerization for minimally invasive implantation *Proc. Natl. Acad. Sci. U. S. A.* **96** 3104–7
24. Hu J, Hou Y, Park H, Choi B, Hou S, Chung A and Lee M 2012 Visible light crosslinkable chitosan hydrogels for tissue engineering *Acta Biomater.* **8** 1730–8
25. Jakubiak J, Allonas X, Fouassier J P, Sionkowska A, Andrzejewska E, Linden L Å and Rabek J F 2003 Camphorquinone–amines photoinitiation systems for the initiation of free radical polymerization *Polymer (Guildf).* **44** 5219–26
26. Mazaki T, Shiozaki Y, Yamane K, Yoshida A, Nakamura M, Yoshida Y, Zhou D, Kitajima T, Tanaka M and Ito Y 2014 A novel, visible light-induced, rapidly cross-linkable gelatin scaffold for osteochondral tissue engineering *Sci. Rep.* **4** 4457
27. Fairbanks B D, Schwartz M P, Bowman C N and Anseth K S 2009 Photoinitiated polymerization of PEG-diacrylate with lithium phenyl-2,4,6-trimethylbenzoylphosphinate: polymerization rate and cytocompatibility *Biomaterials* **30** 6702–7
28. Lin H, Zhang D, Alexander P G, Yang G, Tan J, Cheng A W-M and Tuan R S 2013 Application of Visible Light-based Projection Stereolithography for Live Cell-Scaffold Fabrication with Designed Architecture *Biomaterials* **34** 331–9
29. Shih H and Lin C C 2013 Visible-light-mediated thiol-ene hydrogelation using eosin-Y as the only photoinitiator *Macromol Rapid Commun* **34** 269–73
30. Bahney C S, Lujan T J, Hsu C W, Bottlang M, West J L and Johnstone B 2011 Visible Light Photoinitiation of Mesenchymal Stem Cell-laden Bioreponsive Hydrogels *Eur. Cells Mater.* **22** 43–55
31. Pelin E, Fidan S, Tugba B and Seda K 2018 Gelatin Methacryloyl Hydrogels in the Absence of a Crosslinker as 3D Glioblastoma Multiforme (GBM)-Mimetic Microenvironment *Macromol. Biosci.* **18** 1700369
32. Noshadi I, Walker B W, Portillo-Lara R, Shirzaei Sani E, Gomes N, Aziziyan M R and Annabi N 2017 Engineering Biodegradable and Biocompatible Bio-ionic Liquid Conjugated Hydrogels with Tunable Conductivity and Mechanical Properties *Sci. Rep.* **7** 4345

33. Annabi N, Rana D, Shirzaei Sani E, Portillo-Lara R, Gifford J L, Fares M M, Mithieux S M and Weiss A S 2017 Engineering a sprayable and elastic hydrogel adhesive with antimicrobial properties for wound healing *Biomaterials* **139** 229–43
34. Lim K S, Ramaswamy Y, Roberts J J, Alves M-H, Poole-Warren L A and Martens P J 2015 Promoting Cell Survival and Proliferation in Degradable Poly(vinyl alcohol)-Tyramine Hydrogels *Macromol. Biosci.* **15** 1423–32
35. Fancy D A, Denison C, Kim K, Xie Y, Holdeman T, Amini F and Kodadek T 2000 Scope, limitations and mechanistic aspects of the photo-induced cross-linking of proteins by water-soluble metal complexes *Chem. Biol.* **7** 697–708
36. Lim K S, Levato R, Costa P F, Castilho M D, Alcalá-Orozco C R, Dorenmalen K M A van, Melchels F P W, Gawlitta D, Hooper G J, Malda J and Woodfield T B F 2018 Bio-resin for high resolution lithography-based biofabrication of complex cell-laden constructs *Biofabrication* **10** 34101
37. Muller P and Brettel K 2012 [Ru(bpy)₃]²⁺ as a reference in transient absorption spectroscopy: differential absorption coefficients for formation of the long-lived 3MLCT excited state *Photochem. Photobiol. Sci.* **11** 632–6
38. Bertlein S, Brown G C J, Lim K S, Jungst T, Boeck T, Blunk T, Tessmar J, Hooper G J, Woodfield T B F and Groll J 2017 Thiol–Ene Clickable Gelatin: A Platform Bioink for Multiple 3D Biofabrication Technologies *Adv. Mater.* **29** 1703404
39. Lim K S, Schon B S, Mekhileri N V, Brown G C J, Chia C M, Prabakar S, Hooper G J and Woodfield T B F 2016 New Visible-Light Photoinitiating System for Improved Print Fidelity in Gelatin-Based Bioinks *ACS Biomater. Sci. Eng.* **2** 1752–62
40. Woodfield T B F, Van Blitterswijk C A, De Wijn J, Sims T J, Hollander A P and Riesle J 2005 Polymer scaffolds fabricated with pore-size gradients as a model for studying the zonal organization within tissue-engineered cartilage constructs *Tissue Eng.* **11** 1297–311
41. Schrobback K, Klein T J and Woodfield T B 2015 The importance of connexin hemichannels during chondroprogenitor cell differentiation in hydrogel versus microtissue culture models *Tissue Eng Part A* **21** 1785–94
42. Elvin C M, Brownlee A G, Huson M G, Tebb T A, Kim M, Lyons R E, Vuocolo T, Liyou N E, Hughes T C, Ramshaw J A M and Werkmeister J A 2009 The development of photochemically crosslinked native fibrinogen as a rapidly formed and mechanically strong surgical tissue sealant *Biomaterials* **30** 2059–65
43. Elvin C M, Carr A G, Huson M G, Maxwell J M, Pearson R D, Vuocolo T, Liyou N E, Wong D C C, Merritt D J and Dixon N E 2005 Synthesis and properties of crosslinked recombinant pro-resilin *Nature* **437** 999–1002
44. Martens P and Anseth K S 2000 Characterization of hydrogels formed from acrylate modified poly(vinyl alcohol) macromers *Polymer (Guildf)*. **41** 7715–22
45. Roberts J J, Naudiyal P, Lim K S, Poole-Warren L A and Martens P J 2016 A comparative study of enzyme initiators for crosslinking phenol-functionalized hydrogels for cell encapsulation *Biomater. Res.* **20**
46. Sando L, Danon S, Brownlee A G, McCulloch R J, Ramshaw J A M, Elvin C M and Werkmeister J A 2011 Photochemically crosslinked matrices of gelatin and fibrinogen promote rapid cell proliferation *J. Tissue Eng. Regen. Med.* **5** 337–46
47. Sando L, Kim M, Colgrave M L, Ramshaw J A M, Werkmeister J A and Elvin C M 2010 Photochemical crosslinking of soluble wool keratins produces a mechanically stable

- biomaterial that supports cell adhesion and proliferation *J. Biomed. Mater. Res. - Part A* **95** 901–11
48. Fancy D A and Kodadek T 1999 Chemistry for the analysis of protein–protein interactions: rapid and efficient cross-linking triggered by long wavelength light *Proc Natl Acad Sci U S A* **96** 6020–4
 49. Nichol J W, Koshy S T, Bae H, Hwang C M, Yamanlar S and Khademhosseini A 2010 Cell-laden microengineered gelatin methacrylate hydrogels *Biomaterials* **31** 5536–44
 50. Schuurman W, Khristov V, Pot M W, van Weeren P R, Dhert W J and Malda J 2011 Bioprinting of hybrid tissue constructs with tailorable mechanical properties *Biofabrication* **3** 21001
 51. Parrish J, Lim K S, Baer K, Hooper G J and Woodfield T 2018 A 96-Well Microplate Bioreactor Platform Supporting Individual Dual Perfusion and High-Throughput Assessment of Simple or Biofabricated 3D Tissue Models *Lab Chip* **18** 2757–75
 52. Schuurman W, Levett P A, Pot M W, van Weeren P R, Dhert W J A, Hutmacher D W, Melchels F P W, Klein T J and Malda J 2013 Gelatin-Methacrylamide Hydrogels as Potential Biomaterials for Fabrication of Tissue-Engineered Cartilage Constructs *Macromol. Biosci.* **13** 551–61
 53. Clydesdale G J, Dandie G W and Muller H K 2001 Ultraviolet light induced injury: Immunological and inflammatory effects *Immunol Cell Biol* **79** 547–68
 54. Halliwell B and Chirico S 1993 Lipid peroxidation: its mechanism, measurement, and significance *Am. J. Clin. Nutr.* **57** 715S–724S
 55. Caliari S R, Perepelyuk M, Cosgrove B D, Tsai S J, Lee G Y, Mauck R L, Wells R G and Burdick J A 2016 Stiffening hydrogels for investigating the dynamics of hepatic stellate cell mechanotransduction during myofibroblast activation *Sci. Rep.* **6** 21387
 56. El-Beltagi H S and Mohamed H I 2013 Reactive Oxygen Species, Lipid Peroxidation and Antioxidative Defense Mechanism *Not Bot Horti Agrobo* **41** 44–57
 57. Greenberg M E, Li X-M, Gugiu B G, Gu X, Qin J, Salomon R G and Hazen S L 2008 The Lipid Whisker Model of the Structure of Oxidized Cell Membranes *J. Biol. Chem.* **283** 2385–96
 58. Kaastrup K and Sikes H D 2016 Using photo-initiated polymerization reactions to detect molecular recognition *Chem. Soc. Rev.* **45** 532–45
 59. Levett P A, Melchels F P W, Schrobback K, Hutmacher D W, Malda J and Klein T J 2014 A biomimetic extracellular matrix for cartilage tissue engineering centered on photocurable gelatin, hyaluronic acid and chondroitin sulfate *Acta Biomater.* **10** 214–23
 60. Santini A, Gallegos I T and Felix C M 2013 Photoinitiators in Dentistry: A Review *Prim. Dent. J.* **2** 30–3
 61. Kloxin A M, Tibbitt M W, Kasko A M, Fairbairn J A and Anseth K S 2010 Tunable Hydrogels for External Manipulation of Cellular Microenvironments through Controlled Photodegradation *Adv. Mater.* **22** 61–6
 62. Wang D, Wagner M, Butt H-J and Wu S 2015 Supramolecular hydrogels constructed by red-light-responsive host-guest interactions for photo-controlled protein release in deep tissue *Soft Matter* **11** 7656–62
 63. Lin R-Z, Chen Y-C, Moreno-Luna R, Khademhosseini A and Melero-Martin J M 2013 Transdermal regulation of vascular network bioengineering using a photopolymerizable methacrylated gelatin hydrogel *Biomaterials* **34** 6785–96

Chapter 4

Enzymatically crosslinked gelatin hydrogels for engineering pre-vascularised bone-like tissue analogues

Barbara J. Klotz | Lizette Utomo | Khoon S. Lim | Tim B.F. Woodfield
Antoine J.W.P. Rosenberg | Jos Malda | Debby Gawlitta

Manuscript in preparation



Abstract

Engineering of clinically-relevant sized bone tissue constructs remains challenging due to the required vascular supply throughout the construct. This can be achieved with co-culture of endothelial and multipotent mesenchymal stromal cells (MSCs). To guide the cell differentiation processes, gelatin-based hydrogels are a promising matrix. For the crosslinking of gelatin, currently mainly chemical-based reactions are used which rely on radical-mediated reactions of a photoinitiator and a visible or UV light source. Moreover, gelatin needs to be chemically modified to enable these crosslinking reactions into stable hydrogels for cell culture. Crosslinking under physiological conditions by *e.g.*, transglutaminases (TGs), might be more clinically relevant. Furthermore, this enzymatic crosslinking mechanism offers the possibility to also covalently incorporate other relevant proteins into the 3D matrix to guide cell differentiation without the need of any (biological or chemical) modification.

In the present study, crosslinking of gelatin by microbial TG was characterised by a fast gelation process with high cell compatibility. Both for MSCs and for endothelial-colony-forming cells (ECFCs), TG concentrations up to 3 % did not negatively affect cell viability. Under osteogenic culture conditions for 2 weeks, MSCs and ECFCs formed pre-vascularised, osteogenically differentiated tissue-like constructs. To overcome the fabrication dilemma of needing soft hydrogels for vascularisation and relatively stiff materials for osteogenesis, we propose to add osteogenesis-enhancing proteins to soft, vasculogenesis-supporting hydrogels. Thus, proteins laminin 111 and 211 were incorporated upon hydrogel crosslinking to potentially enhance cellular differentiation. Addition of the two different laminin isoforms resulted in unaltered osteogenic, vasculogenic and pericyte-like cell differentiations demonstrating the feasibility of their incorporation. Consequently, gelatin-TG hydrogels support early vascularised bone tissue engineering with the option of incorporating native proteins.

Introduction

Tissue engineering of bone constructs of clinically-relevant sizes requires the simultaneous development of a dense vascular network. Such a pre-vascularisation approach of an engineered tissue construct was shown to support a faster anastomosis to the host tissue after implantation and thereby leading to an improved implant survival [1, 2]. To simultaneously engineer both the vasculature and a bone-like tissue within a single construct, the use of co-cultures of endothelial cells (ECs) and multipotent mesenchymal stromal cells (MSCs) was proposed [3]. In these co-cultures, endothelial cells undergo self-assembly into capillary-like structures, stabilised by pericyte-like cells, which originate from MSCs [4]. Another fraction of these MSCs in the co-culture can undergo osteogenic differentiation [5-7].

Gelatin-based hydrogels are a promising matrix for tissue engineering approaches and are among the biomaterials most frequently used for tissue engineering purposes due to their inherent bioactivity and favourable properties in terms of biocompatibility [8, 9]. In order to create a matrix for MSC-EC co-cultures, which is stable at a physiological temperature, crosslinking of gelatin is needed. To stabilise gelatin-based hydrogels, conventionally, chemical crosslinking agents have been used [10, 11]. For various tissue engineering strategies, recently crosslinking of gelatin was mainly done by radical-mediated polymerisation of chemically modified gelatin [8]. Modification with methacryloyl groups, but also with phenols or norbornene are often used strategies to fabricate hydrogels [8, 12, 13]. To circumvent their potential cytotoxic nature and also immunological reactions to residual amounts of crosslinking agent in a hydrogel, enzymatic crosslinking with microbial transglutaminase (TG) was introduced [14]. While chemical modification and subsequent photo crosslinking is considered more tuneable for different applications [8], enzymatic crosslinking requires less processing of the material and occurs under physiological conditions. Especially, when considering future clinical applications, it might be beneficial to exploit the body's own crosslinking mechanism of proteins instead of radical-mediated chemical crosslinking methods. Moreover, it is an advantage of using unmodified gelatin since no chemical reactants are needed which therefore also does not need to be purified after the modification process to obtain a clinically-relevant product. Furthermore, using unmodified proteins is timesaving and it can be prevented to potentially introduce immunogenic or non-degradable chemical chains.

Tissue transglutaminase is the enzyme in the human body that is responsible for protein crosslinking during tissue formation. This enzyme catalyses the reaction of the acyl-transfer between the γ -carboxamide group of a glutamine residue and the ϵ -amino group of a lysine residue and thereby leading to a covalent isopeptide bond between proteins [15]. Furthermore, it is suggested that TGs can crosslink native proteins of interest into a hydrogel. Native lysine or glutamine amino acids are commonly present in a majority of proteins, hence varying proteins can be incorporated into a hydrogel via TG-mediated crosslinking.

It has been shown that the use of relatively stiff hydrogels with compressive moduli in the range of 15-30 kPa lead to enhanced osteogenesis [16, 17]. However, to allow for vascular sprouting and formation of a vascular network by endothelial cells within a hydrogel, one is limited to relatively soft materials with a compressive modulus of under 4 kPa [18, 19]. Consequently, the development of a vascular network within a bone-like tissue can only be achieved by using a relatively soft material [5]. To compensate for the less favourable matrix stiffness for osteogenesis in the benefit of vasculogenesis, we suggest to add osteogenesis-stimulating extracellular matrix (ECM)-derived proteins into the matrix, such as laminins. In the present study, gelatin-based TG-crosslinked hydrogels were tailored for vascularised bone tissue engineering. Firstly, the physico-chemical and mechanical properties of the hydrogels were characterised. Secondly, to establish the window for TG-mediated crosslinking, the effect of different TG concentrations was assessed on the viability of endothelial colony forming cells (ECFCs) and MSCs. Moreover, ECFCs and MSCs were co-cultured in gelatin-TG (gelTG) hydrogels to engineer pre-vascularised bone constructs. Additionally, the possibility of the simultaneous incorporation of other lysine and/or glutamine containing proteins, osteogenesis-enhancing proteins, was explored. To accomplish this, different isoforms of laminin (LN111 and LN211), an abundant ECM-derived protein, were covalently crosslinked into gelTG hydrogels and investigated upon their effect on vasculogenesis and osteogenesis in an ECFC-MSC co-culture model.

Materials and Methods

Materials and mould preparations

Type A gelatin from porcine skin was used (MedellaPro, Gelita, Eberbach, Germany). Before use, the pH of gelatin dissolved in PBS was set to 7.5, followed by dialysis against demi water (cellulose membrane, 14 kDa cut-off, Sigma Aldrich), sterile filtration and freeze drying to a porous foam. For compressive testing, disc-shaped moulds were prepared from silicone sheets of 1 mm height (BioPlexus Corporation, Ventura, Ca, USA) and 8 mm diameter. For hydrogel crosslinking microbial transglutaminase (TG; Activa TI[®], Ajinomoto) was used without further purification.

Hydrogel preparation

Gelatin was dissolved at 10% [w/v] in PBS and heated to 50 °C for 15 min and stored at 4 °C until used (maximum of 7 d). TG was dissolved at a concentration of 10 % [w/v] at 50 °C for 10 min, stored on ice and was used within 2 h after preparation. Gelatin at 3 % [w/v] was mixed with TG concentrations ranging from 1 to 3 % [w/v] of TG, supplemented with 20 % of culture medium in PBS and pipetted into either silicone moulds, or as droplets in the centre of culture wells. The mixture was left to crosslink for 1 h at 37 °C in a humidified incubator before medium was added to the hydrogels.

Rheological analysis of hydrogel formation

The crosslinking of 3 % gelatin hydrogels was recorded in the presence of 1, 2, or 3 % [w/v] TG ($n = 3$) using an AR G-2 rheometer (TA Instruments, The Netherlands), equipped with the software TA Instruments Trios V4.3.0.38388. The crosslinking analysis was performed at 0.1 % strain and 1 Hz continuous oscillation at 37 °C under humidified atmosphere. The point of gelation was determined by recording the time when there was a peak in $\tan \delta = G''/G'$, followed by a logarithmic increase of the shear storage modulus (G') compared to the shear loss modulus (G''). Furthermore, after 1 h of crosslinking, the reached G' was recorded.

Compressive testing of swollen hydrogels

Disc-shaped gelTG hydrogels were prepared in silicone moulds (1 × 8 mm; $V = 50 \mu\text{L}$). After 1 h crosslinking, MSC culture medium (as described in following paragraph) was added to the hydrogels, that were subsequently incubated for 24 h at 37 °C. Following, the elastic modulus was determined by means of a dynamic mechanical analyser (DMA, Q800, TA Instruments, New Castle, DE, USA). Compression was applied between – 20 %/ min and – 30 %/ min at room temperature (RT). The elastic modulus was calculated based on the slope from the linear region of stress-strain curves in a strain range between 5 and 10 %.

MSC isolation, culture and characterisation

Bone marrow aspirates were obtained from the iliac crest of patients after informed consent (procedure was approved by the local ethics committee of the University Medical Center Utrecht under 08-001-K). Via density gradient centrifugation on Ficoll-Paque PLUS (1.077 g/mL; GE Healthcare) the white mononuclear cell (MNC) fraction was collected. The cell fraction was cultured in MSC expansion medium at 37 °C/5.0 % CO_2 . For expansion of MSCs the medium was composed of alpha modification minimum essential medium (α -MEM; Gibco), 10 % heat-inactivated foetal bovine serum (FBS; Lonza), 100 U/mL penicillin, 10 mg/mL streptomycin (Gibco), 0.2 mM L-ascorbic acid-2-phosphate (ASAP; Sigma-Aldrich) and 1 ng/mL fibroblast growth factor-2 (FGF-2; 233-FB, R&D Systems). The differentiation potential of the collected cells was tested into the osteo-, adipo- and chondrogenic lineage. Further characterisation of MSCs took place by fluorescence-activated cell sorting (FACS) where cells were negative for the markers CD14 [RPA-M1, fluorescein isothiocyanate (FITC)-conjugated, Abcam], CD34 [4H11, allophycocyanin (APC)-conjugated, Abcam], CD45 [MEM-28, phycoerythrin (PE)-conjugated, Abcam] and CD79a (HM47, PE-conjugated, Abcam) and positive for the established MSC markers CD90 (5E10, FITC-conjugated, Abcam), CD105 (MEM-226, APC-conjugated, Abcam) and CD73 (AD2, PE-conjugated, Abcam). For the co-culture experiments, MSCs up to passage 4 were used.

ECFC isolation, culture and characterisation

Human umbilical cord blood was obtained after approval by the local ethics committee (01-230/K, University Medical Center Utrecht, the Netherlands). The blood was obtained after caesarean section and informed consent from the patient. The blood was diluted at least 1 : 1 with PBS 2 mM EDTA to isolate MNCs by density gradient centrifugation on Ficoll-Paque PLUS. The collected cells were cultured on rat tail collagen I (Corning) coating at a seeding density of $10\text{-}20 \times 10^6$ cells/cm² in EGM-2. For ECFC culture, endothelial growth medium-2 (EGM-2) was used, which was composed of endothelial basal medium-2 (EBM; Lonza), 10 % FBS, 100 U/mL penicillin, 10 mg/ mL streptomycin and EGM-2 SingleQuot (Lonza). During the first 7 days after plating, the culture medium was refreshed daily. Following, the medium was refreshed every 3-4 days. After about 2-3 weeks, colonies with a cobblestone-like morphology were picked and replated for further expansion. Characterisation of ECFCs was done by flow cytometry and were positive for CD105 and CD31 (TLD-3A12, FITC-conjugated, Abcam), partially positive for CD34 and CD309 (VEGFR/KDR, PE-conjugated, MACS, Miltenyi Biotech) and negative for CD45, CD14 and CD133 (AC133-VioBright, FITC-conjugated, Miltenyi Biotech). For co-cultures, ECFCs were used up to passage 10.

Live/dead staining of MSCs and ECFCs

MSCs or ECFCs were encapsulated at a concentration of 5×10^6 cells/mL in 3.5 % gelatin hydrogels crosslinked by 1, 2, or 3 % w/v TG. 20 µl droplets were added on round coverslips in a well-plate and left to crosslink for 1 h. Subsequently, the hydrogels were cultured for 24 h in either MSC expansion medium or EGM-2, respectively. 3 gels were prepared per condition for $N=3$ donors of each cell type. Live and dead cells were stained with 0.5 µg/mL calcein-AM (ThermoFisher Scientific) and 1 µg/mL ethidium homodimer (ThermoFisher Scientific). RGB fluorescence images of the live/dead stainings were taken at the centre of the hydrogel droplets using an upright fluorescence microscope (BX51, Olympus). Images were merged to manually count live and dead cells in 9 fields of view per condition ($N=3$, $n=3$; 1 image per hydrogel droplet). The percentage of dead cells was corrected for the initial cell death after trypsinisation right before encapsulation.

Incorporation of laminins in gelTG hydrogels

To assess the incorporation of laminins in the gelTG polymer network, LN521 (BioLamina, Sweden) was used. LN521 was added at a concentration of 10 µg/ mL to the reaction mixture of 3 % gelatin and 3 % TG. Hydrogels without laminin-addition served as a control. Per condition $n=5$ hydrogel discs (1 x 5 Ø mm; $V=20$ µL) were incubated for 24 h in PBS at 37 °C to remove all laminins which were not covalently bound in the hydrogel network. After fixation, hydrogels were stained with a primary anti-laminin α5 antibody (1:260, clone 4C7, MAB1924, Merck), followed by a goat-anti-mouse antibody Alexa Fluor 546 (4 µg/mL, A-11003, ThermoFisher). Imaging of stained hydrogels was performed with a fluorescence microscope (BX51, Olympus).

Co-cultures in gelTG hydrogels

1.25×10^6 ECFCs and 5×10^6 MSCs were co-cultured in 3 % gelatin hydrogels crosslinked by 3 % TG. Where indicated, 10 $\mu\text{g}/\text{mL}$ LN111 or LN211 (BioLamina, Sweden) were mixed with the cell-gelatin suspension to form covalently crosslinked hydrogels. Hydrogel droplets of 75 μl were placed in the centre of well-plates, left to crosslink for 1 h before addition of osteogenic differentiation medium (ODM). ODM was based on α -MEM which was supplemented with 10 % FBS, 100 U/mL penicillin, 10 mg/mL streptomycin, 10 mM β -glycerophosphate (Sigma-Aldrich) and 10 nm dexamethasone (Sigma- Aldrich). The constructs were cultured for 2 weeks. 3 different donor combinations of MSCs and ECFCs were used. Per experiment 3 hydrogels were used for mRNA isolation and 3 hydrogels were fixed in 4% formaldehyde and cut into 4 pieces for subsequent stainings ($N = 3, n = 3$).

Whole mount (immuno)staining and quantification of pre-vascular networks

After fixation of the samples, one quarter of each construct was stained for ALP activity, an early osteogenic marker, using Fuchsin + Substrate-Chromogen System (K0624, Dako). For fluorescent immunostainings, the hydrogels were permeabilised with 0.2 % Triton-X PBS for 30 min, followed by blocking with 5 % bovine serum albumin (BSA)/PBS for 30 min. To stain capillary-like structures, an anti- CD31 antibody (5.1 $\mu\text{g}/\text{mL}$; M0823, Dako) was combined with a secondary sheep anti-mouse biotinylated antibody (1 : 200; RPN1001v1, GE Healthcare) and a tertiary streptavidin Alexa Fluor 488 conjugated antibody (5.0 $\mu\text{g}/\text{mL}$; S32354, Invitrogen). To detect the stabilising structures of capillary-like networks, a mouse monoclonal Cy3-conjugated α -smooth muscle actin (α SMA) antibody (1 : 300; Clone 1A4, C6198, Sigma- Aldrich) was used. 4, 6-diamidino-2-phenylindole (DAPI; 100 ng/mL; Sigma-Aldrich) was used to stain the cell nuclei. Imaging occurred with a confocal microscope (SP8x Leica, DMi8, Leica).

To quantify the extent of pre-vascular structure formation, hydrogels of co-cultures were imaged in the centre of the hydrogel and 100 μm z-stacks were made (one location per hydrogel, $n = 9$). Projections of these z-stacks were individually adapted in brightness and contrast in ImageJ 1.51a to obtain comparable images for batch-processing using Angioquant software [20] to determine the total and mean vessel-like structure length per projection.

Immunohistochemistry on paraffin sections

The fixed hydrogel constructs were dehydrated in graded ethanol series, cleared in xylene and the hydrogel constructs were embedded in paraffin blocks and sectioned at 5 μm . Osteogenic differentiation of the cells embedded in the hydrogels was assessed by staining for osteonectin. Sections were deparaffinised, hydrated and endogenous peroxidase was blocked in 0.3 % H_2O_2 . Antigens were retrieved in citrate buffer at 80 $^\circ\text{C}$ for 20 min. The primary antibody for osteonectin, AON-1, [4.2 $\mu\text{g}/\text{mL}$; deposited to the Developmental Studies Hybridoma Bank (DSHB) by J.D. Termine [21]] was incubated for 1 h, followed by a horseradish peroxidase-conjugated anti-mouse antibody (EnVision + System- HRP Labelled Polymer, K4000, Dako). Staining of osteonectin was developed by conversion of 3,3'-diaminobenzidine (DAB)

solution (SK-4100, Vector, Burlingame, CA, USA) and nuclei were counterstained with haematoxylin (Merck). Isotype controls were performed using concentration-matched mouse IgG1 monoclonal antibody (ThermoFisher Scientific).

mRNA isolation, cDNA synthesis and qPCR

After 2 weeks of co-culture of MSCs and ECFCs, the hydrogels were digested in 2 mg/mL collagenase A (Roche) for 10 min at 37 °C. Following, the hydrogel-cell pellet was resuspended in TRIzol reagent (ThermoFisher Scientific, USA) and messenger RNA (mRNA) was isolated according to the manufacturer's instructions. DNase treatment (Turbo DNase; Thermo Fisher) was used to remove any DNA contaminations and the extracted mRNA was quantified with a NanoDrop ND-1000 spectrophotometer (ThermoFisher) at 260/280 nm. Complementary DNA (cDNA) was synthesised from 1 µg mRNA using the iScript cDNA Synthesis Kit (Bio Rad, Hercules, USA). qPCR analysis was done with a Bio-Rad CFX96 Real-Time PCR Detection System using FastStart SYBR Green Master mix (Sigma Aldrich) and an input of 20 ng cDNA per reaction. The used primers are presented in table 1 and the amplification efficiencies of all of the primers were between 0.9 and 1.1. Glyceraldehyde 3-phosphate dehydrogenase (*GAPDH*) was used as a housekeeping gene and the relative expression was determined by the $2^{-\Delta CT}$ formula.

Table 1. Primers

Human gene (protein)	Forward primer	Reverse primer
PECAM1 (CD31)	GCAGTGGTTATCATCGGAGTG	TCGTTGTTGGAGTTCAGAAGTG
CDH5 (VE-cadherin)	AAGCAGGCCAGGTATGAGAT	TGTGTACTTGGTCTGGGTGAAG
CSPG4 (NG2)	GAAGGAGGACGGACCTCAAG	GATCAGCTGCTCTTCCACCATT
ACTA2 (α SMA)	ATGCCATCATGCGTCTGGAT	ACGCTCAGCAGTAGTAACGA
BGLAP (osteocalcin)	CCTCACACTCCTCGCCCTAT	GCTTGGACACAAAGGCTGCAC
SPP1 (osteopontin)	GCCGAGGTGATAGTGTGGTT	GTGGGTTTCAGCACTCTGGT
RUNX2 (Runt-related transcription factor 2)	TTACAGTAGATGGACCTCGGGA	AGGAATGCGCCCTAAATCACT
GAPDH (Glyceraldehyde 3-phosphate dehydrogenase)	CAACGGATTTGGTCGTATTGGG	TGCCATGGGTGGAATCATATTGG

Statistical analysis

Differences in physico-chemical properties and cell viabilities were determined by one-way ANOVA and subsequent Tukey honest significant difference (HSD) post-hoc analysis using GraphPad Prism 7.02. For analysis of qPCR and vessel network length, MS Excel 2010 was used for calculations and PASW Statistics 22.0 (SPSS Inc. Chicago, USA) for statistical analysis. A mixed linear model, after log transformation for PCR data, was used to take into account the variations between donors and a Bonferroni's post hoc comparison test to compare the gene expression levels between the different hydrogel compositions. In the used model, the cell donors were considered as random factors and the hydrogel composition as a fixed factor.

Differences were considered statistically significant for $p < 0.05$. Asterisks represent statistical significances according to p -values (* $p < 0.05$; ** $p < 0.01$; *** $p < 0.001$).

Results

Physico-chemical characterisation of gelatin-transglutaminase hydrogels

The formation of 3% [w/v] gelatin-transglutaminase (gelTG) hydrogels was recorded over time by measuring the rheological properties of the crosslinking mixture (Figure 1a). The point of gelation of the hydrogels occurred within minutes and the crosslinking was accelerated by higher TG concentrations (Figure 1b). Although the crosslinking reaction did not plateau within the incubation time of 1 h (Figure 1a), addition of 3 % TG over 2 % did not result in an increased compressive modulus of the swollen hydrogels (Figure 1c). However, when only 1 % TG was used for hydrogel fabrication, they failed to gelate consistently.

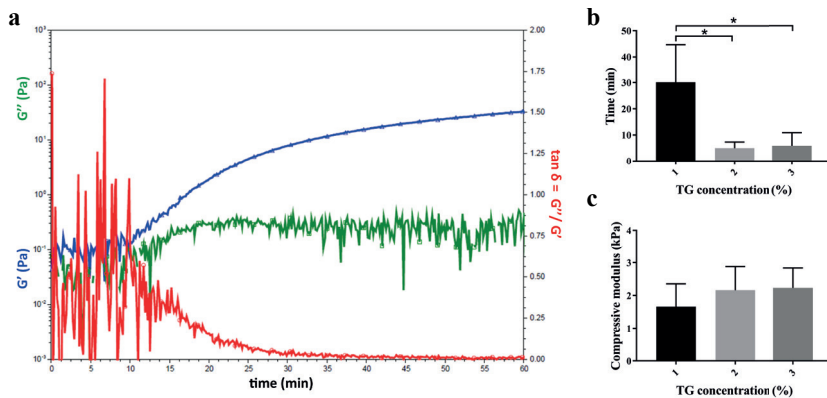


Figure 1. Physico-chemical and mechanical characterisation of gelTG hydrogels. a Representative rheological profile of 3 % (w/v) gelatin crosslinked by 3 % TG (w/v). b Point of gelation of 3 % (w/v) gelatin hydrogels for different TG concentrations (independent experiments with $n = 3$). c Compressive moduli of 24 h swollen gelTG hydrogels for different TG concentrations ($n = 9$).

Formation of pre-vascularised bone-like tissue in gelTG

The effect of the concentration of TG for hydrogel crosslinking on the viability of ECFCs and MSCs was investigated 1 day after encapsulation. Live cells were stained in green (calcein) and nuclei of dead cells in red (ethidiumhomodimer) as shown in a representative image of encapsulated MSCs (Figure 2a). Both ECFCs and MSCs were equally viable at about 90 %, independent of the applied TG concentration (Figure 2b,c). Co-cultures of MSCs and ECFCs for 14 d in osteogenic medium resulted in osteogenic commitment as indicated by positive ALP staining and slightly positive osteonectin staining (Figure 2d,e). Furthermore, the same cultures formed capillary-like structures which were stabilised by α SMA positive cells (Figure 2f-g).

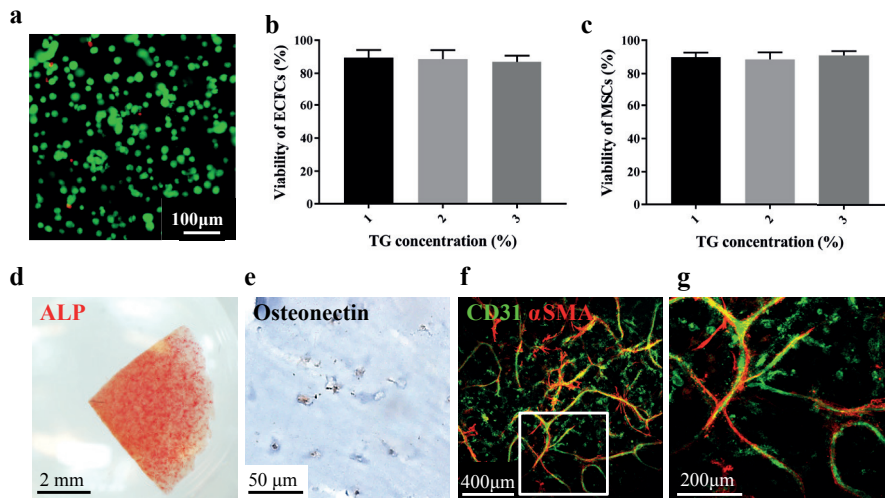


Figure 2. ECFC and MSC cell viability in gelTG hydrogels and formation of a pre-vascularised bone-like tissue. **a** Representative image of a live/dead staining of MSCs 1 d after encapsulation in gelTG hydrogels. **b** ECFC viability in gelTG hydrogels versus TG concentration (w/v). **c** MSC viability in gelTG hydrogels versus TG concentration. **d** ALP expression in a quarter, whole mount hydrogel construct. **e** Osteonectin staining on paraffin sections of the hydrogel. **f,g** 100 μm z-projection of stabilised capillary-like networks with **g** a magnification of the rectangle in **f** (CD31 in green and αSMA in red). $N = 3$ donors, $n = 3$ hydrogels)

Effect of incorporated laminins on MSC-ECFC co-cultures

The successful coupling of LN521 into gelTG hydrogels was confirmed by an immunofluorescence staining against the $\alpha 5$ subunit of LN521, which was incorporated into 3 % hydrogels using 3 % TG. Compared to the empty hydrogel control (insert in Figure 3b), the laminin-containing hydrogel stained homogeneously for $\alpha 5$ (Figure 3b).

LN111 and LN211 were incorporated in gelTG hydrogels with the aim to enhance the osteogenic differentiation in soft hydrogels. After 2 weeks of culture time, intense ALP activity was present in gelTG constructs that were enriched with LN111 or LN211 (Figure 3c,g). Osteonectin, a more mature marker than ALP, was not yet clearly present in the different hydrogels (Figure 3d,h). αSMA -stabilised capillary-like networks were present throughout 100 μm projections in both types of laminin-laden gelTG hydrogels (Figure 3e,i). Quantification of the vascular-like structures, compared to the gelTG hydrogels, indicated no effect on total or mean capillary-like network length (Figure 3f,j). All examined conditions were demonstrated to support formation of pre-vasculature and osteogenic differentiation.

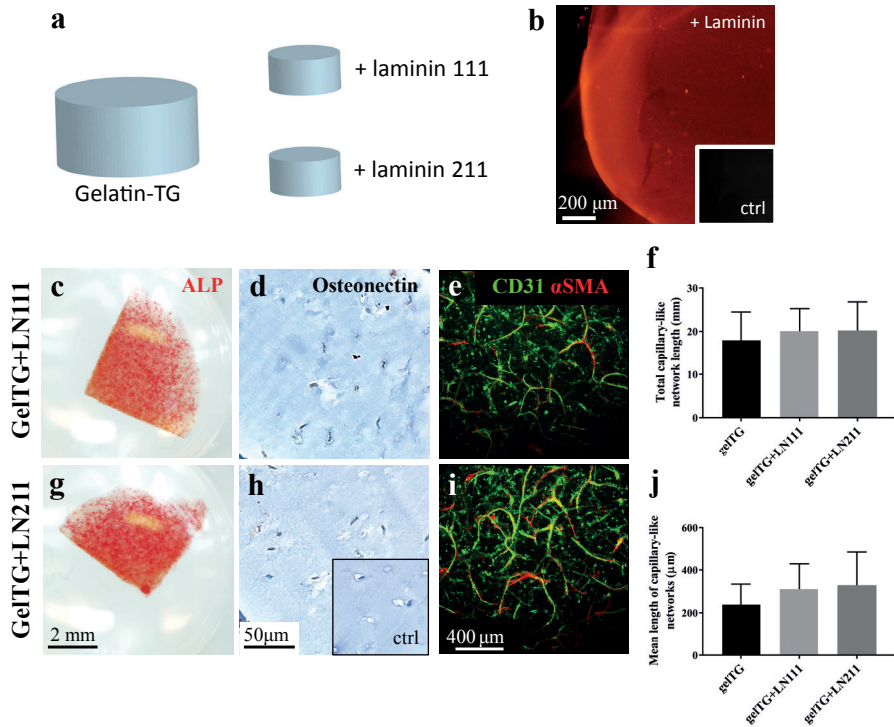


Figure 3. Effect of laminins on osteogenic, vasculogenic and pericyte-like differentiation in gelTG hydrogels after 2 weeks in osteogenic differentiation medium. **a** For cell cultures, gelTG hydrogels were either pure, or enriched with either LN111 or LN211. **b** Immunostaining against the $\alpha 5$ subunit of LN521 showing laminin retention in gelTG hydrogels 24 h after hydrogel fabrication ($n = 5$). **c,g** ALP expression in quarters of whole mount hydrogel constructs. **d,h** Osteonectin staining on paraffin sections of the different hydrogel compositions and of the isotype control (insert). **e,i** stabilised capillary-like networks in 100 μm z-projections. **f** Total, and **j** mean capillary-like network length in the different hydrogels. $N = 3$, $n = 3$

Gene expression levels for osteogenic, vasculogenic and pericyte-like markers were analysed, to detect the cellular differentiation potential when embedded in pure gelTG hydrogels and when laminins were added. For the osteogenic markers, *BGLAP*, *SPP1*, and *RUNX2* no statistical differences in expression levels were observed between the different groups (Figure 4a-c). Furthermore, on vasculogenesis-related genes *CDH5* and *PECAM1* no effect was seen by the added laminins (Figure 4d,e). Also on the pericyte-related genes *CSPG4* and *ACT2*, the addition of laminins did not have any influence (Figure 4f,g).

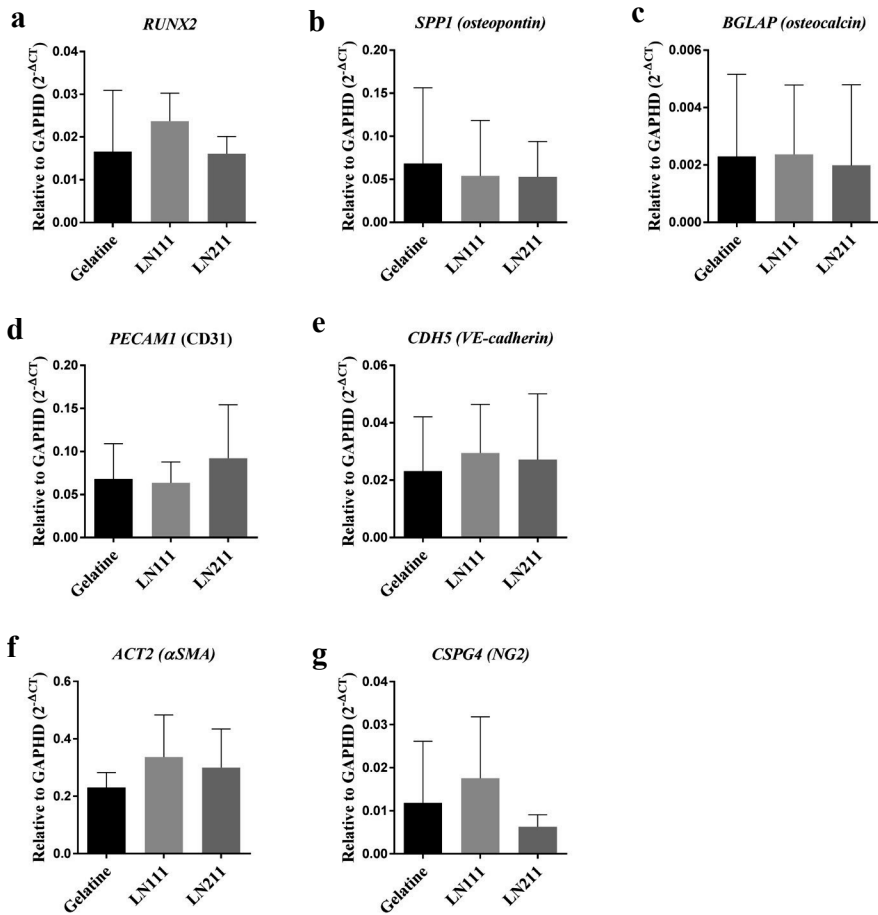


Figure 4. Osteogenic, vasculogenic and pericyte-like gene expression levels in different gelTG hydrogels after 14 d of co-culture in osteogenic differentiation medium. **a-c** Osteogenic gene expression levels for *BGLAP*, *SPP1* and *RUNX2* indicated no significant difference between the different hydrogel compositions. **d, e** Vasculogenic gene expression levels for *CDH5* and *PECAM1* were similar in all hydrogels. **f, g** Pericyte-like gene expression levels *CSPG4* and *ACT2* resulted in no significant differences between the different hydrogel compositions. $N = 3, n = 3$

Discussion

In the present study, we characterised and enriched gelTG hydrogels for pre-vascularised bone tissue engineering. These hydrogels were designed to have a fast enzymatic crosslinking process, high cyto-compatibility and to enable formation of capillary-like structures and simultaneous osteogenic differentiation. Furthermore, it was possible to incorporate unmodified laminins into the hydrogel network.

Physico-chemical and mechanical properties of gelatin-transglutaminase hydrogels

The rate of the crosslinking reaction between gelatin and TG was highly dependent on the TG concentration, where it was observed that a higher TG concentration led to faster gelatin hydrogel formation. This is in line with the observations of Irvine *et al.*, who also observed that the TG concentration had a clear effect on the crosslinking time of gelatin-based hydrogels when using 0.5, 1.5 and 3 % TG [22]. In our study, we observed that at 2 % TG there was a saturation point, where further increasing the TG concentration did not accelerate the crosslinking process any further. Sterical hindrance by relatively high enzyme and maltodextrin concentrations when crosslinking gelatin might be a plausible explanation. The used TG also contains maltodextrin and purification of the enzyme before use [16, 23, 24], might improve the consistency of the speed of crosslinking. While 1 % unpurified TG appeared too low to robustly crosslink 3 % gelatin hydrogels in the tested crosslinking regime, 2 and 3 % TG led to identical compressive moduli of the swollen hydrogels.

Gelatin crosslinking via TG is based on lysine and glutamine residues which are naturally present at approximately 3 and 8 % in the gelatin backbone, respectively [25]. Therefore, this TG-mediated crosslinking is simpler and more efficient compared to other enzyme mediated crosslinking systems for gelatin. To illustrate, the crosslinking reaction of TG and gelatin, which leads to a point of gelation within minutes after initiation, is much faster than those for other enzymes, such as laccase and tyrosinase [26]. Laccase-mediated crosslinking requires extensive crosslinking times of several hours [26]. Such long crosslinking times are impractical for cell incorporation and for clinical use. Horseradish peroxidase (HRP)-mediated crosslinking is characterised by an almost instantaneous reaction. However, gelatin needs to be modified first before it can be crosslinked using HRP and H₂O₂ [27, 28]. HRP and laccase-mediated crosslinking occurs through tyrosine crosslinking which is also naturally present on gelatin but at low concentrations. This would then necessitate the grafting of more tyrosines for stable crosslinking into a hydrogel. For crosslinking systems, as presented by gelatin and TG, potential applications lie in molding of constructs and 3D bioprinting purposes.

Engineering pre-vascularised bone-like tissues in gelTG hydrogels

In order to evaluate possible cell-dependent effects due to TG-mediated crosslinking, materials were evaluated with the relevant primary cell types MSCs and ECFCs. Approximately 90 % of both cell types were viable after 1 day. Moreover, there was also no TG concentration-dependent effect up to 3 % on the viability of the tested cells, highlighting the high cell biocompatibility of the crosslinking process. This high cell biocompatibility was also previously confirmed by others, who found cell viabilities higher than 90 % for MSCs or NIH 3T3 cells [24, 29].

In gelTG hydrogels, ECFCs formed interconnected capillary-like structures, which were stabilised by α SMA-expressing cells. Simultaneously, a fraction of MSCs differentiated towards the osteogenic lineage. While stiffer matrices proved to be more beneficial for inducing osteogenesis, it was also shown previously that osteogenic differentiation can also occur in relatively soft matrices under 4 kPa [16, 30-32], corroborating the outcome of the present study. Osteogenic differentiation in this culture model was assessed after a culture period of 14 d, which is early for bone formation. While there are studies showing osteogenic differentiation after 2 weeks [32], conventionally, osteogenesis is evaluated after 3-4 week culture periods [33] and this may explain the relatively weak staining for osteonectin.

Effect of incorporated laminins on MSC-ECFC co-cultures

Microbial transglutaminase crosslinks lysine and/or glutamine containing proteins, which enables coupling of various (unmodified) ECM-derived proteins, such as laminins, into the gelatin hydrogel network [34]. This direct coupling of unmodified proteins into a polymer network is advantageous over other approaches that require chemical modification of the protein.

Laminins are heterotrimeric proteins that contain an α -chain, a β -chain and a γ -chain and the resulting different isoforms of laminin are named according to their chain composition. They are high molecular weight proteins and as an integral part of the basement membrane they influence cell adhesion, migration and differentiation [35]. For osteogenic purposes, laminins were explored as coatings of calcium phosphates or titanium implants and showed promising results *in-vitro* and *in-vivo* in terms of osteogenic differentiation [36]. For LN111 and for LN211, osteogenesis-enhancing effects were described that might be beneficial for ECFC-MSC co-cultures.

Specifically, LN111-derived peptides were shown to stimulate ALP activity in *in-vitro* cell cultures, as an early osteogenic marker [37]. Furthermore, LN111 increased the precipitation of calcium phosphates *in-vitro* [38, 39]. *In-vivo* it was shown that coating of implant surfaces with LN111 led to significantly higher bone area [40] and bone-related gene expression than in the control groups [41], but only during early bone formation within 2 weeks [42]. Similarly, LN211 was also found to enhance bone cell function *in-vitro* and *in-vivo* [43-45].

In the present study, successful coupling and homogenous distribution of laminin in gelTG was shown. To investigate whether LN111 and LN211 can promote osteogenesis in soft gelatin-based hydrogels, we incorporated these proteins in gelTG. However, addition of these laminins on short term did not result in any added effect on early osteogenic differentiation, neither on the protein nor on the gene expression level. In contrast to the other studies where osteogenesis was stimulated with laminins, the short term of our experiment may have caused this lack of effect. The incorporation of laminins by crosslinking via microbial TG might have led to a transient protein inactivation. Further, the incorporated proteins may have remained inactive while retained in the matrix because on the applied time scale, insufficient degradation and remodelling of the matrix could have taken place by the cells to release the active site of the proteins. It was indeed shown before that, enzymatic crosslinking of bioactive proteins into gelatin can lead to such a reversible inactivation of the protein [23].

Gelatin by itself is a biologically active matrix, and it could also be possible that addition of laminins does not further affect the osteogenic differentiation of our encapsulated cells. It was reported in other studies that laminins have an effect on osteogenesis when incorporated in a (semi) synthetic hydrogel [32, 46]. Another explanation that the laminins did not have an effect in our gelTG hydrogels on the encapsulated cells, might be attributed to the presence of growth factors in the osteogenic culture medium that might have overruled the effect of the added laminins.

Overall, it was demonstrated that it is possible to successfully incorporate laminins into gelTG hydrogels. At short term, laminins in the gelTG hydrogels did not affect cell behaviour towards osteogenesis. It is likely, that the activity of the incorporated laminins was (temporarily) impaired and therefore did not significantly enhance the formation of pre-vascularised bone using the MSC-ECFC co-cultures. However, even though laminins did not have an effect in these hydrogels *in-vitro*, it might still be possible that *in-vivo*, where a faster degradation and remodelling of the hydrogel takes place, the laminins might be released and stimulate osteogenesis. Nevertheless, we demonstrated that the gelTG hydrogels, with or without laminins, were able to support pre-vascular structure formation and osteogenesis simultaneously.

Conclusion

gelTG hydrogels crosslinked by mTG are an easily available and biocompatible biomaterial for cell culture. Via mTG-mediated crosslinking, laminins can be incorporated into these hydrogels to steer cell behaviour. These hydrogels enabled formation of capillary-like structures and early osteogenesis in pure and laminin-enriched gelTG hydrogels using an ECFC-MSC co-culture model. Incorporation of LN111 or LN211 in gelTG hydrogels supported the development of pre-vascularised bone-like microtissues, however, did not further affect the extent of tissue differentiation compared to gelTG hydrogels.

Acknowledgements

The authors thank Maya Wright Clark and Adriana Palom Agustí for their contributions to optimisation of cell cultures in gelTG and Mattie van Rijen for his contributions to histology. This research was partially funded by the European Union FP7- MC-IRSES 'SkelGEN' project under grant agreement Nr. 318553 and by support from the Royal Society of New Zealand Rutherford Discovery Fellowship (RDF-UOO1204; TW), Health Research Council of New Zealand Emerging Researcher First Grant (HRC 15/483; KL).

References

1. Levenberg, S., et al., *Engineering vascularized skeletal muscle tissue*. Nature Biotechnology, 2005. **23**(7): p. 879-884.
2. Butt, O.I., et al., *Stimulation of peri-implant vascularization with bone marrow-derived progenitor cells: Monitoring by in vivo EPR oximetry*. Tissue Engineering, 2007. **13**(8): p. 2053-2061.
3. Unger, R.E., E. Dohle, and C.J. Kirkpatrick, *Improving vascularization of engineered bone through the generation of pro-angiogenic effects in co-culture systems*. Advanced Drug Delivery Reviews, 2015. **94**: p. 116-125.
4. Au, P., et al., *Bone marrow-derived mesenchymal stem cells facilitate engineering of long-lasting functional vasculature*. Blood, 2008. **111**(9): p. 4551-4558.
5. Klotz, B.J., et al., *Engineering of a complex bone tissue model with endothelialised channels and capillary-like networks*. Eur Cell Mater, 2018. **35**: p. 335-348.
6. Kolbe, M., et al., *Paracrine Effects Influenced by Cell Culture Medium and Consequences on Microvessel-Like Structures in Cocultures of Mesenchymal Stem Cells and Outgrowth Endothelial Cells*. Tissue Engineering Part A, 2011. **17**(17-18): p. 2199-2212.
7. Gawlitta, D., et al., *Hypoxia impedes vasculogenesis of in vitro engineered bone*. Tissue Eng Part A, 2012. **18**(1-2): p. 208-18.
8. Klotz, B.J., et al., *Gelatin-Methacryloyl Hydrogels: Towards Biofabrication-Based Tissue Repair*. Trends in Biotechnology, 2016. **34**(5): p. 394-407.
9. Yue, K., et al., *Synthesis, properties, and biomedical applications of gelatin methacryloyl (GelMA) hydrogels*. Biomaterials, 2015. **73**: p. 254-71.
10. Bigi, A., et al., *Mechanical and thermal properties of gelatin films at different degrees of glutaraldehyde crosslinking*. Biomaterials, 2001. **22**(8): p. 763-768.
11. Sisson, K., et al., *Evaluation of Cross-Linking Methods for Electrospun Gelatin on Cell Growth and Viability*. Biomacromolecules, 2009. **10**(7): p. 1675-1680.
12. Munoz, Z., H. Shih, and C.C. Lin, *Gelatin hydrogels formed by orthogonal thiol-norbornene photochemistry for cell encapsulation*. Biomaterials Science, 2014. **2**(8): p. 1063-1072.
13. Lee, Y., et al., *Enzyme-catalyzed in situ forming gelatin hydrogels as bioactive wound dressings: effects of fibroblast delivery on wound healing efficacy*. Journal of Materials Chemistry B, 2014. **2**(44): p. 7712-7718.
14. McDermott, M.K., et al., *Mechanical properties of biomimetic tissue adhesive based on the microbial transglutaminase-catalyzed crosslinking of gelatin*. Biomacromolecules, 2004. **5**(4): p. 1270-1279.
15. Zhu, Y., et al., *Microbial transglutaminase - A review of its production and application in food processing*. Applied Microbiology and Biotechnology, 1995. **44**(3-4): p. 277-282.
16. Tan, S., et al., *The synergetic effect of hydrogel stiffness and growth factor on osteogenic differentiation*. Biomaterials, 2014. **35**(20): p. 5294-306.
17. Wen, J.H., et al., *Interplay of matrix stiffness and protein tethering in stem cell differentiation*. Nature Materials, 2014. **13**(10): p. 979-987.
18. Chen, Y.C., et al., *Functional Human Vascular Network Generated in Photocrosslinkable Gelatin Methacrylate Hydrogels*. Adv Funct Mater, 2012. **22**(10): p. 2027-2039.
19. Occhetta, P., et al., *VA-086 methacrylate gelatine photopolymerizable hydrogels: A parametric study for highly biocompatible 3D cell embedding*. J Biomed Mater Res A, 2015. **103**(6): p. 2109-17.
20. Niemisto, A., et al., *Robust quantification of in vitro angiogenesis through image analysis*. IEEE Trans Med Imaging, 2005. **24**(4): p. 549-53.

21. Bolander, M.E., et al., *Monoclonal antibodies against osteonectin show conservation of epitopes across species*. *Calcif Tissue Int*, 1989. **45**(2): p. 74-80.
22. Irvine, S.A., et al., *Printing cell-laden gelatin constructs by free-form fabrication and enzymatic protein crosslinking*. *Biomedical Microdevices*, 2015. **17**(1).
23. Kuwahara, K., et al., *Enzymatic Crosslinking and Degradation of Gelatin as a Switch for Bone Morphogenetic Protein-2 Activity*. *Tissue Engineering Part A*, 2011. **17**(23-24): p. 2955-2964.
24. Kuwahara, K., et al., *Cell Delivery Using an Injectable and Adhesive Transglutaminase-Gelatin Gel*. *Tissue Engineering Part C-Methods*, 2010. **16**(4): p. 609-618.
25. Paguirigan, A.L. and D.J. Beebe, *Protocol for the fabrication of enzymatically crosslinked gelatin microchannels for microfluidic cell culture*. *Nat Protoc*, 2007. **2**(7): p. 1782-8.
26. Roberts, J.J., et al., *A comparative study of enzyme initiators for crosslinking phenol-functionalized hydrogels for cell encapsulation*. *Biomater Res*, 2016. **20**: p. 30.
27. Thi, T.T.H., et al., *Enhanced tissue adhesiveness of injectable gelatin hydrogels through dual catalytic activity of horseradish peroxidase*. *Biopolymers*, 2018. **109**(1).
28. Sakai, S., et al., *Horseradish peroxidase-mediated encapsulation of mammalian cells in hydrogel particles by dropping*. *J Microencapsul*, 2014. **31**(1): p. 100-4.
29. Chen, P.Y., et al., *Fabrication of large perfusable macroporous cell-laden hydrogel scaffolds using microbial transglutaminase*. *Acta Biomaterialia*, 2014. **10**(2): p. 912-920.
30. Benavides, O.M., et al., *Capillary-Like Network Formation by Human Amniotic Fluid-Derived Stem Cells Within Fibrin/Poly(Ethylene Glycol) Hydrogels*. *Tissue Engineering Part A*, 2015. **21**(7-8): p. 1185-1194.
31. Blache, U., et al., *Dual Role of Mesenchymal Stem Cells Allows for Microvascularized Bone Tissue-Like Environments in PEG Hydrogels*. *Adv Healthc Mater*, 2016. **5**(4): p. 489-98.
32. Klotz, B.J., et al., *A Versatile Biosynthetic Hydrogel Platform for Engineering of Tissue Analogues*. *Adv Healthc Mater*, 2019: p. e1900979.
33. Gotman, I., et al., *Mesenchymal stem cell proliferation and differentiation on load-bearing trabecular Nitinol scaffolds*. *Acta Biomaterialia*, 2013. **9**(9): p. 8440-8448.
34. Paguirigan, A.L. and D.J. Beebe, *Protocol for the fabrication of enzymatically crosslinked gelatin microchannels for microfluidic cell culture*. *Nature Protocols*, 2007. **2**(7): p. 1782-1788.
35. Timpl, R., et al., *Laminin—a glycoprotein from basement membranes*. *J Biol Chem*, 1979. **254**(19): p. 9933-7.
36. Javed, F., et al., *Laminin coatings on implant surfaces promote osseointegration: Fact or fiction?* *Arch Oral Biol*, 2016. **68**: p. 153-61.
37. Vukicevic, S., et al., *Differentiation of canalicular cell processes in bone cells by basement membrane matrix components: regulation by discrete domains of laminin*. *Cell*, 1990. **63**(2): p. 437-45.
38. Bougas, K., et al., *In vitro Evaluation of Calcium Phosphate Precipitation on Possibly Bioactive Titanium Surfaces in the Presence of Laminin*. *J Oral Maxillofac Res*, 2011. **2**(3): p. e3.
39. Bougas, K., et al., *Laminin Coating Promotes Calcium Phosphate Precipitation on Titanium Discs in vitro*. *J Oral Maxillofac Res*, 2012. **2**(4): p. e5.
40. Bougas, K., et al., *In vivo evaluation of a novel implant coating agent: laminin-1*. *Clin Implant Dent Relat Res*, 2014. **16**(5): p. 728-35.
41. Schwartz-Filho, H.O., et al., *The effect of laminin-1-doped nanoroughened implant surfaces: gene expression and morphological evaluation*. *Int J Biomater*, 2012. **2012**: p. 305638.
42. Bougas, K., et al., *Bone apposition to laminin-1 coated implants: histologic and 3D evaluation*. *Int J Oral Maxillofac Surg*, 2013. **42**(5): p. 677-82.

43. Kang, H.K., et al., *The effect of the DLTIDDSYWYRI motif of the human laminin alpha2 chain on implant osseointegration*. *Biomaterials*, 2013. **34**(16): p. 4027-37.
44. Min, S.K., et al., *Titanium surface coating with a laminin-derived functional peptide promotes bone cell adhesion*. *Biomed Res Int*, 2013. **2013**: p. 638348.
45. Yeo, I.S., et al., *Identification of a bioactive core sequence from human laminin and its applicability to tissue engineering*. *Biomaterials*, 2015. **73**: p. 96-109.
46. Becerra-Bayona, S., et al., *Influence of select extracellular matrix proteins on mesenchymal stem cell osteogenic commitment in three-dimensional contexts*. *Acta Biomaterialia*, 2012. **8**(12): p. 4397-4404.

Chapter 5

A versatile bio-synthetic hydrogel platform for engineering of tissue analogues

Barbara J. Klotz | Loes A. Oosterhoff | Lizette Utomo | Khoon S. Lim
Queralt Vallmajo-Martin | Hans Clevers | Tim B.F. Woodfield
Antoine J.W.P. Rosenberg | Jos Malda | Martin Ehrbar | Bart Spee
Debby Gawlitta

Advanced Healthcare Materials 2019 August; online version 1900979



Abstract

For creating functional tissue analogues in tissue engineering, stem cells require very specific 3D microenvironments to thrive and mature. Demanding (stem) cell types that are used nowadays, can find such an environment in a heterogeneous protein mixture with the trade name Matrigel. Several variations of synthetic hydrogel platforms composed of poly(ethylene glycol) (PEG), which were spiked with peptides, were recently developed and showed equivalence to Matrigel for stem cell differentiation. Here we present a clinically relevant hydrogel platform, based on PEG and gelatin, which even outperformed Matrigel when targeting 3D pre-vascularised bone and liver organoid tissue engineering models. The hybrid hydrogel with natural and synthetic components stimulated efficient cell differentiation, superior to Matrigel models. Furthermore, the strength of this hydrogel lies in the option to covalently incorporate unmodified proteins. Our results demonstrate how a hybrid hydrogel platform with intermediate biological complexity, when compared to existing biological materials and synthetic PEG-peptide approaches, can efficiently support tissue development from human primary cells.

Introduction

Shortcomings of autologous tissue transplants and the shortage of donor organs are a major clinical burden to society. Tissue engineering and regenerative medicine are considered as a potential solution to overcome this problem. Considerable advancements over the course of almost 30 years, resulted in therapeutic applications with successes for thin or avascular tissues and organs such as skin ^[1], cartilage ^[2] and bladder ^[3]. For biologically complex tissue analogues and for up-scaling of constructs to clinically relevant size, a major bottleneck for advancement to the clinical setting lies in the lack of vascularization ^[4]. Furthermore, there is a need for clinically relevant, degradable biomaterials that stimulate cell differentiation, matrix secretion and ultimately, functional tissue development ^[5].

Hydrogels play an important role in tissue engineering approaches, since their three-dimensional (3D) polymer network, characterized by a high water content, can closely resemble the native extracellular matrix in the (developing) tissues. In fundamental stem cell culture, the most commonly used biomaterial is isolated from a mouse tumor (Engelbreth-Holm-Swarm), which is rich in extracellular matrix proteins with the trade name Matrigel (or Cultrex) ^[6]. The composition of Matrigel is heterogeneous with more than 1,500 different proteins in its makeup, with the most prevalent proteins being laminin, collagen type IV and entactin ^[7]. This material is especially required for biologically demanding cell cultures, such as organoids ^[5, 8] and vasculogenesis assays ^[9]. Its unique biological composition attributes its value for cell culture to the derivation from the basement membrane and allows cells to proliferate and differentiate. The basement membrane forms a specialized extracellular habitat of multiple organ and tissue systems throughout the body, making it an interesting target matrix for recapitulation.

Furthermore, even though Matrigel might appear as an ideal biomaterial from a biological perspective, there are numerous disadvantages that render it unsuitable for clinical application ^[10]. High variability in composition and also stiffness, limits the batch reproducibility massively ^[11], with a lot-to-lot similarity of only 53% ^[7]. The murine origin of Matrigel will furthermore complicate clinical translation due to immunogenic effects ^[12].

To advance the translation of human tissue analogues to the clinics, new matrices with biological equivalence to the basement membranes are of high relevance. Recent approaches to create these were based on completely defined synthetic hydrogel platforms, coupled with biological components in the form of peptides improving cell adhesion such as RGDs (arginylglycylaspartic acid) ^[13]. In the present study, laminins were chosen for incorporation because these represent the major protein present in Matrigel. Synthetic polymers are advantageous since they are biologically inert and they have highly defined material and mechanical properties. To impart biological characteristics, inert synthetic polymers such as poly(ethylene glycol) (PEG), poly(vinyl alcohol) (PVA), poly-N-isopropylacrylamide (PNIPAAm) require addition of bioactive peptide sequences. For example, in a vascular toxicity screen,

a 2D platform based on poly(ethylene glycol) (PEG) and peptides mimicking the functional groups of large ECM molecules (RGDs) outperformed Matrigel in terms of reproducibility and sensitivity ^[13b]. The screening assay typically involves cell culture periods for up to 24 hours. Also, for stem cell expansion, the tailored PEG-based system with peptides maintained human embryonic stem cell pluripotency during the initial 4 days ^[13b]. Further, another group presented an elegant approach to expand and differentiate intestinal stem cells and organoids in a mechanically dynamic PEG-peptide-based hydrogel to foster fibronectin-based adhesion peptides and compared it to Matrigel ^[13a]. During culture over 4 days, intestinal stem cells survived and proliferated in the PEG-peptide hydrogels. Another variant of PEG hydrogels, spiked with RGDs and protease-degradable peptides even allowed for 14-day cell differentiation protocols, which resulted in comparable levels of differentiation as cultures in Matrigel ^[13c].

These recent hydrogel developments are great achievements towards finding a clinically relevant replacement for Matrigel by showing biological equivalence. The next step lies in the further development of a tissue-specific tailorable material, which allows for enhanced cell differentiation compared to Matrigel in order to more closely mimic the function of a native tissue. However, due to the low number of biologically active sites in synthetic matrices with spiked peptides, they have a reduced cell-driven remodeling capacity when compared to natural materials. Stimulating remodeling of the engineered matrix into a mature biologically functional tissue analogue implies successful long-term performance of encapsulated cells ^[8]. The native extracellular matrix (ECM) is a dynamic material, which provides residing cells with specific physical and chemical cues via binding sites ^[14]. The ECM is ascribed a crucial role in regulating the development, function and homeostasis of residing cells ^[15]. Hence, an ideal scaffold material for engineering of tissues outside the human body, will be one that mimics the natural architecture of the targeted tissue, which remains a significant challenge with the current technology ^[14, 16].

To bridge the gap between minimalistic approaches of synthetic, defined matrices and biological materials, novel hydrogels that provide a matrix with intermediate biological complexity are needed for tissue engineering purposes. Gelatin can serve this purpose, as it is derived from the most abundant protein in the human body, collagen type I, which is highly conserved among species. It is associated with less immunogenicity than collagen while retaining bioactive signals of its native progenitor. Furthermore, gelatin is used, despite its animal origin, routinely in the clinics since several decades ^[17].

In this study, we developed a gelPEG hydrogel platform aimed at recapitulating the biological functionality of the basement membranes, while maintaining the simplicity, tailorability and reproducibility of synthetic hydrogels. This hybrid semi-synthetic gelPEG platform uniquely combines its inherent support of cell performance, tailorability of physicochemical characteristics and highly versatile application by incorporation of natural (unmodified) tissue-specific proteins. A systematic material characterization is presented and tailored towards physico-

chemical parameters favoring multi-tissue differentiation. The biological performance of the novel hydrogel is compared to that of Matrigel. Vasculogenesis, a hallmark process for tissue engineering, is evaluated in gelPEG hydrogels and assessed regarding extent and maturity of the developed vascular network in 3D. To demonstrate the enhanced cell-instructive capacity of the new basement membrane-inspired material, it was applied in engineering of pre-vascularised bone and liver-like tissue analogues.

Results

Systematic evaluation of gelPEG hybrid hydrogels

Hydrogels were fabricated by forming covalent crosslinks between gelatin and PEG via an enzymatic reaction with coagulation factor XIII (FXIIIa). To do so, the specific amino acid substrate sequence (NQEQVSPL) of the enzyme was conjugated to 8-arm PEG (PEG-Gln), which can be crosslinked with the native lysine residues on gelatin (**Figure 1**). Moreover, in the same reaction step, other lysine-containing proteins may be coupled into the gelPEG hydrogel network to create a tissue-specific ECM-like environment. Before crosslinking, cells were resuspended in the gelatin-PEG solution to form a 3D polymer network around the cells.

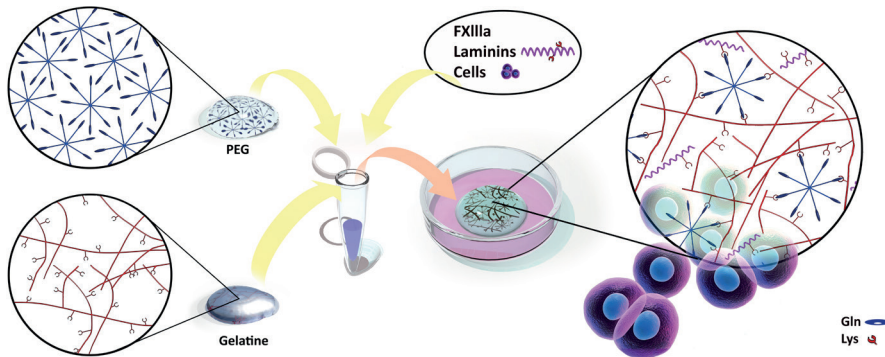


Figure 1. Enzymatic crosslinking reaction between PEG and gelatin. The FXIIIa-specific amino acid sequence for glutamine (gln), NQEQVSPL, was conjugated to 8-arm PEG (PEG-Gln), which can be crosslinked with lysine (lys) residues that are naturally occurring on gelatin. The reaction takes place under physiological conditions and cells can be encapsulated in the same step. It is also possible to immobilize other lysine-containing proteins in the hydrogel network for enhanced tissue specificity (see Supplementary Figure 2).

The optimal crosslinking conditions between gelatin and PEG were established by mixing the two components in molar ratios between 1:1 to 6:1 (gelatin)Lys/(PEG)Gln at a constant overall polymer concentration of 3% w/v (**Figure 2**). Hydrogels with the lowest swelling ratio, indicating efficient crosslinking and therefore the best fabrication window, was from 1:1 to 4:1 gelatin/PEG combination (Figure 2a). Since gelatin can be degraded and remodeled by cells, 4:1 gelatin/PEG was preferred over 2:1 and 1:1

and chosen to proceed within further experiments. The swelling ratio decreased with increasing polymer concentration (Figure 2b). A polymer concentration of 1% w/v gelPEG resulted in mechanically unstable hydrogels that could not be manipulated without destruction. The compressive moduli were 2.6 kPa \pm 0.6 for 2% and 6.8 kPa \pm 2 for 3% w/v gelPEG hydrogels with significant differences ($p= 0.0026$) (Figure 2C). Rheological measurements indicated for 2% gelPEG at 4:1 molar ratio a point of gelation after 2 ± 1.5 minutes and the hydrogel was completely crosslinked after about 15 minutes (**Supplementary Figure 1**). Furthermore, coupling of lysine-containing proteins of interest into the gelPEG network was demonstrated. To do so, laminin (LN) 521 was successfully incorporated in gelPEG hydrogels as indicated by anti- $\alpha 5$ -LN staining in whole mount constructs (**Supplementary Figure 2b**).

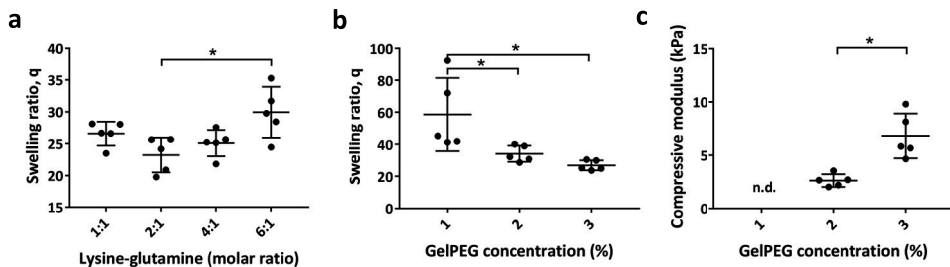


Figure 2. Physical fine-tuning and characterization of gelPEG hydrogels. **a** Hydrogels with the lowest swelling ratio were obtained at a molar ratio (gelatin)Lys/(PEG)Gln of 2:1 for 3% w/v gelPEG. **b** Decreasing gelPEG concentration resulted in higher swelling ratios. **c** Compressive moduli were significantly increased from 2 to 3% gelPEG. n.d., not determined; lys: lysine; gln: glutamine; data is depicted as mean + SD; $n= 5$

Vasculogenesis in gelPEG hydrogels compared to Matrigel

The biological functionality of the novel developed gelPEG hydrogel for 3D vasculogenesis was assessed and compared to Matrigel, the gold standard for vasculogenesis. Low polymer content or crosslink densities resulting in soft hydrogels are needed to allow for cell migration^[18] and enabling capillary network formation^[19]. For this reason, we chose for this application the 2% w/v gelPEG hydrogel formulation, which is relatively stable (compared to 1%) and still relatively soft.

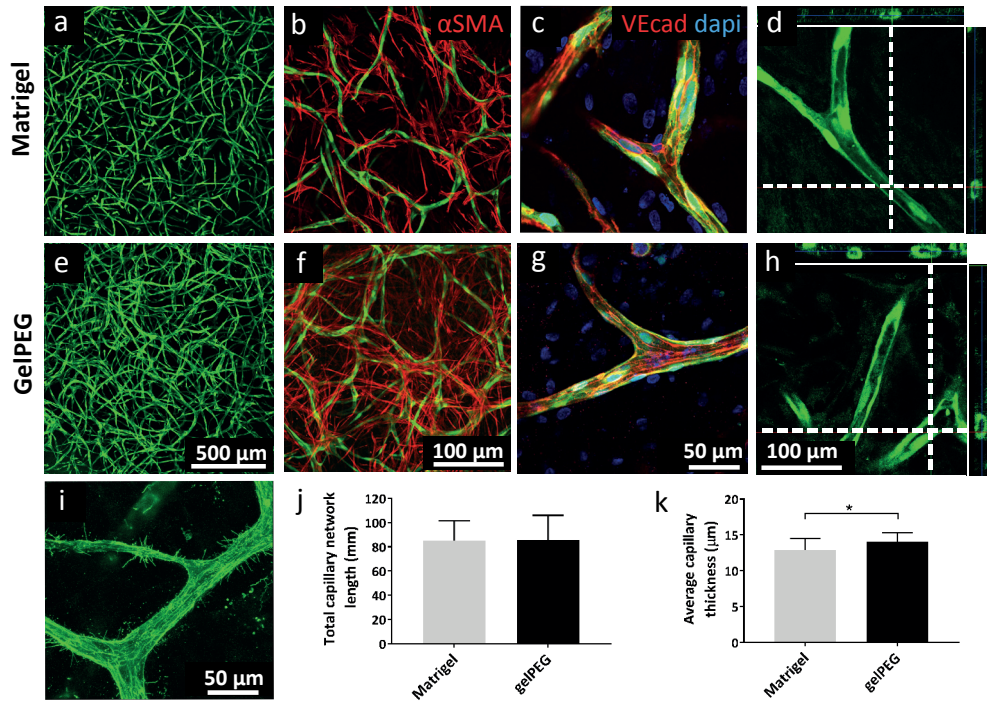
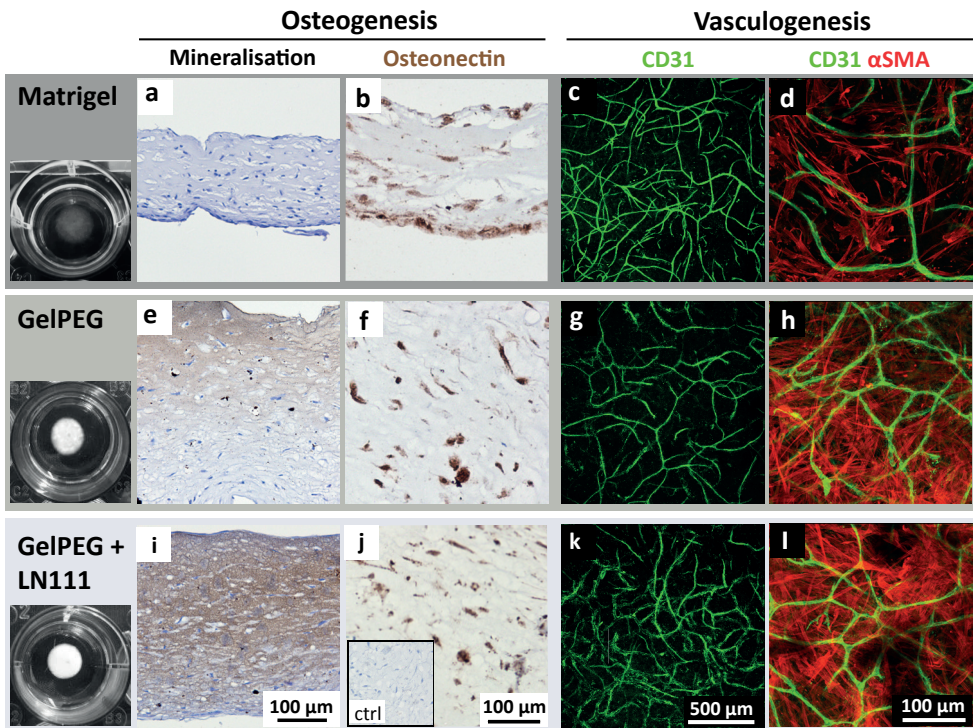


Figure 3. Vasculogenesis in gelPEG and Matrigel characterized by stabilized capillary-like structures with lumen. Human GFP-ECFCs and MSCs were co-cultured for 10 days in EGM-2. **a, e** Projections of 150 μm confocal stacks through a hydrogel. **b, f** Stabilization of vascular networks by pericyte-like cells (red). **c, g** Capillary-like structures were composed of multiple fused endothelial cells indicated by cell-cell contact by lumenization (dotted lines indicate cutting sections). **d, h** Capillary-like structures in gelPEG and Matrigel were characterized by lumenization (dotted lines indicate cutting sections). **i** Capillary-like structures with filopodia at a site of active angiogenesis, here in a gelPEG hydrogel. **j, k** Total vessel length and average vessel thickness in gelPEG hydrogels and Matrigel. Data is depicted as mean + SD; N=3, n=3

Interconnected endothelial cell networks from healthy human endothelial colony forming cells (ECFCs) were observed in Matrigel after 3 days, whereas similar capillary-like network took longer to be formed in gelPEG hydrogels and was observed after 6 days (**Supplementary Figure 3**). After a 10-day co-culture of healthy human ECFCs and MSCs, highly interconnected vascular-like structures were present throughout all hydrogels (N=3 donor combinations, **Figure 3 a, e**; Suppl. Figure 3 c, f). Quantification of total vessel length and average vessel thickness of 150 μm z-projections revealed comparable network formation in gelPEG and in Matrigel (**Figure 3 j, k**). Also, in both matrices, vascular networks were stabilized by pericyte-like cells as indicated by αSMA staining (**Figure 3 b, f**). Moreover, staining of VE-cadherin junctions in the capillary-like structures highlighted the cell-cell contacts of single endothelial cells, which had fused and remodeled into a further matured vessel (**Figure 3 c, g**) containing lumen (**Figure 3 d, h**). A close-up of the capillaries, showed filopodial extensions indicating active angiogenesis at various sites in the hydrogels (here in gelPEG hydrogel) (**Figure 3 i**).

Development of pre-vascularised bone-like tissue analogues

To further demonstrate the versatility and performance of the novel gelPEG hydrogels, pre-vascularised bone-like tissue analogues were cultured with human MSCs and ECFCs in the novel material and compared to Matrigel. Pre-vascularised tissues can be engineered by using endothelial cells that self-assemble into vascular-like networks ^[20]. Furthermore, in a vascularised bone engineering approach, MSCs play a dual role. Firstly, a part of these multipotent cells will differentiate into pericyte-like cells, which are needed for stabilization and maturation of capillary networks. Secondly, another fraction of MSCs will undergo osteogenesis towards the formation of bone tissue ^[19c, 21].



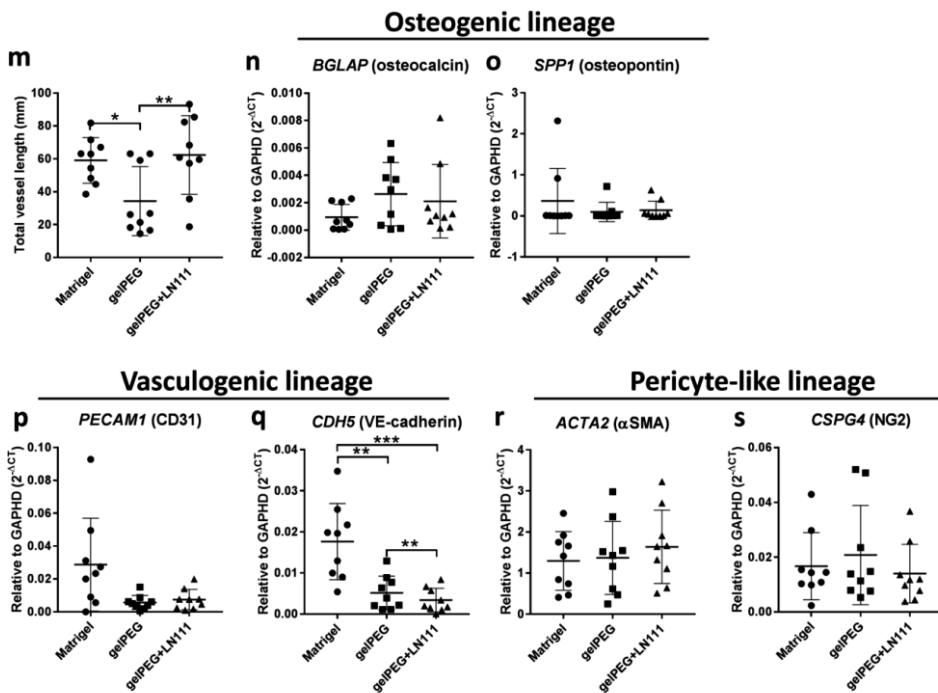


Figure 4. Development of pre-vascularised bone-like tissue analogues in Matrigel and gelPEG-based hydrogels. ECFC-MSC co-cultures were cultured for 2 weeks under osteogenic culture conditions in the different hydrogels before analysis of osteogenesis, vasculogenesis and presence of pericyte-like cells. Expression of *BGLAP* and *SPP1* as osteogenic markers, *CDH5* and *PECAM1* were measured as endothelial markers and *CSPG4* and *ACTA2* as pericyte markers. **a, e, i** Von Kossa staining was positive for gelPEG and gelPEG+LN111 hydrogels highlighting mineralization. **b, f, j** Sections of hydrogels highlighted the presence of the osteogenic marker osteonectin in all groups. **c, g, k** 100 μm z-projections of vascular-like networks (green) in the centre of the hydrogels. **d, h, l** Vascular-like structures, stabilized by αSMA -positive pericyte-like cells (red). **m** Total vessel length was equal in Matrigel and gelPEG+LN111, and significantly longer than in gelPEG hydrogels. **n, o** mRNA expression for osteogenic genes encoding for osteocalcin and osteopontin were comparably expressed in Matrigel, gelPEG and gelPEG+LN111. **p, q** Vasculogenesis-associated genes encoding for CD31 and VE-cadherin were expressed in all hydrogels, with highest VE-cadherin expression in Matrigel, followed by gelPEG and gelPEG+LN111. **r, s** Pericyte-associated genes encoding for αSMA and NG2 were equally expressed in all hydrogels. Data is depicted as mean + SD; $N = 3$, $n = 3$

To increase gelPEG's biological resemblance to Matrigel, one of its major components, laminin 111 (LN111) [6b], was immobilized in the gelPEG networks and taken along in the comparison. After a culture period of 2 weeks under osteogenic conditions, ECFC-MSC co-cultures were analyzed for markers indicating pre-vascularization and osteogenesis. From a macroscopic point of view, gelPEG hydrogels became opaque during the culture period, whereas Matrigel remained rather transparent (**Figure 4**). Matrigel cultures were negative for von Kossa staining, while interestingly, all gelPEG hydrogels were mineralized (Figure 4a, e). Also, gelPEG hydrogels with LN111 showed mineralization in 7 out of 9 constructs, which appeared more homogeneously distributed throughout the hydrogel when compared to pure gelPEG hydrogels (Figure 4i). The majority of cells in co-cultures of all hydrogels were positive for the osteogenic marker osteonectin (Figure 4b, f, j). Late osteogenesis-

related genes encoding for osteocalcin and osteopontin were expressed comparably in all hydrogel systems (Figure 4n, o). Moreover, vasculogenesis was present in all hydrogel compositions as shown in projections of 100 μm in the z-direction (Figure 4c, g, k). The total length of the capillary-like network was comparable between Matrigel and gelPEG+LN111, whereas gelPEG hydrogels had a significantly shorter vascular-like network (Figure 4m). The gene expression levels encoding for CD31 were comparable between all conditions (Figure 3n). However, the gene expression for VE-cadherin was significantly lower in gelPEG and gelPEG+LN111 compared to Matrigel (Figure 4q). The capillary-like networks were supported by αSMA positive pericyte-like cells (Figure 4d, h, l) and pericyte-related genes encoding for αSMA and NG2 had comparable expression levels in all hydrogel compositions (Figure 4r, s).

Notably, Matrigel constructs lost thickness when compared to gelPEG-based constructs as also apparent in paraffin cross-sections of the constructs (Figure 4 a, b, e, f, i, j). At the same time, the diameter of all of the constructs stayed approximately the same (Figure 4, first column).

Development of liver-like tissue analogues

To further assess the biological performance of gelPEG hydrogels for biologically demanding cell cultures, liver organoids were encapsulated in tailored hydrogels and compared to a conventional culture protocol in Matrigel. Since the Matrigel used for this application, typically has a high protein concentration and thus, higher stiffness, in analogy, also gelPEG was used at 3% w/v, to achieve stiffer hydrogels. These hydrogels were further supplemented with LN111, to better resemble Matrigel's composition, or with LN521, since this LN is associated with improved hepatocyte performance ^[22].

H&E staining of liver organoids in the different matrices highlighted cell structures with similar morphology. However, in gelPEG-based hydrogels, the cell nuclei were located more towards the luminal side of the organoid structures (**Figure 5a-d**).

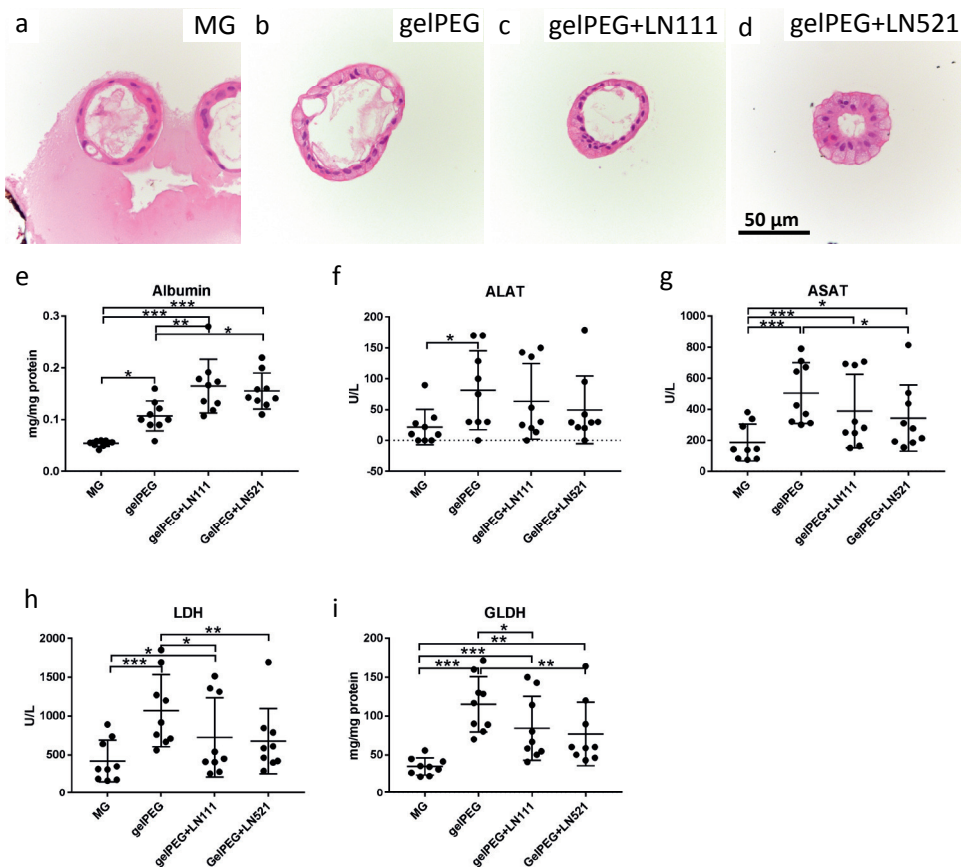


Figure 5. Development of liver-like tissue analogues in Matrigel (MG) and gelPEG-based hydrogels. A functional read-out of protein levels and enzyme activities was performed after 9 day culture of liver organoids. H&E staining of liver organoids in **a** Matrigel, **b** gelPEG, **c** gelPEG+LN111 and **d** gelPEG+LN521. **e** Albumin protein levels in cultured organoid cell lysates. **f, g** ALAT an ASAT enzyme activities of liver organoid cell lysates. **h, i** LDH and GLDH enzyme levels of liver organoid cell lysates. Data is depicted as mean + SD; $N=3$, $n=3$

Functional readout of the liver-like tissue analogues was performed to investigate the quality of the engineered tissue. In terms of albumin production, liver organoids in gelPEG with added laminins performed best, with levels about 2-3 times higher than in Matrigel (Figure 5e). The liver-like tissues in gelPEG produced significantly higher enzyme levels of alanine aminotransferase (ALAT) and aspartate transaminase (ASAT) compared to Matrigel (Figure 5f, g). Lactate dehydrogenase (LDH) and the more liver-specific glutamate dehydrogenase (GLDH) indicate metabolic activity of hepatocytes in the different hydrogels. The same trend as observed for the enzyme levels of ALAT and ASAT could be seen for LDH and GLDH. Again, in Matrigel the levels were lowest compared to gelPEG-based hydrogels (Figure 5h, i). Overall, addition of LN111 or LN521 resulted in intermediate enzyme levels, being higher than in Matrigel (Figure 5). Compared to pure gelPEG hydrogels, overall, the

addition of LN111 did not further enhance the enzyme levels, whereas LN521 had a slightly negative effect.

The metabolic activity as assessed by Alamar Blue (resazurin to resorufin) conversion by hepatocytes was monitored over culture time showing a steep increase from day 1 to day 3. After a culture period of 9 days, the activity was increased by 50% in Matrigel and gelPEG hydrogels, whereas in LN111 and LN521 containing hydrogels, the activity was doubled when compared to day 1 (**Supplementary Figure 4**).

Furthermore, gene expression levels were quantified on day 9. In contrast to the outcomes on protein level, albumin expression levels were highest in Matrigel and gelPEG and lower in gelPEG when LNs were added (**Supplementary Figure 5b**). *KRT7* (CK7), a cytokeratin that is specifically expressed in simple epithelia and can be used to detect bile ducts in the liver^[23], was equally expressed in all hydrogels (Suppl. Figure 5a). The cytochrome family of enzymes CYP2B6, CYP2C19, and CYP3A4, involved in drug metabolism *e.g.*, showed comparable expression levels in Matrigel and gelPEG, whereas with the addition of laminins overall lower expression levels were detected (Suppl. Figure 5d-f). *SLC10A1*, which is encoding for a liver-specific sodium/bile acid cotransporter, was comparably expressed in all hydrogels (Supplementary Figure 5c).

Discussion

In this study, we present a novel, hybrid hydrogel of gelatin and PEG that is easily customized with (native) lysine-containing proteins. The presented tailored hydrogel platform performed as good as Matrigel in terms of 3D vasculogenesis and even outperformed Matrigel when employed for engineering of pre-vascularised bone- or liver-like tissue analogues.

Crosslinking of gelatin and PEG by FXIIIa

The crosslinking strategy that was chosen in the present study was compared to a Matrigel control. The main reason for this was that a direct comparison of the biosynthetic gelPEG platform to pure crosslinked gelatins, such as via microbial transglutaminase or UV crosslinked gelatin methacryloyl (gelMA), is inappropriate. The significant differences in the gelatin concentration, hydrogel stiffness and/or crosslinking density between these systems also affects cell behavior in these materials.

The composition of the herein presented hydrogel-platform is based on a transglutaminase-catalyzed crosslinking mechanism (factor XIIIa), which was adopted from the blood coagulation cascade. The elegant strategy to make use of the recognition sequences of this enzyme for immobilizing instructive peptides in hydrogels was developed by Hubbell and colleagues at the end of the 1990s^[24]. Subsequently, this mechanism was exploited for crosslinking entirely synthetic PEG hydrogels under physiological conditions^[25]. In this approach, two PEG precursors,

one with a glutamine-containing sequence and one with a lysine-containing sequence, served as substrates for factor XIIIa to be coupled.

In the present work, we replaced PEG-Lys with gelatin, which natively contains lysine residues that can serve as a donor substrate without any further modifications. We hypothesized that by using a material with inherent cell-responsive elements, a close mimic of the natural environment of cells could be created. In fact, gelatin is a denatured form of collagen, the most abundant protein in the human body.

The crosslinking agent FXIIIa is an FDA- approved drug for treating patients with a blood coagulation disorder (trade names are Cluvot, CSL Behring; NovoThirteen, Novo Nordisk). These drug formulations of the enzyme are designed for injection into the blood stream. When applied in the gelPEG system, any potentially remaining activity of FXIIIa could be inactivated by plasmin prior to use for implantation purposes ^[26]. Combined, this convincingly highlights the safety of FXIII for hydrogel crosslinking. While PEG is a synthetic polymer, which is on the market for medicinal products ^[27], its conjugated derivatives containing peptides remain to be translated towards the clinics. Furthermore, the incorporated laminins are recombinant and xenogen-free.

Modular approach to integrate non-modified proteins in hydrogels

Hybrid hydrogels that integrate synthetic and biologic materials such as ECM-derived materials, are a promising way for synthesizing next generation hydrogels ^[28]. Therefore, the approach of immobilizing ECM-derived proteins in synthetic materials was undertaken by several groups ^[29]. Such systems present a merger of both, biological complexity in a physico-chemically controllable matrix. These previous modules of PEG platforms could only accommodate incorporation of ECM molecules of interest after their chemical or biological modification. While being elegant, it can be a laborious approach to modify all proteins of interest ^[30]. Therefore, the here taken approach of immobilizing unmodified proteins for tissue specificity presents a simpler hydrogel-platform. Laminins were chosen in this study as model proteins to demonstrate retention of bioactivity after incorporation in gelPEG. Additionally, laminins represent the most abundant protein in Matrigel. The successful incorporation illustrates the flexibility of the platform as tissue-specific isoforms can be used for tailoring the platform's accommodation of various cell types.

Characteristics of gelPEG hydrogels

Optimization of the hydrogel composition revealed the best ratio between gelatin and PEG to be between 2:1 and 4:1 to form most effective hydrogels with low swelling ratio and sol fraction. Increasing the gelatin over PEG concentration still led to reasonable hydrogel formation, an increase of PEG immediately impaired hydrogel formation. This indicates that the availability of lysine residues is the limiting factor in the reaction.

For this study we chose a 4:1 ratio, for which a relatively higher gelatin to PEG concentration ratio was the most ideal. By doing so, less steric hindrance from PEG is expected, which, in contrast to gelatin, cannot be further broken down and replaced by secreted ECM from encapsulated cells. However, the ratio might be further fine-tuned towards a 1:1 Gln:Lys molar ratio, to match the degradation of the hydrogel with the speed of matrix deposition of a specific tissue type of interest. In fact, it was shown previously that degradation of hybrid hydrogels can be further slowed down by the addition of a synthetic polymer ^[31]. While for vasculogenic and osteogenic co-cultures, gelPEG hydrogels roughly retained their initial volume over culture time, this was not the case for Matrigel-based co-cultures. Also, Matrigel constructs of liver organoid cultures appeared very unstable after a culture period of 9 days, which was less apparent in gelPEG hydrogels. For further fine-tuning towards up-scaled, clinically relevant approaches for liver organoids, it might be therefore suggested to slightly increase either the total polymer or PEG-Gln concentration.

Matrigel has a low and highly variable elastic modulus, ranging from approximately 0.4 to 3 kPa ^[32]. The 2% gelPEG hydrogels with a compressive modulus of $2.6 \text{ kPa} \pm 0.6$ were the closest possible (low protein content) Matrigel mimics from a mechanical point of view that could be created. This comparable stiffness of the materials rules out its potential role as effector of the observed cell behavior.

Vasculogenesis in gelPEG matrices

Clinically relevant-sized tissue analogues generally require a pre-vascular network before implantation. The presence of such an engineered capillary-like network throughout the construct can accelerate the connection with the patients' own vasculature, which is critical for implant survival ^[33]. Especially Matrigel is known for its proangiogenic properties that allow for the fast formation of a vascular-like network. Due to this reason it is an often used, highly potent material for vasculogenesis/angiogenesis-related assays ^[11,34].

Pre-vascular network development over time by human ECFCs was initially favoured in Matrigel compared to gelPEG. A thickening of capillary-like structures might indicate further maturation (i.e., arteriogenesis) ^[35]. In the current study, maturity of the networks was shown by the presence of stabilized capillary-like structures and by the presence of lumen. The initial difference in performance between Matrigel and gelPEG might be explained by the proangiogenic properties of Matrigel, which are mediated by proteins such as collagen type IV and LN111 ^[9,36] that might enable faster vasculogenesis. This assumption is supported by the present work where addition of LN111 to osteogenic cultures resulted in improved vascular structure formation. All in all, the gelPEG hydrogel performed equally well as the gold standard Matrigel in terms of long-term pre-vascularization, both in extent and in maturity.

Engineering pre-vascularised bone-like tissue analogues

Following, a bone-like construct was engineered as a model tissue, which requires simultaneous development of a pre-vascular network during bone forming. Early osteogenic differentiation on the protein level of all hydrogel constructs was shown by the presence of osteonectin. Comparable gene expression levels for osteopontin and osteocalcin indicated a comparable extent of osteogenic differentiation in all conditions. However, mineralization, a late phenomenon during osteogenesis, was only present in gelPEG-based hydrogels. While it is known from literature that osteogenesis is supported by Matrigel^[37], the presence of mineralization becomes generally prevalent after 21 days of culture^[38]. Therefore, the absence of mineralization in MG after 14 day culture is in agreement with literature. Whereas 9 out of 9 gelPEG hydrogels were characterized by mineralization after only 14 days, 7 out of 9 gelPEG+LN111 hydrogels were positive for von Kossa staining. Pure gelPEG hydrogels strongly supported early matrix mineralization, which can be explained by the gelatin extraction method. Gelatin is characterized by nucleation sites. Especially, anionic gelatin (obtained by alkaline extraction) enables pronounced calcium binding of the matrix due to its negative charge at physiological pH^[39]. Therefore, due to the nature of the gelatin in gelPEG hydrogels, the matrix is especially favorable as a template for bone development.

The addition of LN111 to gelPEG hydrogels led to an enhanced and more homogenous distribution of minerals throughout the matrix. At the same time, vasculogenesis was stimulated as indicated by a significantly longer vascular network length. LN111 was shown to enhance vasculogenesis, which corresponds to literature^[9]. The influence of LN111 on osteogenesis, especially on mineralization via inducing calcium phosphate precipitation, was established in previous studies^[40]. Together, gelPEG hydrogels appeared as suitable templates for bone development, in which bioactives can enhance tissue development. Specifically, LN111 can be a potent stimulator of vasculogenesis in these constructs. Further fine-tuning of the LN111 concentration, all or not combined with additional factors, might help to optimize the balance between enhanced vasculogenesis and robust mineralization of all hydrogel constructs.

VE-cadherin is an endothelial cell-cell contact marker^[41] and has a key role in endothelial barrier function and angiogenesis^[42]. While the highest VE-cadherin expression is apparent in Matrigel, it might be plausible that downregulation of VE-cadherin in both gelPEG groups was a result of a more complete maturation status of the cells in the pre-vascular structures, supported by the apparent staining of CD31 and α SMA.

In contrast to purely vasculogenic cultures, vasculo-osteogenic cultures resulted in significantly lower vascular network length in pure gelPEG hydrogels compared to Matrigel. This difference can be explained by the added medium. For the osteogenic differentiation with simultaneous vasculogenesis, osteogenic medium was used instead of vasculogenic medium. Thus, in this condition, ECFCs obtain vasculogenic signals from the embedded MSCs^[43] and not from the medium. Therefore, when

the vasculogenic stimulation is not induced by the culture medium, adequate vascularization can be achieved by incorporation of LN111 in the hydrogel.

The novel gelPEG hydrogel platform allowed for the successful engineering of pre-vascularised bone-like tissue analogues. Due to the faster osteogenic differentiation while maintaining simultaneous vasculogenesis, gelPEG hydrogels even outperformed Matrigel for engineering of pre-vascularised bone-like constructs.

Engineering liver-like tissue analogues

GelPEG was tested with hepatic organoids ^[44] to evaluate the potential in comparison to the gold standard, Matrigel. Overall, the addition of LN111 or LN521 did not show a beneficial effect over pure gelPEG hydrogels, apart from albumin expression. However, compared to Matrigel, gelPEG with added laminins improved liver organoid differentiation as shown by elevated albumin expression and both ALAT and ASAT activity levels. This positive effect of LN521 ^[22] and in a mix with LN111, was described previously where efficient hepatocyte differentiation and self-organization occurred on laminin-coated surfaces on pluripotent stem cells ^[22a]. Especially with respect to metabolic function and self-organization of hepatocytes, LN coatings outperformed a Matrigel control. The minor negative effect of the addition of LN521 on hepatic enzymes and CYP-expression compared to gelPEG alone is in contrast with reports by others ^[22]. Since the addition of the LN521 in the pluripotent stem cells is already at the endodermal differentiation stage, this indicates that the effect is not as profound on hepatic organoids which are considered a more mature stem cell type ^[45].

Furthermore, hepatocyte metabolic activity was strongly affected in the different hydrogel compositions. From day 1 until day 3 the cell activity doubled in Matrigel and gelPEG hydrogels, and increased 3.5 and 6 times in hydrogels laden with LN111 and LN521, respectively. This increase in metabolic activity might correlate with cell proliferation. It has been shown that laminins are supporting survival and proliferation of multiple cell types. This strong increase in metabolic activity in gelPEG hydrogels compared to Matrigel in the beginning of the culture period might be due to enhanced proliferation, stimulated by the comparably stiff gelPEG hydrogels. It was shown by Gjorevski *et al.*, that a higher matrix stiffness in PEG hydrogels was associated with intestinal stem cell proliferation, whereas softer hydrogels were needed for cell differentiation ^[13a]. The authors also demonstrated that matrix-metalloproteinase (MMP)-sensitive PEG hydrogels (with RDG-sites) could not be degraded fast enough by the cells to allow for organoid differentiation after an initial proliferation phase. Consequently, they added a hydrolytically degradable polymer to the PEG platform to speed up the degradation process after an initial proliferation phase. In the present hydrogel system, combining gelatin and PEG, this cell-mediated degradation and remodeling of the matrix might naturally occur. After reaching a higher cell number during the initial proliferation phase, secreted MMPs might speed up the degradation process, resulting in a softer hydrogel, suitable for cell differentiation. This assumption can be supported by

the fact that after the initial 3 days the metabolic activity gradually dropped in all hydrogel compositions, which might indicate a phase of cell differentiation.

Furthermore, it was shown recently that natural matrices were characterized by fast stress relaxation properties, a feature that synthetic hydrogels are typically missing and which appeared to be critical in guiding cell differentiation ^[46]. By using hybrid hydrogels as presented here, this natural characteristic of the extracellular matrix might be present and could have contributed to the permission of multiple cell differentiation into the vasculogenic, osteogenic and hepatocyte lineages.

The use of gelPEG hydrogels was demonstrated here for the biological suitability as extracellular matrix of multiple tissue engineering approaches. In the future, gelPEG might also be used as a “bioink” for biofabrication processes due to its fast crosslinking ^[47]. In combination with reinforcing materials, such as offered by thermoplastics ^[48], complex and multi-tissue type tissue analogues might be realized. Furthermore, these complex biofabricated tissue constructs might be characterized by a multiscale vascular tree consisting of engineered macrovessels and self-assembled capillary-like structures ^[21b] throughout the construct.

Outlook

This research demonstrates that a simple hydrogel composed of gelatin and PEG can replace and even outperform Matrigel for complex, long-term tissue engineering approaches. With this, a clinically-relevant, degradable biomaterial was developed, which can efficiently support cell differentiation and matrix secretion towards the development of functional tissue analogues. Moreover, this novel gelPEG platform is easily tailorable with (combinations of) lysine-containing proteins to establish a tissue-specific matrix; illustrated here by addition of tissue-specific laminins. Additional ECM-mimicking cues can prove valuable to create spatial resolution in a hydrogel when aiming at multiple tissue types within one biomaterial, sharing one culture medium.

The presented hybrid hydrogel can be readily applied to other tissue engineering approaches by fine-tuning the ratio between gelatin and PEG, the total polymer concentration and by covalently immobilizing relevant proteins to further stimulate tissue development. Taken together, we suggest that such hybrid hydrogels consisting of PEG-Gln and a relevant biologic material, catalyzed by FXIIIa, will help to overcome the biomaterial-associated bottleneck of implementing complex tissue engineering in the clinics.

Experimental Section

Materials

Alkaline treated porcine skin gelatin (beMatrix™ LS-H high bloom, Nitta Gelatin NA Inc) with an endotoxin count less than 10 endotoxin units (EU) g⁻¹ was used. The gelatin was set to a pH of 7.5, sterile filtered and freeze dried. The peptide was purchased from NeoMPS (Strasbourg, France). Eight-arm PEG-vinyl sulfone (8-PEG-VS, mol wt. 40kDa) was obtained from NOF Europe (Grobendonk, Belgium).

Synthesis of PEG-Gln macromeres

PEG-Gln was synthesized and characterized as described previously [25, 49]. In brief, a glutamine acceptor substrate (H-NQEQVSPL-ERCG-NH₂, TG-Gln) was used. The NQEQVSPL cassette corresponds to a substrate site of FXIII in a α 2-plasmin inhibitor [24b] and the ERCG cassette contains a cysteine that can react with VS [50]. This TG-Gln substrate was coupled to 8-PEG-VS via Michael-type addition at a 1.2-fold molar excess of TG-Gln to PEG-VS in 0.3 M triethanolamine (pH 8.0) at 37°C for 2 h. The reaction product was dialyzed, freeze dried and PEG-Gln conjugation was confirmed by ¹H NMR.

Formation of gelatin-PEG hydrogels

Factor XIII (200 U mL⁻¹, Cluvot, CSL Behring) was activated with 20 U mL⁻¹ thrombin (Baxter) in the presence of 2.5 mM CaCl₂ for 15 minutes at 37°C and stored at -80°C in small aliquots (FXIIIa). Hydrogel formulations consisting of different ratios of PEG-Gln and gelatin were formulated in tris-buffered saline (TBS, pH 7.6, 40 mM) containing 50 mM calcium chloride. Hydrogel cross-linking was initiated upon addition of 10 U mL⁻¹ factor XIIIa. For biomaterial characterizations, disc-shaped hydrogels with 8 mm diameter were prepared in a silicone sheet with 1 mm height (BioPlexus Corporation). The reaction mixture was left to crosslink for 1 h in a humidified incubator when covalent crosslinks were formed between native lysines of gelatin or extracellular matrix-derived proteins and the Gln-conjugates on PEG (Figure 1).

Hydrogel mass loss and swelling analysis

GelPEG hydrogels were prepared in various lysine (Lys) and Gln molar ratios (Lys:Gln) ranging from 1:1 to 6:1 for a 3% w/v total polymer concentration and swelling analysis was performed. Furthermore, gelPEG hydrogels were prepared at a polymer concentration of 1 and 2% w/v at a ratio of 4:1. All hydrogels were characterized by means of swelling and mass loss studies, as described previously [51] for *n* = 5 technical replicates. In brief, immediately after crosslinking, the wet weight of the hydrogels was measured ($m_{\text{initial}, t=0}$). Per experimental group, 10 gels were prepared, from which 5 were directly frozen, lyophilized and weighed ($m_{\text{dry}, t=0}$) and the other 5 were incubated in TBS for 24 h at 37°C before the wet weight (m_{swollen}) and the dry weight were determined ($m_{\text{dry}, t=1}$). The sol fraction describes the polymer concentration that is not crosslinked into the network and is therefore lost

during hydrogel swelling. The hydrogel swelling ratio (q) and the sol fraction were calculated according to the following equations (1-4) ^[52]:

$$\text{Actual macromer fraction} = \frac{m_{\text{dry}, t=0}}{m_{\text{initial}, t=0}} \quad (1)$$

$$m_{\text{initial,dry}} = m_{\text{initial,t=0}} \times \text{actual macromer fraction} \quad (2)$$

$$\text{sol fraction} = \frac{m_{\text{initial,dry}} - m_{\text{dry,t=1}}}{m_{\text{initial,dry}}} \times 100\% \quad (3)$$

$$q = \frac{m_{\text{swollen}}}{m_{\text{dry}, t=1}} \quad (4)$$

Rheological analysis of hydrogel formation

The crosslinking of gelPEG hydrogels at 2% w/v and 4:1 ratio by 10 U mL⁻¹ FXIIIa was investigated ($n=3$). An AR G-2 rheometer (TA-Instruments, The Netherlands) was used with the software TA Instruments Trios V4.3.0.38388. The testing was performed at 0.1% strain and 1 Hz continuous oscillation at 37°C for 30 minutes under a humidified atmosphere. The point of gelation of the reactions was measured by recording the time when the shear storage modulus (G') was equal to the shear loss modulus (G'') by analyzing $\tan \delta = G''/G'$. $n=3$ independent measurements were performed.

Mechanical properties of swollen hydrogels

The elastic modulus of the hydrogels was determined after equilibration for 24 h in PBS at 37°C. By means of a Dynamic mechanical analyzer (DMA 2980, TA instruments), compression was applied between -20%/min and -30% at room temperature (RT). The Elastic modulus was based on the slope from the linear region of the stress-strain curve of a strain range between 5-10% ($n=5$ technical replicates).

Coupling of laminins into gelPEG hydrogels

To investigate the coupling of lysine containing proteins into the gelPEG hydrogel network, laminin 521 (Biolamina, Sweden) served as a model protein. Laminin 521 (LN) was added at a concentration of 10 $\mu\text{g mL}^{-1}$ to the reaction mixture of 3% w/v 4:1 gelPEG in TBS ($n=5$ technical replicates). Hydrogels without LN served as a control ($n=5$ technical replicates). Hydrogel discs (~1x 5 mm) of 20 μL volume were incubated for 24 h at 37°C in TBS. All hydrogels were washed and fixed in 4% formalin and stained with a primary anti-LN $\alpha 5$ antibody (1:260, clone 4C7, MAB1924, Merck), followed by a goat-anti-mouse antibody Alexa Fluor 546 (4 $\mu\text{g mL}^{-1}$, A-11003, Thermofisher). Imaging of control and LN-laden hydrogels occurred with a fluorescence microscope (BX51, Olympus).

Cell isolation, culture and characterization

Multipotent mesenchymal stromal cells (MSCs) were derived from human bone marrow aspirates from the iliac crest of 3 patients after ethical approval and informed consent (University Medical Center Utrecht, 08-001-K). The white mononuclear cell (MNC) fraction was separated via density gradient centrifugation on Ficoll-paque™ PLUS (1.077 g mL⁻¹, GE healthcare). The collected cells were expanded in expansion

medium, composed of α -MEM (Gibco), 10% v/v heat-inactivated fetal bovine serum (FBS, Lonza), 100 U mL⁻¹ penicillin, 10 mg mL⁻¹ streptomycin (Gibco), 0.2 mM L-ascorbic acid-2-phosphate (ASAP, Sigma) and 1 ng mL⁻¹ basic fibroblast growth factor (bFGF, 233-FB R&D Systems), at 37°C/5.0% CO₂. MSCs were identified by their capacity to undergo differentiation towards the osteo-, adipo-, and chondrogenic lineages. Furthermore, FACS characterization of the MSCs was performed showing absence of the hematopoietic markers CD14 (RPA-M1, FITC-conjugated, Abcam), CD34 (4H11, AP-conjugated, Abcam), CD45 (MEM-28, PE-conjugated, Abcam) and CD79a (HM47, PE-conjugated, Abcam) and presence of the established MSC-like markers CD90 (5E10, FITC-conjugated, Abcam), CD105 (MEM-226, AP-conjugated, Abcam) and CD73 (AD2, PE-conjugated, Abcam). Cells were used up to passage 4.

Human endothelial colony forming cells (ECFCs) were derived from 3 human umbilical cord blood donors after caesarean sections according to the local ethical guidelines (University Medical Center Utrecht, METC 01-230/K). The obtained cord blood was diluted 1:1 with PBS 2mM EDTA before density gradient centrifugation on Ficoll-paque. The harvested cells were cultured on rat collagen type I (Corning) at a seeding density of 10-20 x10⁶ cells cm⁻². Endothelial growth medium-2 (EGM-2) was composed of endothelial basal medium-2 (EBM, Lonza), 10% v/v FBS, 100 U mL⁻¹ penicillin, 10 mg mL⁻¹ streptomycin and EGM-2 singlequots (Lonza). During the first 7 days after isolation, the medium was refreshed daily. Colonies with cobblestone-like morphology were picked after 14-21 days and were further expanded. ECFCs were characterized by FACS where they were positive for CD105 and CD31 (TLD-3A12, FITC-conjugated, Abcam), partially positive for CD34 and CD309 (VEGFR/KDR, PE-conjugated, MACS Miltenyi Biotech) and negative for CD45, CD14, and CD133 (AC133-VioBright, FITC-conjugated, Miltenyi Biotech). ECFCs were used up to passage 10. Furthermore, ECFCs were transduced with green fluorescent protein (GFP) in a pHAGE-2 vector with a human EF-1 α promoter as described previously [21b].

Human liver organoid cultures were generated from three donors from surplus material of donor livers used for liver transplantations performed at the Erasmus Medical Centre Rotterdam (courtesy of Dr. Luc van der Laan, approved by the Medical Ethical Council of the Erasmus MC) [45]. The organoids were grown in Matrigel in Expansion Medium (EM), as previously described by Huch *et al.* [45]. 7 to 5 days prior to differentiation towards hepatocyte-like cells the EM was supplemented with 25 ng mL⁻¹ BMP-7 (Peprotech, London, UK). At day 0, the organoids were passaged with a split rate of 1:1 and reseeded in 3% w/v 4:1 gelPEG or Matrigel (Corning, 354230, Growth Factor Reduced Basement Membrane Matrix). Differentiation medium (DM) containing advanced DMEM/F12 (Gibco, Dublin, Ireland) supplemented with 1% v/v Penicillin-Streptomycin (Thermo Fisher Scientific, Waltham, MA, USA), 1% v/v N2, 1% v/v B27, 10 mM HEPES, 1% v/v Glutamax, 50 ng mL⁻¹ EGF (all from Invitrogen, Carlsbad, CA, USA), 1.25 mM N-acetyl cysteine (Sigma-Aldrich, St Louis, MO, USA), 5 μ M A83-01 (Tocris Bioscience, Bristol, UK), 25 ng mL⁻¹ HGF, 10 nM Gastrin, 25 ng mL⁻¹ BMP7 (all from Peprotech), 10 μ M DAPT (γ -secretase inhibitor, Selleckchem, Houston, TX, USA), 100 ng mL⁻¹ FGF19

(R&D Systems, Minneapolis, MN, USA) and 30 μM dexamethasone (Sigma-Aldrich) was added freshly every other day until the samples were collected (day 9).

MSC-ECFC co-culture in hydrogels

MSCs and ECFCs were co-encapsulated in gelPEG (2% w/v 1:4) hydrogels or Matrigel (Corning, 354230, Growth Factor Reduced Basement Membrane Matrix) reaching a final seeding density of 5×10^6 MSCs and 1.25×10^6 ECFCs per ml gel. Besides CaCl_2 , TBS and FXIIIa, the reaction mixture contained 20% of cell culture medium. Furthermore, co-cultures were encapsulated in Matrigel which was 1:1 diluted with TBS including 20% of cell culture medium.

For vasculogenic cultures, GFP-labelled ECFCs were used. For each condition, 3 hydrogel droplets of 75 μL each were placed in the center of wells in a 12-well plate. To track formation of capillary-like structures over culture time, hydrogels were imaged on days 2 and 6 using an inverted fluorescence microscope (IX53 Inverted Fluorescence Microscope, Olympus). Hydrogels were cultured in EGM-2 for 10 days, fixed in formalin and cut in 3 pieces for different stainings. MSCs from 3 different donors were combined with GFP-ECFCs from 1 donor ($N=3$ different donors, $n=3$ technical replicates).

To induce osteogenesis and simultaneous vasculogenesis, hydrogels were prepared as for vasculogenic cultures. MSC-ECFC co-cultures in gelPEG and in gelPEG combined with 10 $\mu\text{g mL}^{-1}$ laminin 111 were compared to cultures in Matrigel. The co-cultures were cultured in osteogenic differentiation medium (ODM) for 2 weeks. ODM was composed of α -MEM, 10% FBS, 100 U mL^{-1} penicillin, 10 mg mL^{-1} streptomycin, 10 mM β -Glycerolphosphate (Sigma) and 10 nM dexamethasone (Sigma). 6 hydrogels per condition were prepared, of which 3 were used for qPCR analysis and 3 were fixed, cut and used for paraffin embedding and whole mount fluorescent stainings. All experiments were performed with 3 MSC-ECFC combinations from different donors ($N=3$, $n=3$).

Liver organoid culture in hydrogels

Liver organoids from three different donors were encapsulated in Growth factor reduced Matrigel (456231, Corning, New York, NY, USA), 3% w/v 1:4 gelPEG, gelPEG with 10 $\mu\text{g/ml}$ LN111 or gelPEG with 10 $\mu\text{g/ml}$ LN521. The gelPEG-cell mixture contained 20% medium, whereas Matrigel was used undiluted. Hydrogel droplets with a volume of 40 μL were placed in the center of culture wells and DM media was added. On day 1, 3, 6, and 9 of differentiation the viability of the organoids was measured with an Alamar Blue assay according to the manufacturer's guide (Invitrogen). 9 days after differentiation samples were collected for gene-expression profiling and enzyme measurements. For gene-expression profiling, organoids were lysed with 350 μl RLT (Qiagen, Hilden, Germany) and stored at -20°C until further analysis. For enzyme measurements, organoids were lysed in Milli-Q water (Merck Millipore) at -20°C until analysis. ALAT, ASAT, LDH, GLDH, albumin and total protein were measured using the AU680 Beckman (Beckman Coulter, Brea, CA, USA) standard protocols, and values were corrected for total protein levels ($N=3$, $n=3$).

mRNA isolation, cDNA synthesis and qPCR analysis

After culture, cell-containing hydrogels were digested using 2 mg mL⁻¹ collagenase A (Roche) for 10 minutes at 37°C. The MSC-ECFC-containing pellet was then homogenized in TRIzol reagent (Thermo Fisher Scientific) and messenger RNA (mRNA) was isolated from the aqueous phase. Potential DNA contamination was removed by a DNase treatment (Turbo DNase; Thermo Fisher) according to the manufacturer's instructions. The organoids were lysed with 350 µl RLT (Qiagen, Hilden, Germany) complemented with 1% v/v 2-Mercaptoethanol (Sigma-Aldrich), and mRNA was isolated using the RNeasy micro-kit (Qiagen), following the manufacturer's guide. The total extracted amount of mRNA was quantified with a NanoDrop ND-1000 spectrophotometer (Thermo Fisher Scientific) at 260/280 nm. Complementary DNA (cDNA) was synthesized from 1 µg mRNA using the iScript cDNA Synthesis Kit (BioRad, Hercules, USA) according to the manufacturer's instructions. qPCR analysis was executed with a Bio-Rad CFX96 Real-Time PCR Detection System (BioRad) using FastStart SYBR Green Master mix (SigmaAldrich) and an input of 20 ng cDNA per reaction. Primers used for qPCR analysis are listed in Suppl. table 1. The amplification efficiency of the used primers was all between 0.9 and 1.1 and the relative expression was determined by the 2^{-ΔCT} formula.

For liver organoid cultures, the same protocol was followed using a Bio-Rad CFX384 Real-Time Detection System and an input of 10 ng cDNA per reaction. A housekeeping index was calculated based on a previously published formula based on GAPDH and YWHAZ^[53].

Whole mount fluorescent stainings

Prior to immunofluorescent stainings, the hydrogel constructs were permeabilized with 0.2% triton-X in PBS for 30 minutes and blocked in 5% BSA/PBS for 30 minutes. Capillary-like structures in the hydrogels were investigated by CD31 staining (5.1 µg mL⁻¹, M0823, Dako), secondary sheep anti-mouse biotinylated antibody (1:200, RPN1001v1, GE Healthcare) and tertiary streptavidin Alexa Fluor 488 conjugate (5.0 µg mL⁻¹, S32354, Invitrogen). In vasculogenic co-cultures, ECFCs with the GFP label were not stained for CD31. The endothelial phenotype was confirmed by a rabbit anti-vascular endothelial cadherin antibody (VE-cad, 1:250, D87F2, Cell Signalling Technology) which was combined with a secondary donkey-anti-rabbit Alexa 647 antibody (5 µg mL⁻¹, ab150075, Abcam). Stabilising cells of the capillary-like structures were identified by a mouse monoclonal Cy3-conjugated αSMA antibody (1:300 µg mL⁻¹, Clone 1A4, C6198 Sigma Aldrich). Furthermore, 4,6-diamidino-2-phenylindole (DAPI, 100 ng mL⁻¹, Sigma) was used to stain cell nuclei. The hydrogels were imaged with a confocal microscope (SP8x Leica, DMi8, Leica).

Immunohistochemistry

Fixed osteogenically differentiated hydrogels were dehydrated in graded ethanol series. After clearance in xylene, the hydrogels were embedded in paraffin and sectioned into 5 μm slices. An osteonectin staining was performed after deparaffinization and rehydration before endogenous peroxidase was blocked in 0.3 % H_2O_2 . Citrate buffer (pH 6) was used for antigen retrieval at 80°C for 20 minutes. The primary antibody for osteonectin (4.2 $\mu\text{g mL}^{-1}$, AON-1, deposited to the DSHB by Termine, J.D.; DSHB Hybridoma Product AON-1 [54]) was incubated for 1 h, followed by a horseradish peroxidase–conjugated anti-mouse antibody (Envision + system-HRP labelled polymer, K4000 Dako). Detection of osteonectin occurred by conversion of 3,3'-diaminobenzidine solution (SK-4100, Vector) with counterstain for nuclei by hematoxylin (Merck). Concentration-matched isotype controls were performed using a mouse IgG1 monoclonal antibody (Thermofisher Scientific).

A von Kossa staining was performed to detect mineralization of the osteogenically differentiated co-cultures. After deparaffinization and rehydration, the samples were incubated with 1% silver nitrate solution (Fisher Scientific) under a light bulb for 1 h. Unreacted silver was removed by rinsing with 5% sodium thiosulfate (Alfa Aesar GmbH) for 5 minutes. Nuclear counterstaining was performed with hematoxylin.

The organoid-containing hydrogels were digested using 2 mg/ml collagenase A (Roche) for 10 minutes at 37°C. The organoids were fixed in 10% neutral buffered formalin, embedded in paraffin and sections of 4 μm were cut. H&E staining (Merck KGaA, Darmstadt, Germany) was routinely performed. Imaging was performed using an Olympus microscope (CKX41) in combination with a Leica DFC425C camera.

Image analysis

Hydrogels of vasculogenically differentiated cultures (GFP-ECFCs), were imaged at the thickest part of the hydrogel (center) on a confocal microscope (SP8x Leica, DMi8). Projections of 150 μm z-stacks were made (one stack per hydrogel, $n=9$ stacks per condition), which were adapted in contrast and intensity with ImageJ 1.51a before batch-processing of the images. Angioquant software [55] was used to analyse the vascular networks' total vessel length as well as average thickness of vessels by dividing the total vessel area by the total vessel length. For osteogenic co-cultures, 100 μm z-stacks were made, processed in ImageJ and the total vessel length was quantified with Angioquant ($n=9$ projections per condition).

Statistics

For mass loss studies, a one-way ANOVA was performed with a Tukey HSD *post hoc* analysis using Graphpad prism 7.02. For the compressive moduli, significance was determined by a Student's t-test in Graphpad prism 7.02. For osteogenic and hepatic cell cultures, MS Excel 2010 (Microsoft, Redmond, USA) was used for calculations and PASW Statistics 22.0 (SPSS Inc. Chicago, USA) for statistical analysis. To take into account donor variations, a mixed linear model (after logtransformation for osteogenically differentiated constructs) was conducted followed by a Bonferroni's

post hoc test to compare gene expressions between the tested hydrogel types. In the model, the hydrogel type was considered as a fixed factor, while the cell donors were considered as random factors ($n=3$ gels per group). Differences were considered statistically significant for $p < 0.05$ and the Bonferroni corrected p-values are depicted in the figures. Asterisks represent statistical significances according to p-values (* $p < 0.05$; ** $p < 0.01$; *** $p < 0.001$), N refers to the number of independent experiments (with different cell donors) and n refers to the technical replicates.

Acknowledgements

The authors are grateful to Mies van Steenberghe who gave support with rheological and compressive measurements at Pharmaceutical Sciences, Utrecht University. Further, Chris van Dijk (RMCU) is acknowledged for help with transduction of ECFCs with GFP. The authors acknowledge Mattie van Rijen (RMCU) for his contributions to histological stainings. This research project was partially funded by the European Union FP7-MC-IRSES 'SkelGEN' project under grant agreement n° 318553 and the European Research Council (ERC) (3D-JOINT, #647426). KL wishes to acknowledge funding by New Zealand Health Research Council Emerging Researcher First Grant (15/483).

References

1. I. V. Yannas, E. Lee, D. P. Orgill, E. M. Skrabut, G. F. Murphy, *Proc Natl Acad Sci U S A* **1989**, *86*, 933.
2. a) D. Saris, A. Price, W. Widuchowski, M. Bertrand-Marchand, J. Caron, J. O. Drogset, P. Emans, A. Podskubka, A. Tsuchida, S. Kili, D. Levine, M. Brittberg, S. s. group, *Am J Sports Med* **2014**, *42*, 1384; b) E. Basad, B. Ishaque, G. Bachmann, H. Sturz, J. Steinmeyer, *Knee Surg Sports Traumatol Arthrosc* **2010**, *18*, 519.
3. A. Atala, S. B. Bauer, S. Soker, J. J. Yoo, A. B. Retik, *Lancet* **2006**, *367*, 1241.
4. a) A. Shafiee, A. Atala, *Annu Rev Med* **2017**, *68*, 29; b) A. Jaklenec, A. Stamp, E. Deweerd, A. Sherwin, R. Langer, *Tissue Eng Part B Rev* **2012**, *18*, 155; c) J. Rouwkema, A. Khademhosseini, *Trends Biotechnol* **2016**, *34*, 733.
5. A. Fatehullah, S. H. Tan, N. Barker, *Nat Cell Biol* **2016**, *18*, 246.
6. a) L. G. Villa-Diaz, A. M. Ross, J. Lahann, P. H. Krebsbach, *Stem Cells* **2013**, *31*, 1; b) H. K. Kleinman, G. R. Martin, *Semin Cancer Biol* **2005**, *15*, 378.
7. C. S. Hughes, L. M. Postovit, G. A. Lajoie, *Proteomics* **2010**, *10*, 1886.
8. X. L. Yin, B. E. Mead, H. Safaee, R. Langer, J. M. Karp, O. Levy, *Cell Stem Cell* **2016**, *18*, 25.
9. Y. Kubota, H. K. Kleinman, G. R. Martin, T. J. Lawley, *J Cell Biol* **1988**, *107*, 1589.
10. E. Polykandriotis, A. Arkudas, R. E. Horch, U. Kneser, *Am J Pathol* **2008**, *172*, 1441.
11. G. Benton, I. Arnaoutova, J. George, H. K. Kleinman, J. Koblinski, *Adv Drug Deliv Rev* **2014**, *79-80*, 3.
12. K. Schneeberger, B. Spee, P. Costa, N. Sachs, H. Clevers, J. Malda, *Biofabrication* **2017**, *9*, 013001.
13. a) N. Gjorevski, N. Sachs, A. Manfrin, S. Giger, M. E. Bragina, P. Ordonez-Moran, H. Clevers, M. P. Lutolf, *Nature* **2016**, *539*, 560; b) E. H. Nguyen, W. T. Daly, N. N. T. Le, M. Farnoodian, D. G. Belair, M. P. Schwartz, C. S. Lebakken, G. E. Ananiev, M. A. Saghiri, T. B. Knudsen, N. Sheibani, W. L. Murphy, *Nature Biomedical Engineering* **2017**, *1*; c) R. Cruz-Acuna, M. Quiros, A. E. Farkas, P. H. Dedhia, S. Huang, D. Siuda, V. Garcia-Hernandez, A. J. Miller, J. R. Spence, A. Nusrat, A. J. Garcia, *Nat Cell Biol* **2017**, *19*, 1326.
14. A. M. Rosales, K. S. Anseth, *Nat Rev Mater* **2016**, *1*.
15. a) R. P. Mecham, *Curr Protoc Cell Biol* **2012**, *Chapter 10*, Unit 10 1; b) P. Lu, K. Takai, V. M. Weaver, Z. Werb, *Cold Spring Harbor perspectives in biology* **2011**, *3*; c) T. Rozario, D. W. DeSimone, *Dev Biol* **2010**, *341*, 126.
16. Y. Kim, H. Ko, I. K. Kwon, K. Shin, *Int Neurorol J* **2016**, *20*, S23.
17. a) A. O. Elzoghby, *J Control Release* **2013**, *172*, 1075; b) M. C. Oz, D. M. Cosgrove, B. R. Badduke, J. D. Hill, M. R. Flannery, R. Palumbo, N. Topic, F. M. S. Grp, *Annals of Thoracic Surgery* **2000**, *69*, 1376.
18. M. Ehrbar, A. Sala, P. Lienemann, A. Ranga, K. Mosiewicz, A. Bittermann, S. C. Rizzi, F. E. Weber, M. P. Lutolf, *Biophysical Journal* **2011**, *100*, 284.
19. a) Y. C. Chen, R. Z. Lin, H. Qi, Y. Z. Yang, H. J. Bae, J. M. Melero-Martin, A. Khademhosseini, *Adv Funct Mater* **2012**, *22*, 2027; b) P. Occhetta, R. Visone, L. Russo, L. Cipolla, M. Moretti, M. Rasponi, *J Biomed Mater Res A* **2015**, *103*, 2109; c) U. Blache, Q. Vallmajo-Martin, E. R. Horton, J. Guerrero, V. Djonov, A. Scherberich, J. T. Erler, I. Martin, J. G. Snedeker, V. Milleret, M. Ehrbar, *EMBO Rep* **2018**, *19*.
20. J. Rouwkema, J. de Boer, C. A. Van Blitterswijk, *Tissue Eng* **2006**, *12*, 2685.

21. a) M. Kolbe, Z. Xiang, E. Dohle, M. Tonak, C. J. Kirkpatrick, S. Fuchs, *Tissue Eng Part A* **2011**, *17*, 2199; b) B. J. Klotz, K. S. Lim, Y. X. Chang, B. G. Soliman, I. Pennings, F. P. W. Melchels, T. B. F. Woodfield, A. J. Rosenberg, J. Malda, D. Gawlitta, *Eur Cell Mater* **2018**, *35*, 335; c) D. Gawlitta, J. O. Fledderus, M. H. van Rijen, I. Dokter, J. Alblas, M. C. Verhaar, W. J. Dhert, *Tissue Eng Part A* **2012**, *18*, 208; d) U. Blache, S. Metzger, Q. Vallmajo-Martin, I. Martin, V. Djonov, M. Ehrbar, *Adv Healthc Mater* **2016**, *5*, 489.
22. a) K. Cameron, R. Tan, W. Schmidt-Heck, G. Campos, M. J. Lyall, Y. Wang, B. Lucendo-Villarin, D. Szkolnicka, N. Bates, S. J. Kimber, J. G. Hengstler, P. Godoy, S. J. Forbes, D. C. Hay, *Stem Cell Reports* **2015**, *5*, 1250; b) L. K. Kanninen, R. Harjumaki, P. Peltoniemi, M. S. Bogacheva, T. Salmi, P. Porola, J. Niklander, T. Smutny, A. Urtti, M. L. Yliperttula, Y. R. Lou, *Biomaterials* **2016**, *103*, 86.
23. C. A. Rubio, *In Vivo* **1998**, *12*, 183.
24. a) S. E. Sakiyama, J. C. Schense, J. A. Hubbell, *Faseb J* **1999**, *13*, 2214; b) J. C. Schense, J. A. Hubbell, *Bioconjugate Chem* **1999**, *10*, 75.
25. a) M. Ehrbar, S. C. Rizzi, R. Hlushchuk, V. Djonov, A. H. Zisch, J. A. Hubbell, F. E. Weber, M. P. Lutolf, *Biomaterials* **2007**, *28*, 3856; b) M. Ehrbar, S. C. Rizzi, R. G. Schoenmakers, B. S. Miguel, J. A. Hubbell, F. E. Weber, M. P. Lutolf, *Biomacromolecules* **2007**, *8*, 3000.
26. W. S. Hur, N. Mazinani, X. J. Lu, H. M. Britton, J. R. Byrnes, A. S. Wolberg, C. J. Kastrup, *Blood* **2015**, *126*, 2329.
27. a) D. F. Torchiana, *J Card Surg* **2003**, *18*, 504; b) J. M. Harris, *Poly (ethylene glycol) chemistry: biotechnical and biomedical applications*, Plenum Press, New York **1992**.
28. a) M. A. Daniele, A. A. Adams, J. Naciri, S. H. North, F. S. Ligler, *Biomaterials* **2014**, *35*, 1845; b) Y. Fu, K. D. Xu, X. X. Zheng, A. J. Giacomini, A. W. Mix, W. Y. J. Kao, *Biomaterials* **2012**, *33*, 48.
29. a) F. Anjum, P. S. Lienemann, S. Metzger, J. Biernaskie, M. S. Kallos, M. Ehrbar, *Biomaterials* **2016**, *87*, 104; b) A. Ranga, M. P. Lutolf, J. Hilborn, D. A. Ossipov, *Biomacromolecules* **2016**, *17*, 1553; c) H. P. Tan, M. Fan, Y. Ma, J. C. Qiu, X. M. Li, J. X. Yan, *Adv Healthc Mater* **2014**, *3*, 1769.
30. a) C. C. Lin, K. S. Anseth, *Adv Funct Mater* **2009**, *19*, 2325; b) P. S. Lienemann, M. P. Lutolf, M. Ehrbar, *Adv Drug Deliv Rev* **2012**, *64*, 1078.
31. a) K. M. Park, Y. Lee, J. Y. Son, D. H. Oh, J. S. Lee, K. D. Park, *Biomacromolecules* **2012**, *13*, 604; b) C. B. Hutson, J. W. Nichol, H. Aubin, H. Bae, S. Yamanlar, S. Al-Haque, S. T. Koshy, A. Khademhosseini, *Tissue Eng Pt A* **2011**, *17*, 1713.
32. S. S. Soofi, J. A. Last, S. J. Liliensiek, P. F. Nealey, C. J. Murphy, *J Struct Biol* **2009**, *167*, 216.
33. S. Levenberg, J. Rouwkema, M. Macdonald, E. S. Garfein, D. S. Kohane, D. C. Darland, R. Marini, C. A. van Blitterswijk, R. C. Mulligan, P. A. D'Amore, R. Langer, *Nat Biotechnol* **2005**, *23*, 879.
34. Y. Mousseau, S. Mollard, H. Qiu, L. Richard, R. Casal, A. Nizou, N. Vedrenne, S. Remi, Y. Baaj, L. Fourcade, B. Funalot, F. G. Sturtz, *Lab Invest* **2014**, *94*, 340.
35. M. Simons, *Circulation* **2005**, *111*, 1556.
36. R. Kalluri, *Nat Rev Cancer* **2003**, *3*, 422.
37. B. J. Kang, H. H. Ryu, S. S. Park, Y. Kim, H. M. Woo, W. H. Kim, O. K. Kweon, *J Vet Med Sci* **2012**, *74*, 827.
38. a) I. Gotman, D. Ben-David, R. E. Unger, T. Bose, E. Y. Gutmanas, C. J. Kirkpatrick, *Acta Biomater* **2013**, *9*, 8440; b) N. Celikkin, S. Mastrogiacomo, J. Jaroszewicz, X. F. Walboomers, W. Swieszkowski, *J Biomed Mater Res A* **2018**, *106*, 201.

39. a) L. Zhou, G. Tan, Y. Tan, H. Wang, J. Liao, C. Ning, *RCS Advances* **2014**, *4*, 21997; b) P. Zhu, Y. Masuda, K. Koumoto, *Biomaterials* **2004**, *25*, 3915.
40. a) K. Bougas, V. F. Stenport, F. Currie, A. Wennerberg, *J Oral Maxillofac Res* **2011**, *2*, e3; b) K. Bougas, V. F. Stenport, F. Currie, A. Wennerberg, *J Oral Maxillofac Res* **2012**, *2*, e5.
41. M. G. Lampugnani, M. Resnati, M. Raiteri, R. Pigott, A. Pisacane, G. Houen, L. P. Ruco, E. Dejana, *Journal of Cell Biology* **1992**, *118*, 1511.
42. E. S. Harris, W. J. Nelson, *Curr Opin Cell Biol* **2010**, *22*, 651.
43. M. Kolbe, Z. Xiang, E. Dohle, M. Tonak, C. J. Kirkpatrick, S. Fuchs, *Tissue Eng Pt A* **2011**, *17*, 2199.
44. a) M. Huch, H. Gehart, R. van Boxtel, K. Hamer, F. Blokzijl, M. M. Versteegen, E. Ellis, M. van Wenum, S. A. Fuchs, J. de Ligt, M. van de Wetering, N. Sasaki, S. J. Boers, H. Kemperman, J. de Jonge, J. N. Ijzermans, E. E. Nieuwenhuis, R. Hoekstra, S. Strom, R. R. Vries, L. J. van der Laan, E. Cuppen, H. Clevers, *Cell* **2015**, *160*, 299; b) M. Huch, C. Dorrell, S. F. Boj, J. H. van Es, V. S. Li, M. van de Wetering, T. Sato, K. Hamer, N. Sasaki, M. J. Finegold, A. Haft, R. G. Vries, M. Grompe, H. Clevers, *Nature* **2013**, *494*, 247.
45. M. Huch, H. Gehart, R. van Boxtel, K. Hamer, F. Blokzijl, M. M. A. Versteegen, E. Ellis, M. van Wenum, S. A. Fuchs, J. de Ligt, M. van de Wetering, N. Sasaki, S. J. Boers, H. Kemperman, J. de Jonge, J. N. M. Ijzermans, E. E. S. Nieuwenhuis, R. Hoekstra, S. Strom, R. R. G. Vries, L. J. W. van der Laan, E. Cuppen, H. Clevers, *Cell* **2015**, *160*, 299.
46. O. Chaudhuri, L. Gu, D. Klumpers, M. Darnell, S. A. Bencherif, J. C. Weaver, N. Huebsch, H. P. Lee, E. Lippens, G. N. Duda, D. J. Mooney, *Nat Mater* **2016**, *15*, 326.
47. J. Groll, T. Boland, T. Blunk, J. A. Burdick, D. W. Cho, P. D. Dalton, B. Derby, G. Forgacs, Q. Li, V. A. Mironov, L. Moroni, M. Nakamura, W. Shu, S. Takeuchi, G. Vozzi, T. B. Woodfield, T. Xu, J. J. Yoo, J. Malda, *Biofabrication* **2016**, *8*, 013001.
48. a) W. Schuurman, V. Khristov, M. W. Pot, P. R. van Weeren, W. J. A. Dhert, J. Malda, *Biofabrication* **2011**, *3*; b) J. Visser, F. P. W. Melchels, J. E. Jeon, E. M. van Bussel, L. S. Kimpton, H. M. Byrne, W. J. A. Dhert, P. D. Dalton, D. W. Hutmacher, J. Malda, *Nature Communications* **2015**, *6*; c) N. V. Mekhileri, K. S. Lim, G. C. J. Brown, I. Mutreja, B. S. Schon, G. J. Hooper, T. B. F. Woodfield, *Biofabrication* **2018**, *10*.
49. N. Gjorevski, M. P. Lutolf, *Nat Protoc* **2017**, *12*, 2263.
50. a) M. P. Lutolf, N. Tirelli, S. Cerritelli, L. Cavalli, J. A. Hubbell, *Bioconjug Chem* **2001**, *12*, 1051; b) M. Ehrbar, A. Sala, P. Lienemann, A. Ranga, K. Mosiewicz, A. Bittermann, S. C. Rizzi, F. E. Weber, M. P. Lutolf, *Biophys J* **2011**, *100*, 284.
51. K. S. Lim, M. H. Alves, L. A. Poole-Warren, P. J. Martens, *Biomaterials* **2013**, *34*, 7097.
52. a) A. Nilasaroya, L. A. Poole-Warren, J. M. Whitelock, P. Jo Martens, *Biomaterials* **2008**, *29*, 4658; b) K. S. Lim, J. Kundu, A. Reeves, L. A. Poole-Warren, S. C. Kundu, P. J. Martens, *Macromol Biosci* **2012**, *12*, 322.
53. M. W. Pfaffl, A. Tichopad, C. Prgomet, T. P. Neuvians, *Biotechnol Lett* **2004**, *26*, 509.
54. M. E. Bolander, P. G. Robey, L. W. Fisher, K. M. Conn, B. S. Prabhakar, J. D. Termine, *Calcif Tissue Int* **1989**, *45*, 74.
55. A. Niemisto, V. Dunmire, O. Yli-Harja, W. Zhang, I. Shmulevich, *Ieee T Med Imaging* **2005**, *24*, 549.

Chapter 6

Engineering of a complex bone tissue model with endothelialised channels and capillary-like networks

Barbara J. Klotz | Khoon S. Lim | Yee Xiang Chang | Bram G. Soliman
Iris Pennings | Ferry P.W. Melchels | Tim B.F. Woodfield
Antoine J.W.P. Rosenberg | Jos Malda | Debby Gawlitta

European Cells and Materials Vol. 35 2018 pp 335-349



Abstract

In engineering of tissue analogues, upscaling to clinically-relevant sized constructs remains a significant challenge. The successful integration of a vascular network throughout the engineered tissue is anticipated to overcome the lack of nutrient and oxygen supply to residing cells. This work aimed at developing a multiscale bone-tissue-specific vascularisation strategy.

Engineering pre-vascularised bone leads to biological and fabrication dilemmas. To fabricate channels endowed with an endothelium and suitable for osteogenesis, rather stiff materials are preferable, while capillarisation requires soft matrices. To overcome this challenge, gelatin-methacryloyl hydrogels were tailored by changing the degree of functionalisation to allow for cell spreading within the hydrogel, while still enabling endothelialisation on the hydrogel surface.

An additional challenge was the combination of the multiple required cell-types within one biomaterial, sharing the same culture medium. Consequently, a new medium composition was investigated that simultaneously allowed for endothelialisation, capillarisation and osteogenesis. Integrated multipotent mesenchymal stromal cells, which give rise to pericyte-like and osteogenic cells, and endothelial-colony-forming cells (ECFCs) which form capillaries and endothelium, were used.

Based on the aforementioned optimisation, a construct of $8 \times 8 \times 3$ mm, with a central channel of $600 \mu\text{m}$ in diameter, was engineered. In this construct, ECFCs covered the channel with endothelium and osteogenic cells resided in the hydrogel, adjacent to self-assembled capillary-like networks. This study showed the promise of engineering complex tissue constructs by means of human primary cells, paving the way for scaling-up and finally overcoming the challenge of engineering vascularised tissues.

Introduction

Engineering of large, clinically-relevant sized tissue analogues remains challenging due to the need for vascularisation. Oxygen and nutrients have to be delivered homogeneously throughout an engineered tissue due to their limited diffusion distance, typically 100-200 μm , and low solubility (Carmeliet and Jain, 2000). Consequently, an engineered multiscale vascular network has to place the residing cells in the bulk material within a limited (diffusion) distance from the nearest perfused vessel (Langer and Vacanti, 1999; Rouwkema and Khademhosseini, 2016). Native bone tissue is characterised by a dense vascular system that regulates bone development, homeostasis and fracture healing (Kanczler and Oreffo, 2008; Lafage-Proust *et al.*, 2015). In addition to delivering oxygen and nutrients, blood flow through the vasculature also transports cells and growth factors to bone defect sites (Lafage-Proust *et al.*, 2015). In vascularised tissues, the vascular network consists of macrovessels branching into a dense bed of capillaries (microvessels). *In vitro* pre-vascularisation strategies, compared to intraoperative preparation of scaffolds, integrate faster with the host vasculature (Levenberg *et al.*, 2005) and prevent necrosis in the central core of the construct (Butt *et al.*, 2007). In principle, pre-vascularisation approaches will allow immediate blood supply throughout the engineered tissue upon its implantation through anastomosis to the host's blood circulation (Rouwkema and Khademhosseini, 2016).

A major advancement in the field is achieved through the biofabrication of a thick bone-like tissue with macrovessel-like structures and subsequent culture under flow perfusion (Kolesky *et al.*, 2016). However, this approach is limited to the macroscale, due to the restricted spatio-temporal resolution in current biofabrication technologies (Lee *et al.*, 2014). Moreover, in order to bring all residing cells close to the perfusing media flow, the presence of dense capillary beds and angiogenic sprouts into the bulk material is essential. Endothelial cells have the ability for self-assembling into capillary-like beds when co-cultured with stabilising cells (Unger *et al.*, 2015). Thus, for the formation of a dense capillary bed, it is a logical approach to exploit the self-assembly capacity of endothelial cells for forming microvessels and connecting with the main channel by sprouting angiogenesis (Lee *et al.*, 2014). This current bottleneck in the field is addressed by seeding endothelial cells into the bulk material surrounding the engineered channels (Lee *et al.*, 2014) or by enabling sprouting from a macrochannel by providing a cell penetrable 3-dimensional (3D) matrix (Miller *et al.*, 2012).

The integration of the abovementioned approaches for pre-vascularisation strategies is the next step in engineering of complex bone tissue constructs. When multiscale pre-vascularised, osteogenically differentiated tissue constructs are engineered, multiple aspects are critical. To date, these have not yet been addressed in a holistic approach for osteogenically stimulated constructs that are pre-vascularised by both capillaries and endothelium-lined macrovessels. Engineering of pre-vascularised bone leads to biological and fabrication dilemmas. A capillary bed requires soft bulk matrices (Occhetta *et al.*, 2015), preferably lower than 4 kPa (Nichol *et al.*, 2010), while

pronounced osteogenic differentiation of progenitor cells is supported by materials with compressive moduli of 15-30 kPa (Tan *et al.*, 2014; Wen *et al.*, 2014). Such stiff hydrogels, which are not cell permissive, are generally used for the fabrication process of macrovessel-like structures (Rouwkema and Khademhosseini, 2016). The resulting structurally stable channel structures are covered with endothelial monolayers (Hasan *et al.*, 2015; Kolesky *et al.*, 2016; Nichol *et al.*, 2010). However, these stiff biomaterial compositions would impair or even exclude cell migration and sprouting into the bulk material.

Besides satisfying the biological requirements of the biomaterial, it also remains challenging to select a suitable culture medium. Choosing one type of medium might affect the differentiation and performance of the combined cell types (Baldwin *et al.*, 2014; Rouwkema and Khademhosseini, 2016). For engineering pre-vascularised bone, the medium has to simultaneously allow for i) endothelialisation on the hydrogel surface, ii) capillarisation and sprouting, iii) osteogenesis. To the best of our knowledge, these three aspects have, so far, not been systematically assessed within one single construct. In tissue engineering, the final aim is to stimulate simultaneous differentiation of multiple cell types within one construct. Therefore, a synergistic combination of media and biomaterial composition that allow for all essential cell lineage commitments is highly desirable.

In this study, an integrated approach was presented – combining multiple human primary cells to engineer a pre-vascularised and osteogenically differentiated tissue construct. A main central macrovessel-like structure covered by endothelium was engineered in a capillarised, early bone tissue. For this purpose, clinically-relevant cell types, being multipotent mesenchymal stromal cells (MSCs) and endothelial-colony-forming cells (ECFCs), were combined in gelatin-based hydrogels. Gelatin-methacryloyl (gelMA) was selected as the base material, due to its tailorable properties for various tissue engineering applications (Klotz *et al.*, 2016). Firstly, gelMA was tuned towards endothelialisation (in 2D) and MSC spreading in 3D bulk hydrogels. Secondly, an optimal culture medium was defined to support multiscale pre-vascularised and osteogenically committed gelMA constructs. Finally, a multiscale pre-vascularised network was fabricated, which was characterised by an endothelium-lined macrochannel, a capillary-like network and a formed bone-like tissue.

Materials and Methods

The outline of the present study is described in Fig. 1, where N refers to the number of experiments conducted with different donor combinations of the MSC-ECFC co-cultures and n to the number of replicates within an experiment.

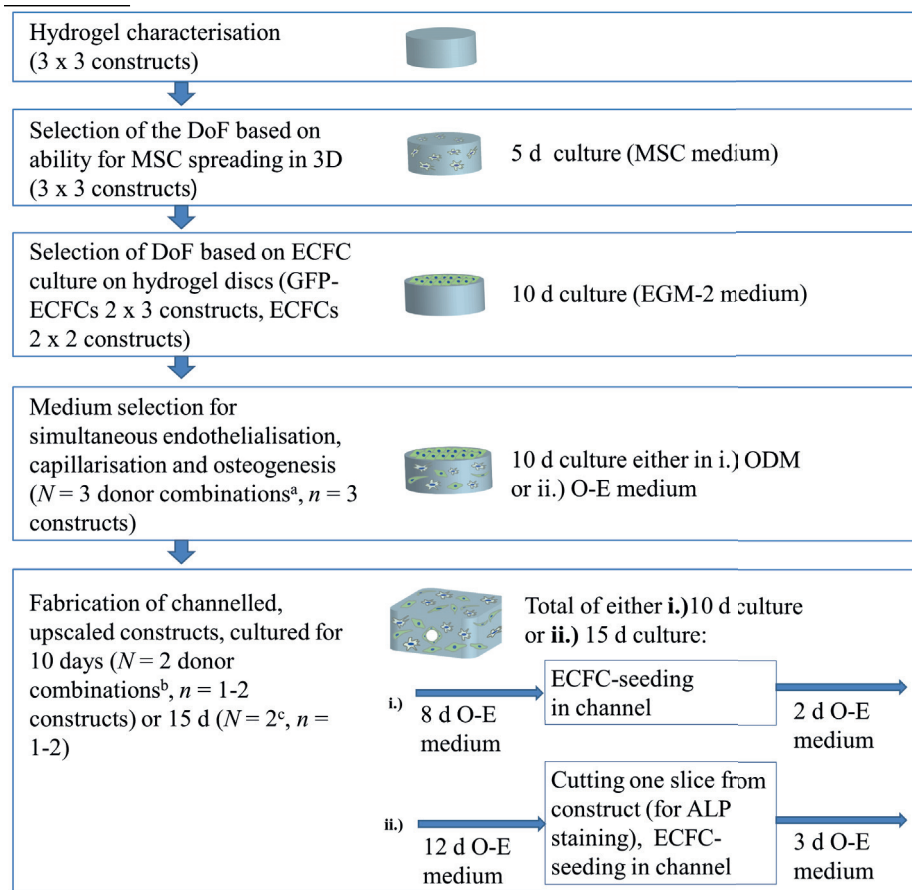


Figure 1. Study outline and replicates. 3 independent experiments were performed for the hydrogel characterisation and MSC encapsulations. Cell seeding on hydrogel discs was performed twice with GFP-ECFCs and twice with non-labelled ECFCs. N refers to different experiments with varying MSC-ECFC combinations from different donors; n to the number of replicates within an experiment. Experiment a: MSC donor 1 + ECFC donor 1, MSC donor 1 + ECFC donor 2, MSC donor 2 + ECFC donor 2. Experiment b: MSC donor 2 + ECFC donor 1, MSC donor 2 + ECFC donor 2. Experiment c: MSC donor 2 + ECFC donor 1, MSC donor 3 + ECFC donor 1.

For the medium selection, 3 different MSC-ECFC donor combinations were tested, with $n = 3$ replicates each. For the channelled constructs, $N = 2$ different MSC-ECFC donor combinations were tested, with $n = 1-2$ replicates and hydrogels cultured for 10 d. Furthermore, the same setup ($N = 2$, $n = 1-2$) was chosen for channelled constructs that were cultured up to 15 d. For the hydrogel characterisation, $n = 3$ independent experiments were performed, with $n = 3$ replicates (3×3 hydrogels). MSCs were encapsulated in hydrogels in $n = 3$ independent experiments, with $n = 3$ replicates (3×3 hydrogels). ECFC seeding on the hydrogel discs was performed twice for $n = 2$ independent experiments, with $n = 3$ replicates for GFP-labelled ECFCs, and twice with $n = 2-3$ replicates for non-labelled ECFCs.

Materials and mould preparations

Disc-shaped silicone moulds were prepared by punching 8 mm-diameter circles into silicone sheets of 1 mm in height (BioPlexus Corporation, Ventura, CA, USA). To make channeled hydrogel constructs, a custom-made mould (Med610, Stratasy, Eden Prairie, MN, USA) was designed with Autodesk Fusion 360 software version 2.0.3253, printed by Cetma (Brindisi, Italy) using an Objet30 3D printer (Stratasy). This mould (8 × 8 × 3 mm as inner dimensions) served as the negative sample to prepare silicone moulds. Inlet and outlet ports in the mould were created by inserting a 0.6 mm-diameter needle into the printed construct. Sylgard 184 silicone elastomer kit (Dow Corning, Midland, MI, USA) was prepared according to the manufacturer's instructions and poured into the custom-designed mould. For hydrogel fabrication, silicone moulds (with needle insert) were placed onto a glass slide, where the gel solution was added and sealed from air by a second glass slide for subsequent UV crosslinking.

GelMA synthesis and characterisation

Gelatin was functionalised with methacryloyl groups to allow for free-radical-mediated photo-crosslinking of a thermally stable hydrogel. The physico-chemical and mechanical properties of the hydrogels can be further tailored by modifying the degree of functionalisation (i.e. number of methacryloyl groups). This is particularly important as the hydrogel microenvironment closely regulates the cell-matrix interaction, affecting cell attachment, spreading and proliferation. GelMA was prepared from type A porcine gelatin (MedellaPro, Gelita, Eberbach, Germany) that was reacted with methacrylic anhydride (Sigma-Aldrich), as described previously (Van den Bulcke *et al.*, 2000). In brief, gelatin was dissolved in phosphate buffered saline (PBS) by heating to 50 °C. Two batches of gelMA were prepared, one with a low- and one with a high- degree of functionalisation (DoF). 0.02 g and 0.6 g of methacrylic anhydride/g of gelatin, respectively, were added drop-wise to the solution and allowed to react for 1 h under constant stirring. Subsequently, unreacted methacrylic anhydride was removed from the reaction mixture by centrifugation. After the pH of the solution was set to 7.4, the gelMA solution was dialysed against distilled water using a cellulose membrane (14 kDa cut-off, Sigma-Aldrich) for 5 d at room temperature. The gelMA solution was sterile filtered, lyophilised and stored at - 20 °C until use. The DoFs of the two gelMA batches were determined by the ninhydrin assay, as described previously (Loessner *et al.*, 2016). The DoF is defined by the percentage of modified lysine residues (Van den Bulcke *et al.*, 2000) and was calculated to be 18.4 % (referred to as 20 %) and 78 % (referred to as 80 %) for the low and high DoF gelMA batches, respectively.

Hydrogel preparation

The gelMA precursor solution was crosslinked by UV-light using 0.1 % (w/v) Irgacure® 2959 (Ciba®, Ludwigshafen am Rhein, Germany). One day before use, GelMA solutions were heated to 70 °C for 15 min and the two batches were mixed in varying ratios to obtain final average DoFs between 30 % and 70 %. For hydrogel preparation, gelMA was dissolved at 60 °C and diluted with PBS to a final concentration of 5 %. Finally, the gelMA precursor solution with 0.1 % Irgacure® 2959 was pipetted into a mould and crosslinked in a UVP CL-1000L UV linker (UVP Cambridge, UK; 365 nm, 7 mW/cm²) for 15 min. Hydrogel constructs containing a channel were crosslinked from both sides for 4.5 min each, with a Superlite S-UV 201AV lamp (350-500 nm, Lumatec, Munich, Germany).

Mechanical analysis of hydrogel

GelMA hydrogels were prepared and incubated for 24 h in PBS at 37 °C (3 independent experiments with $n = 3$) and the compression modulus was determined by a Dynamic Mechanical Analyser (DMA, Q800 TA Instruments, New Castle, DE, USA) at room temperature. Compression was applied between 20 %/min and -30 %/min and the Young's modulus was calculated from the slope of the linear region of the stress/strain curves in the 5-10 % strain range.

Mass loss and swelling studies

Mass loss and swelling studies were performed on GelMA hydrogels, as previously reported (Lim *et al.*, 2013). In short, the wet weight of the hydrogels was determined directly after crosslinking ($m_{initial, t0}$). Then, 3 out of 6 hydrogels per experimental group were frozen and lyophilised to obtain the dry weights of the hydrogels ($m_{dry, t0}$). The other 3 hydrogels were left in PBS at 37 °C for 24 h, frozen and lyophilised to obtain the dry weight ($m_{dry, t1}$). The hydrogel swelling ratio (q) and the sol fraction were calculated as described in the following equations (Lim *et al.*, 2012; Nilasaroya *et al.*, 2008):

Cell culture media

MSC expansion medium was composed of alpha modification minimum essential medium (α -MEM; Gibco), 10 % heat-inactivated foetal bovine serum (FBS; Lonza), 100 U/mL penicillin, 10 mg/mL streptomycin (Gibco), 0.2 mM L-ascorbic acid-2-phosphate (ASAP; Sigma-Aldrich) and 1 ng/mL fibroblast growth factor-2 (FGF-2; 233-FB, R&D Systems). Endothelial growth medium-2 (EGM- 2) was composed of endothelial basal medium-2 (EBM; Lonza), 10 % FBS, 100 U/mL penicillin, 10 mg/ mL streptomycin and EGM-2 SingleQuot (Lonza). Osteogenic differentiation medium (ODM) was composed of α -MEM, 10 % FBS, 100 U/mL penicillin, 10

mg/mL streptomycin, 10 mM β -glycerophosphate (Sigma-Aldrich) and 10 nm dexamethasone (Sigma- Aldrich). For the ODM-EGM combination medium (O-E), the osteogenic components β -glycerophosphate and dexamethasone were 2 \times concentrated and subsequently 1 : 1 diluted with EGM-2.

MSC isolation and culture

Bone marrow aspirates were obtained from the iliac crest of 3 donor patients after informed consent was given and with approval of the local ethics committee (TCBio-08-001-K University Medical Centre Utrecht, the Netherlands). The white mononuclear cell (MNC) fraction was collected after performing a density gradient centrifugation on Ficoll-Paque PLUS (1.077 g/mL; GE Healthcare). Obtained cells were cultured in MSC expansion medium at 37 °C/5.0 % CO₂ and tested for differentiation potential into osteo-, adipo- and chondrogenic lineages. Obtained MSCs were analysed by fluorescence-activated cell sorting (FACS) and were negative for the haematopoietic markers CD14 [RPA-M1, fluorescein isothiocyanate (FITC)-conjugated, Abcam], CD34 [4H11, alkaline phosphatase (AP)-conjugated, Abcam], CD45 [MEM- 28, phycoerythrin (PE)-conjugated, Abcam] and CD79a (HM47, PE-conjugated, Abcam) and positive for the established MSCs markers CD90 (5E10, FITC-conjugated, Abcam), CD105 (MEM-226, AP- conjugated, Abcam) and CD73 (AD2, PE-conjugated, Abcam). For all the experiments, MSCs up to passage 4 were used.

ECFC isolation and culture

Human umbilical cord blood from 2 donors was obtained after approval by the local ethics committee (METC 01-230/K, University Medical Centre Utrecht, the Netherlands) and following patient informed consent after caesarean section. The blood was diluted at least 1 : 1 with PBS 2 mM EDTA and the MNC were isolated by density gradient centrifugation on Ficoll-Paque PLUS. Obtained cells were plated on rat tail collagen I (Corning)-coated plates at a seeding density of 10-20 \times 10⁶ cells/cm² and cultured in EGM-2. The culture medium was refreshed daily during the first 7 d after cell isolation and afterwards every 3-4 d. After 14-21 d, colonies with cobblestone morphology were picked and replated for expansion. Obtained ECFCs were analysed by FACS and resulted positive for CD105 and CD31 (TLD-3A12, FITC- conjugated, Abcam), partially positive for CD34 and CD309 (VEGFR/KDR, PE-conjugated, MACS, Miltenyi Biotech) and negative for CD45, CD14 and CD133 (AC133-VioBright, FITC-conjugated, Miltenyi Biotech). ECFCs were used up to passage 10 for all the experiments.

ECFC transduction with GFP

ECFCs in passage 5 were seeded at a density of 4700 cells/cm² and transduced with a lentiviral green fluorescent protein (GFP) construct (in a pHAGE2 vector combined with a human EF-1 α promoter) in FBS-free medium the following day. After 1 d, fresh EGM-2 was added to the cells. Selection of ECFCs that were successfully transduced with the GFP-construct occurred by addition of 3 μ g/mL puromycin (Sigma- Aldrich) for 10 d. During selection, GFP-ECFCs were expanded for 2 passages to create a batch of fluorescently-labelled cells.

Co-cultures in gelMA and discs covered with ECFCs

ECFCs and MSCs were co-cultured in 5 % gelMA hydrogels and, additionally, ECFCs were seeded on top of the hydrogel discs. Cell-encapsulation occurred in gelMA mixtures of 30 and 50 % DoF, as described above. For these hydrogels, PBS was replaced with the respective culture medium to encapsulate 1.25×10^6 /mL ECFCs and 5×10^6 /mL MSCs. Following hydrogel crosslinking, ECFC suspensions (6.6×10^5 cells/mL) were seeded on top of the disc and left to adhere for 30 min before medium was added. Constructs containing only a (GFP-)ECFC monolayer were cultured in EGM-2, whereas constructs containing a MSC/ECFC co-culture in the hydrogel and ECFCs on top of the disc were cultured in ODM or O-E. After 10 d of culture, gels were fixed and cut in half for vasculogenic and osteogenic stainings ($N = 3, n = 2-3$).

Preparation of MSC-ECFC containing channelled constructs

MSCs and ECFCs were encapsulated at 5×10^6 and 1.25×10^6 cells/mL, respectively, in 50 % DoF, 5% w/v gelMA constructs containing a channel that was seeded with ECFCs as follows. The cell-prepolymer- mixture was injected and cross-linked in silicone moulds with a 0.6 mm-diameter retractable needle in the centre to create the channel in the bulk hydrogel. The gels were cultured in O-E for 8 d before ECFCs, at a concentration of 50×10^6 cells/mL, were seeded into the channel. The cells were allowed to adhere for 15 min before the construct was flipped of 180° and incubated for another 15 min. Next, O-E was added for another 2 d. Alternatively, the gels were cultured for 12 d and a slice was cut from the construct for alkaline phosphatase (ALP) staining. In these gels, ECFCs were seeded at a concentration of 50×10^6 cells/mL on day 12 and the construct was further cultured up to day 15. The constructs were cultured for either 10 or 15 d in O-E, fixed and cut into sections for further analysis.

F-actin staining

MSCs were encapsulated at a concentration of 5×10^6 cells/mL in 30, 50 and 80 % DoF at 5 % w/v gelMA hydrogels (3 independent experiments with $n = 3$ hydrogel discs). After 5 d, the gels were fixed and stained whole mount with 0.2 μm tetramethylrhodamine B isothiocyanate (TRITC)- phalloidin (Sigma-Aldrich) after permeabilisation with PBS-Triton-X and a blocking step in 5 % bovine serum albumin (BSA) in PBS. The central plane in the hydrogels were imaged using a confocal microscope (SP8x Leica, DMi8) to assess cell morphology in 3D.

Histology and immunostaining

After 10 or 15 d of culture, samples were fixed and stained for ALP activity using Fuchsin + Substrate-Chromogen System (K0624, Dako). For immunostainings, the samples were permeabilised with 0.2 % Triton-X in PBS for 30 min and blocked in BSA/PBS for 30 min. The formation of stabilised capillary-like structures was assessed by CD31 staining (5.1 $\mu\text{g}/\text{mL}$; M0823, Dako), secondary sheep anti-mouse biotinylated antibody (1 : 200; RPN1001v1, GE Healthcare) and tertiary streptavidin Alexa Fluor 488 conjugate (5.0 $\mu\text{g}/\text{mL}$; S32354, Invitrogen). Mouse monoclonal Cy3-conjugated α -smooth muscle actin (αSMA) antibody (1 : 300; Clone 1A4, C6198, Sigma- Aldrich) was used to detect the stabilising cells of the capillary-like structures. Furthermore, anti-vascular endothelial cadherin antibody from rabbit (VE-cad, 1 : 250; D87F2, Cell Signalling Technology) was combined with Hilyte fluor 488 (2 $\mu\text{g}/\text{mL}$; AS-28176- 05-H488, AnaSpec, Fremont, CA, USA) and murine anti-von Willebrand factor antibody (vWF, 8 $\mu\text{g}/\text{mL}$; ab194405, Abcam) with secondary Alexa Fluor 546 (A-11030, goat-anti-mouse, 2 $\mu\text{g}/\text{mL}$; ThermoFisher Scientific). 4, 6-diamidino-2-phenylindole (DAPI, 100 ng/mL; Sigma-Aldrich) was used to stain the cell nuclei. The constructs were imaged with an upright fluorescence microscope (BX51, Olympus) or confocal microscope (SP8x Leica, DMi8, Leica).

Immunohistochemistry

After fixation, hydrogels were dehydrated in graded ethanol series, cleared in xylene and embedded in paraffin. An osteonectin staining was performed on 5 μm -thick sections. In short, sections were deparaffinised and hydrated before endogenous peroxidase was blocked in 0.3 % H_2O_2 . Antigen retrieval was performed in citrate buffer at 80 °C for 20 min. Subsequently, the primary antibody for osteonectin [4.2 $\mu\text{g}/\text{mL}$; AON-1 was deposited to the Developmental Studies Hybridoma Bank (DSHB) by J.D. Termine (Bolander *et al.*, 1989)] was incubated for 1 h before addition of a horseradish peroxidase-conjugated anti-mouse antibody (EnVision + System- HRP Labelled Polymer, K4000, Dako). Osteonectin was detected by conversion of 3,3'-diaminobenzidine solution (SK-4100, Vector, Burlingame, CA, USA) and nuclei were counterstained with haematoxylin (Merck). Isotype controls were performed using concentration-matched mouse IgG1 monoclonal antibody (ThermoFisher Scientific).

Image analysis

RGB fluorescence images of the whole hydrogel construct (one field of view per hydrogel, with a random selected plane) were obtained using an upright fluorescence microscope (BX51, Olympus). Images were merged, where contrast and intensity were set to be comparable across all images using Adobe Photoshop CS6 and ImageJ 1.47v and 1.51a. Total and mean lengths of vessel-like structures were quantified by manual processing by AngioQuant software, as per previously published protocols (Niemisto *et al.*, 2005). Quantification of cell-based experiments was based on 3 experiments with different MSC-ECFC donor combinations ($N = 3$) and 2-3 gels ($n = 2-3$) per condition. In total, 9 field of views of 9 different hydrogels were quantified for the O-E condition and 8 hydrogels were imaged for the ODM condition.

Statistical analysis

Difference of the means between O-E and ODM cultures of the AngioQuant data was determined by Student's *t*-tests in GraphPad Prism 7.02. The significance of the differences in the mean compressive moduli, sol fractions and swelling ratios were detected by a one-way ANOVA and subsequent Tukey honest significant difference (HSD) *post-hoc* analysis using GraphPad Prism 7.02. $p < 0.05$ was considered significant.

Results

GelMA hydrogel optimisation by tuning the DoF The DoF was optimised for 5 % gelMA hydrogels, in order to select a composition with suitable physico-mechanical and biological properties to engineer pre-vascularised bone constructs. While a high swelling ratio, indicated by water uptake of the hydrogel, provides cells with freedom to migrate (Ehrbar *et al.*, 2011), it is also associated with loss of material during the crosslinking process (sol fraction), which should be kept minimal (Nandi and Winter, 2005). Hydrogels with a DoF ranging from 20 % to 80 % gradually decreased in swelling ratio from 31.3 ± 13.4 to 16 ± 0.7 ($p < 0.0001$) (Fig. 2a). Also, the sol fraction decreased, with increasing DoF, from 40.5 ± 21.8 % to 5.5 ± 2.7 % ($p < 0.0001$) (Fig. 2b). The compressive modulus indicates the bulk stiffness of the hydrogel and is used to determine the range of mechanical properties that support cell spreading and migration in 3D (Ehrbar *et al.*, 2011). The compressive modulus slightly increased from 1.2 ± 0.5 kPa (30 % DoF hydrogel) to 1.8 ± 0.5 kPa ($p = 0.0966$) and 2.8 ± 0.8 kPa (30 vs. 80 $p < 0.0001$, 50 vs. 80 $p = 0.0052$) for 50 % and 80 % DoF hydrogels, respectively (Fig. 2c). Macroscopically, a difference in swelling behaviour was visible among 30 %, 50 % and 80 % DoF hydrogels (Fig. 2d, upper row). Biologically, a clearly varying cell response was observed among these three hydrogel compositions. After 5 d, MSCs spread in 30 and 50 % DoF hydrogels, which did not occur in 80 % DoF (Fig. 2d, bottom row). Since cell spreading is essential for

the assembly of pre-vascular structures, 30 and 50 % DoF hydrogel compositions were selected for further studies.

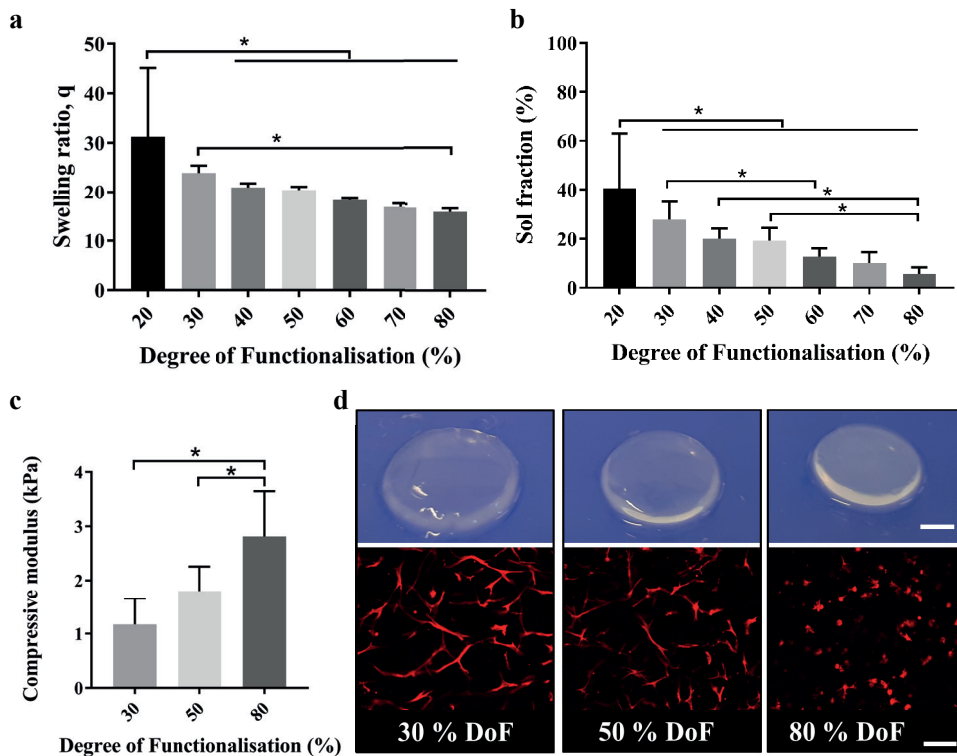


Figure 2. GelMA hydrogel characterisation based on physico-mechanical and biological aspects. 5 % GelMA hydrogels, with average DoF ranging from 20 to 80 %, were characterised. **(a)** Swelling ratio and **(b)** sol fraction gradually decreased from 20 % DoF hydrogels to 80 % DoF. **(c)** Compressive moduli of gelMA hydrogels increased with increasing DoF. **(d, upper row)** A decrease in hydrogel swelling was macroscopically visible with increasing DoF; scale bar: 2 mm. **(d, bottom row)** MSC encapsulation in 30, 50 and 80 % DoF gelMA hydrogels resulted in cell spreading in 30 and 50 % DoF hydrogels, whereas MSCs stayed rounded in 80 % DoF gelMA hydrogels at day 5; TRITC-phalloidin; scale bar: 200 μ m.

Evaluation of endothelium formation

A further selection between 30 and 50 % DoF gelMA was made by evaluating the suitability for formation of endothelial monolayers on the hydrogel surface. ECFCs that were seeded on 30 % DoF hydrogels did not allow for reproducible monolayer formation since the cells detached over time in culture in 2 out of 4 experiments (Fig. 3a-c), whereas on 50 % DoF hydrogels, endothelial cells were able to robustly form confluent monolayers (Fig. 3e,f). Based on these results, 50 % DoF gelMA hydrogels were selected to create multi-scale pre-vascularised bone constructs.

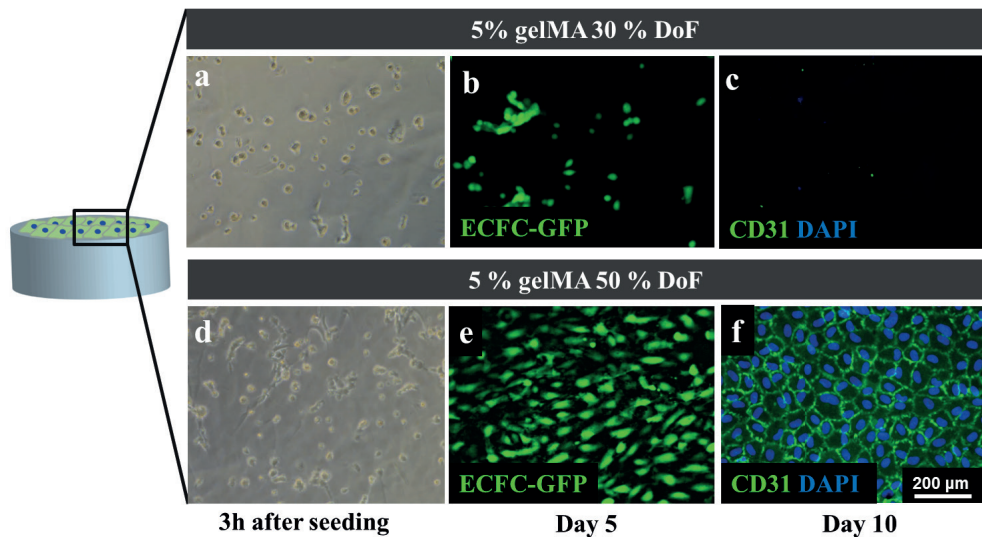


Figure 3. Effect of gelMA DoF on ECFC monolayer formation on hydrogel discs cultured for up to 10 d. (a,b) GFP-labelled ECFCs attached to a 30 % DoF gelMA hydrogel surface 3 h after seeding and after 5 d, however, (c) after 10 d, cells were detached when cultured in EGM-2 (2 out of 4 experiments). (d-f) GFP-ECFCs were able to attach to 50 % DoF gelMA hydrogels and form an endothelial monolayer when cultured in EGM-2 ($N = 2$, $n = 2-3$).

Optimisation of culture medium for pre-vascularisation and osteogenesis

6

The culture medium composition was optimised for pre-vascularisation and osteogenic commitment of encapsulated cells in the bulk hydrogel. Also, the medium had to allow for ECFC monolayer formation on the hydrogel surface, given that any macrovessel or channel in the hydrogel would preferably be covered with endothelium. Whereas the biomaterial selection (Fig. 3) was based on constructs that were cultured in the preferred medium for ECFCs (EGM-2), the MSC-ECFC co-cultures were cultured in either ODM or O-E.

The constructs cultured in ODM resulted in impaired ECFC monolayer formation on the hydrogel surface (Fig. 4a), whereas in the O-E, ECFC-monolayers were obtained reproducibly (Fig. 4d). Pre-vascular network formation in the bulk hydrogel was more pronounced in O-E as compared to ODM (Fig. 4b,e). Also, the total length of vessel-like structures was significantly greater in O-E cultures when compared to ODM ($p = 0.0168$) (Fig. 4g,h). Addition of 50 % EGM-2 to the ODM resulted in an ALP activity comparable to constructs that were cultured in 100 % ODM (Fig. 4c,f).

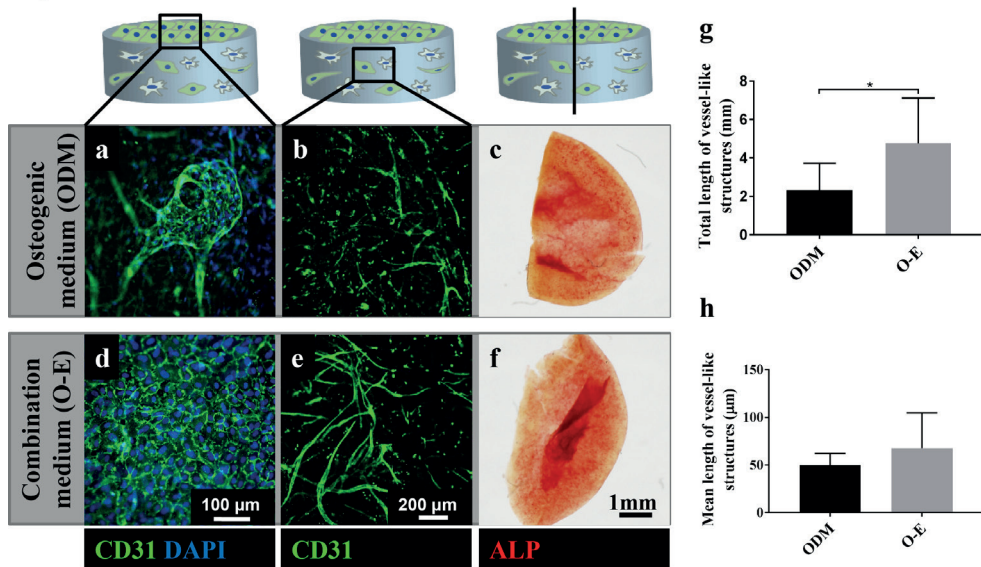


Figure 4. Influence of media composition on ECFC monolayer formation on top of 5 % gelMA discs (50 % DoF) and on capillary-like structure assembly and osteogenic differentiation of ECFC-MSC co-cultures inside gelMA discs. **(a)** Endothelial monolayer formation was impaired in ODM, whereas in **(d)** O-E, endothelial monolayer patches were present after a culture time of 10 d. **(b,e)** Capillary-like structure formation in the bulk hydrogel was dependent on the culture medium. **(c,f)** ALP activity was comparable in both co- cultures. **(g,h)** Quantification of total and mean vessel-like structure length showed the beneficial effect of the combination medium over ODM ($N = 3, n = 2-3$).

Characterisation of endothelium, capillaries and pericyte-like cells

Along with the expression of CD31, indicating the formation of capillary-like structures, the phenotype of the endothelial cells was further investigated after culture for 10 d in O-E.

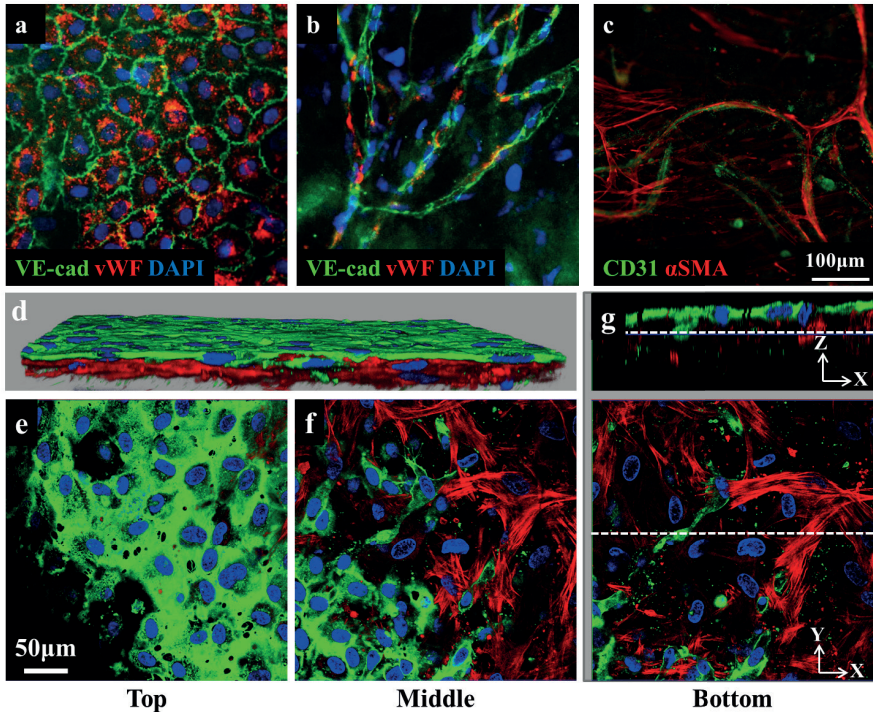


Figure 5. Characterisation of endothelium, capillaries and pericyte-like cells in 5 % gelMA (50 % DoF) hydrogels cultured for 10 d in O-E. (a) Endothelial monolayers on the hydrogel surface show characteristic intercellular junctions enabled by VE-cadherin and vWF in the cytoplasm. (b) Capillary-like structures in the hydrogel expressed VE-cadherin and vWF. (c) Capillary-like CD31 structures adjoined with stabilising α SMA-positive pericyte-like cells. (d) Overview of interface between surface and hydrogel; CD31 in green, α SMA in red and nuclei in blue. (e) Endothelial monolayer forming an endothelium on the surface of gelMA hydrogel discs (X-Y axis). (f) Transition zone between endothelium and underlying capillary-structures and α SMA-expressing stabilising cells. (g) Cross-sections (Z-X and Y-X) showing capillary-like structures and stabilising cells inside the gelMA bulk hydrogel.

VE-cadherin highlighted the presence of intercellular junctions between endothelial cells, both in the endothelium (Fig. 5a) and in the capillary-like structures inside the bulk hydrogel (Fig. 5b). The adhesive glycoprotein vWF, synthesised by endothelial cells, formed globular structures in the cytoplasm (Fig. 5a,b). Pericyte-like cells adjoining the endothelial structures were identified by positive staining for α SMA (Fig. 5c). Furthermore, the interface between the endothelium-covered hydrogel surface and the bulk hydrogel with capillary-like structures was investigated (Fig. 5d). Co-existence of stabilised capillaries in direct contact with an endothelial monolayer could show the feasibility that differentiated MSCs did not impede the formation of the endothelium. Three cross-sections at the level of the endothelium (Fig. 5e), transition zone (Fig. 5f) and capillary-like structures in the hydrogel (Fig. 5g) were analysed. An endothelial monolayer had formed on the hydrogel surface, with capillary-like structures extending from here into the bulk hydrogel (Fig. 5g). At the same time, capillary-like structures and α SMA-positive cells were present inside the hydrogel.

Engineering a macrovessel-like structure in a bulk hydrogel of capillaries and osteogenic cells

Multiscale pre-vascularised and osteogenically differentiated gelMA-based constructs were prepared and cultured for 10 d (Fig. 6a-d) and 15 d (Fig. 6e-j). These constructs contained MSC-ECFC co-cultures in the bulk hydrogel and a confluent ECFC monolayer in the macrochannel (Fig. 6). The luminal side of the channel was prominently covered with endothelial cells, with characteristic cobblestone-like morphology (Fig. 6d,f). Furthermore, sections showed capillary-like structures inside the surrounding bulk hydrogel of the constructs cultured for 10 d (Fig. 6b) and 15 d (Fig. 6e). Sprouting angiogenesis was present from the channel surface into the bulk hydrogel as seen in a cross-sectional projection of the channel (Fig. 6b). Here, α SMA-expressing cells covered the luminal side of the channel, which was additionally covered with endothelial cells (Fig. 6c, originating from the stack shown in Fig. 6b). Early osteogenic differentiation of MSCs, as shown by ALP activity, was observed after 12 d (Fig. 6g). Furthermore, osteonectin was produced by the cells after 15 d of culture (Fig. 6h,i).

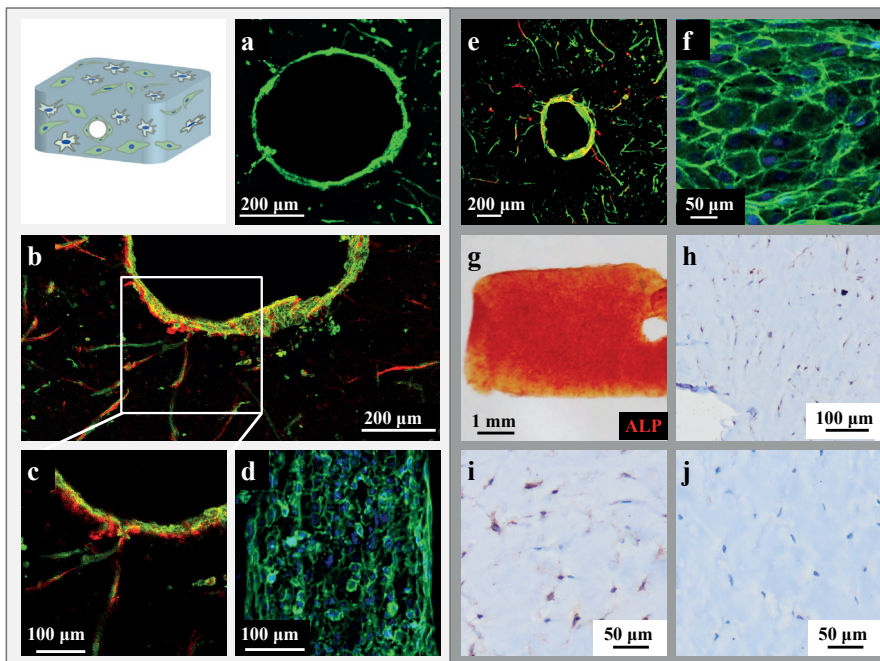


Figure 6. Multiscale pre-vascularised and osteogenically differentiated gelMA constructs. Constructs prepared from 50 % DoF gelMA hydrogels containing ECFC-MS C co-cultures and an ECFC-seeded macrochannel were cultured in O-E for (a-d) 10 d or (e-j) 15 d. (a,e) Cross-section (projection) through the endothelialised channel, (b) projection of close-up of sprouts connecting with the channel-surface and (c) single image of stack in b. (d) Longitudinal section (projection) of endothelialised channel. (f) Projection of an endothelialised channel. (g) Slice of construct harvested after culture for 12 d for ALP staining. (h,i) Osteonectin staining of gelMA construct, cultured for 15 d and (j) isotype control. Staining in green for CD31, in red for α SMA and in blue for nuclei (at day 10 and day 15, each $N = 2$, $n = 1-2$).

Discussion

Vascularisation, in combination with tissue specific maturation, is one of the main challenges in tissue engineering when proceeding towards clinically-relevant sized tissue constructs (Klotz *et al.*, 2016). An often-used strategy is to create vessel-like structures in the form of engineered endothelial-seeded channels to enable vascular supply throughout the construct (Kolesky *et al.*, 2016; Kolesky *et al.*, 2014). Furthermore, endothelial cells have the capacity to self-assemble into a capillary bed, which extends the vascular network through connections with the engineered channels (Lee *et al.*, 2014). This strategy of interconnected macrochannels and capillaries was advanced to the next stage by tailoring it specifically to bone tissue engineering based on clinically-relevant cell sources. In this work, it was demonstrated that multiple sub-cultured primary cell types could be supported within a single construct by means of tailored biomaterial physico-mechanical properties and cell-specific soluble cues in the medium. For the first time, a complex pre-vascularised bone model was realised that allowed for the formation of a multiscale vascular-like network within a developing bone-like matrix.

Fine-tuning of gelMA hydrogel characteristics

GelMA hydrogels can be adjusted for different applications by varying the gelatin source, polymer concentration, DoF or conversion of double bonds (*e.g.* through UV exposure time) (Klotz *et al.*, 2016; Nichol *et al.*, 2010; Van den Bulcke *et al.*, 2000). Even though osteogenesis predominantly occurs in stiff matrices with an elastic modulus of 11-30 kPa (Huebsch *et al.*, 2010; Tan *et al.*, 2014), the need for capillaries infiltrating the developing bone tissue requires the design of a soft gelMA matrix, preferably with an elastic modulus lower than 4 kPa (Nichol *et al.*, 2010). Furthermore, to enable the formation of an endothelium, the hydrogel composition has also to allow the ECFCs to develop a cobblestone-like phenotype on the hydrogel surface (Gimbrone *et al.*, 1974).

To obtain a hydrogel that was suitable for endothelialisation, vascularisation and osteogenesis, the physico-chemical and mechanical properties had to be precisely tailored and extensively characterised. It was possible to form 5 % gelMA hydrogels with a DoF as low as 20 %. However, the sol-gel characteristics of these hydrogels were not as reproducible as at higher DoFs, as shown by high standard deviations for sol fraction and mass swelling ratios. Therefore, 30 % DoF hydrogels with a compressive modulus of 1.2 ± 0.5 kPa were selected for further studies. While 5 % gelMA hydrogels (30 % DoF) performed best in terms of 3D MSC spreading, serving as an indicator of whether ECFCs could migrate and form capillary-like networks, this hydrogel composition is limited by its physico-mechanical characteristics. The pronounced swelling behaviour and the related structural instability excluded this composition for the intended fabrication approaches. Furthermore, and in contrast to 50 % DoF gelMA hydrogels, 30 % DoF gelMA did not allow for reproducible ECFC attachment onto the surface of the hydrogel disc. This behaviour might be

attributed to the considerable swelling of this hydrogel composition, leading to a reduced actual polymer concentration, which does not provide enough cell attachment sites. Pore sizes for gelMA hydrogels increase with decreasing DoF (Chen *et al.*, 2012) and might lead to a pore size that cannot be bridged anymore by residing cells on the hydrogel surface. Furthermore, hydrogels degrade faster with decreasing DoF (Chen *et al.*, 2012; Koshy *et al.*, 2014; Nguyen *et al.*, 2015), favouring, from a structural point of view, the higher DoF of 50 % over 30 %. In addition, no significant difference in compressive modulus was measured when the DoF of 5 % gelMA hydrogels was decreased from 50 % to 30 % ($p = 0.0966$). Therefore, 5 % gelMA at 50 % DoF represented a balance between biological and physico-mechanical requirements, as confirmed by an earlier study using this composition to engineer vascularised hydrogels (Chen *et al.*, 2012). These results highlighted an optimised fabrication window for soft gelMA hydrogels down to 5 % gelMA and 50 % DoF using Irgacure® 2959 as photo-initiator. This composition fulfilled the needed requirements of being relatively form-stable, allowing for endothelialisation on the hydrogel surface and enabling cell spreading within the hydrogel, which is needed for capillarisation.

Optimisation of culture medium composition for pre-vascularised bone

Medium selection is a critical element in culturing of complex tissue constructs containing multiple cell types. Typically, cell culture media are tailored for each individual cell type and vary, for instance, in composition of supplements, salts and vitamins (Baldwin *et al.*, 2014). While many approaches are reported to test the best medium conditions in mesenchymal and endothelial co-cultures for pre-vascularised bone tissue (Baldwin *et al.*, 2014; Bersini *et al.*, 2016; Jin *et al.*, 2015; Kolbe *et al.*, 2011; Ma *et al.*, 2011; Unger *et al.*, 2015), the effect of the same culture medium on endothelialisation of 2D hydrogel surfaces has not yet been reported. ODM performs best in 3D co-cultures of MSCs and endothelial cells for osteogenesis and vasculogenesis/angiogenesis (Gawliotta *et al.*, 2012; Ma *et al.*, 2011). However, in the present study, ODM did not allow for sufficient endothelialisation on gelMA hydrogel surfaces. A possible explanation could lie in the spatial separation of ECFCs and MSCs. Whereas ECFCs inside the hydrogels are stimulated by paracrine signalling from the co-embedded MSCs (Gruber *et al.*, 2005; Hung *et al.*, 2007), on the hydrogel surface (and in the presence of ODM without EGM-specific growth factors) ECFCs may have insufficient stimulating factors to survive and proliferate. Consequently, an alternative culture medium was investigated to allow for endothelialisation under osteogenic stimulation. Besides ODM, a variety of mixtures of ODM and EGM are reported to have been tested on co-cultures (Baldwin *et al.*, 2014; Jin *et al.*, 2015). Since these mixtures lead to a dilution of the osteogenic supplements, in the current study, the effects of a combination medium that contained double concentrated ODM (for β -glycerophosphate and dexamethasone) and standard EGM-2 in a 1 : 1 ratio (resulting in standard ODM component concentrations in the final O-E) were investigated. This medium allowed for more robust endothelialisation on co-culture-seeded gelMA hydrogel surfaces than ODM

alone. VE-cadherin staining highlighted the formation of intercellular junctions between ECFCs and vWF was produced after 10 d. vWF was present in the cytoplasm of ECFCs and appeared as punctate globules, which is a characteristic of endothelial cells (Zheng *et al.*, 2015). These observations demonstrated the maintenance of the endothelial monolayer phenotype during the 10 d of culture in O-E. Furthermore, differentiation of pericyte-like cells under these culture conditions was confirmed by the presence of pericyte-like cells of endothelial structures, which were positive for α SMA. MSCs in co-culture with endothelial cells stabilise capillaries as pericyte-like cells (Au *et al.*, 2008). While the stabilising nature of these cells can be shown using different stainings, the identification of these cells as pericytes remains controversial, since there is a lack of distinct markers (de Souza *et al.*, 2016).

Capillary-like structures were present in constructs cultured in ODM; however, vasculogenesis was enhanced in the combination medium. At the same time, early osteogenesis was confirmed in constructs cultured in ODM and O-E. Previously, 1 : 1 diluted combination media have failed to induce mineralisation of cell-laden constructs (Gawlitta *et al.*, 2012; Ma *et al.*, 2011). Impaired mineralisation could be associated with the dilution of osteogenic supplements and might be a sign that a certain threshold of osteogenic supplements is required (Ma *et al.*, 2011). Lee *et al.* (2013) investigate a medium based on full EGM-2 supplemented with standard concentrations of osteogenic additives. However, this medium fails to induce mineralisation when compared to conventional ODM. Consequently, it is hypothesised that ingredients such as FGF-2, which is present in full EGM-2, might counteract robust osteogenic differentiation (Blache *et al.*, 2016). EGM- 2 contains a complex mixture of different growth factors to support proliferation and maintenance of the endothelial phenotype and might, therefore, influence osteogenesis when used undiluted.

In light of clinical applications, it will be necessary not only to replace the serum, but also to limit the use of growth factors (GFs) to a minimum. Standard EGM-2 contains a cocktail of GFs and might be further fine-tuned and reduced to a few essential vasculogenic supplements in a combination medium. To do so, high-throughput screening platforms, such as presented by Bersini *et al.* (2016), will prove very valuable. Besides screening for 3D co-culture aspects, it will be inevitable to screen the same media as well for 2D endothelialised hydrogel surfaces.

Engineering a macrovessel-like structure in pre-vascularised, osteogenically differentiated hydrogels

To proceed to a multiscale pre-vascularised, osteogenically differentiated construct model, an ECFC-seeded channel was engineered. It was feasible to obtain endothelialised channel surfaces, as well as newly sprouted vessel-like structures into these soft, complex cellular hydrogel constructs. This result differed significantly from previous works where endothelialised channels are created either under purely vasculogenic conditions, with non-clinically- relevant fibroblast or pericyte cell lines (Kolesky *et al.*, 2016; Lee *et al.*, 2014; Miller *et al.*, 2012), or in stiff

osteogenesis-supporting matrices that do not allow for vasculogenic sprouting in the bulk hydrogel (Kolesky *et al.*, 2016).

Besides the characteristic endothelium with cobblestone morphology, capillary-like structures were also observed on the luminal side of the channel surface (not shown). These endothelial cords were only present in constructs containing MSC-ECFC co-cultures and not in ECFC-only (on the surface) constructs (not shown). ECFCs were seeded after an initial pre-differentiation phase, allowing for osteogenic differentiation and vasculogenesis to occur throughout the bulk of the hydrogel. A delay of 8 d appeared most favourable to establish an endothelium in the channel. After a pre-differentiation phase of 12 d, the channels were locally blocked by the cells and required clearing for ECFCs to be seeded. When ECFCs were seeded from the beginning in the channel of the cell-laden constructs, capillary-like monolayers were exclusively detected (data not shown), in agreement with previous studies (Bertassoni *et al.*, 2014; Byambaa *et al.*, 2017; Kazemzadeh-Narbat *et al.*, 2017; Zhu *et al.*, 2017). Surprisingly, this rather undesirable phenomenon of endothelial cords at the gel surface does not attract attention in the literature, while it seems to be an important challenge in the field. A simplified model disc was used to test whether MSC-derived cells would interfere with endothelium formation. On these discs, endothelium co-existed next to capillary-like structures, which were stabilised by α SMA-positive cells. Consequently, cell-cell contact with MSC-derived cells did not lead to disturbance of this monolayer.

The upscaled constructs exhibited an ALP activity level after 12 d that was comparable to hydrogel discs after 10 d. With a comparable hydrogel composition of 5 % gelMA (57 % DoF), the embedded rat MSCs show increased ALP activity on day 14 (Celikkin *et al.*, 2018). In the long term, this gelMA composition outperforms 10 % gelMA hydrogels in terms of the extend of calcium deposition and homogeneous distribution throughout the scaffold after 21 d (Celikkin *et al.*, 2018). In the present study, the presence of osteonectin was observed in constructs cultured for 15 d, highlighting ongoing osteogenesis along with vasculogenesis. The osteonectin staining was rather weak, which could be explained by the early time point for investigating osteogenesis. Matrix mineralisation and elevated osteogenic protein levels are normally assessed after culture periods of more than 3 weeks (Gotman *et al.*, 2013). The aim of the current study was to find a balance between two complex tissue developmental processes, vascularisation and osteogenesis, which required a pre-differentiation phase of the channelled constructs before ECFC-seeding into the channel. While the differentiation phase is relatively short to successfully prime *in vitro* osteogenesis, the optimal pre-differentiation period before implantation of such constructs remains to be investigated. Interestingly, prolonged *in vitro* cultures of MSCs in osteogenic media has a negative effect on the bone regeneration capacity in an orthotopic site (Castano-Izquierdo *et al.*, 2007). Moreover, long-term culture of these pre-vascularised constructs under static condition without perfusion is impractical, as the newly formed vessels will regress and rupture in the absence of a fluid flow (Urbaczek *et al.*, 2017). Hence, future studies will focus on a more thorough assessment of the differentiated osteogenic phenotype and mineralisation,

in combination with perfusion, for successful clinical translation of the pre-vascularised bone model reported here.

The combination of multiple human primary cells in one tissue-engineered construct resulted in a viable approach. To further proceed towards preclinical applications, next steps will lie in upscaling and also mechanically stabilising these soft constructs. For instance, a 3D bioassembly approach can be employed to anatomically populate these soft pre-vascularised gelMA tissue modules into 3D plotted thermoplastic constructs (Mekhileri *et al.*, 2018). Mechanical reinforcement can also be achieved by combining these soft gelMA hydrogels with thermoplastic materials (Schuurman *et al.*, 2011; Boere *et al.*, 2014; Visser *et al.*, 2015; Mekhileri *et al.*, 2018), to withstand the mechanical forces in a bone defect site. To further promote the construct's *in vitro* maturation prior to implantation, flow perfusion might be needed to functionally interconnect the lumina of capillaries and the central channel into an intricate network. Ultimately, the engineered macrovessel-like structures need to be anastomosed to the circulation of a host animal to aid a fast vascularisation of the construct for tissue integration.

The rationale of this study was to advance the strategy of fabricating multi-scale vascularised networks in bone tissue engineering. Subcultured primary cell types were employed to mimic the biological intricacy of this tissue engineering approach, which enabled the investigation of its feasibility and highlighted the challenges towards clinical translation. This work demonstrated the viability of combining multiple sub-cultured primary human cell types in a single relatively soft biomaterial, sharing one culture medium. Multi-cell-differentiation into all relevant lineages was successful in gelatin-based hydrogels, cultured in a tailored endothelial-osteogenic combination medium. Moreover, the presented results were reproducible for MSCs and ECFs isolated from various donors and applied in different combinations in the co-cultures, further underlining the attainability of a clinical translation.

Conclusions

A complex human tissue model was created with an endothelium-covered central channel, surrounded by stabilised capillary-like structures and osteogenic cells. The simultaneous differentiation of multiple cell types required a tailored medium, which was found in a combination of ODM and EGM-2, inducing the desired early differentiations for this tissue model. Furthermore, combining multiple clinically-relevant human primary cells in one tissue-engineered construct resulted in a viable approach. Therefore, the present work showed the feasibility of engineering complex tissue constructs, paving the way for scale-up approaches with the potential to finally overcome the challenge of vascularisation of engineered tissues.

Acknowledgements

The authors are grateful to Joao Garcia, who designed the mould to fabricate the channelled silicone moulds that were printed by Cetma (Brindisi, Italy), and Alessia Longoni for helping with the FACS analysis. Further acknowledgement goes to Chris van Dijk from Dr Caroline Cheng's group for his help in the transduction of ECFCs with GFP and Mattie van Rijen for his contributions to the histology. This research was partially funded by the European Union FP7- MC-IRSES 'SkelGEN' project under grant agreement Nr. 318553.

References

1. Au P, Tam J, Fukumura D, Jain RK (2008) Bone marrow-derived mesenchymal stem cells facilitate engineering of long-lasting functional vasculature. *Blood* 111: 4551-4558.
2. Baldwin J, Antille M, Bonda U, De-Juan-Pardo EM, Khosrotehrani K, Ivanovski S, Petcu EB, Huttmacher DW (2014) *In vitro* pre-vascularisation of tissue- engineered constructs: a co-culture perspective. *Vasc Cell* 6: 13.
3. Bersini S, Gilardi M, Arrigoni C, Talo G, Zamaï M, Zagra L, Caiolfa V, Moretti M (2016) Human *in vitro* 3D co-culture model to engineer vascularized bone-mimicking tissues combining computational tools and statistical experimental approach. *Biomaterials* 76: 157-172.
4. Bertassoni LE, Cecconi M, Manoharan V, Nikkhah M, Hjortnaes J, Cristino AL, Barabaschi G, Demarchi D, Dokmeci MR, Yang Y, Khademhosseini A (2014) Hydrogel bioprinted microchannel networks for vascularization of tissue engineering constructs. *Lab Chip* 14: 2202-2211.
5. Blache U, Metzger S, Vallmajo-Martin Q, Martin I, Djonov V, Ehrbar M (2016) Dual role of mesenchymal stem cells allows for microvascularized bone tissue- like environments in PEG hydrogels. *Adv Healthc Mater* 5: 489-498.
6. Boere KWM, Visser J, Seyednejad H, Rahimian S, Gawlitta D, van Steenberg M, Dhert WJA, Hennink WE, Vermonden T, Malda J (2014) Covalent attachment of a three-dimensionally printed thermoplast to a gelatin hydrogel for mechanically enhanced cartilage constructs. *Acta Biomater* 10: 2602-2611.
7. Bolander ME, Robey PG, Fisher LW, Conn KM, Prabhakar BS, Termine JD (1989) Monoclonal- antibodies against osteonectin show conservation of epitopes across species. *Calcif Tissue Int* 45: 74-80.
8. Butt OI, Carruth R, Kutala VK, Kuppasamy P, Moldovan NI (2007) Stimulation of peri-implant vascularization with bone marrow-derived progenitor cells: monitoring by *in vivo* EPR oximetry. *Tissue Eng* 13: 2053-2061.
9. Byambaa B, Annabi N, Yue K, Trujillo-de Santiago G, Alvarez MM, Jia W, Kazemzadeh-Narbat M, Shin SR, Tamayol A, Khademhosseini A (2017) Bioprinted osteogenic and vasculogenic patterns for engineering 3D bone tissue. *Adv Healthc Mater* 16. DOI: 10.1002/ adhm.201700015.
10. Carmeliet P, Jain RK (2000) Angiogenesis in cancer and other diseases. *Nature* 407: 249-257.

11. Castano-Izquierdo H, Alvarez-Barreto J, van den Dolder J, Jansen JA, Mikos AG, Sikavitsas VI (2007) Pre-culture period of mesenchymal stem cells in osteogenic media influences their in vivo bone forming potential. *J Biomed Mater Res A* 82: 129-138.
12. Celikkin N, Mastrogiacomo S, Jaroszewicz J, Walboomers XF, Swieszkowski W (2018) Gelatin methacrylate scaffold for bone tissue engineering: the influence of polymer concentration. *J Biomed Mater Res A* 106: 201-209.
13. Chen YC, Lin RZ, Qi H, Yang Y, Bae H, Melero-Martin JM, Khademhosseini A (2012) Functional human vascular network generated in photocrosslinkable gelatin methacrylate hydrogels. *Adv Funct Mater* 22: 2027-2039.
14. de Souza LEB, Malta TM, Haddad SK, Covas DT (2016) Mesenchymal stem cells and pericytes: to what extent are they related?. *Stem Cells Dev* 25: 1843-1852.
15. Ehrbar M, Sala A, Lienemann P, Ranga A, Mosiewicz K, Bittermann A, Rizzi SC, Weber FE, Lutolf MP (2011) Elucidating the role of matrix stiffness in 3D cell migration and remodeling. *Biophys J* 100: 284-293.
16. Gawlitta D, Fledderus JO, van Rijen MH, Dokter I, Alblas J, Verhaar MC, Dhert WJ (2012) Hypoxia impedes vasculogenesis of *in vitro* engineered bone. *Tissue Eng Part A* 18: 208-218.
17. Gimbrone MA, Jr., Cotran RS, Folkman J (1974) Human vascular endothelial cells in culture. Growth and DNA synthesis. *J Cell Biol* 60: 673-684.
18. Gotman I, Ben-David D, Unger RE, Bose T, Gutmanas EY, Kirkpatrick CJ (2013) Mesenchymal stem cell proliferation and differentiation on load-bearing trabecular Nitinol scaffolds. *Acta Biomater* 9: 8440-8448.
19. Gruber R, Kandler B, Holzmann P, Vögele-Kadletz M, Losert U, Fischer MB, Watzek G (2005) Bone marrow stromal cells can provide a local environment that favors migration and formation of tubular structures of endothelial cells. *Tissue Eng* 11: 896-903.
20. Hasan A, Paul A, Memic A, Khademhosseini A (2015) A multilayered microfluidic blood vessel-like structure. *Biomed Microdevices* 17: 88.
21. Huebsch N, Arany PR, Mao AS, Shvartsman D, Ali OA, Bencherif SA, Rivera-Feliciano J, Mooney DJ (2010) Harnessing traction-mediated manipulation of the cell/matrix interface to control stem-cell fate. *Nature Materials* 9: 518-526.
22. Hung SC, Pochampally RR, Chen SC, Hsu SC, Prockop DJ (2007) Angiogenic effects of human multipotent stromal cell conditioned medium activate the PI3K-Akt pathway in hypoxic endothelial cells to inhibit apoptosis, increase survival, and stimulate angiogenesis. *Stem Cells* 25: 2363-2370.
23. Jin GZ, Han CM, Kim HW (2015) *In vitro* co-culture strategies to prevascularization for bone regeneration: a brief update. *Tissue Eng Regen Med* 12: 69-79.
24. Kanczler JM, Oreffo ROC (2008) Osteogenesis and angiogenesis: the potential for engineering bone. *Eur Cell Mater* 15: 100-114.
25. Kazemzadeh-Narbat M, Rouwkema J, Annabi N, Cheng H, Ghaderi M, Cha BH, Aparnathi M, Khalilpour A, Byambaa B, Jabbari E, Tamayol A, Khademhosseini A (2017) Engineering photocrosslinkable bicomponent hydrogel constructs for creating 3D vascularized bone. *Adv Healthc Mater* 6. DOI: 10.1002/adhm.201601122.
26. Klotz BJ, Gawlitta D, Rosenberg AJWP, Malda J, Melchels FPW (2016) Gelatin-methacryloyl hydrogels: towards biofabrication-based tissue repair. *Trends Biotechnol* 34: 394-407.
27. Kolbe M, Xiang Z, Dohle E, Tonak M, Kirkpatrick CJ, Fuchs S (2011) Paracrine effects influenced by cell culture medium and consequences on microvessel-like structures in

- cocultures of mesenchymal stem cells and outgrowth endothelial cells. *Tissue Eng Part A* 17: 2199-2212.
28. Kolesky DB, Homan KA, Skylar-Scott MA, Lewis JA (2016) Three-dimensional bioprinting of thick vascularized tissues. *Proc Natl Acad Sci U S A* 113: 3179-3184.
 29. Kolesky DB, Truby RL, Gladman AS, Busbee TA, Homan KA, Lewis JA (2014) 3D bioprinting of vascularized, heterogeneous cell-laden tissue constructs. *Adv Mater* 26: 3124-3130.
 30. Koshy ST, Ferrante TC, Lewin SA, Mooney DJ (2014) Injectable, porous, and cell-responsive gelatin cryogels. *Biomaterials* 35: 2477-2487.
 31. Lafage-Proust MH, Roche B, Langer M, Cleret D, Vanden Bossche A, Olivier T, Vico L (2015) Assessment of bone vascularization and its role in bone remodeling. *Bonekey Rep* 4: 662.
 32. Langer RS, Vacanti JP (1999) Tissue engineering: the challenges ahead. *Sci Am* 280: 86-89.
 33. Lee JH, Kim SW, Kim UK, Oh SH, June-Kim S, Park BW, Kim JH, Hah YS, Kim DR, Rho GJ, Maeng GH, Jeon RH, Lee HC, Kim JR, Kim GC, Byun JH (2013) Generation of osteogenic construct using periosteal-derived osteoblasts and polydioxanone/ pluronic F127 scaffold with periosteal-derived CD146 positive endothelial-like cells. *J Biomed Mater Res A* 101: 942-953.
 34. Lee VK, Lanzi AM, Ngo H, Yoo SS, Vincent PA, Dai GH (2014) Generation of multi-scale vascular network system within 3D hydrogel using 3D bio-printing technology. *Cell Mol Bioeng* 7: 460-472.
 35. Levenberg S, Rouwkema J, Macdonald M, Garfein ES, Kohane DS, Darland DC, Marini R, van Blitterswijk CA, Mulligan RC, D'Amore PA, Langer R (2005) Engineering vascularized skeletal muscle tissue. *Nat Biotechnol* 23: 879-884.
 36. Lim KS, Alves MH, Poole-Warren LA, Martens PJ (2013) Covalent incorporation of non-chemically modified gelatin into degradable PVA-tyramine hydrogels. *Biomaterials* 34: 7097-7105.
 37. Lim KS, Kundu J, Reeves A, Poole-Warren LA, Kundu SC, Martens PJ (2012) The influence of silkworm species on cellular interactions with novel PVA/silk sericin hydrogels. *Macromol Biosci* 12: 322- 332.
 38. Loessner D, Meinert C, Kaemmerer E, Martine LC, Yue K, Levett PA, Klein TJ, Melchels FPW, Khademosseini A, Huttmacher D W (2016) Functionalization, preparation and use of cell-laden gelatin methacryloyl-based hydrogels as modular tissue culture platforms. *Nature Protocols* 11: 727-746.
 39. Ma J, van den Beucken JJ, Yang F, Both SK, Cui FZ, Pan J, Jansen JA (2011) Coculture of osteoblasts and endothelial cells: optimization of culture medium and cell ratio. *Tissue Eng Part C Methods* 17: 349-357.
 40. Mekhileri NV, Lim KS, Brown GCJ, Mutreja I, Schon BS, Hooper GJ, Woodfield TBF (2018) Automated 3D bioassembly of micro-tissues for biofabrication of hybrid tissue engineered constructs. *Biofabrication* 10: 024103.
 41. Miller JS, Stevens KR, Yang MT, Baker BM, Nguyen DH, Cohen DM, Toro E, Chen AA, Galie PA, Yu X, Chaturvedi R, Bhatia SN, Chen CS (2012) Rapid casting of patterned vascular networks for perfusable engineered three-dimensional tissues. *Nat Mater* 11: 768-774. Nguyen AH, McKinney J, Miller T, Bongiorno T, McDevitt TC (2015) Gelatin methacrylate microspheres for controlled growth factor release. *Acta Biomater* 13: 101-110.
 42. Nandi S, Winter HH (2005) Swelling behavior of partially cross-linked polymers: a ternary system. *Macromolecules* 38: 4447-4455.

43. Nichol JW, Koshy ST, Bae H, Hwang CM, Yamanlar S, Khademhosseini A (2010) Cell-laden microengineered gelatin methacrylate hydrogels. *Biomaterials* 31: 5536-5544.
44. Niemisto A, Dunmire V, Yli-Harja O, Zhang W, Shmulevich I (2005) Robust quantification of *in vitro* angiogenesis through image analysis. *IEEE Transactions on Medical Imaging* 24: 549-553.
45. Nilasaroya A, Poole-Warren LA, Whitelock JM, Martens PJ (2008) Structural and functional characterisation of poly(vinyl alcohol) and heparin hydrogels. *Biomaterials* 29: 4658-4664.
46. Occhetta P, Visone R, Russo L, Cipolla L, Moretti M, Rasponi M (2015) VA-086 methacrylate gelatine photopolymerizable hydrogels: a parametric study for highly biocompatible 3D cell embedding. *J Biomed Mater Res A* 103: 2109-2117.
47. Rouwkema J, Khademhosseini A (2016) Vascularization and angiogenesis in tissue engineering: beyond creating static networks. *Trends Biotechnol* 34: 733-745.
48. Schuurman W, Christov V, Pot MW, van Weeren PR, Dhert WJ, Malda J (2011) Bioprinting of hybrid tissue constructs with tailorable mechanical properties. *Biofabrication* 3: 021001.
49. Tan S, Fang JY, Yang Z, Nimni ME, Han B (2014) The synergetic effect of hydrogel stiffness and growth factor on osteogenic differentiation. *Biomaterials* 35: 5294-5306.
50. Unger RE, Dohle E, Kirkpatrick CJ (2015) Improving vascularization of engineered bone through the generation of pro-angiogenic effects in co-culture systems. *Adv Drug Deliv Rev* 94: 116-125.
51. Urbaczek AC, Leao P, Souza FZR, Afonso A, Vieira Alberice J, Cappelini LTD, Carlos I Z, Carrilho E (2017) Endothelial cell culture under perfusion on a polyester-toner microfluidic device. *Sci Rep* 7: 10466.
52. Van den Bulcke AI, Bogdanov B, De Rooze N, Schacht EH, Cornelissen M, Berghmans H (2000) Structural and rheological properties of methacrylamide modified gelatin hydrogels. *Biomacromolecules* 1: 31-38.
53. Visser J, Melchels FPW, Jeon JE, van Bussel EM, Kimpton LS, Byrne HM, Dhert WJA, Dalton PD, Hutmacher DW, Malda J (2015) Reinforcement of hydrogels using three-dimensionally printed microfibrils. *Nat Commun* 6: 6933. Wen JH, Vincent LG, Fuhrmann A, Choi YS, Hribar KC, Taylor-Weiner H, Chen S, Engler AJ (2014) Interplay of matrix stiffness and protein tethering in stem cell differentiation. *Nat Mater* 13: 979-987.
54. Zheng Y, Chen J, Lopez JA (2015) Flow-driven assembly of VWF fibres and webs in *in vitro* microvessels. *Nat Commun* 6: 7858.
55. Zhu W, Qu X, Zhu J, Ma X, Patel S, Liu J, Wang P, Lai CS, Gou M, Xu Y, Zhang K, Chen S (2017) Direct 3D bioprinting of prevascularized tissue constructs with complex microarchitecture. *Biomaterials* 124: 106-115.

Chapter 7

General discussion and future perspectives



Gelatin-based hydrogel platforms: biomaterial perspective

Gelatin-based hydrogels are attractive for tissue engineering purposes due to the intrinsic biological activity of the material, the biodegradability, the limited immunogenicity and its clinical applicability. To form thermally stable hydrogels at body temperature, it is required to crosslink the gelatin chains. In this thesis, multiple ways of crosslinking were optimised and evaluated for application in pre-vascularised bone tissue engineering. Besides the method of gelatin crosslinking, also the source of the material is critical for mechanical and biological properties of the resulting hydrogel.

Currently, functionalisation of gelatin with methacryloyl (gelMA) is probably the most often used method to form stable gelatin hydrogels in tissue engineering. While it is used for engineering of multiple tissue types, ranging from soft to stiff tissues, it was investigated whether the material is equally suitable for engineering of all tissue types (**Chapter 2**) [1]. From this work it became apparent that the latter is not the case, since soft hydrogel designs with relatively low polymer and crosslinking concentrations result in instable hydrogels (**Chapter 6**) [2, 3]. While these soft and instable hydrogels allow for maximum water content and therefore freedom for cells to migrate, the use of these materials is limited. Especially for biofabrication purposes, this shape instability is critical and asks for novel strategies to solve the discrepancy between maximal cell movement in a hydrogel and its shape fidelity [4]. While it was shown in **Chapter 6**, that it is feasible to use gelMA to create soft hydrogels and also for creating macrochannels, there are still numerous challenges left. Construct stability is critically impaired at low concentrations and crosslink density, which is seen by a clear shrinking of the engineered construct over culture time. During the contraction of the hydrogels, pre-vascular networks regressed and initially elongated cells became round. It is suggested that the degradation of the material is faster than the secretion of novel matrix by the residing cells. It is known that biologic materials are associated with fast degradation properties. A solution to overcome this obstacle was presented previously by a combination of gelMA with PEG to slow down the degradation process [5, 6] and by this better balance matrix degradation and deposition.

While UV-induced crosslinking is still the gold standard for crosslinking of gelMA, it might be replaced in the future by visible light-based crosslinking systems. The latter are considered safer, are more flexible with high light intensities and therefore overall faster and more efficient in crosslinking of up-scaled hydrogel constructs (**Chapter 3**) [7]. Moreover, the light penetration depth of UV light is limited and by using photo-initiators in the visible light spectrum both problems could be overcome (**Chapter 3**). A good light penetration depth of the crosslinking system is especially important for upscaling of a hydrogel construct to a clinically relevant size. Moreover, the biological performance of encapsulated cells is increased when the hydrogel is crosslinked by visible compared to UV-light, as discussed below. Overall, gelMA base-material is an easily synthesised material, which is by now commercially available. While the light-induced crosslinking is valuable for multiple

biofabrication approaches, it is limited for moulding approaches. Especially, in combination with non-transparent materials, *e.g.* a rod to create a channel, a “shadow-zone” is created were full crosslinking of the hydrogel is hampered. Based on these named disadvantages of photo-crosslinked gelMA hydrogels for pre-vascularised bone tissue engineering, we moved further towards the exploration of enzymatically crosslinked gelatin hydrogels.

Gelatin crosslinked by microbial transglutaminase (gelTG) was introduced in 2004 by McDermott and colleagues [8]. The beneficial properties of this hydrogel platform are its low cost and the ease of access of the required components [8]. Furthermore, this crosslinking process is occurring under physiological conditions and natural materials, which makes it especially cell-friendly. However, gelTG hydrogels are less tuneable than gelMA, since mainly the gelatin concentration can be varied in order to adapt the physico-mechanical characteristics of the resulting hydrogel. Alternatively it would also be possible to vary the gelatin source. For instance gelatin can be selected based on the average molecular weight of the batch, however, this is an impractical approach. This means that especially for the creation of soft hydrogels, as needed for pre-vascularised tissue engineering approaches, very low gelatin concentrations have to be used. The drawback of these very low polymer concentrations of natural materials is that they are more susceptible to proteolytic attack resulting in the degradation of the material. Furthermore, the reproducibility of the crosslinking speed is limited, which was illustrated by the observed high standard deviations of the gelation points (**Chapter 4**). Moreover, the microbial origin of the transglutaminase might hamper future clinical translation of the hydrogel platform.

To address these challenges of premature hydrogel degradation and to move towards a clinically-relevant material, we developed a novel hydrogel platform. This system was based on gelatin and PEG, crosslinked enzymatically by a very specific transglutaminase, factor XIIIa. PEG was added as a bio-inert base-material for slower degradation properties of the resulting hydrogel. Gelatin was kept as a base-material due to its biofunctionality. For crosslinking between these polymers, factor XIIIa was used due to its safe and highly specific crosslinking mechanism and already existing FDA-approval for its injection into the blood stream.

For soft tissue engineering approaches, these gelPEG hydrogels appeared suitable. It was possible to create hydrogels with polymer concentrations as low as 2% w/v. Such low polymer concentrations allow for maximum water content and therefore freedom for cells to migrate whilst retaining construct integrity. Compared to Matrigel, a completely biologic soft hydrogel that is widely used in 3D tissue culture, it became apparent that gelPEG hydrogels have a significantly better stability over culture time, as shown by having at least twice the height of Matrigel hydrogel droplets after 2 weeks of culture (**Chapter 5**). Moreover, the ease in tuning the mechanical properties at a low polymer concentration is an advantage of the gelPEG platform compared to gelMA or gelTG.

Gelatin-based hydrogel platforms: cell-perspective

Besides the biomaterial aspects the cell performance is key in the different gelatin-based hydrogels. The source of gelatin can be varied and has been shown to have an effect on cell performance. Gelatin is conventionally derived from collagen type I, the most abundant protein in the body. However, besides its source (*e.g.* porcine, bovine, fish) also the extraction procedure is influencing the characteristics. Basic treatment of collagen results in a net negatively charged gelatin at physiological pH, whereas acid treatment results in a positively charged molecule

In this thesis, for gelMA and gelTG hydrogels the same gelatin source from porcine skin was used, which was acid-extracted (type A). For gelPEG hydrogels, however, gelatin type B was used. While vasculogenesis occurred in all hydrogel platforms to some degree, the degree of osteogenesis was clearly different. GelTG hydrogels showed the slowest osteogenic differentiation followed by gelMA. GelPEG showed the most pronounced osteogenic differentiation and was the only hydrogel platform where mineralisation of the matrix was visible over a 2-week culture time. Indeed, it has been shown that the negative charge of gelatin provides nucleation sites for calcium phosphates and therefore might be especially suitable for bone tissue engineering [9]. While gelMA could be prepared from any gelatin source (with lysine residues), TG-mediated crosslinking is not possible with type B gelatin due to the hydrolysed amide groups of glutamine residues [10, 11].

Immobilisation of tissue-specific proteins in gelatin-hydrogels

The immobilisation of extracellular matrix (ECM)-derived proteins into a biomaterial is a promising way to fabricate hydrogels that mimic the native environment of the natural ECM biologically and structurally [12]

There are various strategies to functionalise proteins with crosslinkable chemical groups such as with methacrylate or sulfhydryl groups (also known as thiols) [13, 14]. Moreover, proteins or peptides can be synthetically or recombinantly produced with a linker that can be used for immobilisation in a hydrogel [15, 16]. Generally, the modification of proteins of interest is laborious [17, 18] and might result in inactive proteins due to the chemical processing. Furthermore, the modified proteins might have to be tested separately in FDA-approval procedures before they are admissible for clinical use. Therefore, it is an attractive approach to immobilise unmodified proteins in a gelatin-based hydrogel network. In gelatin hydrogels that were crosslinked with microbial TG, however, it is expected that the immobilisation resulted in an inactivation of the built-in protein (**Chapter 4**). It was described previously, that incorporation of growth factors, for example, can lead to a short term inactivation which could be restored after degradation of the matrix and cleavage of the protein from the hydrogel network [19]. In contrast to gelTG, in gelPEG hydrogels incorporation of laminins led to functional built-in proteins (**Chapter 5**). The difference might lie in the type of the used transglutaminase. FXIIIa

can only crosslink general lysines and not general glutamines, since the very specific sequence around glutamines required for recognition by FXIIIa is naturally not or not much present on laminins. This might result in less extensive coupling of all the lysines of the protein to the network, which might contribute to retaining the bioactivity of the laminins. Therefore, gelPEG hydrogels are an attractive material that offers the option to incorporate any lysine-containing protein to create a hydrogel with a tissue-specific ECM

Soft hydrogel design as an ECM-analogue

Hydrogels with a high water retention capacity are strongly mimicking (developing) biological tissues. During tissue development or repair a soft matrix or callus is remodelled into a mature tissue with varying stiffness ranging from soft brain to stiffer bone tissue/osteoid. In tissue engineering, this developing process might be mimicked by the use of low concentration polymer (soft) hydrogels. While this approach might not be needed for avascular tissues, for the parallel development of a capillary network, a soft matrix with an elastic modulus of under 4 kPa is required. Currently there is a controversy, whether hydrogel stiffness, pore size or anchoring points for cells are determining the stem cell fate- most likely, all of them play a role. While there is a vast amount of literature that shows that higher stiffness of a material is positively correlated with osteogenesis [19, 20], it is also possible to engineer osteogenically differentiated tissue-like constructs starting from soft materials [2, 21]. It is a logical approach to engineer bone starting from a soft material, since also during development bone is starting from osteoid which is softer than mineralised bone. Interestingly, it was shown for gelMA hydrogels, that 5% gelMA outperformed 10% gelMA for osteogenesis. While 10% gelMA had a stiffness of 10 kPa, 5% hydrogels only reached 2.5 kPa. In 5% gelMA hydrogels, a more homogenous, mineralised ECM was detected than in 10% gelMA, which was related to the lower degree of functionalisation [22]. Moreover, recently it was established that stress relaxation properties of a hydrogel are also influencing the differentiation potential of the encapsulated cells [23]. The gelPEG platform presented in this thesis, showed remarkable osteogenic differentiation in soft hydrogels (**Chapter 5**). It is known that endothelial cells enhance the osteogenic potential *in vitro* [24] and the gelatin source probably mostly affects the mineralisation of the matrix. Consequently, it is apparent that a combination of multiple factors influences the development of vascularised bone tissue, however, the use of soft hydrogels to achieve parallel vascularisation is essential

In vivo experiments will show, whether osteogenesis can be enhanced in soft gelPEG hydrogels. For these approaches, the right pre-culturing time of the cell-seeded constructs needs to be determined before implantation to find the optimal window for continued bone-formation *in vivo*. Interestingly, extended *in vitro* pre-culture times were previously shown to have a negative effect on bone formation [25]. Furthermore, osteogenesis might be additionally stimulated in gelPEG hydrogels by the addition of osteoinductive calcium phosphates or osteostimulatory proteins.

Multiscale vascularised bone-like constructs

It is believed that the simultaneous development of vasculature and tissue specific maturation is a promising approach in tissue engineering of clinically-relevant sized constructs [26, 27]. Such large constructs require the presence of a vascular tree, which can be enabled by the fabrication of macrovessels and by the self-assembly of endothelial cells into capillary-like structures [28]

We showed for the first time that it is feasible to create such constructs which are composed of a multiscale vascular network in an osteogenically differentiated bulk hydrogel (**Chapter 6**). It is possible within one material to allow for endothelialisation, vascularisation and osteogenesis using clinically-relevant primary stem cells. Besides selecting a suitable biomaterial, also the choice of culture medium is essential to guide all lineage commitments within one construct simultaneously. To show the feasibility, for this study gelMA hydrogels were used. For future studies it will be beneficial to use hydrogels for this approach that allow for osteogenesis and vascularisation of higher quality compared to the levels obtained in gelMA. Also, it is important to use a hydrogel that has an adequate degradation rate which prevents construct contraction by the embedded cells and stays mechanically stable over culture time. For instance gelPEG hydrogels proved in this thesis to be superior compared to gelMA and meet previously mentioned requirements. Moreover, for the here applied moulding approaches, enzymatic crosslinking would be more practical than light-induced crosslinking, since all areas in the construct can be reached and crosslinked. Further challenges, to be addressed in the future are related to the reproducibility of endothelium formation in the macrochannels and the assessment of their impermeability. Additional challenges are arising when aiming at clinically-relevant sized tissue analogues. Upscaling to cm-size requires enhanced architectural stability and a complex pre-vascular network composed of macrovessels and capillaries. After establishment of such a complex large size tissue analogues, perfusion will allow to achieve matured large tissue analogues, ready for implantation [27].

Towards reinforcement and up-scaling of gelatin-based hydrogels

Biofabrication is an emerging field that integrates the assembly and maturation of complex cell-containing tissue constructs [29]. With these techniques, there is the possibility of creating complex tissue-like constructs with multiple layers and high spatial resolution. In this thesis, the focus was mainly on the cell-material aspects in model tissues with the idea to first address the stimulation of cells towards the desired phenotypes. The next challenge will be to shape these materials with state-of-the-art biofabrication techniques. To do so, the described materials need to be optimised with regard to their printability. Alternatively, moulding approaches could be combined with bioprinting as it is often done [28, 30, 31]. The matrices investigated and engineered in this thesis should ideally represent the ECM-like compartment as suggested by Kolesky and co-workers who distributed different aspects of a

tissue over multiple bioinks [30]. Multiple inks could fulfil different requirements in order to realise up-scaled, complex tissue-like constructs. By this, stabilisation of the construct can be separated from the bulk material in which the cells are residing, which needs to be relatively soft (unstable) for most tissue engineering approaches. Thermoplastic grid-like structures have been shown to enhance the mechanical stability of cell-laden hydrogels [32-34]. To create macrochannels that allow for immediate construct perfusion, pluronics has been successfully employed ([30, 31] *e.g.*) and realised an up-scaled version of the macrovessel fabricated in **Chapter 6**. Alternatively, poly(vinylidene fluoride) (PVDF) was successfully used to build a sacrificial channel template of the main vascular network [35]. After printing a thermoplastic grid for mechanical stability and a sacrificial template for the macrovessels of a vascular bed, an ECM-like material, such as gelPEEG, which was developed in this thesis, could be moulded around these structures. As mentioned before, for such moulding approaches enzymatic crosslinking as applied with gelPEEG will be most ideal, to be able to crosslink the entire construct. There will be no “shadow zone” underneath light-impermeable materials when employing an external light source. Theoretically it might be possible to crosslink the hydrogel in a layer-by-layer approach, however, still there will be zones that cannot be reached by the light and the step-by-step crosslinking will extend the printing time and allow for cell sagging.

After assembly and maturation of such complex tissue analogues *in vitro*, the next step will lie in *in vivo* studies. Such studies will allow answering the question ‘how much predefined architectural complexity such a 3D tissue analogue would require and to what extent the encapsulated cells could take over the tissue formation process to result in a functional tissue replacement’ [1].

Pre-clinical considerations of pre-vascularised bone constructs

When working on the realisation of such complex and up-scaled tissue analogues, it is also important to consider the translatability of the taken approach. Which requirements need to be met in order to be able to proceed ultimately towards clinical application? Such biofabricated tissue constructs, are considered as Advanced Therapy Medicinal Products (ATMPs). The clinical applicability might be more easily achieved by constructs which are printed without cells. The cell-laden hydrogels might be added after the printing process by moulding to circumvent possible restrictions in the additional handling and manipulation of stem cells.

When using gelMA hydrogels, crosslinked by UV light and Irgacure 2959 free radicals will be generated to initiate polymerisation and also non-degradable polymer chains will be developed [36]. However, by using *e.g.* visible light and the Ru/SPS initiation system as introduced in **Chapter 3**, this limitation might be overcome, since it allows for crosslinking at a less energetic irradiation than UV light [7]. Ultimately, however, physiological enzymatic crosslinking might prove safer than radical-induced crosslinking of hydrogels laden with stem cells.

For this thesis, ECFCs and MSCs were chosen as clinically-relevant cell sources. Ideally, autologous MSCs and ECFCs would be used for a patient in need of a vascularised bone tissue analogue. While the use of MSCs is already routine in human clinical trials, the use of ECFCs is not translated yet to the same extent. Currently, the clinical application of ECFCs is limited by challenges regarding time and efficacy of cell isolation and expansion from peripheral blood [37]. Furthermore, the required animal derived reagents (such as growth factors) during cell culture need to be replaced [37].

The use of the gelPEG platform is promising with regard to its translatability. The used gelatin source is already FDA approved and the used crosslinking agent FXIII is a medicinal product (used as an injection into the bloodstream) for patients with blood coagulation disorder. While the here used FXIIIa is derived from human serum which might be a risk for disease-transfer, in future a recombinant version of the enzyme might be preferable. The here used laminins are animal-component-free and the laminin 521 is already available in cell therapy grade. Also, the PEG used in the studies described is medical grade, however, the modification of PEG with a peptide would require clinical translation. Potential regulatory hurdles of translating the gelPEG platform to the clinics might lie in the complexity of the crosslinking platform. It is a multi-component crosslinking system and not just the single factors but also the combination would require a FDA-approval. For above named reasons and in case of successful animal testing, this platform would have a good starting position to fulfill the requirements towards a successful ATMP.

Concluding remarks and future outlook

In this thesis, pre-existing gelatin-based hydrogels were evaluated regarding their suitability as matrices for the engineering of vascularised bone. Moreover, a gelatin-PEG based hydrogel system (gelPEG) was newly developed to address the shortcomings of available gelatin-based hydrogel platforms. While gelMA and gelTG hydrogels were limited for the intended application, the newly developed matrix material proved to be adequately soft with a suitable speed of cell-mediated degradation, which allows for differentiation towards the vasculogenic and osteogenic lineages. Moreover, the developed gelPEG platform could also be applied for other tissue culture techniques, such as for liver organoids, which are currently done in Matrigel, a mouse-tumour-based matrix. Importantly, this novel tailorable hydrogel is easily customised with tissue-specific cues that might prove valuable for other tissue engineering approaches that combine pre-vascularisation approaches with tissue-specific tissue development. Moreover, in this thesis the feasibility was demonstrated to use clinically-relevant stem cells for the generation of complex multiscale vascularised bone-like tissue constructs. The next steps will lie in perfusion of such constructs and *in vivo* models to explore questions, such as how much predeveloped complexity of such tissue engineered constructs is needed to serve the goal to repair and restore the function of damaged tissue platforms, such as the in this thesis developed gelPEG system, might serve as a stepping stone to bridge the gap between tissue engineering at the laboratory bench and clinically relevant *in vivo* models.

References

1. Klotz, B.J., et al., *Gelatin-Methacryloyl Hydrogels: Towards Biofabrication-Based Tissue Repair*. Trends in Biotechnology, 2016. **34**(5): p. 394-407.
2. Klotz, B.J., et al., *Engineering of a complex bone tissue model with endothelialised channels and capillary-like networks*. Eur Cell Mater, 2018. **35**: p. 335-348.
3. Chen, Y.C., et al., *Functional Human Vascular Network Generated in Photocrosslinkable Gelatin Methacrylate Hydrogels*. Adv Funct Mater, 2012. **22**(10): p. 2027-2039.
4. Malda, J., et al., *25th anniversary article: Engineering hydrogels for biofabrication*. Adv Mater, 2013. **25**(36): p. 5011-28.
5. Hutson, C.B., et al., *Synthesis and characterization of tunable poly(ethylene glycol): gelatin methacrylate composite hydrogels*. Tissue Eng Part A, 2011. **17**(13-14): p. 1713-23.
6. Daniele, M.A., et al., *Interpenetrating networks based on gelatin methacrylamide and PEG formed using concurrent thiol click chemistries for hydrogel tissue engineering scaffolds*. Biomaterials, 2014. **35**(6): p. 1845-1856.
7. Lim, K.S., et al., *New Visible-Light Photoinitiating System for Improved Print Fidelity in Gelatin-Based Bioinks*. ACS Biomaterials Science & Engineering, 2016. **2**(10): p. 1752-1762.
8. McDermott, M.K., et al., *Mechanical properties of biomimetic tissue adhesive based on the microbial transglutaminase-catalyzed crosslinking of gelatin*. Biomacromolecules, 2004. **5**(4): p. 1270-1279.
9. Zhu, P.X., Y. Masuda, and K. Koumoto, *The effect of surface charge on hydroxyapatite nucleation*. Biomaterials, 2004. **25**(17): p. 3915-3921.
10. Rosseinsky, D.R., *Encyclopedia of Polymer Science and Engineering, 2nd Edition - Kroschwitz, Ji. Nature*, 1989. **339**(6222): p. 268-269.
11. Crescenzi, V., A. Francescangeli, and A. Taglienti, *New gelatin-based hydrogels via enzymatic networking*. Biomacromolecules, 2002. **3**(6): p. 1384-1391.
12. Daniele, M.A., et al., *Interpenetrating networks based on gelatin methacrylamide and PEG formed using concurrent thiol click chemistries for hydrogel tissue engineering scaffolds*. Biomaterials, 2014. **35**(6): p. 1845-56.
13. Visser, J., et al., *Crosslinkable Hydrogels Derived from Cartilage, Meniscus, and Tendon Tissue*. Tissue Engineering Part A, 2015. **21**(7-8): p. 1195-1206.
14. Bertlein, S., et al., *Thiol-Ene Clickable Gelatin: A Platform Bioink for Multiple 3D Biofabrication Technologies*. Adv Mater, 2017. **29**(44).
15. Zisch, A.H., et al., *Cell-demanded release of VEGF from synthetic, biointeractive cell-ingrowth matrices for vascularized tissue growth*. Faseb Journal, 2003. **17**(13): p. 2260+.
16. Metzger, S., et al., *Cell-Mediated Proteolytic Release of Growth Factors from Poly(Ethylene Glycol) Matrices*. Macromol Biosci, 2016. **16**(11): p. 1703-1713.
17. Lin, C.C. and K.S. Anseth, *Controlling Affinity Binding with Peptide-Functionalized Poly(ethylene glycol) Hydrogels*. Adv Funct Mater, 2009. **19**(14): p. 2325.
18. Lienemann, P.S., M.P. Lutolf, and M. Ehrbar, *Biomimetic hydrogels for controlled biomolecule delivery to augment bone regeneration*. Adv Drug Deliv Rev, 2012. **64**(12): p. 1078-89.
19. Tan, S., et al., *The synergetic effect of hydrogel stiffness and growth factor on osteogenic differentiation*. Biomaterials, 2014. **35**(20): p. 5294-5306.
20. Sun, M., et al., *Effects of Matrix Stiffness on the Morphology, Adhesion, Proliferation and Osteogenic Differentiation of Mesenchymal Stem Cells*. Int J Med Sci, 2018. **15**(3): p. 257-268.

21. Blache, U., et al., *Dual Role of Mesenchymal Stem Cells Allows for Microvascularized Bone Tissue-Like Environments in PEG Hydrogels*. *Adv Healthc Mater*, 2016. **5**(4): p. 489-98.
22. Celikkin, N., et al., *Gelatin methacrylate scaffold for bone tissue engineering: The influence of polymer concentration*. *J Biomed Mater Res A*, 2018. **106**(1): p. 201-209.
23. Rosales, A.M. and K.S. Anseth, *The design of reversible hydrogels to capture extracellular matrix dynamics*. *Nature Reviews Materials*, 2016. **1**(2).
24. Thebaud, N.B., et al., *Whatever their differentiation status, human progenitor derived - or mature - endothelial cells induce osteoblastic differentiation of bone marrow stromal cells*. *J Tissue Eng Regen Med*, 2012. **6**(10): p. e51-60.
25. Castano-Izquierdo, H., et al., *Pre-culture period of mesenchymal stem cells in osteogenic media influences their in vivo bone forming potential*. *J Biomed Mater Res A*, 2007. **82**(1): p. 129-38.
26. Schneeberger, K., et al., *Converging biofabrication and organoid technologies: the next frontier in hepatic and intestinal tissue engineering?* *Biofabrication*, 2017. **9**(1): p. 013001.
27. Rouwkema, J. and A. Khademhosseini, *Vascularization and Angiogenesis in Tissue Engineering: Beyond Creating Static Networks*. *Trends Biotechnol*, 2016. **34**(9): p. 733-745.
28. Lee, V.K., et al., *Generation of Multi-Scale Vascular Network System within 3D Hydrogel using 3D Bio-Printing Technology*. *Cell Mol Bioeng*, 2014. **7**(3): p. 460-472.
29. Groll, J., et al., *Biofabrication: reappraising the definition of an evolving field*. *Biofabrication*, 2016. **8**(1): p. 013001.
30. Kolesky, D.B., et al., *3D bioprinting of vascularized, heterogeneous cell-laden tissue constructs*. *Adv Mater*, 2014. **26**(19): p. 3124-30.
31. Kolesky, D.B., et al., *Three-dimensional bioprinting of thick vascularized tissues*. *Proc Natl Acad Sci U S A*, 2016. **113**(12): p. 3179-84.
32. Schuurman, W., et al., *Bioprinting of hybrid tissue constructs with tailorable mechanical properties*. *Biofabrication*, 2011. **3**(2): p. 021001.
33. Boere, K.W., et al., *Covalent attachment of a three-dimensionally printed thermoplastic to a gelatin hydrogel for mechanically enhanced cartilage constructs*. *Acta Biomater*, 2014. **10**(6): p. 2602-11.
34. Visser, J., et al., *Reinforcement of hydrogels using three-dimensionally printed microfibrils*. *Nat Commun*, 2015. **6**: p. 6933.
35. Tocchio, A., et al., *Versatile fabrication of vascularizable scaffolds for large tissue engineering in bioreactor*. *Biomaterials*, 2015. **45**: p. 124-31.
36. Stichler, S., et al., *Thiol-ene Clickable Poly(glycidol) Hydrogels for Biofabrication*. *Ann Biomed Eng*, 2017. **45**(1): p. 273-285.
37. Paschalaki, K.E. and A.M. Randi, *Recent Advances in Endothelial Colony Forming Cells Toward Their Use in Clinical Translation*. *Front Med (Lausanne)*, 2018. **5**: p. 295.

Appendices

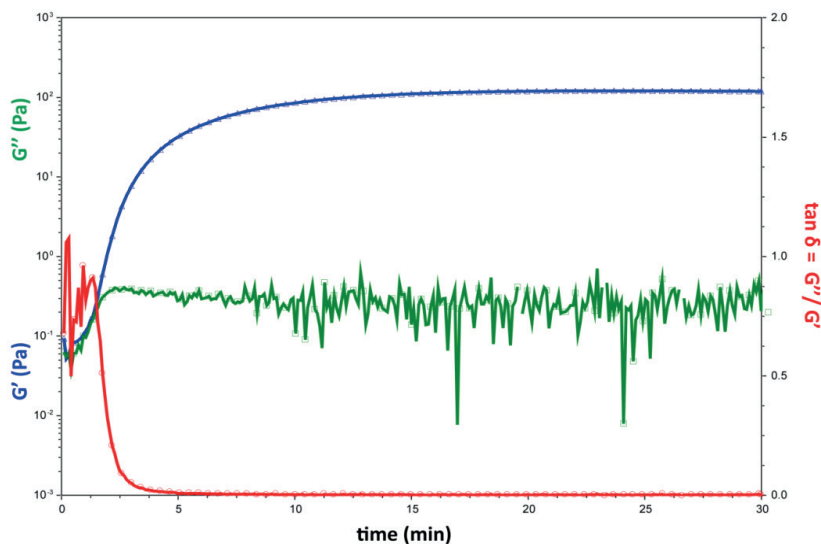


Supporting Information Chapter 6

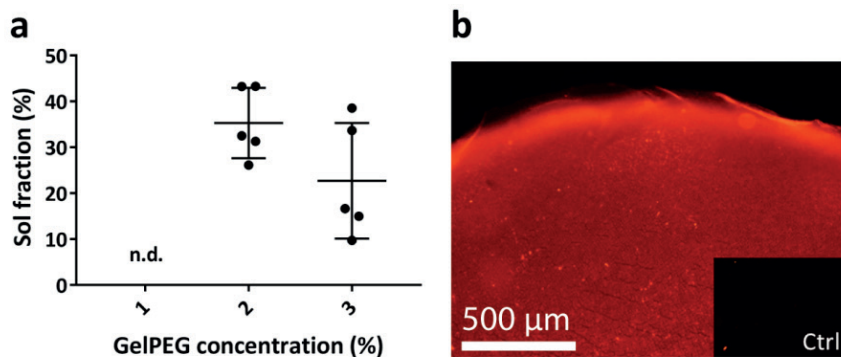
Copyright WILEY-VCH Verlag GmbH & Co. KGaA, 69469 Weinheim, Germany, 2018.

Supplementary comment 1.

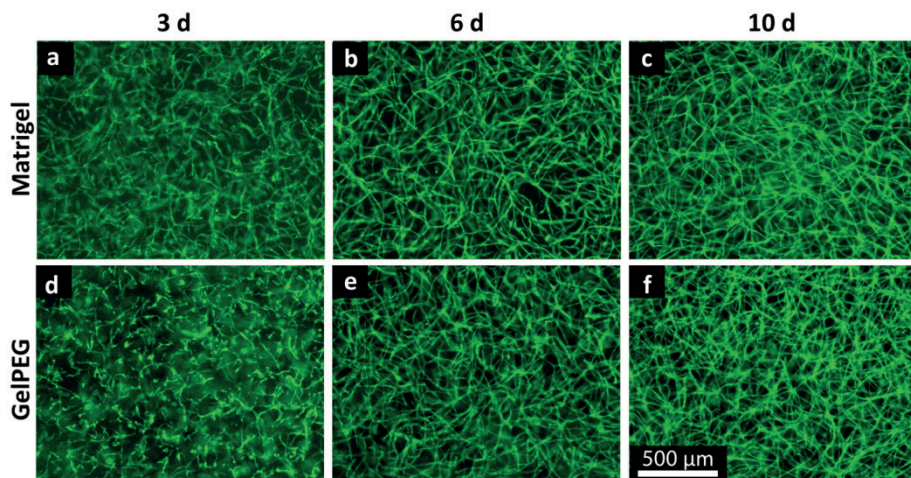
We hypothesized, that while the amino acid sequence containing a glutamine is a very specific sequence that the lysine (Lys) containing sequence is more generic. Indeed, hydrogels did not form in the absence of PEG-Gln when PEG-Lys was combined with gelatin. To exclude the formation of intramolecular crosslinks, pure gelatin was crosslinked at a concentration of 10% w/v with FXIIIa. Under present crosslinking conditions, pure gelatin did not form a hydrogel and the polymer solution remained at a low viscosity (data not shown), demonstrating the need for the substrate-specific Gln-sequence for FXIIIa mediated crosslinking.



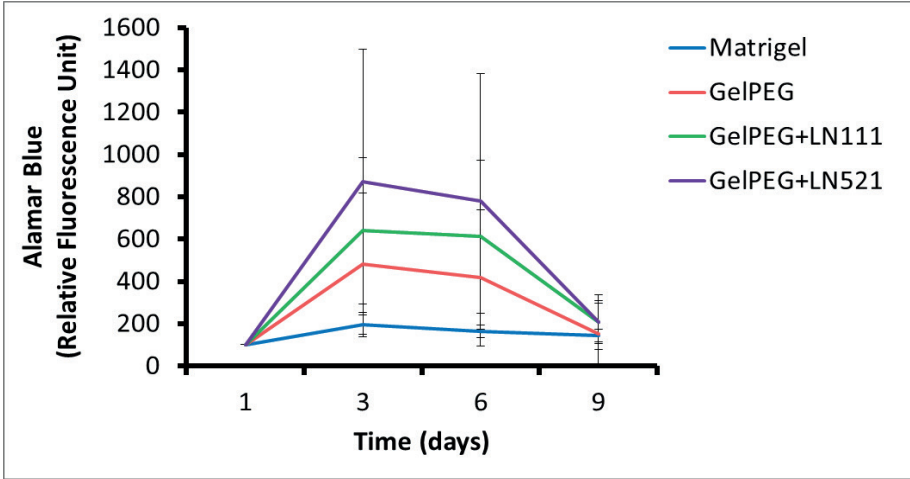
Supplementary Figure 1. Hydrogel formation of gelatin and PEG mediated by FXIIIa. The point of gelation occurred at about 2 minutes and the crosslinking was completed after about 15 minutes, when G' reached a plateau. Depicted data are from a representative measurement; $n=3$ independent experiments



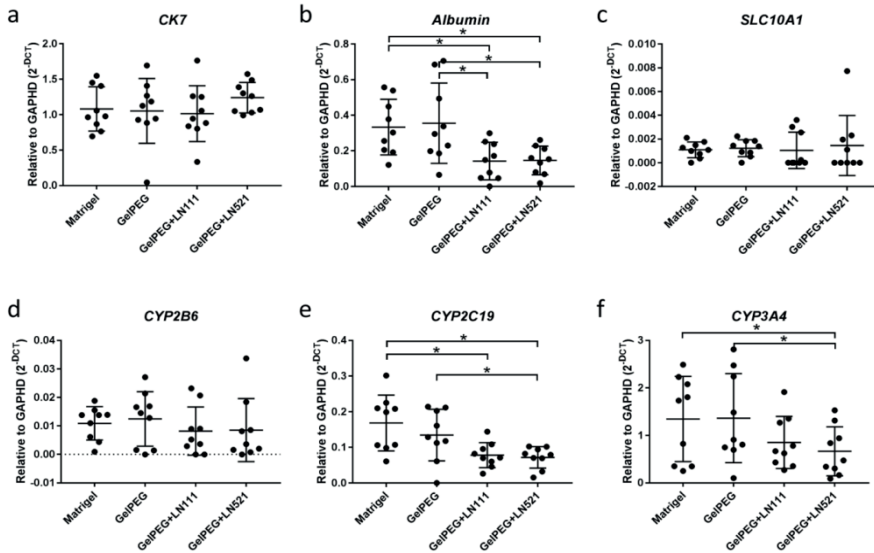
Supplementary Figure 2. Hydrogel sol fraction and LN binding in gelPEG hydrogel networks. **a** Sol fraction in dependence of gelPEG concentration. **b** Anti-LN-subunit $\alpha 5$ staining of LN521-laden 3% w/v gelPEG hydrogel compared to unloaded hydrogel (insert) after 1 d swelling in TBS. Data is depicted as mean + SD, $n = 5$



Supplementary Figure 3. Pre-vascular network formation in GFP-ECFC and MSC co-cultures under vasculogenic culture conditions. **a-c** GFP-ECFCs in Matrigel form vascular-like networks on day 3 which are remodeled up to day 10. **d-f** GFP-ECFCs in gelPEG hydrogels form vascular-like structures with an initial temporal delay, resulting in comparable networks to Matrigel on day 6 and 10. (widefield fluorescence, $N = 3$, $n = 3$)



Supplementary Figure 4. Metabolic activity of liver organoids over culture time in Matrigel and gelPEG-based hydrogels. Liver organoids exhibited an increase in metabolic activity from day 1 to 3, which gradually decreases over culture time, resulting in comparable activity levels as liver organoids cultured in Matrigel after 9 days culture. Data is depicted as mean \pm SD; $N=3$, $n=5$



Supplementary Figure 5. Gene expression levels of liver organoids that were cultured for 9 days in Matrigel and gelPEG-based hydrogels. **a** The cytokeratin *KRT7* (*CK7*) was equally expressed in all hydrogels. **b** Albumin expression was decreased in LN-laden gelPEG hydrogels. **c** *SLC10A1*, encoding a liver-specific sodium/bile acid cotransporter, was comparably expressed in all hydrogel compositions. The cytochrome family of enzymes **d** CYP2B6 **e** CYP2C19 and **f** CYP3A4 were comparably expressed in Matrigel and gelPEG, whereas LN-laden hydrogels showed partially lower expression levels. Data is depicted as mean \pm SD; $N=3$, $n=3$

Tables

Supplementary table 1. Primer sets used for qPCR analysis

Human gene	Forward primer	Reverse primer
Pre-vascularised bone:		
<i>PECAM1</i>	GCAGTGGTTATCATCGGAGTG	TCGTTGTTGGAGTTCAGAAGTG
<i>CDH5</i>	AAGCAGGCCAGGTATGAGAT	TGTGTA CTGGTCTGGGTGAAG
<i>CSPG4</i>	GAAGGAGGACGGACCTCAAG	GATCAGCTGCTCTTCCACCATT
<i>ACTA2</i>	ATGCCATCATGCGTCTGGAT	ACGCTCAGCAGTAGTAACGA
<i>BGLAP</i>	CCTCACACTCCTCGCCCTAT	GCTTGGACACAAAGGCTGCAC
<i>SPP1</i>	GCCGAGGTGATAGTGTGGTT	GTGGGTTTCAGCACTCTGGT
<i>GAPDH</i>	CAACGGATTTGGTCGTATTGGG	TGCCATGGGTGGAATCATATTGG
Liver organoids:		
<i>YWHAZ</i>	ACTTTTGGTACATTGTGGCTTCAA	CCGCCAGGACAAACCAGTAT
<i>GAPDH</i>	TGCACCACCAACTGCTTAGC	GGCATGGACTGTGGTCATGAG
<i>KRT7</i>	GGACATCGAGATCGCCACCT	ACCGCCACTGCTACTGCCA
<i>CYP2C19</i>	GGGACAGAGACAACAAGCA	CCTGGACTTTAGCTGTGACC
<i>ALB</i>	GTTCGTTACACCAAGAAAGTACC	GACCACGGATAGATAGTCTTCTG
<i>SLC10A1</i>	GATATCACTGGTGGTTCTC	ATCATCCCTCCCTTGATGAC
<i>CYP3A4</i>	CACAGGCTGTTGACCATCAT	TTTTGTCCTATAAGGGCTTT
<i>CYP2B6</i>	CTACCAAGATCAAGAGTTCCTG	ATTCAAGAAGCCAGAGAAGAG

List of abbreviations

2D	Two-dimensional
3D	Three-dimensional
α -MEM	Alpha minimal essential medium
α -SMA	Alpha smooth muscle actin
ALP	Alkaline phosphatase
Asap	L-ascorbic acid-2-phosphate
ATMP	Advanced therapy medicinal product
bFGF	Basic fibroblast growth factor
BSA	Bovine serum albumin
cDNA	Complementary deoxyribonucleic acid
DAB	Diaminobenzidine
DAPI	4, 6-diamidino-2-phenylindole
DMA	Dynamic mechanical analyser
DNA	Deoxyribonucleic acid
DoF	Degree of functionalisation
EBM	Endothelial basal medium
EC	Endothelial cell
ECFC	Endothelial colony forming cell
ECM	Extracellular matrix
EDTA	Ethylenediaminetetraacetic acid
EGM-2	Endothelial growth medium-2
EM	Expansion medium
FACS	Fluorescence-activated cell sorting
FBS	Fetal bovine serum
FGF-2	Fibroblast growth factor-2
FXIIIa	Activated factor XIII
GelMA	Gelatin-methacryloyl
GelPEG	Gelatin-poly(ethylene) glycol
GelTG	Gelatin-transglutaminase
GF	Growth factor
GFP	Green fluorescent protein
Gln	Glutamine
GMP	Good manufacturing practice
H&E	Haematoxylin and eosin
LN	Laminin
Lys	Lysine
MG	Matrigel
MMP	Matrix metallo proteinase
MNC	Mononuclear cells

MSC	Multipotent mesenchymal stromal cell
NG-2	Neural/glial antigen-2
ODM	Osteogenic differentiation medium
O-E	Osteogenic- endothelial combination medium
PBS	Phosphate-buffered saline
PCL	Poly(ϵ -caprolacton)
PCR	Polymerase chain reaction
PEG	Poly(ethylene) glycol
PVA	Polyvinylalcohol
RGD	Arginylglycylaspartic acid
RT	Room temperature
TBS	Tris-buffered saline
TG	Transglutaminase
UV light	Ultraviolet light
VE-cad	Vascular endothelial cadherin
VIS light	Visible light
vWF	Von willebrand factor
w/v	Weight/volume

Nederlandse samenvatting

Construeren van biomaterialen voor pre-vascularisatie van botanalogen

Bot is het op één na meest getransplanteerde weefsel in het menselijk lichaam. De huidige behandeling om een ontbrekend botsegment te vervangen is de transplantatie met autoloog bot. Hoewel kleinere botdefecten kunnen worden vervangen door een niet-gevasculariseerd stuk botweefsel van het patiënt, vereisen defecten van meer dan ongeveer 5 cm in lengte in de onderkaak onmiddellijke vascularisatie van het getransplanteerde bot. Daarom zijn voor dergelijke grote botdefecten zogenaamde gevasculariseerde botflappen nodig. Conventioneel worden deze gevasculariseerde lappen geoogst uit de fibula van het onderbeen, de rand van het schouderblad, of uit de kam van het bekken. Anastomose van een dergelijk relatief groot implantaat is van cruciaal belang om een onmiddellijke bloedtoevoer door de volledige dikte van het geïmplanteerde implantaat te verkrijgen en dus overleving van het implantaat mogelijk te maken. Deze reconstructieve operaties gaan gepaard met nadelen zoals morbiditeit van de donorplaats en lange operatietijd, die een belasting voor de patiënt vormen.

Het vakgebied van de tissue engineering heeft als doel om weefselsubstituten te ontwikkelen om zo de functies van het aangetaste weefsel van een patiënt te behouden, te herstellen of te verbeteren.

In de afgelopen bijna 30 jaar zijn successen geboekt in de tissue engineering van dunne, niet doorbloede weefsels en organen zoals kraakbeen, huid en blaas. Voor tissue engineering van botweefsel en andere weefsels is het belangrijkste knelpunt de benodigde vascularisatie om grotere weefselconstructen te kunnen maken. Een andere uitdaging bij het construeren van gevasculariseerde botweefsels ligt in de compositie van het dragermateriaal dat een efficiënte weefselontwikkeling mogelijk moet maken. Bovendien is, naast de gewenste biologische, mechanische en chemische kenmerken van een biomateriaal, ook de klinische toepasbaarheid cruciaal. Om deze reden werd gelatine gebruikt als basismateriaal omdat het klinisch toepasbaar geproduceerd kan worden. Daarbij worden verschillende methoden voor crosslinking van een hydrogel onderzocht en hoe, met de verschillende methoden, gevasculariseerd bot gekweekt kon worden.

In dit proefschrift wordt onderzocht of het mogelijk is om een complex botweefsel met bloedvaten te maken in het laboratorium.

In dit proefschrift is aangetoond dat het mogelijk is om met behulp van klinisch toepasbare stamcellen uit het beenmerg (multipotente mesenchymale stromale cellen, MSCs) en uit navelstrengbloed (endotheliale kolonievormende cellen, ECFCs) een complex gevasculariseerd botconstruct te kweken (**Hoofdstuk 6**). Tot dusver werd niet eerder aangetoond dat met deze primaire cellen één construct gecreëerd kon worden met de volgende eigenschappen: een met endotheelcellen

bekleed kanaal; haarvat-achtige structuren door de gehele dikte van het construct; en osteogeen (richting bot) gedifferentieerde cellen rondom de haarvatachtige structuren. Het hiervoor gebruikte dragermateriaal bestond uit gemethacryleerde gelatine (gelMA) dat gecrosslinked werd met een photoinitiator en UV licht.

In een vervolgstudie werd onderzocht, of het crosslinken met een alternatief systeem bestaande uit een photoinitiator en zichtbaar licht voordelen biedt voor celoverleving en -gedrag (**Hoofdstuk 3**). Het crosslinken met zichtbaar licht en de geselecteerde fotoinitiatoren resulteerde in een betere celfunctionaliteit dan met UV licht en fotoinitiator. Verder bleek zichtbaar licht geschikter dan UV licht om grote constructen van gelMA te crosslinken. Dit is voornamelijk van belang wanneer constructen van klinisch relevante afmetingen worden gemaakt, omdat zichtbaar licht een betere diepte penetratie heeft.

In **Hoofdstuk 4** wordt de mogelijkheid onderzocht om geprevasculariseerde bot-achtige constructen te maken door gelatine enzymatisch te crosslinken. Het voordeel van enzymatisch crosslinken met het gebruikte transglutaminase is dat dit een onderdeel is van het fysiologische collageen crosslink proces. Ook komen hierbij geen radicalen vrij zoals tijdens het photocrosslinken. Hierbij werd duidelijk, dat met transglutaminase gecrosslinkte gelatine, net als met photoinitiator en UV licht gecrosslinkt gelMA, differentiatie van de stamcellen toelaat. Echter, het bleek niet mogelijk om proteïnen functioneel in te bouwen in het hydrogel en de botvorming additioneel te kunnen stimuleren.

Verder deed zich het probleem voor dat gelMA, net als gelatine-transglutaminase gelen die puur op gelatine gebaseerd zijn, te snel afbreken om een evenwicht van gelafbraak en weefselaanmaak door de stamcellen te kunnen waarborgen. Om deze reden werd vervolgens een nieuw klinisch toepasbaar materiaal ontwikkelt, dat de biologische kenmerken vertoont van de gouden standard (Matrigel) met excellente biofunctionaliteit, toepasbaar voor verschillende weefseltypen, (**Hoofdstuk 5**), en minder snel afbreekt dan pure gelatine door de toevoeging van een synthetische component (polyethylene glycol, PEG). Dit nieuwe semi-synthetische dragermateriaal wordt door een klinisch relevant enzym, bloedstollingsfactor XIII, gecrosslinkt. De weefselontwikkeling van bot, vaten en ook leverweefsel was vergelijkbaar en gedeeltelijk zelfs beter dan de gouden standaard Matrigel. Verder bleek het mogelijk om eiwitten in het nieuwe dragermateriaal te immobiliseren die de biofunctionele eigenschappen van het materiaal verbeterden. Vaatvorming en celdifferentiatie richting bot konden in deze materialen zelfs verder verbeterd worden door actieve eiwitten in de constructen te incorporeren.

Conclusie

In dit proefschrift werden bestaande, op gelatine gebaseerde, hydrogelen onderzocht en vergeleken met een nieuw ontwikkeld hydrogelsysteem wat betreft geschiktheid om matrix gevasculariseerd botweefsels te kunnen creëren. Er werd aangetoond dat het haalbaar is om complexe gevasculariseerde botachtige weefselconstructen te maken op basis van klinisch relevante stamcelbronnen. GelMA en gelTG-gebaseerde hydrogelen bleken beperkingen te hebben voor de beoogde toepassing. De ontwikkeling van een klinisch relevante hydrogel maakte het mogelijk om een matrix voor cellen te verkrijgen, die voldoende zacht is en een optimale snelheid van celgedieerde afbraak vertoont. Het nieuw ontwikkelde materiaal bleek geschikt te zijn voor celdifferentiaties richting de vasculogene, osteogene maar ook voor andere tissue engineering strategieën zoals voor het kweken van mini-levers. Bovendien kan de nieuwe hydrogel geoptimaliseerd worden door toevoeging van weefselspecifieke eiwitten. Hierdoor is dit materiaal uitermate interessant voor toepassingen voor uiteenlopende weefsels.

Deutsche Zusammenfassung

Konstruktion von Biomaterialien zur Vaskularisation von Knochenanaloge

Knochen ist das am zweithäufigsten transplantierte Gewebe im menschlichen Körper. Die derzeitige Behandlung zum Ersatz eines fehlenden Knochensegments ist die autologe Knochentransplantation. Obwohl kleinere Knochendefekte durch ein nicht vaskularisiertes Stück Knochengewebe des Patienten ersetzt werden können, erfordern Defekte mit einer Länge von mehr als ungefähr 5 cm im Unterkiefer eine sofortige Vaskularisation des transplantierten Knochens. Daher erfordern solche großen Knochendefekte sogenannte vaskularisierte Knochenlappen. Herkömmlicherweise werden diese vaskularisierten Lappen aus der Fibula des Unterschenkels, der Kante des Schulterblatts oder aus dem Kamm der Hüfte entnommen. Die Anastomose eines solch relativ großen Implantats ist entscheidend, um eine sofortige Blutversorgung durch die volle Dicke des implantierten Implantats zu erhalten und somit das Überleben des Implantats zu ermöglichen. Diese Rekonstruktionsoperationen gehen mit Nachteilen wie Morbidität der Spenderstelle und langen Operationszeiten einher, die den Patienten belasten.

Das Gebiet des Tissue Engineering zielt darauf ab, Gewebeersatz zu entwickeln, um die Funktionen des betroffenen Gewebes eines Patienten zu erhalten, wiederherzustellen oder zu verbessern.

In den letzten fast 30 Jahren wurden Erfolge beim Tissue Engineering von dünnen oder nicht durchbluteten Geweben und Organen wie Knorpel, Haut und Blase erzielt. Beim Tissue Engineering von Knochengewebe und anderen Geweben besteht der Hauptengpass in der Vaskularisation, die zur Herstellung größerer Gewebekonstruktionen erforderlich ist. Eine weitere Herausforderung beim Aufbau von vaskularisierten Knochengeweben besteht in der Zusammensetzung des Trägermaterials, das eine effiziente Entwicklung des Gewebes ermöglichen soll. Darüber hinaus ist neben den gewünschten biologischen, mechanischen und chemischen Eigenschaften eines Biomaterials dessen klinische Anwendbarkeit von entscheidender Bedeutung. Aus diesem Grund wird Gelatine als Basismaterial verwendet, da sie klinisch anwendbar hergestellt werden kann. Verschiedene Methoden zur Vernetzung eines Hydrogels werden untersucht und wie mit den verschiedenen Plattformen vaskularisierter Knochen kultiviert werden kann.

In dieser Dissertation wurde untersucht, ob es möglich ist, im Labor ein komplexes Knochengewebe mit Blutgefäßen herzustellen.

Diese Dissertation hat gezeigt, dass klinisch anwendbare Stammzellen aus Knochenmark (multipotente mesenchymale Stromazellen, MSCs) und Nabelschnurblut (endotheliale koloniebildende Zellen, ECFCs) verwendet werden können, um ein komplexes vaskularisiertes knochenähnliches Konstrukt zu züchten

(**Kapitel 6**). Bisher wurde nicht nachgewiesen, dass mit diesen Primärzellen ein Konstrukt mit den folgenden Eigenschaften erzeugt werden kann: ein mit Endothelzellen bedeckter Kanal; kapillarähnliche Strukturen über die gesamte Dicke des Konstrukts; und osteogene (in Richtung Knochen) differenzierte Zellen die die kapillarartigen Strukturen umgeben. Das hierfür verwendete Trägermaterial bestand aus methacrylierter Gelatine (gelMA), die mit einem Photoinitiator und UV-Licht vernetzt wurde.

In einer Folgestudie wurde untersucht, ob die Vernetzung mit einem alternativen System aus Photoinitiator und sichtbarem Licht Vorteile für das Überleben und Verhalten der Zellen bietet (**Kapitel 3**). Die Vernetzung mit sichtbarem Licht führte zu einer besseren Zellfunktionalität als mit UV-Licht. Darüber hinaus schien sichtbares Licht für die Vernetzung großer GelMA-Konstrukte geeigneter zu sein als UV-Licht. Dies ist besonders wichtig, wenn Konstrukte mit klinisch relevanten Abmessungen hergestellt werden, da sichtbares Licht eine bessere Tiefenwirkung hat.

In **Kapitel 4** wurde die Möglichkeit untersucht, vaskularisierte knochenähnliche Konstrukte durch enzymatische Vernetzung von Gelatine herzustellen. Die enzymatische Vernetzung mit der hier verwendeten Transglutaminase hat den Vorteil, dass sie Teil des physiologischen Kollagenvernetzungsprozess ist. Auch werden keine Radikale freigesetzt, wie beispielsweise bei der Photovernetzung. Es wurde deutlich, dass mit Transglutaminase vernetzte Gelatine sowie mit Photoinitiator und UV-Licht vernetztes gelMA eine Differenzierung der Stammzellen ermöglicht. Es stellte sich jedoch heraus, dass es nicht möglich war, Proteine funktionell zu integrieren und zusätzlich die Knochenbildung zu stimulieren.

Ferner trat das Problem auf, dass Gele die ausschließlich auf Gelatine basieren (wie gelMA und Gelatine-Transglutaminase), zu schnell abgebaut werden, um ein Gleichgewicht zwischen Gelabbau und Gewebeproduktion durch die Stammzellen zu gewährleisten. Aus diesem Grund wurde ein neues klinisch anwendbares Material entwickelt, das die biologischen Eigenschaften des Goldstandards (Matrigel) mit hervorragender Biofunktionalität für verschiedene Gewebetypen zeigt (**Kapitel 5**); und weniger schnell als reine Gelatine zerfällt durch Zusatz einer synthetischen Komponente (Polyethylenglykol, PEG). Dieses neue halbsynthetische Material ist mithilfe eines klinisch relevanten Enzyms, den Blutgerinnungsfaktor XIII, vernetzt. Die Gewebeentwicklung von Knochen, Gefäßen und auch Lebergewebe in dem neuen Material war vergleichbar und zum Teil sogar besser als in dem Goldstandard Matrigel. Darüber hinaus konnten Proteine in dem neuen Trägermaterial immobilisiert werden, die dadurch die biofunktionellen Eigenschaften verbesserten. Die Gefäßbildung und Zelldifferenzierung in Richtung Knochen konnte in diesen Materialien noch weiter verbessert werden, indem aktive Proteine in die Konstrukte eingebaut wurden.

Fazit

In dieser Dissertation wurden existierende Hydrogele auf Gelatinebasis untersucht und mit einem neu entwickelten Hydrogelsystem hinsichtlich der Eignung als Trägermaterial zur Herstellung von vaskularisierten Knochengewebe verglichen. Es wurde gezeigt, dass es möglich ist, komplexe vaskularisierte knochenähnliche Gewebekonstrukte basierend auf klinisch relevanten Stammzellquellen herzustellen. Es wurde festgestellt, dass GelMA- und GelTG-basierte Hydrogele Einschränkungen für die beabsichtigte Anwendung aufweisen. Die Entwicklung eines klinisch relevanten Hydrogels ermöglichte es, eine Matrix für Zellen zu erhalten, die ausreichend weich ist und eine optimale Geschwindigkeit des zellvermittelten Abbaus aufweist. Das neu entwickelte Material erwies sich als geeignet für die vaskulogene und osteogene Zelldifferenzierung Tissue-Engineering-Strategien wie die Kultivierung von Mini-Lebern. Darüber hinaus kann das neue Hydrogel durch Zugabe von gewebespezifischen Proteinen optimiert werden. Dies macht dieses Material für Anwendungen für verschiedene Gewebe äußerst interessant.

Acknowledgements

Prof. Rosenberg, beste Toine, wat was het fijn om zo warmhartig op de afdeling Kaakchirurgie opgenomen te worden. Je vraagt altijd hoe het gaat en je toont interesse in zowel onderzoek als ook in de persoon. Het is mooi om te zien dat het fundamentele onderzoek zo veel waardering van een clinicus krijgt, die iedere dag de échte patiënten ziet.

Prof. dr. ir. Malda, beste Jos, dank je dat ik ook onder jouw begeleiding mijn promotie mocht doen. Dankzij jou heb ik twee keer de grote mogelijkheid gekregen om (heel spontaan) naar Nieuw Zeeland te gaan. Deze tijd heeft mijn promotie ruimte en vorm gegeven en gaf me de gelegenheid om geweldige mensen te leren kennen. Ik genoot van onze progress meetings, waar je met een frisse blik op de data kon kijken en mijn (te?) hoge verwachtingen wat hebt kunnen relativeren. Dank voor je hulp om de promotie in de gegeven tijd grotendeels af te ronden.

Dr. ir. Gawlitta, beste Debby, ik wist al bij het eerste interview voor de PhD positie dat het een match was en ik graag met je wilde samenwerken en deelgenoot wilde zijn van het opstarten van een nieuw onderzoeksteam. Ik waardeer je enthousiasme en tegelijkertijd ook je oprechte kijk op onderzoek, wat discussies met je heel erg leuk maakt. Je maakte altijd tijd voor me en naast onderzoek was er ook de tijd om de kleine en grote levensvragen te bediscussiëren. Wat een geluk, dat je zo open bent, ik kon hierdoor veel van je leren! Ik wens je het allerbeste op het werk en ook met jullie kleine meidenteam thuis.

Dr. Lim, dear Khoon, I am super happy I got to know the most crazy and lovely Asian. I will never forget your warm welcome after my two-day flight to the other site of the world- without luggage- and you drove me straight to the mall to be able to survive the first days. Thanks to you, I had great stays in NZ, talking a lot about science and even more about life. You were always reachable as my personal chemist. You were also the person that kept me going when the PhD appeared too difficult and seemed to lead nowhere. I had also the honor to join your Team Hydrogel and the Brunch Club. I am happy that we met so many times again in the Netherlands, Switzerland and in Scotland. And let's hope next time will be soon!

Thanks also to your (former) lab-members Gabby, Naveen, Tiemen, Jonathan, Pau and Jonas for the company on the awesome trips together in NZ.

Dr. Woodfield, dear Tim, thank you for hosting me in your lab in New Zealand. I felt as part of the group and had the pleasure to join all your lab activities. Good to see that so many collaborative efforts came from these visits to New Zealand and thanks for your support with the valuable feedback on the manuscripts.

Dr. Melchels, beste Ferry, ook al heb ik niet lang onder je supervisie gewerkt, ben ik je toch heel dankbaar. Je hebt me geïntroduceerd in de wereld van gelMA en

hydrogel crosslinking. Jammer dat je niet langer in Utrecht bleef, maar het was erg leuk om je met jullie meidenkwartet zo gelukkig in Edinburgh te zien.

Dr. Ehrbar, lieber Martin, meinen ersten Kontakt zum Tissue Engineering habe ich Dir zu verdanken. Ich habe es wirklich genossen während meiner Masterarbeit im schönen Zürich Teil Deines Teams zu sein. Wie schön, dass uns die Wege während meiner Promotion wieder gekreuzt haben. Ich weiß Deine Offenheit und Einstellung zur Zusammenarbeit sehr zu schätzen. Also thanks to the good soul in your lab, Queral, for making and sending all the valuable material to us!

Very important during my PhD and for sure the reason why it became such a nice place to work once you were there: Alessia, Iris, Luuk and Lizette. Ale, you have always the best stories to tell and it is lovely how much you can laugh about yourself "being goofy". I enjoyed our bouldering sessions on Sunday evenings and to end the week with a tea afterwards- very peaceful moments. Iris, ik vond het fijn dat je in de groep kwam en op het gebied van gepre-vasculariseerd bot werkte, waardoor ik veel ondersteuning heb gevonden. Ook waardeer ik dat je mij eraan herinnerde om soms toch weer wat positiever te zijn, wanneer ik me door het onderzoek te veel liet deprimeren. Luuk, wat fijn om met je te werken en ook van je verhalen te horen als je weer je bucket lijst hebt "afgewerkt". Ik vond het heel verfrissend, dat je je niet te gek liet maken door de beruchte promotiestress en gewoon je ding doet. Lizette, wat ben ik blij en dankbaar dat jij in de groep bent gekomen. Je hebt me gered door je hulp met PCR, statistiek en met je positieve, warmhartige instelling. Je weet te goed hoe waardevol het is als iemand je aan het einde van de promotie ondersteuning biedt. Ik vind het jammer, dat je niet veel eerder in het team kwam, want je bent geweldig!

Bedankt aan iedereen van de afdeling Kaakchirurgie voor de interactie bij de RM-childmeetings, beer and pizza-meetings en de gezellige uitjes- op de boot, bij het midgetgolf of een van de borrels. Speciale dank ook aan Iris, Monique en Harmien voor alle ondersteuning bij de organisatorische dingen.

Thanks to all the Orthopaedic people, who adopted me from the beginning in their lab, Jetze, Loek, Vivian, Maarten, Willemijn, Michiel, Behdad, Tommy, Dino, Mechtheld, Anita, Yvonne, Angela and Lucienne. And the newer generation Irina, Joao, Imke, Maaïke, Koen, Chella, Flor, Mylene, Riccardo, Miguel, Saber, Kim, Joost, both Inges, Iris, Paweena, Yang, Susanna, Anneloes, Lotte, Margot, Jasmijn and most importantly of course Mattie!

Beste Mattie, dank voor al je hulp, voor mijn gevoel had ik iedere dag je raad nodig! Jij bent het hart van de hele groep. Naast bier en bitterballen moet jij erbij zijn voor een geslaagde borrel- waarvan er gelukkig vele waren.

Dank aan Loes en Bart van de afdeling Diergeneeskunde voor de leuke samenwerking op het gebied van lever organoïden. Wat fijn, dat we ons enthousiasme konden delen en er mooie resultaten uit ons onderzoek kwamen.

Thanks also to my students, who I had the chance to supervise during their master internship. I learned a lot from you, Bram, Yee Xiang, Maya, Marijke, Gregor and Adriana. I wish the best to all of you wherever your paths may go!

Mies, van de Afdeling Farmacie, dank voor alle ondersteuning bij diverse hydrogelkarakterisaties. Je was een grote hulp bij veel van mijn vragen en het was altijd fijn om bij je langs te komen omdat je zo een vrolijk persoon bent.

Liebe Giga, was für ein Geschenk, dass wir einander schon so lange haben. Obwohl ich seit mehr als 10 Jahren im Ausland lebe, finden wir uns immer wieder als wäre nichts gewesen.

Beste Tineke en Gert, Judith en Dennis, wat fijn om een tweede familie in Nederland te hebben. Ik geniet van de tijd met jullie, ook al betekend het, dat ik gedichtjes in Nederlands moet verzinnen. Dank Gert, voor je interesse ook aan de inhoudelijke aspecten van mijn promotie.

Meine Familie, ich bin froh, dass ich euch alle habe. Während meiner Promotion konnte ich so immer wieder den nötigen Abstand bekommen und das wirklich Wichtige im Leben vor Augen behalten.

Mama, du glaubst immer an mich und ermutigst mich dennoch auch aufgeben zu dürfen. Es ist großartig ein Vorbild zu haben wie man unkonventionell und abseits der ausgetretenen Pfade seinen eigenen Weg gehen kann. Deinem Schubs aus dem Haus habe ich es zu verdanken, dass ich den großen Schritt nach Holland gewagt habe (wo ich doch nicht einmal wusste, wo auf der Karte dieses Land liegt).

Papa, es ist unbezahlbar jemanden an seiner Seite zu wissen, den man immer um Rat fragen kann. Sei es was die Bahn angeht oder ob man das tote Pferd das man reitet, endlich für tot erklären sollte. Heimlich warst du immer mein Vorbild, als du beruflich auf der ganzen Welt unterwegs warst und auf Konferenzen vor vielen Leuten präsentiert hast. Vielleicht habe ich deswegen den Weg der Forschung eingeschlagen und ich ins Ausland gezogen.

Peter, du verstehst die Kunst zu gut wie man am Meisten aus dem Leben macht, es anpackt und feiert. Es ist bewundernswert, wie viel Biss du hast, etwas Neues zu erlernen- egal ob Motorrad reparieren, künstlerische Projekte, Häuserrestauration oder neue Sportarten. Und das alles neben einer Weiterbildung und einer Vollzeitstelle. Da kann ich viel von dir lernen.

Anna, wunderbar, dass du so rebellisch und dickköpfig bist und am Ende das erreichst, wovon du überzeugt bist. Mit deinem starken Gerechtigkeitsinn lässt sich die Welt ganz sicher zu einem besseren Ort machen.

Isi, ich finde klasse wie du dein Ding machst und zwischen den Optionen deiner vielen Geschwister, deinen Weg gehst. Du kämpfst dich durch das Ingenieurstudium und ich wünsch dir, dass auch bald wieder freudigere Zeiten für dich kommen.

Lori, du bist genial und als Jüngste von uns profitierst du sicher von einem guten Bonus in Sachen Unkompliziertheit. Ich bin echt gespannt, wo dich dein Leben in ein paar Jahren hinführt ;)

Liebe Oma, danke, dass du mich immer so verwöhnst mit schwäbischem Essen und Vitaminen, wenn ich wieder auf Heimaturlaub bin.

Endlich ist unser Schlössle keine Träumerei mehr und können wir unter italienischer Sonne Dornen hacken, bohrhammern oder von morgens bis abends brunchen.

Liefste Thijs, wat heb ik een ontzettend groot geluk en ben ik dankbaar dat jij in mijn leven bent gekomen! Tijdens mijn promotie was ik te vaak niet de mooiste versie van mezelf, maar jij wist er gelukkig goed mee om te gaan. Ook had ik profijt, dat je nieuwe onderzoeksvragen wilde bediscussieren en de een of andere presentatie kon ik ook geduldig met je doorspreken. Ik waardeer je kritische en analytische kijk op alles – ook op wat ik vertel, ook al ben ik op het moment zelf niet altijd even blij over. Je ongecompliceerde, nieuwsgierige en vrolijke kijk op het leven is een genot. Ik was altijd een fan van grote plannen die ik (ver) in de toekomst omzet. Jij bent een meester van het leven in het nu. Met jou verspil ik geen tijd met grote plannen maken maar geniet ik van onze tijd samen. Daardoor gaat niet alles efficiënt en volgens plan, maar door die “omleidingen” is mijn leven met jou vol met leven- en er kan niets leukers zijn. Ook zonder veel te plannen is er weer tijd voor een nieuw avontuur en kijk ik er naar uit om samen met z’n drieën naar Duitsland te verhuizen!

Curriculum Vitae

Barbara Judith Klotz was born on 26th of November 1988 in Filderstadt, Germany. After finishing high school in 2008, she moved to the Netherlands, where she started her B.Sc degree in Biology at Radboud University Nijmegen, the Netherlands. She stayed in Lambaréné, Gabon, for a clinical research internship at the Albert Schweitzer Research Unit. The study focused on the effect of helminth infections on the efficacy of vaccines in school children. For her M.Sc degree in Medical Biology, Barbara continued the program at Radboud University Nijmegen. In 2012, she started a Master project in the group of Dr. Ehrbar in the Cell and Tissue Engineering Lab at the University Hospital Zurich, Switzerland. During this project she got first insights into hydrogel platforms and stem cell culture. For her second Master internship, she joined Prof. Habibovic at the Tissue Regeneration group at the MIRA Institute at University Twente, Enschede, the Netherlands. The work focused on the preparation of calcium-laden microspheres for osteogenic differentiation of mesenchymal stromal cells. In June 2014, Barbara finished her M.Sc degree and accepted a PhD position at the University Medical Center Utrecht, the Netherlands. The topic of the PhD project was vascularised bone tissue engineering with a special focus on the biomaterial aspects. During the course of her PhD, Barbara got the chance to stay in New Zealand for two consecutive visits, at the Christchurch Regenerative Medicine and Tissue Engineering research group, with Dr. Woodfield and Dr. Lim, at the University of Otago, Christchurch. The results of the four-year PhD studies are presented in this thesis.

